

**Landslide Risk to Railway Operations and Resilience in the Thompson River Valley
near Ashcroft, British Columbia**

by
Kristen Michelle Tappenden

A thesis submitted in partial fulfillment of the requirements for the degree of

Doctor of Philosophy
in
Geotechnical Engineering

Department of Civil and Environmental Engineering
University of Alberta

© Kristen Tappenden, 2017

Abstract

This thesis investigates the hazard frequency and associated risk posed by twelve large landslides in the Thompson River Valley south of Ashcroft, British Columbia, which are collectively referred to as the Ashcroft Thompson River landslides. The Canadian National and Canadian Pacific railways operate busy main lines within the subject 10 kilometer corridor south of the village of Ashcroft, traversing the lower portions of many of the landslides. These landslides have resulted in significant, recurring disruptions to Canada's Class 1 railways, and affect numerous other groups located within the valley, including First Nations communities, residents of the villages of Ashcroft and Spences Bridge, salmonid populations within the Thompson River, and owners/operators of upland agricultural areas. While the Ashcroft Thompson River landslides are typically inactive or very slow moving, numerous periodic reactivations have been documented in the past 150 years, some of sufficient magnitude to temporarily dam the Thompson River.

The objectives of the research are to characterize the risks posed by the Ashcroft Thompson River landslides to the Canadian railway network and to the numerous stakeholders in the Thompson River Valley, and to investigate strategies for managing the risks and improving the overall resilience of the system. The research methodology includes an examination of the history and ongoing activities of the landslides, with an emphasis on the dynamic climatic and anthropogenic factors which have contributed to the slope movements over time. Recent landslide activity in the corridor is correlated to snow pack and stream flow in the Thompson River basin. Trends in the discharge of the Thompson River over the past century are, in turn, related to the phase of the high-level climate phenomenon termed the Pacific Decadal

Oscillation (PDO). An awareness of the interannual and interdecadal fluctuations in climate regimes and their hydrologic implications is presented as an essential component for contextualizing historic landslide frequency and future landslide risk. The anticipated hydrologic impacts of climate change and their potential effects on landslide activity in the corridor are also discussed. The qualitative risk assessment which follows distinguishes the different modes of failure which have been demonstrated by the landslides in the corridor, to elucidate the unique causal factors, consequences and associated risk scenarios. A risk management strategy is presented which integrates an understanding of climate factors which may portend landslide activity in the corridor, a kinematic understanding of the landslide failure modes, and an observational approach to geotechnical monitoring and inspection. It is recommended that contemplated risk reduction measures favor flexible options which would be suited to a range of future climate conditions, improve adaptive capacity through more effective anticipation and forward planning, and integrate active monitoring and regular site inspections of slope movements with effective strategies for the documentation, communication and dissemination of hazard and risk information.

The economic consequences of a landslide which impacts the railway infrastructure in the Thompson River Valley can grow exponentially with the duration of the outage; given the diverse cross-section of stakeholders involved, the consequences of a rapid landslide in this corridor may also include significant safety, environmental, and cultural impacts. The application of a resilience paradigm for managing critical infrastructure and enhancing a community's ability to cope with disruptions is presented in the context of the Ashcroft Thompson River landslides. The high-consequence, low-probability nature of a rapid landslide

necessitates a flexible, resilient response by all stakeholders. To this end, case studies summarizing and evaluating the risk communication and public involvement efforts in the District of North Vancouver, British Columbia, and Canmore Alberta, are presented to convey lessons learned and highlight current best practices stakeholder involvement in risk management and decision making. It is hoped that the research contributions in the area of risk management and system resilience will impact how Canada's railway industry and its regulator will monitor and mitigate landslides along the Thompson River Valley, with broader implications for the risk management of natural hazards interacting with the built environment.

Preface

This thesis is an original work by Kristen Tappenden. The research has been conducted in cooperation with the Canadian Rail Research Laboratory (CaRRL) at the University of Alberta, under the supervision of the chair, Professor C. Derek Martin.

The description and evaluation of the District of North Vancouver's Landslide Management Strategy, presented in Chapter 7, forms a portion of the manuscript which has been published in the journal *Natural Hazards*:

Tappenden, K.M. 2014. The district of North Vancouver's landslide management strategy: Role of public involvement for determining tolerable risk and increasing community resilience. *Natural Hazards*, 72(2): 481–501.

Portions of Chapters 2, 3 and 4 have been published as papers in the following conference proceedings:

Tappenden, K.M. 2014. Climatic influences on the Ashcroft Thompson River Landslides, British Columbia, Canada. *In Proceedings of the 6th Canadian Geohazards Conference*, Kingston, Ontario.

Tappenden, K.M. 2016. Impact of climate variability on landslide activity in the Thompson River Valley near Ashcroft, B.C. *In Proceedings of the 69th Canadian Geotechnical Conference*, Vancouver, British Columbia.

Dedication

To my Grandmother,

Edith Maria Gruber
1975 MA, 1990 PhD

and my children,

Avery Frederick Tappenden

&

Clara Edith Tappenden

You inspired me to undertake this project and motivated me to complete it.

Acknowledgements

I would like to acknowledge and sincerely thank the following individuals and organizations for facilitating the realization of this thesis in a variety of ways, including:

For their supervision and guidance of this research, including numerous meetings, conversations and reference letters, which opened many doors and ushered me forward in my professional and personal development:

Derek Martin, David Cruden, and Norbert Morgenstern, University of Alberta

For her engaging course on risk communication, which presented a seminal learning experience, challenging and ultimately persuading me to understand risk management as a social process:

Cindy Jardine, University of Alberta, School of Public Health

For their enthusiasm for research, readily sharing their knowledge, experiences and relevant information on the Ashcroft landslides and the British Columbia climate:

Peter Bobrowsky and David Huntley, both of the Geological Survey of Canada

Chris Bunce and Eddie Choi, both formerly of Canadian Pacific Railway

David Campbell, B.C. River Forecast Centre

Tom Edwards, Canadian National Railway

Tim Keegan, Klohn Crippen Berger

Pete Quinn, BGC Engineering

David Wood, David Wood Consulting

For sharing their experiences of public involvement and Canmore's Mountain Creek Hazard Mitigation Program:

Julia Eisl and Andy Esarte, Town of Canmore

For their ongoing friendship, for wandering the desert with me, and when needed, extending empathy as only former PhD students can:

Renato Macciotta, University of Alberta

David Elwood, University of Saskatchewan

For her wonderfully loving and compassionate care of my children, which allowed me to pursue my education and research:

Doreen Niles

For always believing I was capable, my parents, siblings and extended family:

Mike and Sandy Gruber

Lisa, Garth, Andrea and Carla Gruber

Alan and Connie Tappenden

For their enduring support, which extends beyond my research endeavours and into my everyday life, and for enthusiastically coming along for the ride, my family:

Andrew, Avery and Clara Tappenden

This research project received funding from the Natural Sciences and Engineering Research Council of Canada (NSERC), Alberta Innovates: Technology Futures, the University of Alberta and the Canadian Rail Research Laboratory—a collaborative initiative involving numerous public and private sector partners, which include the University of Alberta, Transport Canada, and the Canadian National and Canadian Pacific Railways.

Table of Contents

1. Introduction	1
1.1. Objectives and Significance of the Research	1
1.2. Scope and Limitations	2
1.3. Organization of the Thesis	3
2. Geology	5
2.1. Geomorphology	5
2.2. Stratigraphic Sequence	6
2.2.1. Glacio-Isostatic Rebound and Elevation of Rupture Surfaces	7
2.2.2. Geologic Controls on Extent of Landsliding	10
2.3. Regional Hydrogeology	11
2.3.1. Impact of Groundwater Flow and Seepage Pressures on Slope Stability	11
2.3.2. Groundwater and Surface Water Isotopes	18
2.4. Conditionally Collapsible Soils	20
2.5. Conclusion	23
3. History of Ongoing Landslide Activity	32
3.1. Overview and Evolution of Slope Instabilities	32
3.2. Inventory and Description of Historical Landslide Events	35
3.2.1. Landslide No.1 (CN 50.4)	40
3.2.2. Landslide No.2 (CN 50.9)	41
3.2.3. Landslide No.3 (Unnamed)	44
3.2.4. Landslide No.4 (Goddard)	45
3.2.5. Landslide No.5 (CN 53.4/53.7)	49
3.2.6. Landslide No.6 (North Slide)	50
3.2.7. Landslide No.7 (South Slide)	53
3.2.8. Landslide No.8 (Red Hill / Hammond Ranch)	56
3.2.9. Landslide No.9 (Barnard)	59
3.2.10. Landslide No.10 (Nepa)	60
3.2.11. Landslide No.11 (CN/CPR Nepa Crossover)	62
3.2.12. Landslide No.12 (Basque)	63

3.2.13.	Landslide Near Spences Bridge	64
3.3.	Conclusion	69
4.	Influence of Weather and Climate on Landslide Frequency	79
4.1.	Introduction	79
4.2.	Local Climate of Ashcroft, British Columbia	80
4.3.	Seasonal and Inter-Annual Fluctuations in Thompson River Flow	81
4.4.	Annual Basin-Wide Snow Pack	84
4.5.	Pacific Decadal Oscillation (PDO)	89
4.5.1.	Introduction	89
4.5.2.	Definition of the Pacific Decadal Oscillation	89
4.5.3.	PDO Regimes	90
4.5.4.	Impacts of PDO on Snow Pack and Streamflow in North America	93
4.5.5.	Impacts of PDO on Snow Pack and Thompson River Flow	95
4.5.6.	Association of PDO with Landslide Activity	97
4.6.	Hydrologic Effects of the El Niño Southern Oscillation (ENSO)	98
4.7.	Weather and Climate Conditions Associated with the 1982 Goddard Landslide	101
4.8.	Climate Change and Hydrologic Impacts in British Columbia	103
4.8.1.	Historic Trends in Canadian Climate and Streamflow	104
4.8.2.	Climate Change Forecasts for British Columbia	106
4.8.3.	Implications of Climate Trends and Forecasts for the Thompson River	109
4.9.	Conclusion	109
5.	Landslide Mechanics	125
5.1.	On Accelerations of Slow-Moving Landslides	125
5.2.	Interpreted Modes of Movement	127
5.2.1.	Complex Earth Slide–Debris Flow (North Slide, Spences Bridge Slide)	128
5.2.2.	Reactivated Rapid Compound Earth Slide (Goddard)	134
5.2.3.	Alternate Hypotheses for the Rapid Acceleration of the Goddard Slide	147
5.2.4.	Use of Inverse Velocity Method for Forecasting Rapid Failure (Goddard)	152
5.2.5.	Reactivated Very/Extremely Slow Earth Slide (CN 50.9)	154
5.3.	Conclusion	158

6.	Landslide Risk Assessment and Management Strategy _____	169
6.1.	Risk Assessment and Management Concepts _____	169
6.2.	Importance of Railway Ground Hazards and Risk Management _____	170
6.3.	Spectrum of Landslide Failure Modes, Causes and Effects _____	171
6.3.1.	Mode III: Reactivated Very/Extremely Slow Earth Slide _____	173
6.3.2.	Mode II: Reactivated Rapid Compound Earth Slide _____	174
6.3.3.	Mode I: Complex Very Rapid Earth Slide-Debris Flow _____	176
6.4.	Risk Scenarios and Risk Management Strategy _____	177
6.4.1.	Direct Operational Effects _____	177
6.4.2.	Slope Monitoring Strategy and Kinematic Threshold Criteria _____	181
6.5.	Indirect Effects _____	185
6.6.	Conclusion _____	188
7.	Risk Management Within a Resilience Framework _____	193
7.1.	Resilience Concepts and Frameworks for Managing Complex Risks _____	193
7.2.	Engineering Mitigation and Stakeholder Perspectives _____	195
7.3.	Case for Public Involvement in Risk Management _____	198
7.3.1.	Mountain Creek Hazard Mitigation Program, Canmore, Alberta _____	202
7.3.2.	Landslide Management Strategy, District of North Vancouver _____	204
7.4.	Adaptation Strategies for Risk Reduction _____	211
7.5.	Conclusion _____	213
8.	Conclusions and Future Research _____	218
8.1.	Summary _____	218
8.2.	Conclusions and Significant Contributions _____	219
8.2.1.	Landslide Failure Modes, Causes and Effects _____	219
8.2.2.	Integrated Risk Management Strategy and Adaptive Actions _____	222
8.3.	Opportunities for Further Research _____	224
	List of References _____	225

List of Tables

Table 2.1: Investigated rupture surface elevations at several landslides in the Thompson River Valley south of Ashcroft (modified from Eshraghian et al. (2007)).	24
Table 2.2: Estimated horizontal and vertical hydraulic conductivities of dominant Quaternary valley fill sediments in the Thompson River Valley south of Ashcroft (modified from Bishop (2008)).	24
Table 3.1: Recorded movements of large landslides in the Thompson River Valley within approximately 10 km south of Ashcroft. The number assigned to each landslide in the table corresponds to the location shown on Figure 3.1.	71
Table 4.1: Summary of hydrologic years with cumulative flow departure from normal exceeding 3400 Mm ³ for Thompson River flow at Spences Bridge from 1913 to 2011.	112
Table 4.2: Snow survey sites utilized in snow pack versus river flow analysis; modified from Province of British Columbia (2014)	113
Table 4.3: Summary of Pacific and North American climate anomalies associated with extreme phases of the PDO (Mantua 2002). Reproduced with permission.	113
Table 4.4: Summary of snow monitoring stations with readings in excess of 500% of normal for the spring of 1982.	114
Table 4.5: Climate change projections for British Columbia (seven models and eight emission scenarios). Data are the changes from 1961 to 1990 climate as a change in mean temperature or a percentage change in total precipitation (PPT) (Moore et al. 2010).	114
Table 4.6: GCM ensemble medians of April 1 st SWE volume and annual discharge changes (2050s versus 1970s) for emissions scenarios B1, A1B and A2 (modified from Shrestha et al. (2012)).	114
Table 6.1: Summarized landslide monitoring and risk management strategy for the Ashcroft Thompson River Landslides.	189
Table 7.1: Comparison of traditional engineering approach to system management with resilience concepts.	215

List of Figures

- Figure 2.1: Characteristic semi-arid, terraced landscape used for ranching and farming along the Thompson River Valley, as seen looking east from Highway 1 between Ashcroft and Spences Bridge (November 2015). _____ 25
- Figure 2.2: Generalized stratigraphy of Quaternary sediment fill in the Thompson River Valley at Ashcroft (modified from Clague and Evans 2003). _____ 25
- Figure 2.3: Characteristic exposure along the Thompson River Valley between Ashcroft and Spences Bridge (looking east from Highway 1, November 2015). The surficial late-glacial lacustrine silt deposits (unit 7) are readily identifiable as the upper light-coloured band of sediment. _____ 26
- Figure 2.4: Depiction of groundwater seepage vector of magnitude, i , and direction, λ , relative to an infinite slope inclined at angle, β (modified from Iverson and Major (1986)).__ 26
- Figure 2.5: Effect of stratigraphic layering on the seepage force within a slope due to contrasting permeabilities between two soil strata (modified from Reid and Iverson (1992)). _____ 26
- Figure 2.6: Effect of seepage gradient magnitude and direction on factor of safety for a hypothetical infinite cohesionless slope with $\phi'=\beta=16^\circ$. _____ 27
- Figure 2.7: Vertical pore pressure gradients between deep and shallow piezometers measured at the toe of the CN 51 landslide, close to the Thompson River (modified from Quinn et al. 2012). _____ 27
- Figure 2.8: Results of groundwater isotope testing from samples at the Ripley landslide; (a) Deuterium (^2H) concentration with depth– stratigraphic columns are from Schafer (2016), (b) Oxygen-18 concentration with depth, (c) Deuterium versus Oxygen-18 concentration with meteoric water line and slope of enrichment line shown. _____ 28
- Figure 2.9: Evolution of $\delta^{18}\text{O}$ and $\delta^2\text{H}$ in snow during evaporation under controlled conditions; f is the fraction of snow remaining during sublimation (modified from Moser and Stichler (1975), as reproduced in Clark and Fritz (1997)). Reproduced with permission. ____ 29
- Figure 2.10: Cross section locations and interpreted stratigraphy of the Quaternary fill in the study area, from Clague and Evans (2003). _____ 29

Figure 2.11: Interpreted stratigraphy of the Quaternary fill along an east-west section A-A', 3 km north of Ashcroft, from Clague and Evans (2003).	30
Figure 2.12: Aerial view of Bonaparte confluence north of Ashcroft, with evidence of historic irrigation practiced on river terrace above the confluence (NRC Roll A291, #69, July 15, 1928).	30
Figure 2.13: Irrigated field on the upper terrace of the Thompson River Valley north of Ashcroft at the Bonaparte River confluence (looking east from Highway 1, November 2015).	31
Figure 3.1: Map of the study area showing large landslides along the Thompson River Valley within approximately 10 km south of the village of Ashcroft (BC map modified from www.worldatlas.com). The number assigned to each landslide in the figure corresponds to Table 3.1.	72
Figure 3.2: Timeline of recorded landslide events.	73
Figure 3.3: Cambie [...] & survey party. Caption reads: "The first expedition sent out to explore the Northern British Columbian passes thro' the Rockies for the Canadian Pacific Railway. Photo taken by Cambie at Fort McLeod– 1879 I was [laid?] off by the H.B.Co. as guide to the party. HBW. This route was finally abandoned for one further south." (Bullock-Webster 1879). Reproduced with permission.	73
Figure 3.4: Cambie's (1895) map of landslides in the Thompson River Valley south of Ashcroft (as reproduced by EBA Engineering (1984)).	74
Figure 3.5: Stanton's (1898a) map of landslides in the Thompson River Valley south of Ashcroft.	75
Figure 3.6: 2015 aerial photo of the Goddard landslide on the east bank of the Thompson River (courtesy of CN rail); shaded area corresponds to the limits of the 1982 reactivation (as per Eshraghian et al. (2007)), dashed line delineates broader extents of an older, possibly ancient landslide feature.	76
Figure 3.7: 1928 aerial photo showing the Goddard landslide and upslope ditch-and-furrow irrigation (east bank on the outside river bend); NRC roll A291 #55.	76
Figure 3.8: Photograph of The Anglican Church of St. Michael and All Angels (looking northeast from Highway 1); taken at Spences Bridge, B.C. in November 2015.	77

Figure 3.9: 1928 aerial photo showing the 1905 Spences Bridge landslide; Natural Resources Canada, Roll A682, No. 8. _____	77
Figure 3.10: 2015 aerial photos showing the 1905 Spences Bridge landslide; courtesy of Canadian National Railway. _____	78
Figure 3.11: Photograph of the 1905 landslide south of the village of Spences Bridge, B.C. (looking west from Highway 1), taken in November 2015. _____	78
Figure 4.1: Latitudinal cross-section of southern British Columbia, illustrating the physiographic diversity and associated climatic regimes (Chilton 1981). _____	115
Figure 4.2: Ashcroft North weather station; temperature and average precipitation, 1980-1986 (Environment Canada 2015b). _____	115
Figure 4.3: Ashcroft North weather station; temperature and annual precipitation, 1980-1986 (Environment Canada 2015b). _____	116
Figure 4.4: Spences Bridge Nicola weather station; temperature and precipitation normals, 1981-2002 (Environment Canada 2015b). _____	116
Figure 4.5: Thompson River cumulative flow departure from normal, Spences Bridge station 08LF022 (1912-1951) and station 08LF051 (1952-2011), with 20 th century landslide activity indicated. _____	117
Figure 4.6: Annual cumulative flow departure from normal by hydrologic year (October – September), Thompson River at Spences Bridge; 1913-2011. _____	117
Figure 4.7: Overview of manual and automated snow survey sites, with boundaries of the North Thompson and South Thompson administrative basin areas as shown; modified from the Province of British Columbia (2016c), and Quinn et al. (2012). _____	118
Figure 4.8: Relationship between peak snow pack (snow water equivalent) measured in the North and South Thompson River basins and annual and maximum Thompson River flow, 1952-2011. _____	118
Figure 4.9: Time series of anomalies exhibiting coherent inter-decadal climate changes (thin solid curve), with temporal averages of the anomalies for the periods 1870-1889, 1890-1924, 1925-1947, 1948-1976 and 1977-1990 (thick dashed lines). (a) Spring (Mar-May) air-temperature anomalies in western North America averaged over 130°W-105°W, 30°N-55°N. (b) Spring SST anomalies in the eastern North Pacific average over 140°W-110°W, 30°N-55°N. All differences in the temporal average between successive periods	

are significant at the 95% confidence level in each time series (Minobe 1997). Reproduced with permission. _____	119
Figure 4.10: Outer extents of Minobe’s (1997) study area (140°W-105°W and 30°N-55°N), with location of Ashcroft indicated. _____	119
Figure 4.11: British Columbia winter (Dec-Feb) temperature and precipitation anomalies during neutral, positive and negative phases of the PDO (Stahl et al. 2006). Reproduced with permission. _____	120
Figure 4.12: Normalized winter mean (November—March) time histories of Pacific Climate indices, with stream flow time series for Skeena, Fraser and Columbia Rivers (shading convention is reversed). Dotted vertical lines are drawn to mark the PDO polarity reversal times in 1925, 1947, and 1977 (Mantua et al. 1997). © American Meteorological Society; reproduced with permission. _____	121
Figure 4.13: Times series of normalized annual flow departure from normal for hydrologic (October to September) years 1913 to 2011, with 3-, 5-, and 10-year running averages overlain. _____	121
Figure 4.14: Comparison of Pacific Decadal Oscillation (PDO) index to Thompson River cumulative flow departure from normal at Spences Bridge, with number of landslides indicated; 1912-2011. _____	122
Figure 4.15: Strong/very strong ENSO events, landslide activity, and cumulative Thompson River flow departure from normal, with PDO regimes indicated; 1950-2011. _____	123
Figure 4.16: Locations of snow survey sites within approximately 100 km of Ashcroft with SWE in excess of 500% of normal on May 1, 1982. Province of British Columbia (2016c). _____	123
Figure 4.17: Baseline (1970’s) and future (2050’s) discharge for three emissions scenarios for the Thompson River at Spences Bridge. Each box plot shows the median and inter- quartile range, with whiskers denoting upper and lower limits of the 30-year means of GCM ensembles (Shrestha et al. 2012). Reproduced with permission. _____	124
Figure 4.18: Fraser River average daily flows at Hope, B.C.; base, observed and projected (Morrison et al. 2002). Reproduced with permission. _____	124
Figure 4.19: Thompson River summer temperatures at Spences Bridge; base and projected (Morrison et al. 2002). Reproduced with permission. _____	124

Figure 5.1: Five kinematic stages in the development of a compound translational slide (modified from Soe Moe et al. (2006)).	159
Figure 5.2: Composite photograph (top) of the North slide, June 2016, with interpretation (bottom). Note weathered rear scarp and mid-slope uphill-facing scarps; irrigated plateau above the Goddard slide is visible in the background; vantage point is standing above the south flank looking north, as indicated on Figure 5.4.	160
Figure 5.3: Cross-section through the North slide, based on 2015 LiDAR data (courtesy of CN). Stratigraphy and rupture surface after Eshraghian et al. (2007).	161
Figure 5.4: 1928 aerial photo of the North slide (left), with interpretation (right). Photo courtesy of Natural Resources Council (NRC), Roll A291, No. 54.	161
Figure 5.5: Carbonate (?) precipitates at slope face in seepage area south of the South slide; location shown in Figure 5.7 (June 2016).	162
Figure 5.6: Derivation of the stable slope angle for a wedge of frictional soil sliding on a horizontal rupture surface, with cleft water pressure at the rear crack.	163
Figure 5.7: 1928 aerial photo of the Red Hill slide (left), with interpretation (right). Photo courtesy of Natural Resources Canada (NRC), Roll A291, No. 46.	164
Figure 5.8: Composite photograph of the Red Hill slide, taken from the opposite bank of the Thompson River, looking west (June 2016).	164
Figure 5.9: Cross-section through the Red Hill slide, based on 2015 LiDAR data (courtesy of CN). Stratigraphy and rupture surface interpolated from data at the South slide (after Eshraghian et al. (2007)).	164
Figure 5.10: Composite image of the Red Hill slide in 1928 (centre of image), with older scarp visible to the left (south) of the main slide area. Photos courtesy of Natural Resources Canada (NRC), Roll A0291, No. 45 & 46.	165
Figure 5.11: Schematic cross sections of the 1982 Goddard landslide before, during and after failure (from Wood (1982)); location shown on Figure 5.13.	165
Figure 5.12: Simplified stratigraphic cross-section of the 1982 Goddard landslide, with pre-slide surface profile indicated by the dashed line (Eshraghian et al. 2007); location shown on Figure 5.13.	166
Figure 5.13: Sketch plan view of the 1982 Goddard landslide; note location of monitoring point MP-1 on the north flank of the landslide (modified from Wood (1982)).	166

Figure 5.14: Cumulative surface displacement at north flank of 1982 Goddard slide, as determined from surface offset displacements recorded by Wood (1982); inset figure modified from Wood (1982).	167
Figure 5.15: Inverse velocity of surface offset displacements during 1982 Goddard slide, with linear trendline established using surface displacements recorded by Wood (1982) from approximately 27 hours prior to onset of major failure.	167
Figure 5.16: Relationship between CN50.9 landslide displacement (deep shear zone), Thompson River elevation, and deviation of bedrock pore pressure elevation from river level. Figure prepared based on instrumental data provided by BGC Engineering Inc., with the permission of Canadian National Railway.	168
Figure 6.1: Risk management framework (modified from Canadian Standards Association (1997)).	190
Figure 6.3: Landslide risk scenarios and adaptive responses.	192
Figure 7.1: Properties of resilience (modified from Maguire and Hagan (2007), as adapted from Adger, 2000). Reproduced under: https://creativecommons.org/licenses/by-nc/4.0/	216
Figure 7.2: Spectrum of philosophical approaches to risk management.	216
Figure 7.3: Resilience framework for managing critical infrastructure (modified from National Infrastructure Advisory Council (2010)).	216
Figure 7.4: Role of adaptation responses for risk reduction through reduced vulnerability (modified from United Nations Environment Programme (2009)).	217

1. INTRODUCTION

“As I resided and travelled on the Cariboo Road for years, I know it at first hand. ...it was an atmosphere sui generis, something quite distinct and apart from any other.”

— Wade (1979)

1.1. Objectives and Significance of the Research

This thesis is concerned with the risk posed by large landslides located in the Thompson River Valley south of Ashcroft, British Columbia, Canada. The valley contains main lines of both the Canadian Pacific and the Canadian National Railways, forming an important transportation corridor which links directly to Canada’s west coast shipping industry via the port of Metro Vancouver. The railways traverse several active landslides along the base of the valley, which are among twelve large landslides located along the 10-kilometer (km) reach south of the village of Ashcroft, collectively referred to herein as the Ashcroft Thompson River landslides. While the Ashcroft Thompson River landslides are typically inactive or very slow moving, approximately nine rapid slope failures have occurred in the past 150 years, some of sufficient volume to temporarily dam the Thompson River. As the largest tributary of the Fraser River, the Thompson River is also an important Pacific salmon spawning waterway, comprising a resource with an annual commercial value in excess of \$100 million (Clague and Evans 2003). Periodic reactivations of the Ashcroft Thompson River landslides may impact operations of the Canadian National and Canadian Pacific railway lines, residents of the villages of Ashcroft and Spences Bridge, transportation and utility assets, upslope agricultural lands and salmon populations within the Thompson River Valley. Considering the diverse stakeholders involved, the consequences of a rapid landslide reactivation in this corridor present significant safety, environmental, and economic implications.

The objectives of the research are to assess the risk posed by the landslides to the Canadian railway network and the numerous stakeholders in the Thompson River Valley, and to formulate strategies for managing the risk and improving the overall resilience of the system. The study documents the long history of slope movements in the corridor, and proceeds to

investigate the complex interrelationships between the slope movements and natural (climatic) and anthropogenic factors, which have themselves evolved over time. Inter-annual and inter-decadal fluctuations in climate conditions, and their effect on stream flow in the Thompson River Valley, are presented as a potential tool for better anticipating future landslide activity. Past landslides which have been documented in this corridor are classified based on the interpreted modes and velocities of movement, from which relevant risk scenarios are derived. An inverse-velocity analysis of unpublished slope displacement measurements from the 1982 reactivation of the Goddard landslide offers important insights for the risk management of future landslide reactivations in the valley. Strategies are recommended for management of the risk scenarios based on an integrated approach to anticipating, monitoring and inspecting active slopes in the corridor. The final stage of the research offers resilience concepts for integrating adaptation and public involvement into the risk management framework. The high-consequence, low-probability nature of a large landslide necessitates a flexible, resilient response by all stakeholders. The research contributions will facilitate Canada's railway industry and its regulator in monitoring, anticipating and coping with landslides along the Thompson River Valley, with broader implications for the management of natural hazards interacting with the built environment.

1.2. Scope and Limitations

The subject area of this research is limited to large landslides identified along the Thompson River Valley within 10 kilometers south (downstream) of the village of Ashcroft, British Columbia, as identified in Figure 3.1. While the research methodology and general principles of the risk management and resilience strategies may be broadly applicable to other areas, the specific findings and recommendations contained in this thesis are applicable only to the study area. This study attempts to incorporate a wide range of existing historical and contemporary technical information, field observations and climate data, to illuminate the interrelationships between the landslides and the natural and social environments in which they have occurred, in the context of risk management and resilience strategies. As would be expected for natural hillslopes which have been subject to landslide activity, anecdotal inspection and technical study for nearly 150 years, there is a wealth of often conflicting and conflated information

concerning the Ashcroft Thompson River landslides; as the author, I have presented my interpretation of the available information supplemented by my own additional inquiries, inspections and analyses, and have sought to justify my recommendations as fully as possible. Notwithstanding, the findings contained herein remain a matter of judgement and interpretation from which others may differ.

1.3. Organization of the Thesis

This thesis is organized into eight chapters as summarized below:

Following these introductory remarks, **Chapter 2** describes the complex geologic setting of the Ashcroft Thompson River landslides, with specific reference to geologic and hydrogeologic factors which predispose the valley walls to instability.

Chapter 3 provides a detailed discussion of the history of the Ashcroft Thompson River landslides, drawing upon historical documents, contemporary technical information and my own field inspections and aerial photograph interpretations of the twelve landslides shown on Figure 3.1; the chapter culminates with a landslide inventory presented in Table 3.1.

Chapter 4 presents local and regional climate data for the Thompson River basin, and illustrates novel relationships between the documented slope movements and inter-annual and inter-decadal climate phenomena, including an examination of the hydrologic impacts of the Pacific Decadal Oscillation and the El Niño Southern Oscillation; the chapter concludes with a discussion on the potential impacts of climate change to hazard frequency in the corridor.

Chapter 5 offers an interpretation of the mechanics of past landslide movements, and how these kinematics have evolved and changed over time in response to environmental and anthropogenic influences. A case study of the 1982 Goddard landslide, drawing upon previously unpublished field observations, is analyzed using an inverse-velocity approach for identifying the time to failure of an accelerating landslide in the corridor, from which salient risk management observations arise.

Based on the diverse information presented in the preceding sections, **Chapter 6** offers an assessment of the future likelihood and potential consequences of a rapid acceleration of a slow-moving landslide in the corridor, based on the relevant landslide failure modes and risk scenarios captured in Chapter 5. An integrated risk management strategy is then presented, synthesizing climate relationships with displacement monitoring and field observations of kinematic thresholds for landslide reactivations.

While the estimation of landslide frequency relationships is primarily a scientific exercise, **Chapter 7** acknowledges the importance of public involvement for effectively communicating and managing the risk associated with natural hazards impacting the built environment. Resilience concepts for coping with the transient disruptions associated with landslide movements are presented in the chapter, drawing upon stakeholder perspectives on the Ashcroft Thompson River landslides, and recent case studies of public involvement from the District of North Vancouver's landslide management strategy and the Town of Canmore's mountain creek hazard mitigation program.

Chapter 8 closes the thesis with a summary of the research conclusions, substantial contributions, and suggested areas for future inquiry.

2. GEOLOGY

“Unfortunately, soils are made by nature and not by man, and the products of nature are always complex...”

—Karl Terzaghi (Goodman 1999)

2.1. Geomorphology

In few other regions of North America is there preserved as complete a record of changing environments as in the Pacific Northwest (Schultz and Smith 1965). The Thompson River Valley is located within the Thompson Plateau (part of the Interior Plateau) in the central interior of British Columbia; the Thompson Plateau is a late Tertiary (late Miocene–early Pliocene) erosion surface that was dissected by stream and glacial erosion after mid-Pliocene uplift (Ryder 1976). Figure 2.1 displays the low-lying, semi-arid valley of the Thompson River south of Ashcroft; the valley contains a variety of Quaternary sediments which have been dissected and terraced by postglacial downcutting of the river (Ryder 1976). The Quaternary valley fill near Ashcroft consists of deposits from three glaciations dating from the Early to Middle Pleistocene (Clague and Evans 2003).

Recent reconstruction work by Tribe (2005) indicated the modern landscape of the southern Interior Plateau to be similar to its Eocene counterpart, except that regional drainage was broadly to the north, rather than the south, from Eocene to early Quaternary time. The preservation of Eocene landform remnants suggests that glacial erosion was highly spatially variable, with only a modest effect at regional scales (Tribe 2005). Pertinent to the study area, Tribe (2005) found the Thompson River Valley, from Kamloops to Spences Bridge, dates to at least Middle Eocene time, with southward drainage along the modern Thompson River Valley established after the Miocene. Regional uplift during the late Miocene–Pliocene resulted in valley incision; during the Quaternary, valleys were widened and deepened somewhat by glaciation, and although drainage rearrangement may have resulted at the local scale due to thick glacial deposits and postglacial landslides, the modern drainage pattern is much the same as it was in late Tertiary (Miocene) time (Tribe 2002).

2.2. Stratigraphic Sequence

As illustrated in Figure 2.2, the Quaternary sediment fill in the Thompson River Valley near Ashcroft comprises deposits from three glaciations; the glacial sequences are separated by unconformities produced by erosion and mass wasting during intervening interglaciations (Clague and Evans 2003). Pre-Fraser sediments are exposed in a 15 km stretch of the Thompson River Valley from approximately 3 km north of Ashcroft to approximately 12 km south of Ashcroft; glacial lake sediments of the Fraser glaciation overlie Fraser till and are commonly overlain by Holocene terrace gravel and loess (Johnsen 2004); the bedrock comprises andesite, rhyolite and pyroclastic beds that are fractured and well-drained (Huntley et al. 2017a).

Unit 1 (Figure 2.2) consists of cemented sand and gravel, possibly representing ancient river deposits corresponding to paleo-valleys, which, based on the work of Tribe (2005, 2002) may be of Tertiary age. Unit 1 also contains minor lenses of diamicton (till) which are believed to be ice-contact materials deposited at the end of an Early to Middle Pleistocene glaciation (Clague and Evans 2003). South of Ashcroft, unit 1 is overlain conformably by rhythmically bedded silt and clay couplets, ranging from less than 1 centimetre (cm) to tens of centimetres thick, which are believed to be glaciolacustrine sediments of Early to Middle Pleistocene age (unit 2 in Figure 2.2) (Clague and Evans 2003). A second, younger, glaciolacustrine sequence (unit 3), unconformably overlies unit 2. Unit 3 consists of poorly sorted, intertonguing silt, sand, gravel and diamicton with weak horizontal stratification; graded and laminated beds occur within the finer facies of the unit (Clague and Evans 2003). The unconformity between units 2 and 3 probably represents one or more interglaciations during which the sediments were dissected by the Thompson River (Clague and Evans 2003).

Units 4–7 represent sediments deposited during the most recent (Fraser) glaciation; at most sections in the study area, the Fraser sequence is incomplete, consisting of only one or two of the four units (Clague and Evans 2003). Clague and Evans (2003) interpret unit 4 to be braided-river channel gravels deposited by meltwater streams during the initial advance of the Fraser

glaciation; the horizontally bedded silt and sand of unit 5 probably represents glaciolacustrine sediments deposited when glaciers impounded a lake in the Thompson Valley. Unit 6 is glacial till dating to Late Wisconsin time; unit 7 consists of gravel grading up into sand and silt—these glaciolacustrine sediments were deposited when the regional drainage was blocked by stagnating ice (Clague and Evans 2003). The depositional environment of the late-glacial ribbon lakes produced relatively low to extremely high rates of sedimentation that were likely energetic throughout the year (Johnsen 2004). The rarity of clay resulting in the absence of classic varves is attributed to a sediment stratified water column and energetic lake conditions throughout the year (Johnsen 2004); this is in contrast to the relative abundance of clay in the sedimentary record of aerially expansive de-glacial lakes (Johnsen 2004). There is a general upward fining in sediment (i.e. over time), resulting in laminated silt deposits predominating upsection. Deposits within the area formed in at least two ribbon-shaped de-glacial lakes that occupied, and extended beyond, the study area: Glacial Lake Thompson and Glacial Lake Deadman; Glacial Lake Thompson was deeper and older compared to Glacial Lake Deadman (approximately 140 metres (m) versus 50 m deep) (Johnsen 2004). Both lakes were dammed by ice south of Spences Bridge and drained eastward (Johnsen 2004). Glacial Lake Deadman drained catastrophically when the ice dam failed; drainage then reversed, flowing west and south, and former shorelines of both lakes have been tilted (up to 1.8 m/km) by differential glacio-isostatic uplift (Johnsen 2004). The unit 7 glaciolacustrine deposits are identified in the photo of Figure 2.3, taken south of the study area between the villages of Ashcroft and Spences Bridge.

Unit 8 is bedded, pebble-cobble gravel deposit by the Thompson River and its tributaries during the Pleistocene-Holocene transition (Clague and Evans 2003).

2.2.1. Glacio-Isostatic Rebound and Elevation of Rupture Surfaces

Flowing south through the study area, the Thompson River has incised to a depth of approximately 150 m below the late-glaciolacustrine and outwash surfaces during post-glacial time, cutting extensive terraces into the Pleistocene valley-fill sediments (Ryder 1976, Porter et al. 2002). The landslides are situated on the steep walls of an inner valley that was incised

in the broader Thompson River Valley during Holocene time (Clague and Evans 2003, Eshraghian et al. 2007). As described above, the valley fill sequence consists predominantly of permeable sediments, with the exception of the rhythmically bedded glaciolacustrine silt and clay (unit 2) near the base of the Pleistocene sequence (Ryder 1976, Clague and Evans 2003). Large landslides have occurred in areas where this clayey glaciolacustrine layer is present, with the failure plane located within, or along the surface of, this unit (Clague and Evans 2003). Clague and Evans (2003) observed that clayey glaciolacustrine sediments older than the Fraser Glaciation play a significant role in the stability of many of valley slopes in the Pacific Northwest, including portions of the Fraser River Valley in central British Columbia and at the Grand Coulee Dam in Washington.

The clay beds of unit 2 are highly plastic, with plasticity indices in the order of 15 to 55 percent, and liquid limits ranging from 45 to almost 90 percent (Porter et al. 2002). Residual friction angles estimated using the empirical correlation of Stark and Eid (1994) are in the order of 11 to 15 degrees (Eshraghian 2007). Bishop (2008) measured residual friction angles of 10 to 15 degrees in laboratory ring shear tests on samples of the clay interbeds from the Ashcroft slides (assuming a cohesion intercept $c = 0$), which are in agreement with those determined by Porter et al.'s (2002) back-analyses of the North and CN 50.9 landslides, and recently measured in ring shear and direct shear tests on samples from the rupture surface at the Ripley landslide (11 and 12 degrees, respectively (La Meil, personal communication 2016)). Bromhead (2013) noted that the residual strengths collected from numerous back-analyses of three British clays (London clay, Gault, Lias), were all strikingly similar when plotted in the same τ - σ' space, falling between 10 and 11 degrees. He attributed this to a similar process of formation for these “slide-prone horizons”, involving increased smectite content resulting from the deposition and decomposition of a thin layer of fine-grained volcanic ash—not implying that the clays were the same, but noting that the *weakest* parts of the clays were strikingly similar (Bromhead 2013). The apparent laterally-extensive nature of the deeper rupture surfaces for the Ashcroft Thompson River landslides, combined with their positions above the base of the unit 2 deposit (not at the contact with the underlying gravel and bedrock) suggests that Bromhead's (2013) explanation of the predisposition of these clay layers to sliding is perhaps more enticing than the competing “junction hypothesis.”

Disturbance by overriding ice, substantial post-glacial valley rebound (as described by Johnsen and Brennand (2004)) and/or early slope movements may have created pre-sheared discontinuities operating at or near residual strength. Clague et al. (1987) commented that the terraces in this part of the Thompson River valley are underlain by truncated, back-tilted landslide blocks, possibly indicating that there were extensive slope movements in the glaciolacustrine sediments before the present valley was incised. They suggest the recent landslides have occurred in these displaced, sheared sediments, with river erosion and excess pore-water pressure from groundwater flow acting as contributing factors (Clague et al. 1987).

Eshraghian et al. (2005) documented the elevations of the rupture surfaces, as indicated by slope inclinometers, at the CN50.9, Goddard, North and South slides as shown in Table 2.1 (Landslide locations are indicated on Figure 3.1). The deepest rupture surfaces for the landslides decreased towards the south by approximately 12 m from the CN50.9 slide to the South slide. Measured tilt directions in the Thompson basins suggest that crustal load, and consequently the rebound, was greatest to the north-northwest (330° – 350° azimuth) and less to the south-southeast (Johnsen and Brennand 2004). Thus, despite the measured elevation differences between the rupture surfaces, the landslides may be moving along a clay layer with similar mineralogy resulting from a consistent depositional environment within the glaciolacustrine clay-silt sequence. Johnsen and Brennand (2004) employed a paleogeographic reconstruction procedure to show that differential glacio-isostatic rebound has caused the former shorelines of Glacial Lake Thompson and Glacial Lake Deadman to have among the highest tilts that have been measured in the world (1.7–1.8 m/km). Schafer et al. (2015) located the failure surface within the smaller Ripley landslide at an elevation of 257.3 m, which is again consistent with the deep failure surfaces of the large landslides to the north determined by Eshraghian et al. (2007) when considering the isostatic tilt given by Johnsen and Brennand (2004).

2.2.2. Geologic Controls on Extent of Landsliding

Ryder (1976) determined the pattern of ice flow during the Fraser glaciation to be dominantly from west to east across the Fraser Valley, Clear Range, and Upper Hat Creek valley towards the Thompson Valley, with this pattern probably continuing further east. She noted that relatively little erosion by glacial ice occurred within those parts of the Fraser and Thompson Valleys which were transverse to the direction of ice advance, resulting in the preservation of earlier Pleistocene deposits under the Fraser till in the Thompson River Valley south of Ashcroft (Ryder 1976). Later deglaciation of the region resulted in glacier lobes remaining in major valleys whilst upland areas became ice-free, with evidence of valley-controlled ice flow parallel to the Thompson Valley (Ryder 1976). The north-south orientation of the Thompson Valley south of Ashcroft thus acted as a critical factor in preserving the earlier glaciolacustrine sediments during overriding by Fraser ice. Unit 2 glaciolacustrine sediments, as previously noted, form the rupture surfaces for the numerous large landslides south of Ashcroft; the north-south orientation of this section of the Thompson Valley transverse to the direction of the Fraser ice advance likely explains the preservation of these sediments and the extensive landsliding which is evident along this reach.

It is evident that the form of many of the landslides south of Ashcroft are controlled by bedrock outcroppings such as between the North and South slides at Black Canyon. The toe of the Goddard landslide is also bedrock controlled at river level immediately upstream and downstream of the slide (Golder, Brawner & Associates Ltd. 1969). Based on an extensive geophysical investigation at the smaller Ripley landslide, Huntley et al. (2017a) suggested that the landslide toe extends under the Thompson River, where greater than 20 m of clay-rich colluvial, glaciolacustrine and till deposits are confined to a bedrock basin, with the largest slope movement rates measured adjacent to areas of active toe erosion. It is hypothesized that the shape and size of the numerous other landslides south of the Ashcroft are also controlled by the bedrock surface, likely conforming to abandoned paleo-valleys. Interestingly, Stanton (1898a) suggested that prior to the last glaciation, the ancient river ran to the east of the present Black Canyon, and that when downcutting through the glacial till, the river relocated to the west, forming great bays where the boulder clay was washed out, and subsequently filled with

silt. These are the conditions at the North and South slides, which he described as “great bays of white silt”, extending back from the river into the original mass of boulder clay, stating “The silt deposit in these two bays accounts clearly for the peculiar form and action of these two great slides, and for the immense vertical drop in each case” (Stanton 1898a).

2.3. Regional Hydrogeology

2.3.1. Impact of Groundwater Flow and Seepage Pressures on Slope Stability

Popescu (1994) underscored that all landslides are caused by a combination of preparatory and triggering factors. Preparatory factors bring the slope into a state of marginal stability without actually initiating movement, while triggering factors act to initiate movement on the marginally stable slope (Cruden and VanDine 2013). Clague and Evans (2003) stated that the stratigraphy of the Thompson River Valley “predisposes it to failure.” They identified that clayey strata are confined to a single unit—the rhythmically bedded glaciolacustrine sediment (unit 2) near the base of the Quaternary sequence, which confines and is also overlain by, non-plastic, more permeable sediments (Clague and Evans 2003). Based on groundwater flow simulations, Hodge and Freeze (1977) demonstrated that the presence of a low-conductivity unit at depth can be extremely detrimental to valley wall stability, especially where it confines a unit of higher conductivity; they further noted that this contrast in hydraulic conductivity need not be more than two orders of magnitude to have a marked detrimental effect on slope stability. The effect of this sequencing is to produce wetting and softening of the clayey layer as well as elevated pore water pressures along the base of the unit as a result of artesian water pressures confined within the more permeable underlying strata (Hodge and Freeze 1977). The presence of a buried aquifer has a profound effect on the movement of groundwater and hence the slope stability in the vicinity of the valley walls (Lafleur and Lefebvre 1980, Bishop 2008), acting as a “highway” that transmits water to the principal discharge area (Freeze and Witherspoon 1967).

Tutkaluk et al. (1998) illustrated the importance of regional hydrogeology in controlling riverbank stability along the Red River in Winnipeg, where the river banks are composed

primarily of glacially-derived sediments overlying a carbonate aquifer. Riverbank movements typically occur in the fall as a result of two factors which conspire to reduce the stability of the banks: the Red River is allowed to drop from a regulated river level to its natural unregulated level, and at approximately the same time, piezometric levels in the bedrock aquifer increase significantly as urban demand for groundwater seasonally decreases (Tutkaluk et al. 1998). The artesian pore pressure conditions and associated upward flow of groundwater from the bedrock towards the clay serves to de-stabilize the slopes (Tutkaluk et al. 1998).

Lafleur and Lefebvre (1980) underscored the importance of the geological environment in controlling the movement of groundwater in the vicinity of Champlain clays slopes using finite element modeling. They found that “In relation to deep failures, the parametric study of the groundwater regime surrounding slopes shows that the lower aquifer has a maximal influence on the distribution of pore pressures in the intact clay, and that this distribution can be altered significantly from the so-called hydrostatic conditions” (Lafleur and Lefebvre 1980). They found the magnitude of the upward gradients to be inversely proportional to the vertical distance between the toe of the slope and the top of the aquifer (Lafleur and Lefebvre 1980); this is of course the result of the gradient, i , being inversely proportional to the distance over which the change in head occurs; the resulting uplift pressure is equal to i multiplied by the unit weight of water (Harrison 2014).

Záruba and Mencl (1976) described a large composite landslide (approximately 40 Mm³) along the Váh river valley near Súčany, Slovakia, moving at 80-100 millimetres (mm) per year. They noted an artesian water pressure of 13 atmospheres (atm) (1317 kilopascals, kPa) contained within basal conglomerates was responsible for uplift of the moving mass along ancient fault planes. By relocation of the river channel, the movement of the landslide ceased as soon as the toe of the slide was no longer undermined by river erosion (Záruba and Mencl 1976).

The preceding examples illustrate the importance of the complex interaction between groundwater pressures, river erosion, and ancient failure planes in contributing to river bank instability. The importance of regional groundwater flow patterns, and their impact on slope stability, has been demonstrated with the assistance of finite element modelling in several

studies including Hodge and Freeze (1977), Lafleur and Lefebvre (1980), Iverson and Major (1987), Iverson and Reid (1992), Reid and Iverson (1992), and Iverson (1992). Despite the critically important role that groundwater flow may play in provoking slope instability, the relationship between groundwater flow, effective stress and deformation that may lead to slope failure is not always obvious, and has represented a “missing link” in the chain of principles uniting hydrology and geomorphology (Iverson 1992). According to Bromhead (1987):

“In many investigations of natural slopes and their associated landslides, engineers and geologists have confined themselves to the measurement of what groundwater pressures exist, without attempt to explain why. Hence they have failed to provide a rational basis for the prediction of the likelihood of future change, and its resulting impact on the behavior of the slope” (p. 147).

Iverson and Reid (1992) employed finite element modeling of saturated homogenous hillslopes to demonstrate that gravity-driven groundwater flow produces a spatially variable body force field that influences the effective stress distribution in hillslopes, and that shear stresses, as well as effective normal stresses in a porous medium can be influenced by groundwater flow¹. Where groundwater conditions within a slope deviate from hydrostatic conditions, gradients produced in the slope will result in the movement of groundwater and the corresponding unbalanced seepage force, as defined in Equation 2-1, which is borne by the mineral skeleton of the soil by virtue of effective stress (King 1989, Iverson et al. 2015).

$$F_s = i\gamma_w V \quad [2-1]$$

where:

F_s = seepage force per unit volume of soil [M/V]

i = hydraulic gradient [L/L]

γ_w = unit weight of water [M/V]

V = unit volume of soil [V]

¹ Spatially uniform pore pressure changes, which induce no groundwater flow, also have no influence on effective stress distributions and failure potential in slopes characterized by frictional materials— a cohesionless slope will have the same factor of safety in a dry state as it does in a uniformly saturated state with no groundwater flow, such as at the edge of a lake (Lambe and Whitman 1969).

Haefeli (1948) showed that for a given material which is characterized by its unit weight at saturation and its angle of internal friction, the limiting angle of an infinite slope with seepage depends solely on the hydraulic gradient along a normal to the slope. For the special case of slope-parallel seepage, there can be no gradient at a right-angle to the slope, and Haefeli's (1948) formulations reduce to the well-known maxim for an infinite slope with surface-parallel seepage:

$$\beta_{\text{critical}} = \gamma_b/\gamma_t \cdot \tan\phi' \cong 1/2 \cdot \tan\phi' \quad [2-2]$$

where:

β_{critical} = steepest stable slope angle [degrees]

γ_b = bouyant unit weight of soil [M/V]

γ_t = bulk unit weight of soil [M/V]

ϕ' = effective angle of internal friction of soil [degrees]

Where contrasts in the hydraulic conductivity of layered materials are introduced, these can profoundly modify the groundwater flow field and produce locally large gradients which will increase the seepage force and failure potential, particularly in near-surface discharge areas where seepage forces are directed outward from the slope (Reid and Iverson 1992). Bishop (2008) estimated the contrast in vertical permeability between unit 2 and unit 3 in the Thompson River Valley to be three orders of magnitude, as shown in Table 2.2; Eshraghian et al. (2008) estimated one order of magnitude contrast in permeability between these layers.

For gravity-driven groundwater flow, Iverson and Major (1986) demonstrated that minimum slope stability occurs when seepage is directed such that $\lambda - \phi' = 90^\circ$ (symbols defined in Figure 2.4); on landslide-prone slopes, where the slope angle, β , differs little from the internal friction angle, ϕ' , minimal slope stability is thus achieved under conditions of horizontal seepage (Iverson and Major 1986). This may occur near an interface of contrasting permeability that impedes flow and daylights at the slope surface; a contrast of hydraulic conductivity of even one order of magnitude can have an appreciable effect on the hydraulic head and the slope failure potential or factor of safety, as depicted in Figure 2.5 (Reid and Iverson 1992). The

slope stability can be reduced even further under artesian groundwater conditions where the directional seepage emerges from the slope with a significant upward component (i.e. $\lambda < 90^\circ - \beta$) (Ghiassian and Ghareh 2008). *Both* of these detrimental conditions exist in the hydrologic regime of the Thompson River Valley south of Ashcroft; gravity-driven groundwater flow through Quaternary fill sediments is directed horizontally out-of-the-slope as it percolates down through higher permeability units (8–3) and until it encounters the lower-permeability unit 2 which reorients the seepage direction towards the slope face. In addition, the stability of the valley walls is reduced even further by the artesian groundwater which emerges with a significant upward component from the toe of the slope into the Thompson River.

The general physical significance of steady seepage effects on the potential for slope instability was quantified by Iverson and Major (1986) who derived a normalized solution of the limiting stable slope angle, β , of a semi-infinite mass of cohesionless soil subject to a seepage a gradient of magnitude i in the direction λ , governed by the Coulomb equation for incipient failure, $\tau = \sigma \cdot \tan\phi'$, as:

$$\tan\phi' = \frac{\left[\left(\frac{\gamma_t}{\gamma_w}\right)-1\right]\sin\beta + i \cdot \sin\lambda}{\left[\left(\frac{\gamma_t}{\gamma_w}\right)-1\right]\cos\beta - i \cdot \cos\lambda} \quad [2-3]$$

The factor of safety for an infinite cohesionless slope can thus be expressed as (Ghiassian and Ghareh 2008):

$$F.S. = \frac{\cos\beta - A_b \cdot \cos\lambda}{\sin\beta + A_b \cdot \sin\lambda} \tan\phi' \quad [2-4]$$

where:

$$A_b = i \frac{\gamma_w}{\gamma_t}$$

The implications of seepage gradient magnitude i , and direction, λ , on the stability of an infinite cohesionless slope with internal friction angle $\phi' = 16^\circ$ and slope angle $\beta = 16^\circ$ are plotted on Figure 2.6 using the formulae of Ghiassian and Ghareh (2008). It can be appreciated

that for marginally-stable cohesionless slopes where the slope angle is approximately equal to the angle of internal friction, the factor of safety is substantially reduced as the magnitude of the gradient increases and is directed out-of-the-slope, compared to hydrostatic and slope-parallel seepage conditions.

Bishop (2008) modelled the regional hydrogeology of the Thompson River Valley south of Ashcroft, incorporating transient boundary conditions in the flow system model to simulate precipitation, irrigation, and fluctuation in the stage of the Thompson River level. Though his analyses produced unrealistically high porewater pressures in the basal materials, his groundwater simulations affirmed the critical role of the glaciolacustrine silt and clay (unit 2) in controlling groundwater flow patterns, and producing artesian pore water pressures in the valley bottom (Bishop 2008). Bishop's (2008) work suggested that surface water that originates further upslope is channeled underneath unit 2, through the more permeable underlying units, and migrates upwards to the surface closer to river level. This regional flow regime is capable of generating elevated pore pressures in the glaciolacustrine silt and clay, fractured bedrock, and bedrock units, which discharge from the slope in an outward and upward direction in the lower region of the valley near the Thompson River.

Field investigations at several of the large landslides in the Thompson River Valley have confirmed the presence of artesian groundwater pressures beneath the toes of the slides, contained within the fractured bedrock underlying the laminated silt and clay (unit 2) which forms the rupture surface (Porter et al. 2002, BGC Engineering Inc. 2005). Shallow piezometers installed near the base of the valley walls respond readily to fluctuations in the Thompson River level, while deeper-seated piezometers respond to variations in river level to a much lesser degree. The artesian water pressures in the fractured bedrock control the pore pressures at the base of the silt and clay unit (unit 2 in Figure 2.2), while river levels exert a controlling influence on the pore pressures measured at the top of unit 2 near the toes of the landslides (Porter et al. 2002). Quinn et al. (2012) described the importance of the fluctuating Thompson River levels and pore water pressures in presenting the vertical gradients produced below the toe of the CN50.9 landslide. The seasonally high river levels serve to substantially reduce, if not equilibrate, the upward gradient of pore water pressures measured near the base

of the landslide, while upon recession of the river, the upward gradient rapidly increases, aggravating the instability of the marginally stable slope (Figure 2.7). Seasonal recharge of the fractured bedrock and overlying gravels on a regional scale would therefore be important in controlling the artesian water pressures below the failure surface, and could potentially trigger reactivation of the existing landslides in the subject corridor. BGC Engineering (2005) recorded nearly identical artesian porewater elevations of approximately 292 m in ancient river gravels below the South slide and the Basque slide, despite a 17 m difference in piezometer tip elevation and a distance of approximately 3 km between the two sites. These data suggest that confined, basal aquifers in the area are likely subject to recharge via a common regional source (BGC Engineering Inc. 2005).

Groundwater may also pool on the surface of unit 2 through infiltration of the more-permeable overlying sediments; unconformities which separate the three glacial sequences, and buried paleo-valleys (containing unit 4 gravels) incised into the older Quaternary sediments may also provide ready transport of groundwater (Clague and Evans 2003). Huntley et al. (2017a) utilized terrestrial and waterborne geophysical surveys to describe the geology and groundwater conditions of the bedrock and surficial materials at the Ripley landslide. Their findings suggest complex patterns of groundwater migration via downward percolation through the permeable surficial units, and preferential travel through fractures, partings and porous beds within the glaciolacustrine units and the fractured bedrock and overlying gravel (Huntley et al. 2017a). While the complex structure and stratigraphy of the Quaternary sediment in the Thompson River Valley make it difficult to predict groundwater flow in detail, the stratigraphic sequence promotes development of de-stabilizing pore water pressures in the lower part of the valley fill sequence, coincident with the rupture surfaces of the landslides (unit 2) (Clague and Evans 2003).

2.3.2. Groundwater and Surface Water Isotopes

Based on the preceding discussion of regional groundwater flow in relationship to the Ashcroft Thompson River landslides, I hypothesize that there exist two groundwater flow regimes which act to destabilize the valley walls. The first is the artesian groundwater pressure which is confined below unit 2 in the ancient river gravels; I believe this to be the result of regional groundwater flow from a distant source, and hence reflective of the broader climate conditions reflected in the snow pack and river levels in any given year. The second is the groundwater contained within the Quaternary valley fill materials, which I believe to be the result of more localized weather patterns (including local precipitation), water inputs at the terrace level by agricultural irrigation, and recharge of shallow groundwater near the base of the slopes by seasonal river flood levels. This two-tiered groundwater system is supported by the results of groundwater isotope testing that was undertaken at the site of the Ripley landslide, approximately 8 km south of Ashcroft, as described below.

Isotopes are used in hydrologic studies to estimate the age and history of a water sample, providing specific insight into the source of the water and the groundwater flow regime. The stable isotopes of oxygen (^{18}O) and hydrogen (^2H) were measured in core samples collected during a geotechnical drilling investigation at the Ripley landslide in February 2015 (conducted and described by Schafer (2016)). The drilling was accomplished using 1.5 m long HQ size continuous coring with water as the drilling fluid (Schafer 2016). The samples were prepared by cutting approximately 300 mm thick discs from the bottom of each 1.5 m core run, which were trimmed to remove any contamination from drilling fluid; the samples represented glacial till (unit 6), glacio-lacustrine clay and silt (unit 2) and andesite bedrock from various depths between 6.4 m and 15.4 m below the ground surface.

The core samples were analyzed using a Picarro L1102-I isotopic water liquid analyzer, following the method of sample preparation and testing outlined in Hendry et al. (2013a). The stable isotopes of oxygen (^{18}O) and hydrogen (^2H) were measured in the core samples, and in samples of the drilling fluid (water) and a sample of surface water collected from the Thompson River. Laboratory testing was performed by the University of Saskatchewan, and I

have presented and interpreted the results in Figure 2.8 (a)–(c). Samples from depths of 4.9 m and 7.9 m in Borehole 15-01 were omitted from the plots due to their contamination with drilling water. The analytical results are expressed in terms of $\delta^{18}\text{O}$ and $\delta^2\text{H}$, indicating the relative enrichment (positive values) or depletion (negative values) of the isotopes in a water sample, compared to Vienna Standard Mean Ocean Water (VSMOW) in units of parts per thousand called per mil (‰) (Clark and Fritz 1997, Golder Associates 2004).

The proportions of $\delta^{18}\text{O}$ and $\delta^2\text{H}$ in precipitation will generally follow a linear relationship particular to the study area, defined for the Ashcroft area by the Western Interior Meteoritic Water Line (MWL) given by Equation [2-5] below (Clark and Fritz 1997):

$$\delta^2\text{H} = 7.6 \delta^{18}\text{O} + 0.6 \quad [2-5]$$

The $\delta^{18}\text{O}$ and $\delta^2\text{H}$ in precipitation and hence in fresh waters generally plot along the meteoritic water line (Drever 1997). This isotopic signature of precipitation is generally also maintained in shallow groundwater systems with short residence times; differences between the isotopic signatures of groundwater samples suggests a different point of recharge (Golder Associates 2004). When water undergoes evaporation, the residual water becomes progressively enriched in ^{18}O and ^2H ; however, the composition of the residual water does not follow the MWL, but evolves along a line of lesser inclination, typically with a slope of approximately 3–5, dependent upon the temperature and humidity at which the evaporation occurs (Clark and Fritz 1997, Drever 1997).

The isotopic composition of groundwater in arid regions can be considerably modified from that of local precipitation, due to strong isotopic enrichment by evaporation, which is a highly fractionating process (Clark and Fritz 1997). Evaporation during runoff and infiltration in arid landscapes is generally associated with groundwater traveling along ephemeral streams or drainage courses that are typically dry (Clark and Fritz 1997). Isotopic enrichment can also result from recharge by snowmelt; unlike evaporation, the high humidity within the snowpack facilitates a greater degree of equilibrium exchange between solid and vapor; the slope of the isotopic enrichment trend is therefore steeper than for evaporation of water (Clark and Fritz

1997). When melting of the snowpack occurs, isotope exchange between the meltwater and snow as it infiltrates from the melting upper surface through to the base of the snowpack will also produce isotopic enrichment in the meltwater, as shown in Figure 2.9 (Clark and Fritz 1997). While isotopic exchange with rock minerals may produce enrichment in ^{18}O in groundwater, the ^2H value will be unaffected because rock contains a large amount of oxygen, but very little hydrogen (Drever 1997).

As shown in Figure 2.8 (a) and (b), the $\delta^{18}\text{O}$ and $\delta^2\text{H}$ values are consistent for all of the soil samples collected from the surficial sediments above a depth of 15.4 m, and plot very near to the relevant meteoric water line (Figure 2.8 (c)), along with the fresh water sample collected from the Thompson River. The $\delta^{18}\text{O}$ and $\delta^2\text{H}$ measurements of approximately -17 and -140 conform to the expected values for meteoric water in the southern interior of British Columbia (Drever 1997). The single groundwater sample collected at a depth of 17.1 m from within the andesite bedrock is significantly enriched in both ^{18}O and ^2H , with little mixing evident between the shallower samples and this deeper groundwater (Figure 2.8 (a) and (b)). Moreover, this bedrock water sample does not plot on the MWL, but along a line of slope 4.4 from the surface water sample.

These findings suggest the groundwater within the surficial sediments to be meteoric and of similar composition to the river water, while the groundwater within the deeper bedrock aquifer likely derives from a different source which has been subject to isotopic enrichment by evaporation, or perhaps as a result of water derived from snowmelt, as depicted in Figure 2.9.

2.4. Conditionally Collapsible Soils

Numerous authors, including the writer, have previously hypothesized that the large landslides south of Ashcroft may have originated as earth flows resulting from structural collapse of the late-glacial lacustrine silt deposits (unit 7), induced by water-intensive irrigation of the terraces. However, cross sections of interpreted stratigraphy of Quaternary fill in the study area by Clague and Evans (2003) show a general paucity of late-glacial silt deposits in the stratigraphic sequence on the east bank of the Thompson River immediately north of the

Goddard slide and Landslide No.3 (Sections B and C, Figure 2.10). Unpublished field notes by D.M. Cruden also indicate limited thicknesses (2–3 m) of late-glacial silts observed in the vicinity of the Ashcroft landslides (personal communication, 2016). Thicker exposures of the surficial glaciolacustrine deposits are evident along the Thompson River valley north of Ashcroft (unit 7 in Section A, Figure 2.11 below, located 3 km north of Ashcroft in an east-west direction), and are the dominant Quaternary deposit in other parts of the valley, exceeding 150 m in thickness in some places (Johnsen 2004). Notwithstanding the abundance of unit 7 deposits and ample irrigation on the terrace north of Ashcroft, as seen on the 1928 air photo (Figure 2.12) and in a contemporary view (Figure 2.13), slope instability is *not* evident along this portion of the valley.

The surficial glaciolacustrine deposits of the Southern Interior are dominated by silt varves, which are sensitive and collapsible under certain moisture and loading conditions (Evans 1982). Quigley (1976) illustrated the open fabric of silts from the South Thompson and Penticton areas, and Lum (1979) established their collapse potential under certain moisture and loading conditions in laboratory oedometer testing. He concluded that the high strength of the silts under low degrees of saturation, typical of the semi-arid environments in which they occur, is due to substantial apparent cohesion, the magnitude of which is controlled by the degree of saturation (Lum 1979). Lum (1979) described the Kamloops glaciolacustrine silt as “conditionally collapsible soil” as defined by Reginatto and Ferrero (1973). Whether or not the soil structure will collapse when flooded with water depends upon its stress state. At low confining pressures, the soil exhibits heave when flooded; at higher stress levels, in excess of approximately 6 kg/cm² (589 kPa), collapse occurs (Lum 1979). Though it is possible that the surficial glaciolacustrine soils south of Ashcroft may be conditionally collapsible, the limited overburden thicknesses of the late-glacial deposits in the study area would not produce the “sufficiently large load” of approximately 6 kg/cm² (590 kPa) required for structural collapse at depth as described by Lum (1979). The deeper-seated glaciolacustrine deposits (units 2 and 3) would not have the open fabric required for collapse due to their consolidation by subsequent advances of glacial ice. The lack of landslide activity on slopes dominated by unit 7 glaciolacustrine deposits is probably due to the notable absence of unit 2 sediments as per Clague and Evans’ (2003) cross section in Figure 2.11. This further corroborates the critical

destabilizing role of the pre-Fraser glaciolacustrine sediments (unit 2), which serve as the rupture surfaces for the large landslides.

Stanton's (1898a) account of the historic landslides south of Ashcroft, and subsequent correspondence concerning his paper, indicate that the slope movements of the late-1800's were deep-seated, rather than surficial, failures: "...it seemed that the mass of silt under the slides extended below the present bed of the Thompson River, and was being forced up into the river at its edge" (Stanton 1898b). He indicated the height of the scarp to be over 400 feet at the North Slide, and over 300 feet at the South slide (Stanton 1898a). His description suggested that water from irrigated fields and crudely-constructed irrigation ditches on the benchlands penetrated overlying sand and gravel and "re-arranged boulder clay" to reach the underlying "white silt deposits," which were described as "generally fine and uniform in texture, and are usually well bedded in perfectly horizontal layers from ¼ inch to 4 inches in thickness, with occasional sandy seams and small pockets of coarse sand, formed locally, appearing in places" (Stanton 1898a). After some years of agricultural irrigation on the terraces, he speculated, the silt became sufficiently saturated, such that it took on the consistency of "thick pea-soup", and the great mass of earth above it dropped vertically and slid out towards the river, with back-tilted blocks angled at about 45 degrees (Stanton 1898a). Stanton's (1898a, 1898b, 1904) descriptions of these early landslides are more consistent with compound earth slides, as opposed to earth flows induced by structural collapse. The mechanics of the Ashcroft Thompson River landslides are discussed in detail in Chapter 5.

2.5. Conclusion

The slopes of the Thompson River Valley south of Ashcroft are predisposed to failure as a result of the presence of a low strength, clayey glaciolacustrine unit at depth (unit 2 on Figure 2.2); this unit serves two detrimental purposes, in acting as the rupture surface for the landslides due to its pre-sheared, residual strength characteristics, and, by confining regional groundwater flow to promote artesian pore water pressures (and associated uplift forces) below the rupture surfaces by virtue of its low permeability. The artesian groundwater pressures are confined below unit 2 in the fractured bedrock and overlying gravels; the form of the landslides appear to be controlled by the high-relief bedrock surface (Huntley et al. 2016), perhaps conforming to abandoned paleo-valleys. In Cruden and VanDine's (2013) terminology of landslide causes, these preparatory factors can be generally categorized as ground conditions (sensitive materials, contrast in permeability, contrast in stiffness), and geomorphologic processes (glacial rebound, fluvial erosion of the slope toe).

The destabilizing role of the complex groundwater flow regime, which results from the preservation of an Eocene-age drainage network (Tribe 2005) and contrasts in material permeabilities of the Quaternary fill in the Thompson River Valley, appears to play a significant role in controlling the stability of the valley walls. Results of groundwater isotope testing support the hypothesis of a two-tiered groundwater system, whereby groundwater in the Quaternary fill materials is replenished by precipitation and/or irrigation (meteoric water), and groundwater in the underlying gravels and fractured bedrock is replenished by more distant regional sources. The complex stratigraphy and groundwater flow regime within the Thompson River Valley south of Ashcroft have conspired to produce marginally stable slopes on which a variety of triggering factors have acted to produce a long history of movement, as will be discussed in the next chapter. While conditionally collapsible late-glacial lacustrine silt sediments of the South Thompson area may produce earth flows when saturated under sufficiently large loads, the form of the slope movements in the Thompson River Valley south of Ashcroft are generally consistent with compound earth slides, or complex earth slide-debris flows, as will be further described in Chapter 5.

Table 2.1: Investigated rupture surface elevations at several landslides in the Thompson River Valley south of Ashcroft (modified from Eshraghian et al. (2007)).

Landslide Name	River elevation (based on May 2003 LiDAR data)	Deeper rupture surface elevation (m)	Shallower rupture surface elevation (m)
CN 50.9	282.6	275.7	280.9
Goddard	275.8	270.6	278.1
North	273.2	264.2	269.4
South	269.2	263.7	272.7

Table 2.2: Estimated horizontal and vertical hydraulic conductivities of dominant Quaternary valley fill sediments in the Thompson River Valley south of Ashcroft (modified from Bishop (2008)).

Unit	K horizontal (cm/s)	K vertical (cm/s)
Terrace gravels (unit 8)	1.0×10^{-3}	1.0×10^{-3}
Glaciolacustrine silt (unit 3)	1.0×10^{-5}	1.0×10^{-5}
Glaciolacustrine clay-silt (unit 2)	5.0×10^{-7}	5.0×10^{-8}



Figure 2.1: Characteristic semi-arid, terraced landscape used for ranching and farming along the Thompson River Valley, as seen looking east from Highway 1 between Ashcroft and Spences Bridge (November 2015).

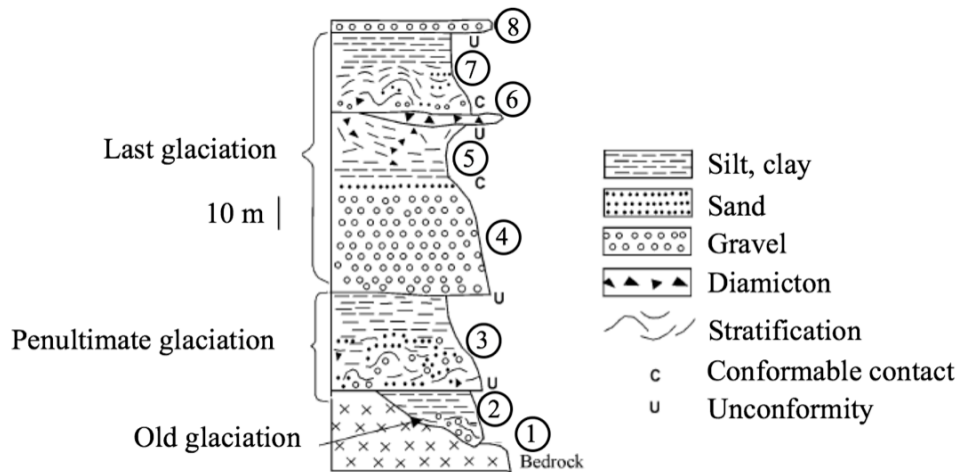


Figure 2.2: Generalized stratigraphy of Quaternary sediment fill in the Thompson River Valley at Ashcroft (modified from Clague and Evans 2003).



Figure 2.3: Characteristic exposure along the Thompson River Valley between Ascroft and Spences Bridge (looking east from Highway 1, November 2015). The surficial late-glacial lacustrine silt deposits (unit 7) are readily identifiable as the upper light-coloured band of sediment.

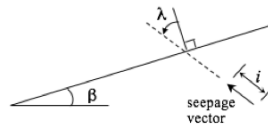


Figure 2.4: Depiction of groundwater seepage vector of magnitude, i , and direction, λ , relative to an infinite slope inclined at angle, β (modified from Iverson and Major (1986)).

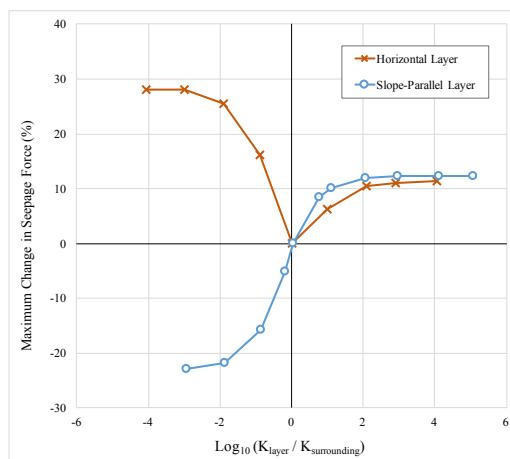


Figure 2.5: Effect of stratigraphic layering on the seepage force within a slope due to contrasting permeabilities between two soil strata (modified from Reid and Iverson (1992)).

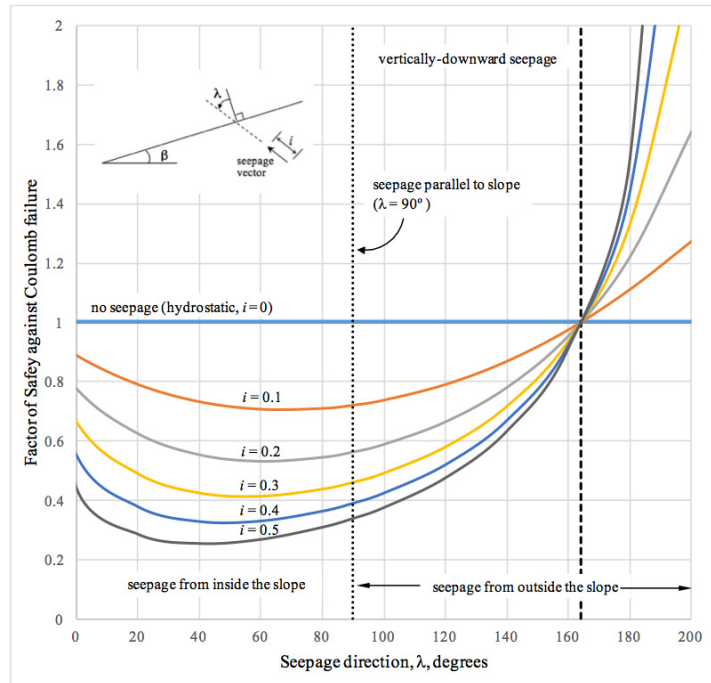


Figure 2.6: Effect of seepage gradient magnitude and direction on factor of safety for a hypothetical infinite cohesionless slope with $\phi' = \beta = 16^\circ$.

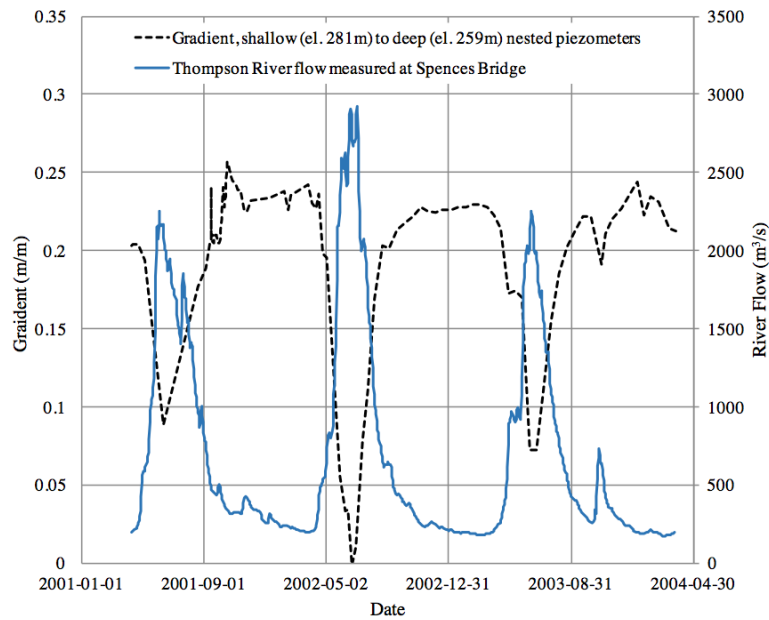
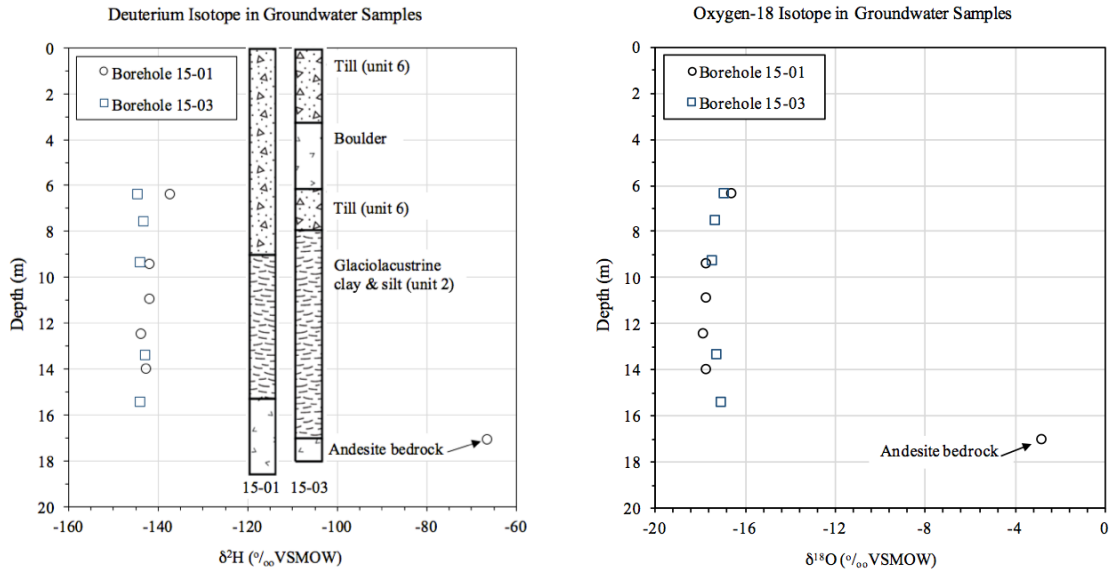
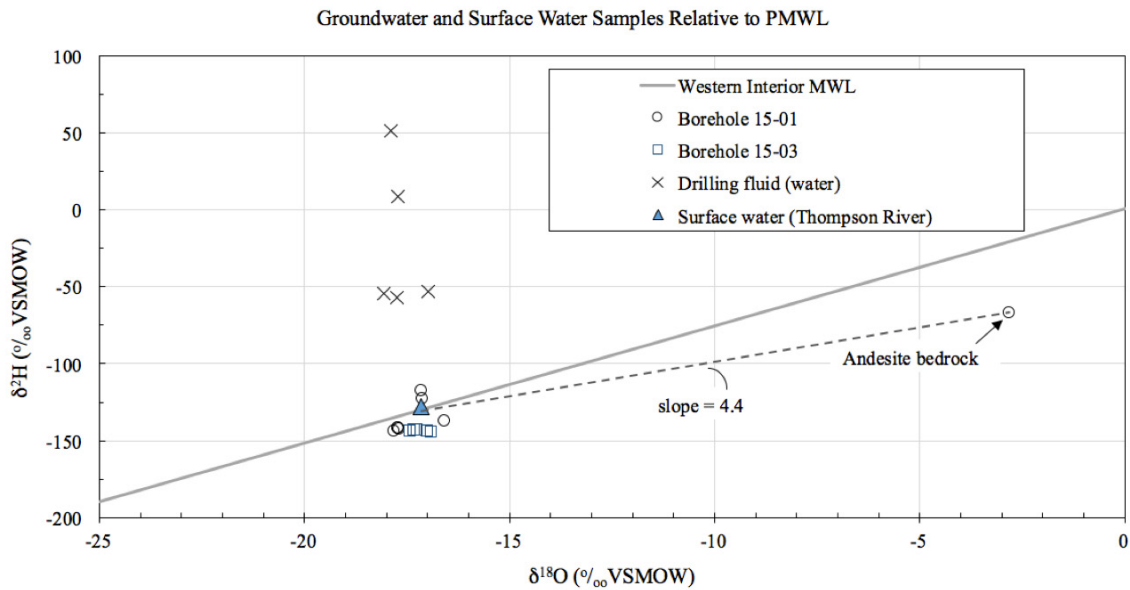


Figure 2.7: Vertical pore pressure gradients between deep and shallow piezometers measured at the toe of the CN 51 landslide, close to the Thompson River (modified from Quinn et al. 2012).



(a)

(b)



(c)

Figure 2.8: Results of groundwater isotope testing from samples at the Ripley landslide; (a) Deuterium (^2H) concentration with depth— stratigraphic columns are from Schafer (2016), (b) Oxygen-18 concentration with depth, (c) Deuterium versus Oxygen-18 concentration with meteoric water line and slope of enrichment line shown.

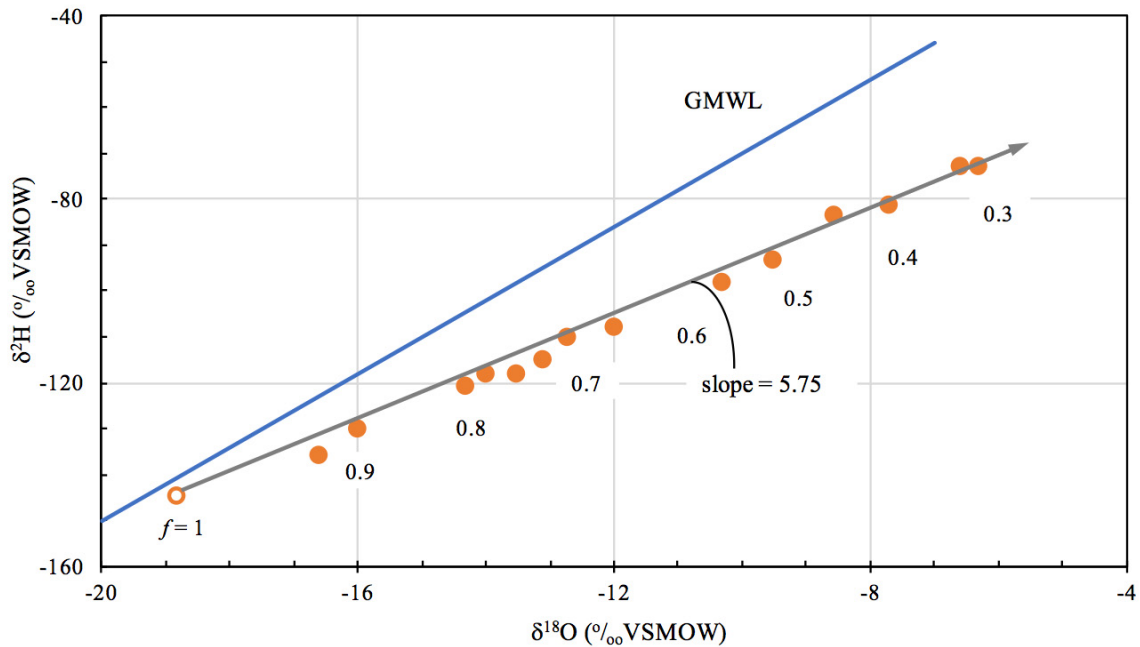


Figure 2.9: Evolution of $\delta^{18}\text{O}$ and $\delta^2\text{H}$ in snow during evaporation under controlled conditions; f is the fraction of snow remaining during sublimation (modified from Moser and Stichler (1975), as reproduced in Clark and Fritz (1997)). Reproduced with permission.

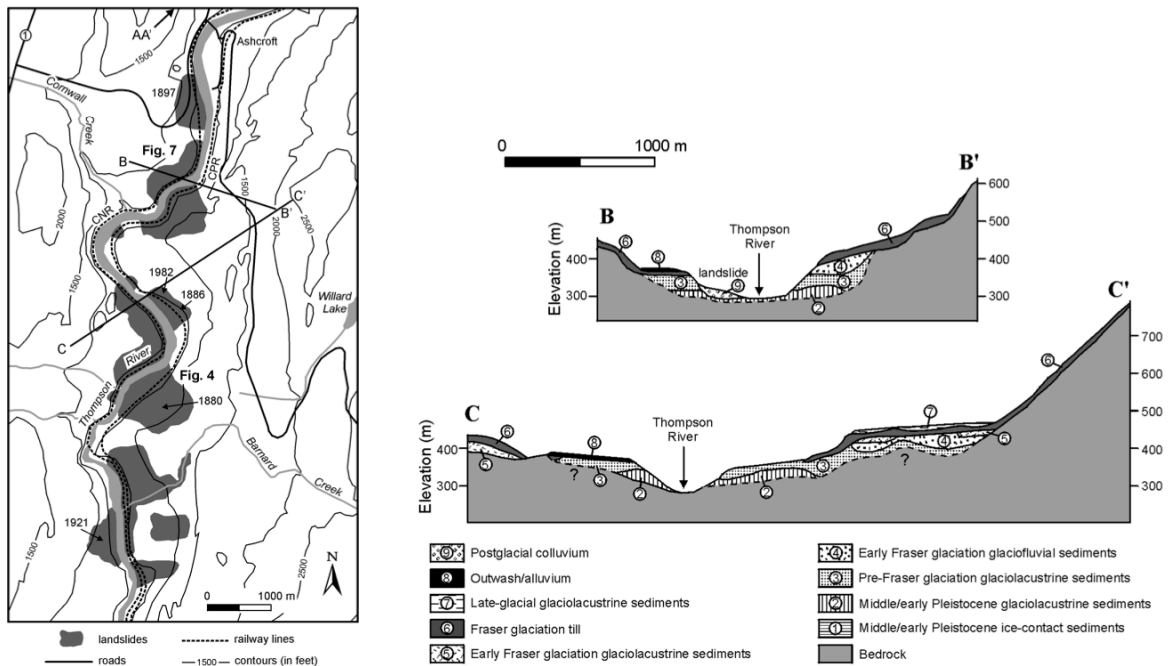


Figure 2.10: Cross section locations and interpreted stratigraphy of the Quaternary fill in the study area, from Clague and Evans (2003).

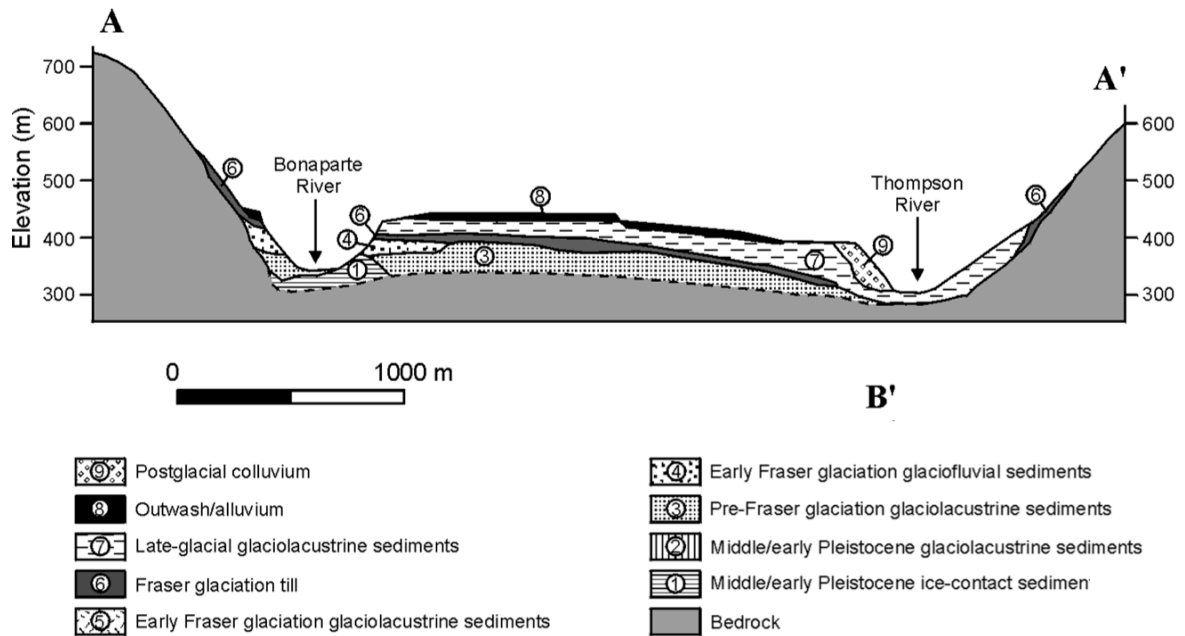


Figure 2.11: Interpreted stratigraphy of the Quaternary fill along an east-west section A-A', 3 km north of Ashcroft, from Clague and Evans (2003).



Figure 2.12: Aerial view of Bonaparte confluence north of Ashcroft, with evidence of historic irrigation practiced on river terrace above the confluence (NRC Roll A291, #69, July 15, 1928).



Figure 2.13: Irrigated field on the upper terrace of the Thompson River Valley north of Ashcroft at the Bonaparte River confluence (looking east from Highway 1, November 2015).

3. HISTORY OF ONGOING LANDSLIDE ACTIVITY

“...in addition to full information on the geology and other aspects of the environment, the importance of a good database of case records of failures, their behaviour, their effects and their frequency cannot be over-emphasised. In such events, Nature shows her hand, revealing where, and to some extent when landslides and other mass movements are prone to occur, the style of these failures and the damage that they can cause.”

— Hutchinson (2001)

3.1. Overview and Evolution of Slope Instabilities

The Thompson River Valley south of Ashcroft, which forms the subject corridor of this research, has a complex and varied history. In addition to the richly preserved geology discussed in Chapter 2, the area also has a storied anthropogenic history which has evolved substantially over time. Figure 3.1 identifies the extents of the study area: the Thompson River Valley from the village of Ashcroft to approximately 10 km south, and the 12 large landslides that are present in this corridor. While the landslides today are typically inactive or very slow moving, approximately nine rapid slope failures have been documented in the past 150 years. In examining the long history of landslide activity in this corridor, it is evident that the landslides have impacted, and in turn been affected by, the natural and social environments in which they have occurred (and recurred). Before proceeding with a detailed discussion of each of the landslides identified in Figure 3.1, some understanding of the social evolution of the area is helpful for contextualizing the documented landslide events.

As described in Chapter 2, the geology of the Thompson River Valley south of Ashcroft predisposes the valley walls to instability; moreover the work of Tribe (2005, 2002) dates this section of the Thompson River Valley to at least Middle Eocene time. Several authors have identified evidence of prehistoric landslide activity in the corridor due to the complex geomorphologic processes of valley incision and widening with attendant stress relief (Clague 1998; Clague et al. 1987; Morgenstern 1986), which would have preceded any written accounts of these landslides.

The first peoples to enter this area following the glacial retreat were the Interior Salish aboriginals (VanDine 1983). The Interior Salish people arrived approximately 9000 thousand years ago according to radiocarbon dating of artifacts excavated from the Drynoch landslide, located on the Thompson River approximately 8 km south of Spences Bridge (40 km south of Ashcroft) (VanDine 1983). VanDine (1983), citing Brawner and Readshaw (1963), notes that “Indian legend, which goes back hundreds of years, describes the [Drynoch] landslide but no reference is made of its beginning.” I am not aware of any comparable early oral histories referencing the landslides in the Ashcroft area. During his early investigation of the Ashcroft landslides in 1897, engineering geologist Robert Stanton (1898a) stated that:

“By the testimony of Indians who had lived in the country all their lives and that of some of the original white settlers, no slides had ever occurred at any point along the Thompson River before the white men began to irrigate the land, although one or two small cave-downs existed before that time.” (p. 16)

The earliest documentation of the Ashcroft landslides that I am aware of is a letter and accompanying map dated January 2, 1895, from Mr. H.J. Cambie to Mr. J. Abbott, Esq., General Superintendent of Canadian Pacific (CP) Railway, Vancouver (Cambie 1895). He wrote (Cambie 1895):

“When I first became familiar with this district in 1877 there was only one land slide, that marked No. 5 on the plan [the South Slide], and I have lately learned that even that one did not commence to move till after the bench above it had been irrigated for some years by W.R. Puckett,... so that all slides are directly traceable to irrigation waters.” (p. A1)

In the second half of the 1800’s, the lower Thompson River became a popular transportation route for the fortune-hunters of the Cariboo gold rush which commenced in 1858 (VanDine 1983). The building of the Cariboo wagon road followed the older migration trails of the Salish people (VanDine 1983). European settlement of the Ashcroft area followed; according to Clague and Evans (2003), ditch-and-furrow irrigation commenced in the area in 1868, eventually evolving to sprinkler techniques by the mid 1960’s.

In 1877, H.J. Cambie carried out a location survey along the Fraser and Thompson Rivers for the proposed Canadian Pacific Railway route (VanDine 1983); construction of the CP line at

Ashcroft was completed in 1885, followed by the Canadian Northern (now Canadian National) railway line in 1915. The Cariboo Road was upgraded in the early 1900's and eventually formed the route for the Trans Canada Highway which was constructed through the area in the early 1960's (VanDine 1983).

The inventory which I have compiled of reported landslide events in the Thompson River Valley south of Ashcroft is presented in Table 3.1, and described in detail in the following sections. It is worth noting that the majority of the recorded rapid landslide movements occurred in the late 1800's, coincident with the introduction of primitive ditch-and-furrow irrigation methods to the otherwise semi-arid benchlands along the Thompson River. Cambie (1895) and Stanton (1898a) both contended that these early landslides were directly caused by irrigation, with detrimental effects to the CP railway which traversed the lower portions of many of the landslides, as shown in Figure 3.1. The natural and human systems within the Thompson River Valley are necessarily intertwined, and there is certainly an anecdotal connection between the timing of these early landslides and the introduction of agricultural irrigation, which will be explored further in Chapter 5. However, consider that both Cambie (1895) and Stanton (1898a) were employed by the CP railway, on whose infrastructure the ongoing landslide movements exerted substantial detrimental effects, and their perspectives should be understood in this context. Morgenstern (1986) cautioned that "large landslides seldom have a single and unambiguous cause", suggesting that the slope failures of the late-1800's were likely reactivations of prehistoric landslides, the forms of which may not have been recognizable by Cambie (1895) and Stanton (1898a) without the assistance of aerial photography. We do know that Landslide No.2, the CN 50.9 slide, which occurred in 1897, could not be attributed to irrigation, as the *Victoria Daily Times* (1897) reported that there were "no streams within a long distance and no irrigation is being done within several miles."

Chronologically, as identified in Table 3.1, the earliest landslide, the South slide (No.7), reportedly occurred sometime between 1865 and 1877; this was followed by at least six (probably rapid) landslides in the corridor between 1865 and 1898; the only rapid slope movements recorded in the 20th century were the Red Hill Landslide (No.8) of 1921 and the Goddard Landslide (No.4) of 1982. Compared to the initial clustering of landslides which

occurred in the corridor during the late 1800's, a period of relative inactivity followed during the early 1900's. The paucity of reported landslide events in the first half of the 20th century (Table 3.1) is likely related to several factors, including:

- lack of record keeping of slow-moving (low-consequence) landslides prior to 1970 (Eshraghian et al. 2005);
- overarching dry climate conditions from 1925–1947 (refer to Chapter 4);
- sediment from previous landslides of the late 1800's acting as buttresses to river erosion;
- changes in irrigation locations and practices due to: loss of arable land near the valley wall, the imposition of court-ordered irrigation restrictions, and the evolution in irrigation methods (from ditch-and-furrow techniques to more water-efficient sprinkler methods).

In the latter half of the 20th century, the railways constructed a rip rap toe berm at the CN 50.9 slide and two large rock groynes extending into the river at the South Slide, as described in Section 7.2. Since 1970, better record-keeping by the railways has provided information on the frequency of reactivation of the landslides, which have since moved at very/extremely slow rates, with the exception of the Red Hill slide of 1921 and the rapid reactivation of the Goddard landslide in 1982. An approximate timeline of the recorded landslide events, in relation to anthropogenic influences described above, is presented in Figure 3.2. The following sections describe what details have been recorded or can be interpreted for each of the landslide events in Table 3.1.

3.2. Inventory and Description of Historical Landslide Events

An important first step in the assessment of hazard frequency is the preparation of an inventory of historical landslides which have occurred along the Thompson River Valley south of Ashcroft. One cannot make an educated assessment of the likelihood, nature or consequence of future events until a reasonable understanding of the past is established. Figure 3.1 identifies 12 large landslides present in the Thompson River Valley within approximately 10 km south of Ashcroft. Table 3.1 summarizes the nature, reported frequency, estimated velocity, and approximate size of each of the landslides in turn; a listing of the literature sources which make

reference to each landslide event are also given in the table. The number assigned to each landslide in Table 3.1 corresponds to the numbered location on Figure 3.1. The following paragraphs discuss the history of each landslide in detail, describing the literature sources cited and any inconsistencies between sources, justifying how the values and descriptions given in Table 3.1 were ultimately arrived at. The landslides are referenced by number (north to south) and name, as assigned in Table 3.1. It may be noted that smaller landslides exist along the corridor, but these are not addressed in this study for the sake of brevity. The most active of these, the Ripley landslide (approximate volume 400,000 m³ (Huntley et al. 2016)), is identified for reference on Figure 3.1, and is the subject of ongoing monitoring and study by others (Hendry et al. 2013b, Macciotta et al. 2014, Hendry et al. 2015, Schafer et al. 2015, Huntley et al. 2016, Journault et al. 2016, Macciotta et al. 2016, Schafer 2016, Huntley et al. 2017a). Relevant findings arising from these studies of the Ripley landslide will be referenced where applicable. This thesis, however, focuses primarily on the large landslides which may present greater consequences to the railways from an operational standpoint, and are of interest to a broad cross-section of stakeholders.

Based on railway maintenance records available for the 30-year period from 1970 to 2000, Eshraghian (2007) compiled a list of years in which existing large compound translational landslides along the Thompson corridor south of Ashcroft displayed a “noticeable increase in their rate of movement.” This statement refers to landslides that may be moving at an extremely slow rate (undetectable without instrumentation), but then exhibit a more substantial step-wise displacement in a given year, as evidenced by surface cracking or other readily identifiable indications of differential movement. Eshraghian’s (2007) findings are included in Table 3.1, and pertain to the Basque, CN 50.9, Goddard, North and South slides; his work forms the starting point for the historical landslides inventory.

More recently, Journault (2016) and Journault et al. (2016) presented the results of InSAR mapping of the Thompson River Valley south of Ashcroft. Their study utilized east-facing data from 2011-2016, and west-facing data from 2013-2016. Journault (2016) found that several of the landslides have exhibited coherent downslope movement rates in the order of approximately 10mm-44mm/year since 2011/2013. His findings relate to the Goddard, North,

South, Barnard and Red Hill slides. The movement rates identified were relatively consistent year over year, and generally confined to the toes of the landslides subject to active erosion by the river; these may be termed the background creep rates of the landslides. Journault's (2016) findings are described in the relevant subsections below, but are *not* listed as landslide events in Table 3.1; the purpose of the table is to identify years in which anomalous landslide movements occurred, in excess of extremely slow background activity.

It was a challenging task to find accounts of historical landslide events that occurred along the subject corridor prior to 1970, as reliable records of landslide movements were not maintained by the railways before this time (Eshraghian et al. 2005). In preparing the historical landslide inventory given in Table 3.1, I accessed many sources of information as cited in the table and further described in the following subsections for each particular landslide location. Whenever possible, I retrieved original sources to resolve often-conflicting information from more contemporary reports. These included archived newspaper columns from the *Ashcroft Journal* and the *Daily British Colonist*, and documents by Cambie (1895), Stanton (1898a) and Wade (1979). Mr. Cambie was directly involved with locating and surveying the rail route in British Columbia in the late 1800's, and was subsequently employed with Canadian Pacific as a construction engineer (EBA Engineering Ltd. 1984). A photograph of Cambie's survey party, dated 1879, is presented in Figure 3.3 below. The earliest first-hand documentation of the Ashcroft Thompson River landslides that I am aware of is a letter and accompanying map dated January 2, 1895, from Mr. H.J. Cambie to Mr. J. Abbott, Esq., General Superintendent of Canadian Pacific (CP) Railway, Vancouver (Cambie 1895). I was unable to access the original document, but reviewed the letter as re-typed by EBA Engineering Ltd., along with the accompanying map which was also electronically redrawn by EBA, and presented in Figure 3.4 (EBA Engineering Ltd. 1984). Mr. Robert Stanton was an engineering geologist commissioned by the CPR in 1897 to conduct an assessment of the landslides in the corridor, which had proven problematic to railway operations since the completion of the line in 1885 (Stanton 1898a, Porter et al. 2002). Stanton's paper was presented to, and published by, the (British) Institution of Civil Engineers in 1898, and represents the first major paper related to engineering geology in the province of British Columbia (VanDine et al. n.d.). A map of the

landslides on the Canadian Pacific Railway in the Thompson River Valley as drawn by Stanton (1898a) is presented in Figure 3.5.

Dr. Mark S. Wade lived in the Cariboo from the late 1800's until his death in 1929, and was employed as a physician by Andrew Onderdonk, chief contractor for the CPR (Wade 1979). Though first published posthumously in 1979, Wade's (1979) book *The Cariboo Road* is a manuscript that he wrote near the end of his life in the 1920's, telling of his life in the region and recounting some of the large landslides which occurred following completion of the Canadian Pacific Railway in 1885 and the Canadian National (CN) Railway in 1915.

In seeking to verify the accuracy and improve the completeness of the historical landslide inventory presented in Table 3.1, I also reviewed two retrospective chronologies of landslides in the broader region, which were produced by Peckover (1972) and Septer (2007) as described below.

In 1972, F.L. Peckover, Engineer of Geotechnical Services for CN, produced a report on the treatment of rock falls on the CN Jasper to Vancouver main line, in response to a formal inquiry into the safety of CN and CP mountain region operations by the Canadian Railway Transport Committee (Peckover 1972). The inquiry was the result of a fatal derailment which occurred west of the subject corridor, at Mileage 118.9 on CN's Ashcroft Subdivision on February 15, 1971 (Keegan 2007). Based on unpublished information from Peckover's investigation, Keegan (2007) provided a summary of injuries and fatalities resulting from rockfalls and landslides between 1937 and 1971 on mainlines of the CN and CP railways in British Columbia (Table 3-8 in Keegan 2007). Through personal communication with Keegan (2015), I obtained the location information and hazard type for each of the entries in his summary table, and verified that between 1937 and 1971, there were no landslides which resulted in injury or death along the 10-km corridor south of Ashcroft (CP Thompson Subdivision, approximate mileage 47-54, CN Ashcroft Subdivision approximate mileage 50-58); any reported incidents along the subject reach were related to rock falls, which are outside the scope of this study. This does not preclude the occurrence of slow-moving landslide activity which did not produce bodily harm but nonetheless required track maintenance by the railway. Such maintenance records

were not reliably kept by the railways prior to the Railway Transport Committee Inquiry. Again based on unpublished information, Keegan (2003) stated that slope movements occurred and railway maintenance repairs were required at the location of the Landslide No.2 (CN 50.9) following significant river flood events in the years 1921, 1948, 1972, 1997 and 1999, and these have been included as landslide events in Table 3.1.

Septer (2007) compiled an inventory of flooding and landslide events in Southern British Columbia from 1808 to 2006. He cited numerous original sources such as newspaper accounts, as well as unpublished information from geologist Stephen Evans (formerly of the Geological Survey of Canada). I reviewed Septer's (2007) chronology in order to validate the thoroughness of Table 3.1, and to add additional details to the landslide descriptions where available. While his chronology is very thorough, the stated intent of Septer's (2007) report was to produce a chronological list of flood events for the southern British Columbia, including descriptions of weather/storm induced landslides, and therefore his chronology includes some, but not all, of the landslides listed in Table 3.1. In addition, Septer (2007) presented the recorded landslide information as originally reported and without additional interpretation, such that there are several erroneous statements and conflated events as described in the relevant subsections below.

Finally, to supplement the written information described above and to aid in my interpretation of the history of the landslides, I retrieved and viewed stereo pairs of the earliest aerial photographs available for the Thompson River Valley south of Ashcroft from the National Air Photo Library, a division of Natural Resources Canada (NRC), dated July 15 and 16, 1928 (roll A291 # 39-64 and roll A300 # 35-50, respectively).

The following subsections describe each landslide in detail, citing the available historical information and any written accounts of the event(s) arising from the sources identified above and aided by more contemporary published literature and my own aerial photograph interpretations.

3.2.1. Landslide No.1 (CN 50.4)

Landslide No.1 (CN 50.4) is depicted by several authors (Clague et al. 1987, Clague 1998, Clague and Evans 2003, Bishop 2008, BGC Engineering Inc. 2012) on landslide maps of the Thompson River Valley south of Ashcroft. This landslide is, however, absent from Ryder's (1976) and Cambie's (1895) maps of the corridor, and from the landslide map accompanying Stanton's (1898a) report which does not extend as far north as CN mileage 50.4. No original sources give any date nor description of the landslide movement. Landslide No.1 is visible on the 1928 aerial photos for the area, and is therefore interpreted to have occurred prior to 1928, as stated in Table 3.1. By stereo examination of the 1928 air photos, Landslide No.1 appears to be ancient in origin, with a noticeably subtle, more subdued morphology compared to other, more contemporary landslide features visible to the south; this may explain its omission from Ryder's (1976), Stanton's (1898a) and Cambie's (1895) maps. It is also quite possible that the feature labeled Landslide No.1 is simply an abandoned terrace of the Thompson River; in either case, the subdued slope morphology does not show evidence of any recent instability.

Landslide No.1 has frequently been conflated with Landslide No.2 in more contemporary literature. Clague and Evans (2003) described a large compound translational landslide which took place on the west bank of the Thompson River on September 22, 1897. Figure 2 in Clague and Evan's (2003) paper unfortunately misrepresents the location of the 1897 slide as coincident with Landslide No.1. The 1897 landslide in fact occurred approximately 0.5 km to the south (Landslide No.2, CN 50.9 slide). This is verified by the location given for the 1897 landslide on Figure 19 in Clague (1998) and Figure 32 in Clague et al. (1987), the original sources on which Clague and Evans' (2003) Figure 2 was based. In addition, if one persists in reading the full Clague and Evans (2003) paper, Figure 7 makes it apparent that the 1897 landslide which they describe is indeed the CN 50.9 slide, *not* Landslide No.1 (CN 50.4). Bishop (2008) and BGC (2012) understandably conflated Landslide No.1 with the 1897 CN 50.9 slide, as they both make reference to Clague and Evans (2003); their descriptions of the origin of Landslide No.1 have therefore been ignored. BGC (2012, Table 3) indicated that a reactivation of the CN 50.4 landslide occurred in the year 2000. I suspect, however, that this

information is also correctly attributed to the CN 50.9 slide, as reported in several other sources (Porter et al. 2002, Kosar et al. 2003, Eshraghian et al. 2008).

3.2.2. Landslide No.2 (CN 50.9)

Landslide No.2 (CN 50.9) is depicted by numerous authors (Clague 1998; Clague et al. 1987; Clague and Evans 2003; Bishop 2008; BGC Engineering Inc. 2012; Eshraghian et al. 2008; Eshraghian et al. 2007; Ryder 1976) on landslide maps of the Thompson River Valley south of Ashcroft. Landslide No.2 is not mentioned in Stanton's (1898a) report; his field visit likely preceded the occurrence of the most recent large-scale movement of the slide, which occurred in September 1897. Landslide No.2 is also absent from Cambie's (1895) map of the corridor, which was prepared prior to the 1897 event.

Based on field inspection of the landslide and stereo examination of aerial photos, the CN 50.9 landslide appears to be predominantly compound² translational in nature, with minor backwards rotation of some large blocks within the debris mass, as per Clague and Evans' (2003) description. Eshraghian et al. (2007) hypothesized that the 1897 event represented a rapid retrogression of an existing landslide, which had originally occurred due to downward incision of the Thompson River Valley since deglaciation, exposing the weak glaciolacustrine seams which served as the rupture surfaces for the initial event and subsequent retrogressions. They speculated that the major scarp was likely developed during the 1897 event, which translated the existing minor scarps from previous retrogressions (Eshraghian et al. 2007). Eshraghian et al. (2007) presented a cross-section through the CN 50.9 slide, based on a compilation of LiDAR data, geological information, inclinometer readings (BGC Engineering Inc. 2001a), borehole information (BGC Engineering Inc. 2001a, 2003), modeling of the sliding stages, aerial photos and site visits. The slide is moving on two rupture surfaces as a multiple translational earth slide (Eshraghian et al. 2007). The lower rupture surface is located in the glacio-lacustrine clay and silt (unit 2), with a second, shallower surface of rupture in the

² According to Skempton and Hutchinson (1969), *compound* refers to slope movements in which the rupture surface is formed of a combination of curved and planar segments, whereby the movements exhibit a part-rotational, part-translational character.

overlying colluvium and till; the rupture surfaces, as determined by inclinometer readings, are located at elevation 275.7 m and 280.9 m, respectively (Eshraghian et al. 2007). Eshraghian et al. (2007) reported the rate of movement for the most recent reactivations to be 3-20 mm/year with the higher movement rate measured along the deeper rupture surface.

Landslide No.2 is somewhat anomalous compared to the other large landslides in the corridor, in that it was not adjacent to any irrigated agricultural areas. Newspaper reports of the 1897 landslide indicate that “The present slide can in no way be attributed to the use of water as there are no streams within a long distance and no irrigation is being done within several miles” (Victoria Daily Times 1897). Landslide No.2 is located directly across the river from Landslide No.3, which occurred earlier, probably between 1886–1894, as indicated in Table 3.1. It is therefore possible that Landslide No.2 was initiated by increased river scour and bank erosion, resulting from constriction of the river channel by Landslide No.3. The *Daily British Colonist* (1897) reported that Landslide No.2 commenced on Wednesday, September 22, 1897 as “rumblings in the near by hills”, saying:

“At one o’clock in the night a large portion of the pine clad mountain broke off, and started with a rumble like thunder toward the Thompson river. The section first in motion was about half a mile square and some 400 or 500 feet high. Its motion was slow at first, but increased as the immense strip of land advanced towards the water, and there found its progress arrested. Within two hours from the time the first contribution was made to the river bed, the Thompson is said to have raised nine inches...”. (p. 6)

This account would suggest that the 1897 slide constricted the Thompson River without completely blocking it, which is corroborated by the article in the *Victoria Daily Times* (1897). Based on these reports, the rate of movement of the landslide appears to have varied from slow (as reported by Clague and Evans (2003)) to rapid (as suggested by Eshraghian et al. (2007)), over a period of several days. The *Victoria Daily Times* (1897) implies the disturbed mass to have been generally dry, with the major movement producing “... a great volume of dust rising from the river bank.” The description of the landslide, (“The top of the middle section of the slide is higher than the ground immediately behind...”) is consistent with the formation of a graben and counterscarp characteristic of a compound translational mode of movement (Victoria Daily Times 1897). While there were no reported casualties or impact to the CP

railway (located on the opposite side of the river), the *Victoria Daily Times* (1897) noted that the subsidence encompassed an aboriginal burial ground, and the bodies were removed and re-buried several days later when the movement of the landslide had all but ceased. In describing the 1897 landslide, Septer (2007) mistakenly cited the *Daily Colonist* of September 27, 1897 (which was not published on September 27, 1897), instead of the *Victoria Daily Times* (1897) of the same date.

The CN 50.9 landslide has experienced several reported reactivations (out-of-slope movements along existing rupture surfaces) within the last century, including in 1921 and 1948 (Keegan et al. 2003), 1972 and 1977 (Porter et al. 2002, Keegan et al. 2003, Eshraghian et al. 2008), 1997 (Keegan et al. 2003, Eshraghian et al. 2007, 2008), 1999 (Keegan et al. 2003), 2000 (Porter et al. 2002, Kosar et al. 2003, Eshraghian et al. 2008), and 2001 (Porter et al. 2002, Kosar et al. 2003) as recorded in Table 3.1. Septer (2007) noted that on June 3, 1948, the Thompson River at Spences Bridge set an all-time record with a daily discharge of 4130 m³/s, which may have contributed to the reported landslide reactivation that year. Eshraghian et al. (2007) estimated the volume of the most recently active (northern) portion of the landslide (at CN mileage 50.9) to be 3.3 Mm³.

Both the northern (CN mileage 50.9) and southern (CN mileage 51.2) portions of the landslide are visible in the 1928 air photos. Ditch and furrow irrigation is evident above the southern portion of the slide, with dark patches of ponded water or vegetation visible in the southernmost portion of the disturbed slide mass. The southern boundary of the landslide is confined by a rock outcropping where the CN railway tunnels through.

The northern, most recently active portion of the landslide (at CN mileage 50.9) is protected against river erosion by a toe berm that was constructed below the rail grade in the late 1970's (Eshraghian et al. 2008). Monitoring in the summer of 2001 showed an increase in the slide movement rate, and a 6m extension was added to the existing berm (Porter et al. 2002, Kosar et al. 2003). In response, movements reportedly slowed above the rail grade but continued near the crest of the toe berm. The face of the berm extension was constructed at a relatively steep angle to minimize the impact on the waterway (Porter et al. 2002).

3.2.3. Landslide No.3 (Unnamed)

Though Landslide No. 3 is depicted on numerous maps of the Thompson River Valley south of Ashcroft (Cambie 1895, Stanton 1898a, Ryder 1976, Clague et al. 1987, Clague 1998, Clague and Evans 2003, Bishop 2008, BGC Engineering Inc. 2012), none of the above-noted authors discuss this particular slide in detail. Moreover, there do not appear to be any records of ill effects to the CP railway which traverses the toe of the slide, which suggests the Landslide No.3 has been largely inactive over the last century. Landslide No.3 is visible on the 1928 aerial photos and has a subdued appearance consistent with this presumed inactivity.

The best source of information concerning Landslide No.3 appears to be a letter and accompanying map dated January 2, 1895, from H.J. Cambie to J. Abbott, General Superintendent of CPR, Vancouver (Cambie 1895). Cambie (1895) confirmed that Landslide No.3 had occurred since a previous communication of August 27, 1886, in which he had apparently expressed concern about an irrigation stream and dams that J.E. Barnes was constructing on recently-purchased terrace land along the east side of the Thompson River about 4 miles (6.4 km) south of Ashcroft. Says he: “In talking to you August 27th, 1886 I mentioned this stream and the dams they were then erecting and expressed a fear that the irrigation would cause landslides at the Railway line. Since then my fears have been more than realized” (Cambie 1895). By the time of writing this letter on January 2, 1895, Landslide No.3 had occurred, and, along with a smaller landslide to the south, had since that time had cost the railway upwards of \$1000 per annum in Cambie’s estimation (Cambie 1895). As such, the date of Landslide No.3 is given as 1886-1894 in Table 3.1. The map accompanying Cambie’s (1895) letter, as reproduced in EBA’s 1984 report on the Goddard landslide (EBA Engineering Ltd. 1984), shows the footprint of Landslide No.3 at that time to be similar in size to that depicted on Stanton’s (1898a) landslide map, being somewhat smaller than shown on more recent maps, and visible in the earliest (1928) air photos of the area. Cambie (1895) directly attributed the cause of Landslide No.3 to aggressive irrigation of the terrace above by construction of a 15-foot-high (4.6 m) dam at the west end of Lower Barnes Lake, and the diversion of a portion of Barnes Creek into the lake to fill it to the height of the dam each

spring. It is worth noting that Cambie (1895) attributed the cause of all of the landslides shown on his map to irrigation, which, along with some smaller landslides, include Landslide No.'s 3, 4, 5, 6, 7 and a larger slide possibly representing Landslide No.'s 9 and 10 combined (Figure 3.4).

Cambie (1895) went on to recommend that CP acquire as much land as possible along this stretch of the railway, as well as water rights to Barnes Creek, so as to prevent irrigation and further damage to the railway by landslides. I do not know what, if any, actions were taken by CPR in this regard, though I did not detect any evidence of irrigation above the slide in the 1928 aerial photo. It is possible that the apparent enlarging of the slide from Cambie's (1895) time until 1928 resulted in a loss of the arable terrace lands, or that CP did indeed acquire ownership of the adjacent land and water rights.

3.2.4. Landslide No.4 (Goddard)

Landslide No.4, the Goddard slide, has been relatively well-documented due to historical litigation over irrigation of the upslope terrace lands between CP Rail and the agricultural landowners. The first recorded movement of the Goddard landslide took place on October 19, 1886, and is described by numerous authors (Cambie 1895, Clague 1998, Porter et al. 2002, Clague and Evans 2003, Eshraghian et al. 2007, Septer 2007, Eshraghian et al. 2008). The location of the Goddard landslide is shown on numerous landslide maps of the Ashcroft Thompson River Valley south of Ashcroft (Cambie 1895, Stanton 1898a, Ryder 1976, Clague et al. 1987, Clague 1998, Clague and Evans 2003, Bishop 2008, BGC Engineering Inc. 2012); the footprint depicted on Stanton's (1898a) and Cambie's (1895) maps is considerably smaller than that shown by more recent authors. By stereo examination of aerial photos, it is evident that the most recent reactivation of the Goddard landslide, in 1982, comprised only about the northern one-third of a larger landslide, as shown on Figure 3.6. The northern portion, corresponding to the area depicted on Stanton's (1898a) and Cambie's (1895) maps, is hummocky in appearance, indicative of its more recent activity. The southern, possibly ancient portion of the Goddard slide is distinguished in aerial photos by a more subdued morphology (Thurber Consultants Ltd. 1984). It is likely that the 1886 landslide also represented a

reactivation of the northern portion of this ancient slide (Eshraghian et al. 2007), which would not have been readily recognizable (at the time) without the assistance of aerial photography. Large swaths of ditch and furrow irrigation are evident above the Goddard slide in the 1928 aerial photo (Figure 3.7), as depicted on Stanton's (1898a) map of the area (Figure 3.5).

The *Daily British Colonist* reported on Wednesday, October 20, 1886, that "a large land-slide occurred near Ashcroft on Monday night [October 18], washing away a large quantity of track and leaving a deep gully. The engine, tender and baggage car of the Pacific express went off the embankment. The engineer was scalded and the fireman hurt" (1886). The article speculated that "owing to the exceptionally dry season, the high banks at this point near the track, which are of a very gravelly nature, would easily be moved by the first heavy rain that fell" (Daily British Colonist 1886). Stanton (1898a), however, implicated ditch-and-furrow irrigation on the upland areas as the cause of the 1886 Goddard landslide (and of all the others depicted on his map in Figure 3.5).

Cambie (1895) corroborated Stanton's claim, asserting that the Goddard landslide occurred "just after" an extra quantity of water had been brought there for irrigation purposes, and entailed a loss of \$15,000 or more to the CP railway. In a later paper for the Transactions of the Canadian Society of Civil Engineers, Cambie (1902) alluded to a slower-moving slide that has required constant watching as it included a portion of the railway line:

"...although its forward progress has been slow, it has begun to move, year after year, at a date about three months after the beginning of the irrigation season, and has continued moving for about the same period of time. In 1886 the Canadian Pacific Railway Company took legal proceedings against the parties irrigating the fields above this slide, and it devolved upon the writer to furnish the legal advisers for the Company with evidence to prove that the slide was due to the action of irrigation water." (p. 198)

The timing of the litigation in 1886 suggests that Cambie (1902) was describing the Goddard landslide. This is an important observation, as it would indicate that the Goddard slide of 1886 was not a first-time event, but rather the culmination of seasonal movements that had been occurring for some time. The lawsuit was successful, and Cambie (1902) noted that "In all probability the jury was influenced by the evidence that no slides had occurred before the commencement of irrigation, and that there was irrigated land in the rear of each slide."

Clague (1998) suggested that the 1886 Goddard slide represented a relatively slow-moving, rotational slump in which multiple, back-tilted slide blocks were preserved. Notwithstanding, Clague and Evans (2003) described the 1886 event as a “sudden-onset flowslide, which happened only minutes after a railway trackman passed the spot.” This is presumably based on Stanton’s (1898a) dramatic description of a fatal landslide that occurred a few years prior to his report, which H.J. Cambie subsequently clarified as a landslide that occurred in 1886, during which the engine driver was scalded, not killed, and asserted that the CPR did *not* have a watchman on that part of the railway at that time. Eshraghian et al. (2007) asserted that the 1886 movement was likely very rapid, based on Clague and Evans’ (2003) description. However, the fact that there was no reported landslide dam nor significant constriction of the river, and the apparent similarity of the 1886 event to the 1982 reactivation (Eshraghian et al. 2007), lead me to favor a description of the 1886 Goddard landslide as a compound translational landslide, probably of moderate to rapid velocity.

On September 24, 1982, a rapid landslide occurred within the displaced material of the 1886 landslide mass (Clague 1998, Eshraghian et al. 2007). The 1982 slide had an estimated volume of 2 Mm³ (Eshraghian et al. 2007) to 3 Mm³ (Clague 1998). The CP railway track was severed by the slide, requiring six days of closure for emergency remedial construction, with damages estimated to be about \$1 million (Clague 1998, Porter et al. 2002). CP brought a legal action against the owner of the agricultural land above the slide, claiming that the landslide was triggered by excessive irrigation (Clague 1998). Lengthy litigation followed, with both the Supreme Court of British Columbia and the British Columbia Court of Appeal ruling in favour of the landowner (BC Court of Appeal 1990, Clague 1998, Eshraghian et al. 2007). The repaired CP track was relocated somewhat upslope of its original position (Edwards 2015), but is still located within the disturbed slide mass.

Activity of the Goddard landslide prior to 1982 included minor reactivations in 1974 (Morgenstern 1986) and October 1976 (Golder Associates 1977, Morgenstern 1986, Porter et al. 2002). Movement rates during this period were generally very slow, in the range of 20mm/year up to 400 mm/year in 1976 (Eshraghian et al. 2007). In 1982, the reactivated slide mass moved rapidly, commencing at a rate of 30 mm/hour on September 23, and accelerating

to a maximum rate of 6 m/hour on September 24, 1982 according to Krahn (1984). Eshraghian et al. (2007) presented a cross-section of the 1982 Goddard landslide based on borehole information from Krahn (1984), with the bedrock depth interpolated from the adjacent CN 50.9 and South slides. The cross section depicts four sliding blocks moving on two surfaces of rupture located within, and along the surface of, the glaciolacustrine silt and clay (unit 2); the rapid 1982 Goddard reactivation is thus described as a multiple translational earth slide (Krahn 1984, Eshraghian et al. 2007). Based on unpublished information from Wood (1982), indicating the formation of a distinct graben feature during the failure, I would suggest that multiple *compound* translational earth slide would be a more complete description of the 1982 reactivation.

Bank erosion at the toe of the slope may have contributed to the rapid 1982 reactivation of the Goddard landslide. Morgenstern (1986) estimated the toe erosion rate of the Thompson River bank at the Goddard slide to be approximately 0.25 to 0.33 m/year, which was accompanied by a 6-m-deep scour hole in the Thompson River bed at the location of the 1982 landslide (Krahn 1984, Eshraghian et al. 2007). Active river erosion and new cracks developing at the toe of slide were evident during a May 2005 site visit by Eshraghian et al. (2007). Eshraghian et al. (2008) argued that continuous river erosion at the toe of the slope, along with increased pore pressure on the slide rupture surface associated with fluctuations in the Thompson River level, were responsible for the 1982 reactivation of the Goddard landslide. Moreover, he postulated that the slow movement which began at the toe of the slide opened cracks within the slide body, which were readily filled with water from the perched water table connected to the crown terrace (Eshraghian et al. 2008). Leroueil (2001) distinguished between “active landslides” and “reactivated landslides”; in contrast to active landslides, where the rate of displacement varies with seasonal changes in pore pressures, reactivated landslides may be associated with sudden and fairly rapid displacements. He cited Hutchinson (1987) and D’Elia et al. (1998) in observing that these movements may be precipitated by, among other mechanisms, river erosion at the toe or a rapid pore pressure increase due to infilling of cracks in the soil mass with water (Leroueil 2001).

Eshraghian et al. (2008) suggested that the improved stability since the 1982 reactivation is due to a flatter slope geometry and the fact that the movement disrupted the connection between the perched water table and the slide's crown terrace. As previously mentioned, others (e.g. Krahn (1984)) argued that the landslide was caused by irrigation, although this theory was not successful in court. Various theories notwithstanding, the 1982 Goddard retrogression remains an anomaly, in that it represents the only reported rapid landslide movement which has occurred in the corridor in modern times (since the 1921 slide at Red Hill/Hammond Ranch). Anomalous weather and climate conditions which preceded, and may have contributed to, the 1982 reactivation are discussed in detail in Chapter 4. Eshraghian et al. (2008) suggested that toe berm construction could significantly improve the stability of the marginally-stable toe block by minimizing the effects of river erosion, thus preventing the development of new tension cracks by minimizing stress relief and extension at the slide toe. However, while the construction of a toe berm may reduce erosion locally, it may also have the undesirable effects of increasing scour in the riverbed and erosion on the opposite (west) bank of the river (where the CN track is located). Journault (2016) estimated the Goddard slide to be moving at a consistent (extremely slow) downslope rate of approximately 10 mm/year based on InSAR data from 2011-2016.

3.2.5. Landslide No.5 (CN 53.4/53.7)

Landslide No.5 is delineated by numerous authors (Cambie 1895, Stanton 1898a, Clague et al. 1987, Clague 1998, Clague and Evans 2003, Bishop 2008, BGC Engineering Inc. 2012) on landslide maps of the Thompson River Valley south of Ashcroft. Details of the landslide, however, remain largely unknown. The southern portion of Landslide No.5 (CN mileage 53.7) is located directly across the river from the largest landslide in the corridor, the North Slide, and likely dates from approximately the same time. This southern portion of the slide must have occurred prior to 1898, as it is included on Stanton's (1898a) map, and its inclusion on Cambie's (1895) map would suggest it occurred sometime between 1877 and 1894, as indicated in Table 3.1. Although Cambie's (1895) letter and Stanton's (1898a) assessment both implicate irrigation of the upslope terrace as the cause of the movement, the temporary landslide dam formed by the North slide of 1880 most likely acted as a trigger for the

movement as a result of concentrated erosion caused by displacement of the river. For this reason Porter et al. (2002) surmised that Landslide No.5 may have also occurred in 1880. The northern portion of Landslide No.5 (CN mileage 53.4) is not mapped in Cambie's (1895) letter nor Stanton's (1898a) report, and likely represents a separate event or events which occurred at a different time. On the 1928 aerial photos, the northern portion of the slide has a smoother, more subtle appearance in comparison to the more hummocky southern portion, which exhibits ridge-like features consistent with the grabens and counterscarps of a compound translational earth slide. It is possible that the northern portion represents an older, possibly ancient slope movement which, similar to the outer extents of the Goddard landslide, was not recognized by early authors such as Stanton (1898a) and Cambie (1895) without the assistance of aerial photography. It is possible, though unlikely, that the northern portion of the slide failed later, in connection with the Goddard landslide of 1886 (which is located directly across the river); but given the subdued morphology, and as there was no reported landslide dam associated with the 1886 Goddard slide, this is unlikely. Ditch-and-furrow irrigation is visible west of Landslide No.5 in the 1928 aerial photo, though it is set back a minimum distance of about 300 m from the crest of the valley wall.

3.2.6. Landslide No.6 (North Slide)

“The great north slide”, to borrow from Stanton's (1898a) terminology, occurred on the evening of October 14, 1880 (Daily British Colonist 1880b, Wade 1979). Evans (1984) noted that Stanton (1898a) incorrectly gave the date of this landslide as 1881; Drysdale (1914) also reported the date of the slide as October 1881, referencing Stanton (1898a). Septer (2007) recorded this event three times in his landslide chronology, in October 1880 (referencing numerous authors and newspaper reports) October 1881 (primarily referencing Stanton (1898a)), and in 1888 (referencing Evans (1992), p.82, where the date is mistyped as 1888, instead of 1880 as stated in the text of the manuscript). The North slide is the largest landslide recorded in Table 3.1, estimated to be between 15 Mm³ (Clague and Evans 2003) and 21.4 Mm³ (Eshraghian et al. 2007) in volume. The extent of the landslide is shown on all of the landslide maps referenced in this thesis (Cambie 1895; Stanton 1898b; BGC Engineering Inc. 2012; Ryder 1976; Bishop 2008; Clague and Evans 2003; Clague et al. 1987; Clague 1998),

and the landslide has been described by numerous authors (Stanton 1898a, 1904, Engineering News 1909, Drysdale 1914, Wade 1979, Evans 1984, 1986, 1992, Clague and Evans 1994, Clague 1998, Porter et al. 2002, Clague and Evans 2003, Eshraghian et al. 2007, Septer 2007). The rate of the 1880 movement is believed to have been very rapid; the landslide was felt and heard in Ashcroft, where it was thought to be an earthquake (Clague and Evans 2003, Eshraghian et al. 2007). The 1880 landslide dammed the Thompson River completely for approximately 44 hours (Daily British Colonist 1880b, Stanton 1898a, Wade 1979, Evans 1986). Wade (1979) recounted the North slide and the subsequent damming of the Thompson River as follows:

“About nine o’clock on the night of the 14th a huge landslip occurred suddenly and a great barrier of earth and gravel completely blocked the Thompson River at a point about three miles below the present town of Ashcroft, which, at that time, was not in existence. So thoroughly was the river dammed that for over forty hours not a drop of water passed beyond the obstruction; from there to the mouth of the Nicola the dry channel of the Thompson was exposed to view. Above the barrier, the water steadily rose higher and higher and a great lake spread over the banks, the depth of water at the dam being between fifty and sixty feet. The flat upon which the town of Ashcroft is built was covered with water to a depth of sixteen inches. ... the barrier would have held intact several hours longer had not men been put to work cutting a channel through which the water was allowed to flow. Once it began to run it soon eroded a deeper channel, great masses of earth were washed away, an ever widening breach in the barrier grew moment by moment, and within a few hours the Thompson pursued its wonted way as if nothing untoward had ever occurred to impede its progress.” (p. 120–121)

Upon investigating the cause on the North slide, Stanton (1898a) wrote that:

“Irrigation had been carried on above it for some years, and some time before the final catastrophe occurred, a reservoir 2 miles distant in the hills from which the irrigation water came, broke its dam, and most of the water liberated spread over the upper benches of this land, already well soaked. The whole tract of 150 acres sank vertically in one movement to a depth, at the back edge, of over 400 feet. The lower portion, about 2,000 feet wide, was forced entirely across the river, a distance of 800 feet to 1,000 feet; and coming against the steep bluff on the opposite side, it filled the whole inner gorge of the valley, and formed a dam fully 160 feet high, completely stopping the flow of the river for several days, so that men walked dry-shod across the river-bed below the dam.” (p. 5)

Cambie (1895) attributed the cause of the North slide to irrigation. Stanton (1898a) observed that the North slide destroyed all of the arable benchland immediately above it, and hence

irrigation ceased following the 1880 event; the loss of the irrigation dam was likely also a factor in the cessation of irrigation. The movements of the disturbed mass practically ceased within a few years following the initial slide, which Stanton (1898a) attributed to cessation of irrigation and drainage of the slide material. He noted that “The railway crosses this slide 500 feet or 600 feet back from the river, and since the water has drained out, little trouble has been experienced, for the land has settled firm and dry” (Stanton 1898a). This was corroborated by Cambie’s (1895) letter, in which he identified the Goddard slide, the South slide, and one smaller slide to have cost the CP railway company at least \$35,000 in the 8 years between 1886 and 1894, but did not mention the North slide as having caused any issues in rail transport during that period. Though no casualties were reported at the time, an 1897 newspaper article concerning the CN 50.9 slide suggested that the North slide resulted in the loss of one life, in addition to “great damage to property” (Daily British Colonist 1897).

The North slide of 1880 is distinct from the other landslides in the corridor, in that it was the only slide reportedly preceded by the breach of an irrigation reservoir (Stanton 1898a, 1904). A working hypothesis is that the North Slide was a complex³, rapid, very wet, earth slide-debris flow, as indicated in Table 3.1. The rapidity of the movement and the reach of the landslide, inundating the valley and damming the Thompson River, supports this hypothesis, which is further articulated in Chapter 5.

Since the 1880 event, the North slide has experienced minor reactivations. In the fall of 2000, a reactivation with maximum displacement rate of 150 mm/year (very slow) was documented at the North slide (BGC Engineering Inc. 2001b, Porter et al. 2002). Eshraghian et al. (2007, 2008) also suggested the North slide was reactivated due to river flooding in 1997, citing BGC Engineering Inc. (2001b); though Eshraghian et al. (2007) estimated that rate of movement in 1997 to be extremely slow (<16 mm/year). 1997 was a year of exceptionally high Thompson River discharge, and other authors documented very/extremely slow movements at the CN 50.9, South and Nepa Crossover slides that year (Table 3.1). Journault (2016) estimated the

³ According to Varnes (1978) *complex* refers to slope failures that exhibit more than one of the major modes of movement.

North slide to be moving extremely slowly at a consistent downslope rate of approximately 10 mm/year based on InSAR data from 2011-2016.

Inclinometer measurements have revealed that the reactivated North slide is moving on two rupture surfaces (el. 269 m and 264 m) in the highly plastic glaciolacustrine clay-silt layer (unit 2) as a retrogressive, multiple, translational earth slide (Eshraghian et al. 2007). Piezometer measurements indicated an artesian groundwater condition near the toe of the slide (BGC Engineering Inc. 2001b).

The North slide is clearly evident in the 1928 aerial photos, with dark (irrigated) farmland visible on the terrace immediately above the scarp of the slide. I detected smaller, active-looking slumps at the toe of the slide along the riverbank (below the railway track) in the 1928 aerial photos; these are likely the result of ongoing river erosion, as the northern portion of the slide coincides with an outside bend of the river (Figure 3.1). Porter et al. (2002) estimated contemporary river bank erosion at the toe of the North slide to be in the order of 0.7 m/year.

3.2.7. Landslide No.7 (South Slide)

Landslide No.7, the South slide, is located downstream of the North slide on the east bank of the Thompson River. Its volume is estimated to be 9 Mm³ (Eshraghian et al. 2007), making it second in size only to the North slide. The central portion of the slide, which has historically been more active, encompasses approximately 3.2 Mm³ (Bishop 2008). The northern margin of the South slide abuts the bedrock ridge known as Black Canyon, which forms a constriction in the Thompson River (Porter et al. 2002). The South slide is shown on all of the landslide maps of the Thompson River Valley south of Ashcroft reference herein (Cambie 1895, Stanton 1898a, Ryder 1976, Clague et al. 1987, Clague 1998, Clague and Evans 2003, Bishop 2008, BGC Engineering Inc. 2012), and has been described by several authors (Cambie 1895, Stanton 1898a, BGC Engineering Inc. 2001b, Porter et al. 2002, Kosar et al. 2003, Eshraghian et al. 2007, BGC Engineering Inc. 2012). The landslide reportedly occurred prior to construction of the CP railway, which was completed in 1885 (Porter et al. 2002). While Eshraghian et al. (2007) suggested the South slide likely occurred in 1881, they may be

conflating it with the North slide which Evans (1984) noted was misreported by Stanton (1898a) as having occurred in 1881, rather than 1880; others (e.g. BGC Engineering Inc. (2001b)) have made the same error based on Stanton's (1898a) account. Bishop (2008) suggested the South slide occurred between 1865 and 1877; this is the date range indicated in Table 3.1, based upon Cambie's (1895) observation that the South slide was the only landslide which already existed when he first became familiar with the district in 1877, and that he had learned that the South slide occurred after the benchland above it had been irrigated for some years by W.R. Puckett, who purchased it in 1865⁴.

While there is no report of the movement rate during the South slide of the late 1800's, Stanton (1898a) likened it to the other landslides which occurred in the corridor during that time; he attributed the cause of the landslide to irrigation on the benchland above it, and noted that irrigation continued following the initial movement, perpetuating ongoing displacement of the disturbed mass towards the river, and necessitating continual maintenance and slow orders along this portion of the CP railway. Stanton (1898a) noted that the ongoing movements were concentrated in the center of the slide (the central, circular scarp is still visible on the 1928 air photos), and described the ongoing movements as "continuous, though it is greatest in the months of July, August and September" (Stanton 1898a). This would suggest the slide was most active during the driest months, when irrigation would be at its peak, in contrast to the more recent reactivations which have been recorded in September/October upon seasonal recession of the Thompson River (Table 3.1).

However, in response to Stanton's (1898a) assertion that the South slide had been moving continually since its initiation ("at times the road-bed has sunk 4 feet, and has moved out twice that distance in a night"), Cambie subsequently contended that "A movement had occurred in 1894, but it was not nearly so rapid as that described, and no such motion had occurred before or since that time" (Stanton 1898b). This apparent reactivation of the South slide in 1894 is included in Table 3.1. Septer (2007) corroborated that record snowfalls in the interior mountains accompanied by a cold and wet spring, followed by a sudden warm spell in late

⁴ This date is erroneously typed as 1965 in the reproduction of Cambie's (1895) letter in Appendix A of EBA Engineering Consultants Ltd. (1984) report.

May, resulted in great flooding of the Thompson River in 1894, which may well have contributed to reactivation of the South slide. Such flooding was not seen again until 1948 (Septer 2007). The apparent reactivation of the South slide in 1894 is also corroborated by the fact that in the following year, 1895, the CPR sought an injunction to prevent the landowners from irrigating the property above the slide (Clague 1998). While the British Columbia Supreme Court ruled for the landowners, the injunction was ultimately granted on appeal by the Privy Council of London, “restraining the Respondents... from so irrigating the... lands as to cause a landslide or slip, and thereby to injure the Appellant Company’s line of railway” (Privy Council, 1899, p.14, as cited in Clague (1998)).

The South slide is visible on the 1928 aerial photos. The central portion of the slide is evidently more active, with a sharper, circular slide scarp. Relatively fresh scarps also show evidence of slope instability along Nelson Creek to the south. Active irrigation is visible above the North slide in the 1928 photo, set back approximately 550 m from the crest of the South slide. Irrigation ditches, perhaps abandoned, are visible above the South slide in 1928, set back a minimum distance of about 200 m from the scarp of the slide. The CN railway crosses the Thompson River from the west to east bank at the northern edge of the South slide, traversing the toe of the landslide about 20 m below the CP rail line (Porter et al. 2002).

Since Stanton and Cambie’s time, contemporary authors have documented several reactivations of the central portion of the South slide. This central, more active portion is depressed, and filled to varying levels with runoff water; it likely coincides with the centre of a buried thalweg (K.W. Savigny, personal communication 2017). Porter et al. (2002) and Eshraghian et al. (2007) reported that the South slide was reactivated in the winter of 1977 and the fall of 1997; Eshraghian et al. (2008) also suggested the South slide was active in 1999. An InSAR map presented by Kosar et al. (2003) indicated that 16 mm of total ground movement occurred at the South slide between August 1997 and August 1998; on this basis, Eshraghian et al. (2007) classified the 1997 rate of movement as very slow. BGC Engineering Inc. (2012) also reported the movement rates in 1997 and 1977 to be very slow (between 20 mm/year to 60 mm/year), based on unpublished CP documentation. Examining InSAR data from 2011–2016, Journault et al. (2016) observed the southern portion of the South slide to be

moving at a consistent rate of approximately 20 mm/year, while the historically more-active central portion did not show any coherent movement. A field inspection of the southern portion of the slide by Journault (2016) did not reveal any open cracking other surficial indications of movement.

Two large groynes (rock breakwaters extending into the river to protect against bank erosion) were constructed in the Thompson River below the South slide in the 1950's (Edwards 2015), suggesting the slide may also have been active at that time. Porter et al. (2002) reported that one of the groynes was damaged during the 1997 flooding, resulting in extensive erosion at the toe of the South slide. A scour hole also formed in the Thompson River bed below the South slide (Eshraghian et al. 2007). Repairs to the groyne and the addition of a toe berm to replace the material eroded during the 1997 flood event were undertaken the following year, and credited with slowing the movement rate of the South slide to an acceptable level from an railway operations standpoint (Porter et al. 2002, Eshraghian et al. 2007).

Similar to the North slide, Eshraghian et al. (2007) described the South slide as a retrogressive, multiple, translational earth slide. Based on borehole information and inclinometer readings reported by BGC Engineering Inc. (2005), Eshraghian et al. (2007) presented a simplified cross-section of the South slide, showing three sliding blocks moving on two planar rupture surfaces located within the glacio-lacustrine silt and clay unit 2 at elevations of 273 m and 264 m, respectively.

3.2.8. Landslide No.8 (Red Hill / Hammond Ranch)

Landslide No.8 is located on the west bank of the Thompson River in the southern portion of the corridor, where both the CN and CP railway tracks are situated on the opposite (east) bank. Bishop (2008) and BGC Engineering Inc. (2012) referred to the landslide as the “Red Hill Slide”, named for the nearby Red Hill. Apart from the 1982 Goddard landslide, Landslide No.8 is the only other documented rapid landslide south of Ashcroft which occurred in the 20th century. It temporarily dammed the Thompson River, though only for a few hours.

Landslide No.8 occurred on August 13, 1921, as briefly described by Wade (1979): “The cause of this most recent landslip was seepage of irrigation water. The area affected was about half a mile in length and completely dammed the river which, however, speedily cut its way through the obstruction.” The landslide is visible in the 1928 aerial photos, with some remaining constriction of the river still evident. There has been some confusion between subsequent accounts as to the location of the 1921 landslide, owing to Wade’s (1979) ambiguous description of its whereabouts: “On 13th August 1921, a landslide occurred on the Thompson River about two miles below the site of the above slide and on the opposite side of the river.” By “the above slide”, Wade (1979) could have been referring to the catastrophic landslide on the west bank of the Thompson River near Spences Bridge which occurred on August 13, 1905, described in his manuscript immediately prior, or he could perhaps be referencing the North slide of October 14, 1880, which precedes his description of the Spences Bridge slide. An article in the Ashcroft Journal of Friday, August 19, 1921, serves to clarify the issue: “A landslide with about half a mile frontage came down without warning on the west side of the Thompson river at Basque, about six miles [9.6 km] south of Ashcroft on Saturday morning last...” (Ashcroft Journal 1921). The article confirmed that the landslide completely blocked the flow of the river, impounding a lake up to 3.7 m (12 feet) deep. The landslide did not damage the railways, as both lines are located on the east side of the Thompson River at this location (Ashcroft Journal 1921).

Subsequent to Wade’s (1979) account, several authors have noted the 1921 landslide, although the location attributed to the landslide has varied, presumably due to the ambiguity of Wade’s (1979) original description. Evans (1984) stated the location of the 1921 landslide to be 2.6 km below Spences Bridge, presumably based on the first interpretation of Wade’s (1979) account. Evans (1986) included the 1921 landslide in his Table 1, and gives the location as “Basque Ranch.” Clague and Evans (1994) also gave the location as “Basque Ranch”, in their Table 2 of historical landslide dams. Clague (1998) gave the location of the landslide as 8 km south of Ashcroft, and suggested that the landslide was predominantly translational in nature and was seated in the clayey glaciolacustrine sediments (unit 2). Clague and Evans (2003) described the location of the landslide as occurring 9 km downstream of Ashcroft, on the west bank of the Thompson River, as shown on their Figure 2. They misstate the date of the

landslide, however, as August 21, 1921. In their Table 1 on the same page, Clague and Evans (2003) correctly stated the date of the landslide as August 13, 1921, but gave the location as “South of Spences Bridge.” Septer (2007) also made note of the August 13, 1921 landslide, giving the correct location as “near the Hammond Ranch at Basque, 6 mi. (9.6 km) south of Ashcroft”, referencing the Ashcroft Journal (1921), Evans (1986), and Clague and Evans (1994).

Stanton’s (1898a) report and Cambie’s (1895) letter pre-date the 1921 landslide, and it is therefore not depicted on either of their maps of landslides along the Thompson River Valley. Several other authors (BGC Engineering Inc. 2012; Ryder 1976; Bishop 2008; Clague and Evans 2003; Clague et al. 1987; Clague 1998), however, have included Landslide No. 8 on their maps of the Thompson River Valley south of Ashcroft, in agreement with the location shown on Figure 3.1. The 1921 landslide has been interpreted by several authors (Clague and Evans 2003, Bishop 2008) to represent a rapid earth flow, presumably based on the fact that it completely dammed the Thompson River. BGC Engineering Inc. (2012) also described the 1921 movement as a very rapid flow slide, based on unpublished CPR documentation. Based on field inspection and an examination of the 1928 air photos, I interpret the mode of movement to be a rapid compound translational slide, as described in Chapter 5. The Ashcroft Journal (1921) reported that, following the initial movement, “during the afternoon the ground was still falling down at intervals.” This manner of initial subsidence followed by ongoing, lesser cave-downs, is consistent with a compound translational landslide comprising the rapid descent of the active block, followed by ongoing outward movements at the steep backscarp and stress redistribution within the slide mass. Based on stereo examination of aerial photos from 1928 and 2015, I estimated the maximum rate of river erosion at the base of the Red Hill slide to be approximately 0.3 m/year, which is in agreement with Morgenstern’s (1986) estimate of river erosion at the Goddard slide, underscoring the potential similarities between these two rapid 20th century slope movements.

I am not aware of any contemporary reports concerning reactivation of Landslide No.8; however, this lack of reporting is probably related to the fact that the landslide has not affected any railway infrastructure (located on the opposite side of the river), and therefore any

ongoing, slow movements of the slide material would likely pass unnoticed. Based on InSAR data for the period of 2013-2016, Journault et al. (2016) found the toe area of Landslide No.8 to be moving at a downslope rate of approximately 25 mm/year, likely as the result of active river erosion of the displaced material.

Landslide No. 8 is visible on the 1928 aerial photos, at which time minor constriction of the Thompson River resulting from the landslide and temporary dam of 1921 still appears to be evident; active irrigation of the upland area is visible to the southwest of the fresh-looking backscarp of the landslide. The occurrence of Landslide No.8 in August, at the height of summer, supports Wade's (1979) notion that irrigation contributed to the landslide in some way; however, the narrative of the Ashcroft slides being the result of irrigation was well-entrenched by 1921, and may have obfuscated other contributing factors. In addition to the deleterious effects of ditch-and-furrow irrigation, it is possible that the natural river erosion at the base of the slope was accelerated in the preceding years by the rock groynes constructed below the South slide (immediately to the north on the opposite bank) and the recent construction of the CN railway on the opposite bank (completed 1915).

3.2.9. Landslide No.9 (Barnard)

Little is known of the history of Landslide No.9 (Barnard slide). BGC Engineering Inc. (2012) suggested the landslide occurred between 1877 and 1895 (referencing BGC Engineering Inc. (2005)). Bishop (2008) suggested the Barnard slide was prehistoric (occurring up to several thousand years before present), and was reactivated between 1877 and 1895. Cambie's (1895) map depicts a large slide at the approximate location of the Barnard slide (denoted Landslide No.6 on Figure 3.4), likely encompassing both the Barnard slide and the Nepa slide to the south. Although Cambie (1895) did not provide any specific description of the slide, its inclusion in his figure suggests that it occurred sometime post-1877 (as stated in his letter), and prior to the time of writing (January 2, 1895). The date of the Barnard slide in Table 3.1 is therefore given as between 1877–1894.

The Barnard landslide is not depicted on Stanton's (1898a) landslide map of the Thompson River Valley south of Ashcroft; it is, however, shown on more recent maps by several other authors (BGC Engineering Inc. 2012; Bishop 2008; Clague and Evans 2003; Clague et al. 1987; Clague 1998), as well as on Ryder's (1976) map, where it is lumped together with the adjacent South and Nepa slides. Eshraghian et al. (2005) unfortunately mislabelled the Landslide No.10 (Nepa) as the "Barnard Slide" on their Figure 1, which may lead to some confusion in terminology. This is repeated in Figure 2.1 of Eshraghian's (2007) thesis.

Bishop (2008) described the Barnard slide as most likely a rapid flow, while BGC Engineering Inc. (2012) suggested it represents a compound translational/rotational slide of unknown velocity, with which I am inclined to agree. The Barnard slide is visible on the 1928 air photos—its subdued morphology is consistent with the lack of any reported movements since Cambie's (1895) documentation of it in the late 1800's. However, due to its location on an upper terrace above the railway lines and its lack of impact on the railway infrastructure, it is quite possible that undocumented slow movements or reactivations of the disturbed slide mass may have gone unnoticed. Based on InSAR data from 2011-2016, Journault et al. (2016) estimated the Barnard slide to be creeping at a downslope rate of approximately 10 mm/year. Whether the origins of the Barnard landslide are related to ditch-and-furrow irrigation of the late 1800's, or stem from more ancient river downcutting on a now-abandoned terrace remains unclear. It is also possible that the movements at the Barnard slide are related to Landslide No.10 (the Nepa landslide), located immediately downstream.

3.2.10. Landslide No.10 (Nepa)

There is a paucity of information concerning the origins of Landslide No.10 (the Nepa slide). The landslide is delineated on landslide maps of the Thompson River Valley south of Ashcroft by several authors (BGC Engineering Inc. 2012; Bishop 2008; Clague and Evans 2003; Clague et al. 1987; Clague 1998), as well as on Ryder's (1976) map, where it is lumped together with the South and Barnard slides to the north, and Cambie's (1895) map, where it appears lumped together with the Barnard slide to the north. Stanton (1898a) also depicted the Nepa slide on his landslide map of the Thompson River Valley south of Ashcroft, although the shape

of the landslide shown does not extend as far upslope as seen on the more recent landslide maps, and visible on the 1928 air photos. It is possible that the slide retrogressed somewhat between the late 1800's and 1928, although this is speculative. Stanton's (1898a) map also depicts an irrigated field located on the benchland above the location of the Nepa slide.

BGC Engineering Inc. (2012) suggested the landslide originated as an extremely rapid flow slide which occurred between 1877 and 1895, (referencing BGC Engineering Inc. (2005)). Bishop (2008) concurred that the slide occurred between 1877 and 1898 as a rapid earth flow. Cambie's (1895) map depicts a rather large slide at the approximate location of the Nepa slide, probably encompassing both the Nepa slide and the Barnard slide to the north. Although Cambie (1895) did not provide any specific description of the slide, its inclusion in his figure suggests that it occurred sometime post-1877 (as stated in his letter), and prior to the time of writing (January 2, 1895). The date in Table 3.1 is therefore given as between 1877-1894.

Landslide No.10 is mislabelled as the "Barnard Slide" on Figure 1 of Eshraghian et al. (2005), and on Figure 2.1 of Eshraghian (2007), with both figures giving the name "Nepa" to Landslide No.12 (Basque). Therefore, when Eshraghian et al. (2005) referred to reactivations of the Nepa slide in 1977 and 1997, it is clear from their Figure 1 that they were referencing Landslide No.11 (the CN/CPR Nepa Crossover slide). Table 3.1 therefore attributes these two reactivations to the CN/CPR Nepa Crossover slide (Landslide No.11). Given this conflation of names, both BGC Engineering Inc. (2012) and Bishop (2008) noted Landslide No.10 to have been active in February 1977 and Fall 1997, citing Eshraghian (2007) and Porter et al. (2002). Porter et al. (2002) stated that in February 1977 and Fall 1997, a landslide of approximately 6 hectares in areal extent was reactivated at the location of the CN/CPR Crossover in the Basque/Nepa area (presumed to have developed in the late 1800's). The location of the Nepa Crossover slide is shown in BGC Engineering Inc.'s (2012) Figure 01, corresponding to the location given for Landslide No.11 on Figure 1 above (its position is incorrectly depicted on Porter et al.'s (2002) Figure 2).

The Nepa slide is visible on the 1928 aerial photos. The appearance of the slide is hummocky and appears to have been more recently active compared to the adjacent Barnard slide. The

Nepa slide is located on an outside bend of the Thompson River and as such, would be subject to ongoing river erosion at its toe. I did not observe any evidence of irrigation in the immediate vicinity of the Nepa slide in the 1928 aerial photos. Given the general lack of information on the origins of Landslide No.10, I am inclined, based on stereo aerial photo interpretation, to categorize it as a compound translational landslide as indicated in Table 3.1. The Nepa landslide is traversed by both the CN and CP railway lines.

3.2.11. Landslide No.11 (CN/CPR Nepa Crossover)

Landslide No.11 (CN/CPR Nepa Crossover) is located approximately 600 m to the south of the Nepa slide on the east bank of the Thompson River; the southern flank of the landslide coincides with an unnamed intermittent stream (BGC Engineering Inc. 1998). Little is known of the origins of Landslide No.11.

Landslide No.11 is plotted on Stanton's (1898a) landslide map of the Thompson River Valley south of Ashcroft, and on this basis is presumed to have occurred prior to 1898, as indicated in Table 3.1. Stanton (1898a) also depicts an irrigated field above Landslide No.11, although it is located approximately 1.6 km (1 mile) upslope of the landslide. The omission of Landslide No.11 from Cambie's (1895) map could suggest that the landslide occurred between 1895-1898. The location of Landslide No. 11 was also mapped by BGC Engineering Inc. (2012); it is, however, absent from Ryder's (1976) and Bishop's (2008) landslide maps, and is south of the area captured on maps by Clague and Evans (2003), Clague (1998) and Clague et al. (1987). It should be noted that the location of the CN/CPR Nepa Crossover slide is incorrectly shown on Porter et al.'s (2002) Figure 2, with its correct position given in BGC Engineering Inc. (2012) Figure 01, corresponding to the location shown on Figure 3.1. Landslide No. 11 is visible on the 1928 aerial photos; its subdued morphology may be indicative of ancient origins. I did not observe any evidence of irrigation in the immediate vicinity of Landslide No. 11 in the 1928 aerial photos.

In 1998/1999, CN and CP undertook the construction of a railway crossover near the Basque/Nepa area, approximately 10 km south of Ashcroft (Porter et al. 2002). During the

site investigation for the crossover design, fresh tension cracks were identified upslope of the rail grade near the southern limit of Landslide No.11 (BGC Engineering Inc. 1998, Porter et al. 2002). Porter et al. (2002) recorded that the CN/CPR Nepa Crossover slide was reactivated in February 1977 and Fall 1997, as indicated in Table 3.1. Eshraghian et al. (2005) also referred to reactivations of Landslide No.11 in 1977 and 1997; (it should be noted that they referred to Landslide No.11 as the “Nepa” slide, rather than the CN/CPR Nepa Crossover slide). In keeping with the nature of the landslide reactivations which occurred in the corridor during the later 1900’s, these are assumed to represent extremely slow or very slow translational movements. Porter et al. (2002) noted that a toe berm and riverbank armoring were incorporated into the final crossover design to improve stability and limit the potential for future river erosion.

3.2.12. Landslide No.12 (Basque)

Landslide No.12, the Basque slide, is located immediately south of the CN/CPR Nepa Crossover slide; the two features are separated by an intermittent stream located at approximately CP Thompson Subdivision track mileage 55.0 (CN Ashcroft Subdivision track mileage 57.4). The location of the Basque slide was mapped by Eshraghian (2007), Eshraghian et al. (2007), BGC Engineering Inc. (2012), Bishop (2008). Landslide No.12 is not shown on Stanton’s (1898a), Cambie’s (1895) nor Ryder’s (1976) landslide maps of the Thompson River Valley south of Ashcroft, and is south of the area captured on maps by Clague and Evans (2003), Clague (1998) and Clague et al. (1987).

Eshraghian et al. (2007) noted that the most recent retrogressions of the Basque slide occurred before the construction of the CP railway in 1885. The absence of the Basque slide, however, from Stanton’s (1898a) and Cambie’s (1895) landslide maps would seem to contradict this assessment. Notwithstanding, the date of Landslide No.12 has been given as pre-1885 in Table 3.1. BGC Engineering Inc. (2012) did not indicate a date for the original movement. Bishop (2008) suggested Landslide No.12 may be a prehistoric feature, having occurred up to several thousand years before the present, which may explain why Stanton (1898a) and Cambie (1895)

did not recognize the slide as such. The Basque slide is clearly visible on the 1928 air photos; no irrigation is visible in the immediate vicinity.

BGC Engineering Inc. (1998) observed that the Basque slide showed no signs of recent activity during 1997 field traverses for design of the proposed CN/CPR Nepa Crossover. However, in Figure 3 of Eshraghian et al. (2008) and Figure 4.2 of Eshraghian (2007), it is shown that the “Basque” slide was reactivated in 1977 and 1997; I presume that these reactivations are correctly attributed to the CN/CPR Nepa Crossover slide immediately to the north (Landslide No.11), in accordance with Eshraghian et al. (2005), Porter et al. (2002) and BGC Engineering Inc. (1998), and as indicated in Table 3.1. Based on InSAR data from 2011-2016 Journault (2016) did not observe any coherent indications of movement at the Basque slide.

Eshraghian et al. (2007) and Bishop (2008) characterized the Basque slide as a translational movement. BGC Engineering Inc. (2012) characterized the movement as a compound translational/rotational slide (referencing BGC Engineering Inc. (2005)). Eshraghian et al. (2007) estimated the volume of the Basque slide to be approximately 1.8 Mm^3 . Based on four boreholes advanced by BGC Engineering Inc. (1998) for the design of the proposed CN/CPR Nepa Crossover, Eshraghian et al. (2007) presented a schematic cross-section of the Basque slide, extrapolating a single, planar surface of rupture located in the glacio-lacustrine clay and silt unit 2.

3.2.13. Landslide Near Spences Bridge

On August 13, 1905, a catastrophic landslide occurred on the west bank of the Thompson River 40 km downstream of Ashcroft, just south of the village of Spences Bridge. The slide killed at least 15 Salish aboriginals who had a settlement (“rancherie”) on the lowermost terrace on the opposite side of the river. This landslide, though located outside of the study area, is significant due to its potential similarities to the North slide, as articulated in Chapter 5. The 1905 landslide near Spences Bridge is also significant due to the number of casualties involved, and the complete damming of the Thompson River and reported displacement wave which ensued as a result of the slide. The displacement wave associated with the Spences Bridge slide is a

phenomenon not mentioned in accounts of the Ashcroft slides to the north. However, unlike the slides near Ashcroft, many of which occurred at night, the 1905 Spences Bridge landslide occurred in the middle of the day and was witnessed first-hand by many people. The lack of displacement waves in descriptive accounts of the Ashcroft slides may simply be due to a lack of eye-witnesses. The 1905 landslide near Spences Bridge remains one of Canada's deadliest landslides (Evans 2000), and an event on the Thompson River which should not be forgotten when seeking to objectively evaluate future landslide risk in the corridor. It is described in detail below.

At 3:20 pm on Sunday, August 13, 1905, a catastrophic landslide occurred on the northwest bank of the Thompson River at the mouth of Murray Creek, about 1 km southwest of the village of Spences Bridge, 40 km downstream of Ashcroft (Daily Ledger 1905, Daily Colonist 1905a, Wade 1979). The rapid landslide and resulting displacement wave killed at least 15 Salish aboriginals who had a settlement on a low flat opposite the slide—twelve more were reported injured; there were reportedly thirty houses in the encampment, all of which were destroyed (Daily Ledger 1905, Daily Colonist 1905a).

An initial newspaper report described the slide as follows: “Just after 3 o'clock there was a rumble from the mountain side and three minutes later it was all over. A few of the natives ran down along the river when they saw the slide approaching, but no more than seven or eight got away. ... The main slide covered the centre of the village with forty feet of rocks and trees” (Daily Colonist 1905a). The slide occurred just as the CPR's Atlantic express passenger train was approaching Spence's Bridge, and so was seen by numerous eye-witnesses; a passenger on the train described the slide to the *Daily Colonist* newspaper as follows (Daily Colonist 1905b):

“The towering bluff on the north side of the Thompson river, about 200 feet high, suddenly became detached and swept down into the river. The river is a quarter of a mile wide at this point, and the banks are about 40 feet high, but the channel was completely filled up with the mass of earth and debris that came down. The Indians had not a moment of warning, and many were buried with their buildings. The force of water was so terrific that the railway track, although nearly 100 feet above the bed of the river and 400 feet from the channel, was covered with mud and debris. There are water marks high up on the hill above the track. ...Just as the Atlantic express approached the spot, a vast cloud of dust was observed rolling down the bluff toward

the river, marking the course of the slide. As it reached the water, the spray and debris were flying right by, the terrific force affording an awful spectacle and one rarely witnessed by so many people. The huge slide swept on the rancherie without a moment's notice and with no warning sound, the dry earth rolling silently and rapidly save for a "munching" sound that could be heard above the roar of the train." (p. 2)

The landslide produced a "tidal wave" which was responsible for many of the fatalities (Daily Colonist 1905a). A displacement wave 10 to 15 feet (3 to 4.6 m) high swept across and up the river, destroying everything in its path, including the Anglican Church at the aboriginal settlement, and drowning 10 people—five more were buried in the slide debris (Daily Ledger 1905, Drysdale 1914, Evans 1992, Clague 1998); the elderly Chief Lillooet was among the dead (Clague et al. 1987, Clague 1998). Drysdale (1914) reported that the force of the wave was sufficient to carry a granite and marble headstone 200 yards (183 m) from its original location, while a horse tied to a hitching post had its rope broken and was carried upstream 300 yards (274 m). The church was lifted and carried 100 yards (91 m) by the impact of the water, and reduced to "kindling wood" (Daily Ledger 1905). The slide dammed the Thompson River for five hours to a depth of approximately forty feet before the waters overtopped the debris; flooding of lower-lying properties occurred upstream as a result of the temporary dam (Daily Ledger 1905, Daily Colonist 1905a, Evans 1984, Clague 1998). Septer (2007) stated the aboriginal village had a population of approximately 100 Salish people, and that the slide occurred about 10 minutes after most of the inhabitants had left the church service; had the slide occurred 10 minutes earlier, the death toll would have undoubtedly been much higher. The aboriginal village was located on the east bank of the Thompson River, near the bank yet sufficiently elevated above the high-water level; on a higher bench on the same side of the river was the railway station and the nearby town of Spences Bridge (Wade 1979). The course of the Thompson river was altered by the slide, earth being piled high in the center of the old channel; the CPR track was undamaged, but the train was stopped for half an hour at the scene (Daily Colonist 1905b). The landslide occurred during the salmon run, and thousands of salmon were stranded in shallow water by the slide (Daily Colonist 1905b, Wade 1979).

The 1905 event was preceded by at least two other landslides that occurred near the same location, but did not produce any fatalities (Daily Colonist 1905a, Drysdale 1914, Wade 1979, Evans 1984). Evans (1984) and (1992), Clague (1998) and Clague and Evans (1994) and

(2003) reported these precursory events occurred on August 1, 1880 and December 31, 1899, both landslides partially damming the Thompson River. Septer (2007) also reported a landslide occurred at Spences Bridge on December 31, 1899, and a large landslide occurred on August 1, 1880 at Cook's Ferry near Spences Bridge, though some of the information he presents is conflated with details from the North Slide of 1880. An article in the August 19, 1880 edition of the *Daily British Colonist* (1880a) confirmed that a landslide of "unusual magnitude" occurred near Cook's Ferry about three weeks prior: "A huge mass of Shawnikan mountain was suddenly observed to be moving and without a moment's warning thousands of tons of earth and rock were precipitated into the channel of Thompson river. So violent was the decision that not only was the course of the river impeded but a large portion of the flat on the opposite covered by the slide." This slide also occurred during the salmon run, as it was reported that numerous fish were washed out of the river by the displacement, the aboriginal people saving and drying them for consumption (Daily British Colonist 1880a). The *Daily Colonist* article of August 14, 1905 stated that similar slides occurred in 1882 and 1897, but were not attended by loss of life (Daily Colonist 1905b). Wade (1979) provided medical assistance to the victims of the 1905 slide, and recorded that previous slides had occurred on December 31, 1899, and in 1877, saying "Twice before, there had been slides from that same place but they had gone far from the village" (p. 122). Clague (1998) stated a small slide took place at the same location on January 1, 1905, though it may be he is conflating the events of December 31, 1899 and August 13, 1905. Whether these dates all represent separate events at the same location, or at other locations in the near vicinity is unclear. Following the devastating 1905 slide, the aboriginal village was rebuilt on higher ground, away from the river (Wade 1979). A contemporary photograph of The Anglican Church of St. Michael and All Angels, rebuilt about 1906 (Veillette and White 1977), is included as Figure 3.8 below.

Officials of the CPR engineering department attributed the cause of the 1905 landslide (and its predecessors) to irrigation on the bench lands above; apparently the aboriginal people had been "pouring large quantities of water on these bench lands in order to get a heavy second crop of hay, and this unusual amount of moisture undoubtedly caused the catastrophe" (Daily Colonist 1905b). Citing unpublished notes by H.J. Cambie, consulting engineering to the CPR, Clague (1998) and Evans (1992) noted that the 1880, 1899 and 1905 slides were thought to be Cambie

to have been caused by irrigation of the benchland behind the slide; a wide irrigation ditch behind the 1905 landslide was noted by Cambie to be “the cause of the trouble” (Clague et al. 1987). Ryder (1981) noted that the 1905 slide occurred after a period of heavy rainfall when the adjacent Murray Creek was in flood; she also confirmed that irrigation was practiced on the delta-terrace at this time, and undoubtedly excess water percolating into the silt from one or all of these sources contributed to the slope instability. Clague et al. (1987) cautioned that landslides in the Spences Bridge area, as at Ashcroft, have also occurred on slopes that have never been irrigated, in materials with a long history of instability.

Similar to the landslides near Ashcroft, the 1905 Spences Bridge landslide occurred in Pleistocene sediments dominated by a glacio-lacustrine silt unit; a pre-existing shear zone 1- to 13-cm-thick is located near the base of the silt unit (Clague et al. 1987, Clague 1998). The slide debris occupies an area 1300 m wide by 1000 m long, comprising an irregular mass of hummocky silt and gravel in front of a steep slide scar (Ryder 1981). The outward-sloping basal contact of the lacustrine silt is underlain by deltaic gravels (Ryder 1981). Several other landslides in Quaternary materials are present in the Thompson River Valley southwest of Spences Bridge, as identified in Clague (1998) and Ryder (1981); some of these may represent historical/ancient landslides which occurred as a result of river downcutting and the presence of this pre-existing shear zone at depth.

The Spences Bridge landslide is clearly visible on the 1928 aerial photos (Figure 3.9); the tortuosity of the river at this location as a result of the slide can be clearly seen. A composite aerial photo of the landslide in 2015 is shown in Figure 3.10; while the diverted course of the river is still evident, the angle of the river channel diverted by the slide has softened somewhat. A photo of the slide area taken in November 2015 is included as Figure 3.11 below. I am not aware of any evidence to indicate the slide has been active since the catastrophic 1905 event; it would appear that the 1905 slide resulted in the destruction of all the arable agricultural land above it. The current presence of a house at the base of the landslide (Figure 3.11) would suggest that the area is now stable, perhaps further corroborating the interpretation of the historic 1905 landslide as being caused by ditch-and-furrow irrigation, rather than by an ongoing, natural process. Similar to the North Slide of 1880, I surmise that the 1905 Spences

Bridge landslide involved the extremely rapid remobilization of previously disturbed (contractant), water saturated deposits, in the form of a complex earth slide-debris flow, the mechanics of which are more fully articulated in Chapter 5.

3.3. Conclusion

The Thompson River Valley south of Ashcroft has a storied history from both a geologic and anthropogenic perspective. Twelve large landslides have been identified in the 10-km reach south of the village of Ashcroft, as presented in Figure 3.1. Substantial changes in land use along the naturally semi-arid terraces of the Thompson River Valley occurred with European settlement of the area following the Cariboo gold rush of the mid-1800's. Flooding of the upland areas by ditch-and-furrow irrigation in the mid- to late-1800's probably served as the catalyst for dramatic landslides along these valley walls that were geologically predisposed to failure. The earliest documented landslide, the South slide, occurred between 1865 and 1877; this was followed by at least six (probably rapid) landslides recorded in the corridor between 1865 and 1898. The only reported rapid slope movements of the 20th century were the Red Hill Landslide of 1921 and the Goddard Landslide of 1982. The cluster of rapid slope failures which occurred in the late 1800's, coincident with the introduction of irrigation, and in an overarching dry climate regime (as will be described in the following chapter), suggests that many of these were indeed related to irrigation of the terraces by primitive methods.

Notwithstanding the connection between the historic landslides and primitive irrigation methods, the CN 50.9 landslide of 1897 occurred in the absence of any nearby irrigation indicating that other factors, including river erosion, served to undermine the stability of the valley walls and will continue to present future risk to the corridor. From an examination of historic (1928) aerial photographs and consideration of original written accounts, most of the landslides appear consistent with compound translational slope movements of moderate to rapid velocity; many were likely reactivations of ancient landslides. I have argued that the largest, the North slide, was a unique mode of failure, and probably represented a complex earth slide-debris flow; it was preceded by the breaching of a nearby irrigation reservoir, and was the most mobile of all the landslides, fully damming the Thompson River for nearly two

days. It may have been of a similar nature to the 1905 landslide which occurred south of the village of Spences Bridge, approximately 40 km downstream, which created a displacement wave in the river and resulted in 15 deaths.

Presently, remote sensing indicates that the twelve landslides identified on Figure 3.1 are either inactive or very/extremely slow moving. Notwithstanding the evolution in irrigation methods, rapid renewals of movement are likely to continue to occur periodically in the corridor, which are of concern to multiple stakeholders from a risk management perspective. The most recent rapid landslides may have been partly affected by irrigation, but cannot be solely attributed to it: the CN 50.9 landslide of 1897, the Red Hill landslide of 1921, and the Goddard landslide of 1982. As such, in addition to the very/extremely slow slope movements which must be addressed by ongoing railway maintenance, I would suggest that rapid renewals of movement pose future risk to the corridor. The following chapters will investigate relationships between the slope reactivations and regional climate factors, and contextualize the historic movements within a contemporary understanding of landslide processes, leading to an integrated strategy for effective risk management and infrastructure resilience in the Thompson River Valley south of Ashcroft.

Table 3.1: Recorded movements of large landslides in the Thompson River Valley within approximately 10 km south of Ashcroft. The number assigned to each landslide in the table corresponds to the location shown on Figure 3.1.

#	Landslide Name	Dates of Recorded Movement	Estimated Rate of Movement	Probable Mode of Movement	Current State of Activity	Approx. Volume (Mm ³)	Ref.
1	CN 50.4	Unknown (possibly ancient)	Unknown	Unknown	Inactive, possibly relict	—	a,b
2	CN 50.9	1897 (September 22)	Probably Rapid	Compound earth slide	Inactive, stabilized	—	a,b,c,d,e,f,g,h
		1921	Probably Extremely Slow			—	i
		1948	Probably Extremely Slow			—	i
		1972 (Fall)	Extremely Slow			3	a,c,e,i
		1977 (Winter)					a,c,e,i
		1997					a,c,d,i
		1999					i
2000 (Fall)	a,c,e,j						
3	Unnamed	Between 1886–1894	Unknown	Unknown	Inactive	—	a,k,l
4	Goddard	1886 (October 19)	Probably Rapid	Compound earth slide	Reactivated	>3	a,b,c,d,e,g,k,l
		1974	Very Slow			—	c,d
		1976 (October)	Rapid			—	a,c,d,e
		1982 (September 24)				2	a,b,c,d,e
5	CN 53.4 / CN 53.7	Between 1877-1894, Possibly 1880	Unknown	Unknown	Inactive, possibly abandoned	—	a,e,k,l
6	North	1880 (October 14)	Very Rapid	Complex earth slide-debris flow	Reactivated	15	a,b,d,e,f,h,k,l,m,n
		1997	Extremely Slow			21	c,d
		2000 (October)	Very Slow			a,c,d,e	
7	South	Between 1865-1877	Probably Rapid	Compound earth slide	Main body inactive, repaired; southern flank reactivated	—	a,e,d,g,k,l
		1894	Probably Slow/ Moderate			—	o
		1977 (Winter)	Very Slow			9	a,c,d,e,p
		1997 (Fall)	Very Slow				a,c,d,e,p
		1999	Probably Very Slow				c
8	Red Hill/ Hammond Ranch	1921 (August 13)	Rapid	Compound earth slide	Reactivated	—	a,b,m,n?,f,h?,l,p,q
9	Barnard	Between 1877–1894	Probably Rapid	Compound earth slide	Reactivated	—	a,k,p
10	Nepa	Between 1877–1894	Probably Rapid	Compound earth slide	Inactive	—	a,g,k
11	CN/CPR Nepa Crossover	Pre-1898	Probably Rapid	Compound earth slide	Inactive	—	e,g,p
		1977 (February)	Probably Very Slow				e,c?
		1997 (Fall)	Probably Very Slow				e,c?
12	Basque	Unknown, pre-1885	Unknown	Unknown	Inactive, possibly relict	2	a,d,p

- | | | |
|-----------------------------|---------------------------|--------------------------------|
| a. Bishop (2008) | g. Stanton (1898a) | m. Evans (1986) |
| b. Clague and Evans (2003) | h. Wade (1979, p.120-123) | n. Evans (1984) |
| c. Eshraghian et al. (2008) | i. Keegan et al. (2003) | o. Stanton (1898b) |
| d. Eshraghian et al. (2007) | j. Kosar et al. (2003) | p. BGC Engineering Inc. (2012) |
| e. Porter (2002) | k. Cambie (1895) | q. Ashcroft Journal (1921) |
| f. Septer (2007) | l. Ryder (1976) | |

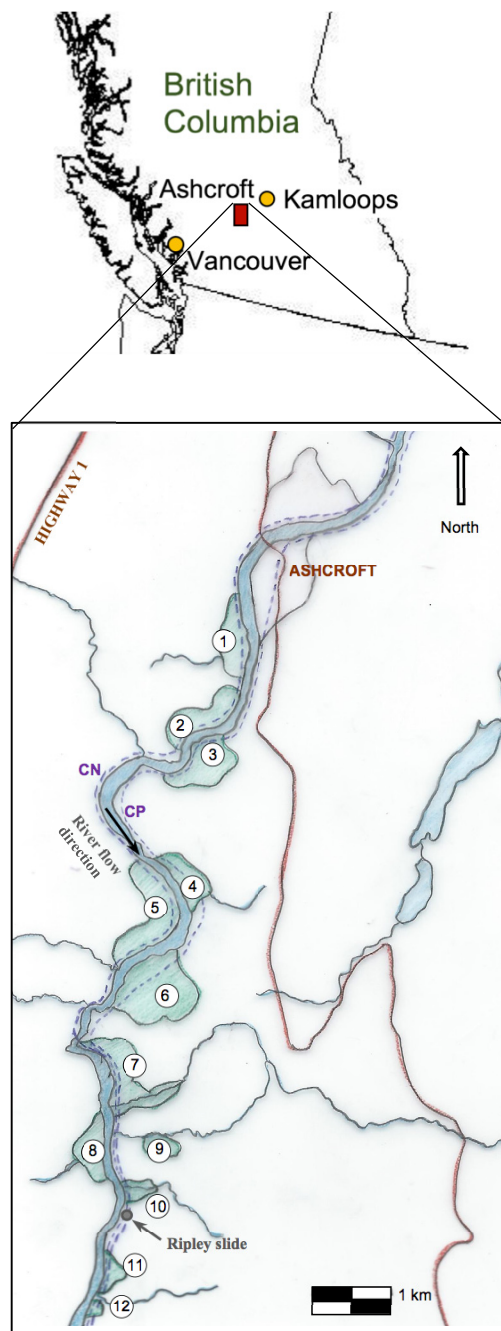


Figure 3.1: Map of the study area showing large landslides along the Thompson River Valley within approximately 10 km south of the village of Ashcroft (BC map modified from www.worldatlas.com). The number assigned to each landslide in the figure corresponds to Table 3.1.

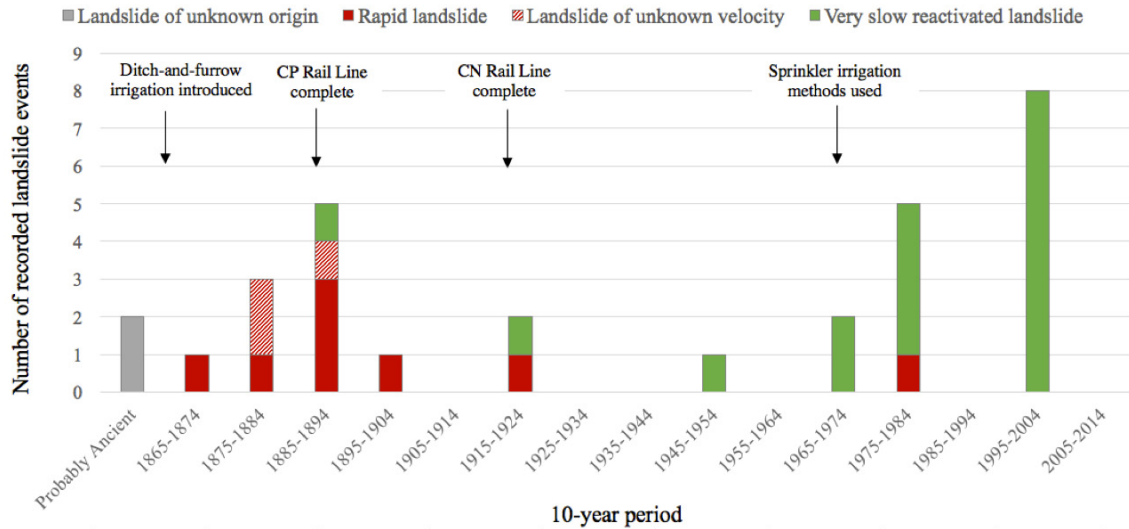


Figure 3.2: Timeline of recorded landslide events.



Figure 3.3: Cambie [...] & survey party. Caption reads: "The first expedition sent out to explore the Northern British Columbian passes thro' the Rockies for the Canadian Pacific Railway. Photo taken by Cambie at Fort McLeod- 1879 I was [laid?] off by the H.B.Co. as guide to the party. HBW. This route was finally abandoned for one further south." (Bullock-Webster 1879). Reproduced with permission.

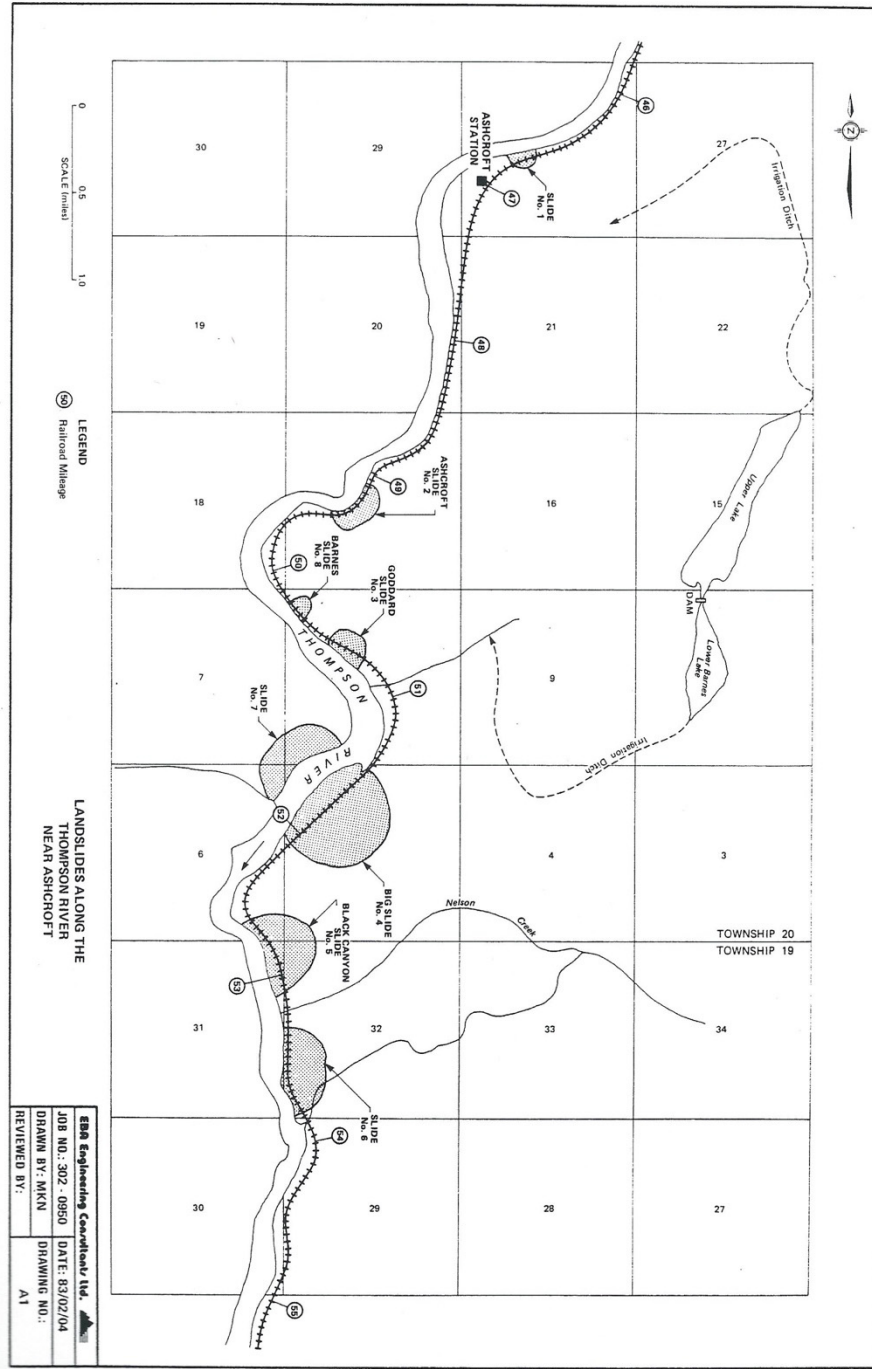


Figure 3.4: Cambie's (1895) map of landslides in the Thompson River Valley south of Ashcroft (as reproduced by EBA Engineering (1984)).



Figure 3.5: Stanton's (1898a) map of landslides in the Thompson River Valley south of Ashcroft.



Figure 3.6: 2015 aerial photo of the Goddard landslide on the east bank of the Thompson River (courtesy of CN rail); shaded area corresponds to the limits of the 1982 reactivation (as per Eshraghian et al. (2007)), dashed line delineates broader extents of an older, possibly ancient landslide feature.

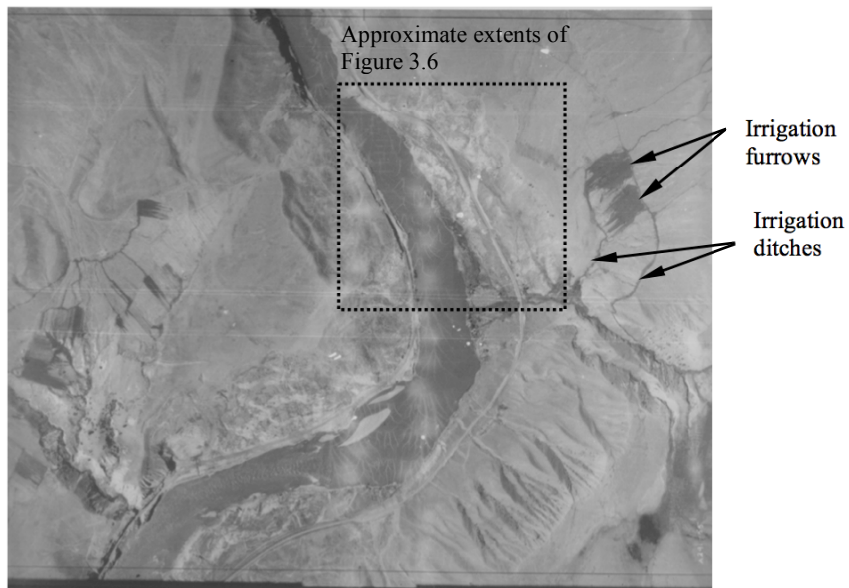


Figure 3.7: 1928 aerial photo showing the Goddard landslide and upslope ditch-and-furrow irrigation (east bank on the outside river bend); NRC roll A291 #55.



Figure 3.8: Photograph of The Anglican Church of St. Michael and All Angels (looking northeast from Highway 1); taken at Spences Bridge, B.C. in November 2015.



Figure 3.9: 1928 aerial photo showing the 1905 Spences Bridge landslide; Natural Resources Canada, Roll A682, No. 8.



Figure 3.10: 2015 aerial photos showing the 1905 Spences Bridge landslide; courtesy of Canadian National Railway.



Figure 3.11: Photograph of the 1905 landslide south of the village of Spences Bridge, B.C. (looking west from Highway 1), taken in November 2015.

4. INFLUENCE OF WEATHER AND CLIMATE ON LANDSLIDE FREQUENCY

“Most people do not differentiate very carefully between weather, climate (average weather over time), and climate variability (variations in weather over time). People confound climate and weather in part because they have personal experience with weather and weather abnormalities but little experience with climate change...”

—IPCC (2014)

4.1. Introduction

Portions of this chapter have been published in the conference paper *Impact of climate variability on landslide activity in the Thompson River Valley near Ashcroft, B.C.* (Tappenden 2016).

This chapter investigates the influences of weather, climate and climate change on the 20th century landslide activity in the Thompson River valley south of Ashcroft, particularly, the roles that weather and climate may play in reactivating and accelerating the slope movements. While the balance of evidence suggests that the rapid landslides which occurred along the Thompson River Valley in the late 1800’s were likely induced by anthropogenic factors (ditch-and-furrow irrigation), I hypothesize the periodic 20th century reactivations of the landslides are related to weather and climate influences, as discussed in the following sections; these may be characterized as triggering factors using the terminology of Popescu (1994). Regional meteorological conditions potentially portending landslide movement, such as depth of snow pack and annual discharge of the Thompson River, are examined.

The hydrologic impacts to the Thompson River basin of high-level climate phenomena including the Pacific Decadal Oscillation and the El Niño Southern Oscillation are also investigated in this chapter. Current climate change predictions for British Columbia, and their potential impacts to snow pack and river flow levels, are discussed in Section 4.8. Given climate change, an understanding of climatic influences on the risk posed by the Ashcroft Thompson River landslides is more relevant today than ever before. While a changing climate

does not, in itself, constitute a hazard, it may substantially affect the frequency of occurrence of hazards that are triggered by weather and climate conditions. This non-stationarity of hazard frequency, and its implications for risk management and resilience, will be explored in subsequent chapters.

4.2. Local Climate of Ashcroft, British Columbia

The interaction of large-scale weather systems with British Columbia's topography produces distinctive climatic patterns that vary with elevation, distance from the coast, exposure to the prevailing winds, and season (Moore et al. 2010). The village of Ashcroft is in the southern Interior Plateau of British Columbia, between the Coast and the Columbia Mountains, as illustrated by Chilton (1981) in Figure 4.1. Ashcroft is located within the low-lying, semi-arid valley of the Thompson River, where deep Quaternary fill has been dissected and terraced by postglacial downcutting (Ryder 1976). The Coast Mountains serve as an effective barrier to the moist westerly air flow, creating a much drier and more continental climate on the Interior Plateau in comparison to the coast (Chilton 1981). Summer temperatures are often higher in the Interior than on the Coast, with the reverse being true for winter temperatures (Moore et al. 2010). In contrast to wet coastal locations, dry interior sites such as Ashcroft have high levels of evaporation that, combined with low summer precipitation, result in a high cumulative moisture deficit (Moore et al. 2010). The landscape of the Thompson-Nicola region contains large tracts of arid ranchland, requiring extensive irrigation the cultivation of a variety of crops (Province of British Columbia 2016a).

A weather monitoring station named Ashcroft North was operational in Ashcroft (lat. 50.73, long. -121.27) for the seven-year period between September 1980 and September 1986. Data are missing from April through August of 1986 (Environment Canada 2015a). Figure 4.2 and Figure 4.3 display the average and annual total precipitation (rain and snow), and the daily maximum, minimum, and average temperature for each month over the limited period of record.

There is a longer period of record for weather conditions (temperature and precipitation) at Spences Bridge, also located in the Thompson River Valley approximately 40 km south of Ashcroft, where Environment Canada maintained a weather station for the 22-year period from 1981-2002 (weather station #1167637, latitude 50.42 N, longitude -121.31) (Environment Canada 2015b). Figure 4.4 displays the average total precipitation (rain and snow), and the daily maximum, minimum, and average temperature for each month over the period of record. The average annual rainfall was 233.3 mm, snowfall 30.4 cm, for a total average precipitation of 263.7 mm at this station (Environment Canada 2015b). An extreme snow depth of 23 cm was recorded at the Spences Bridge station on January 24, 1982 (Environment Canada 2015b). Extreme daily precipitation was 30.5 mm on May 9, 2000, and extreme daily snowfall was 22.0 cm on December 29, 1996 (Environment Canada 2015b). It can be observed from Figure 4.4 that the highest periods of precipitation occur as rain during the months of May, June and July, and as snow during the months of November and December. By comparison with Figure 4.2, it can be seen that daily temperature normals in Ashcroft are similar but cooler than those measured over the longer period of record at Spences Bridge. There is a greater degree of variation in precipitation trends year over year, as evidenced by Figure 4.3, such that the short period of record at the Ashcroft North station differs somewhat from the longer 22-year means at the Spences Bridge weather station.

4.3. Seasonal and Inter-Annual Fluctuations in Thompson River Flow

Eshraghian (2007) identified the importance of the fluctuating Thompson River levels in exacerbating the very slow landslide movements in the corridor south of Ashcroft. In years when the Thompson River level was higher than normal, and remained high for an appreciable period of time, a noticeable increase in movement of one or more of the landslides was observed to occur upon recession of the river, typically in early fall. He plotted the cumulative river level difference from average for each calendar year (as measured upstream of the site at Kamloops), as a means of capturing both the magnitude and duration of the seasonal high water levels. Eshraghian (2007) identified that reported landslide movements between 1970 and 2000 occurred in years when the maximum cumulative river level difference from average was significantly greater than zero, or in the year immediately following.

A year of above-average river discharge may affect the landslides in at least three ways: controlling the degree of saturation at the toes of the landslides; reflecting the overall climate conditions, especially the degree of recharge of the underlying aquifer and the extent of the artesian water pressures acting on the rupture surface; and controlling the amount of erosion occurring at the toes of the landslides. The mechanics of the landslide movements will be discussed in Chapter 5. However, it is worth noting that river flows exceeding certain thresholds may produce sufficient bank erosion to reactivate a landslide, but the landslide itself must also be in a state to be reactivated in its own morphological cycle. This cycle appears to consist of the toe of the landslide pushing out into the river, the landslide colluvium being eroded by the river, and finally river erosion acting on the toe of the landslide itself to facilitate further movement. Therefore, a possible explanation for the paucity of recorded landslide events in the early 20th century may be that sediment from the previous large landslides of the late 1800's was still in the process of being eroded by the river, such that active erosion, even in high-flow years, was not taking place at the toes of the landslides themselves, but rather acting to remove the colluvium of the previous earth slides.

Building on the work of Eshraghian (2007), I obtained archived Thompson River discharge records for the flow monitoring stations near the village of Spences Bridge, approximately 40 km downstream of Ashcroft (Environment Canada 2014). While Eshraghian (2007) examined river level data from 1970-2000, I obtained daily discharge readings (m^3/s) for the Thompson River at Spences Bridge (stations 08LF051 and 08LF022) for the 100 years from November 1911 to December 2011 (Environment Canada 2014); data are missing from hydrologic years 1932, 1933, and 1934. I utilized river flow (discharge) data for this study rather than river level measurements; due to the century-long length of record, the river level at Kamloops contains a downward trend in the average due to ongoing river downcutting, while the average river flow data at Spences Bridge is more stable in this regard. Moreover, the Kamloops river monitoring station is located upstream of Kamloops Lake, a body of water which has a significant attenuating effect on the downstream flow; river data downstream at Spences Bridge is likely more representative of the subject site in this regard (D. Campbell, personal communication 2016).

I retrieved the archived Spences Bridge daily discharge data and calculated daily average flow values for each measurement station over their respective periods of record (Station 08LF022: 1911-1951, and Station 08LF051: 1952-2011). As Station 08LF022 was located upstream of the contemporary Station 08LF051, the two sets of records were treated as separate domains, with separate daily flow averages calculated. Assuming the daily measured discharge rate to be reasonably representative of the 24-hour period, the cumulative daily discharge (m^3) was calculated and compared to the average daily value for each day of the year. In order to better contextualize the results, the volume of daily flow (in millions of cubic meters) was plotted, rather than the measured daily flow rate (m^3/s). Figure 4.5 displays the cumulative river flow departure from average (in millions of cubic metres) since 1913, along with the number of large landslides showing a noticeable increase in their rate of movement between 1970 and 2000, as listed in Table 3.1. It can be observed that the landslides are most likely to demonstrate an increased rate of movement in years when the cumulative river flow rises sharply compared to average conditions. The average annual river discharge at Spences Bridge is approximately $24,400 \text{ Mm}^3$ (Environment Canada 2014); it was $23,451 \text{ Mm}^3$ at station 08LF022, and $24,358 \text{ Mm}^3$ at station 08LF051 over their respective periods of record.

The powerful aspect of relating landslide activity to river flow levels is that there exists a much longer record of river flow data compared to the landslide movement records. Nearly-complete daily river discharge measurements are available for the Thompson River near Spences Bridge for the past 100 years. These flow measurements provide insight into a century of climate conditions, which may serve as a proxy for estimating the frequency of landslide reactivations back in time. Figure 4.6 shows the cumulative river flow difference from average for each hydrologic year (October of the previous year to September of the year indicated), based on the daily Thompson River discharge measurements near Spences Bridge. This is the algebraic summation of the daily flow departures from normal over the entire hydrologic year (as calculated from the daily flow rates measured at Spences Bridge). The dashed line in Figure 4.6 represents a potential threshold value of $3,400 \text{ Mm}^3$, which when exceeded, has historically portended landslide activity in the corridor.

When the annual cumulative Thompson river flow difference from average exceeds 3,400 Mm³ (or approximately 14% above average annual flow), the large landslides in the corridor have historically displayed a noticeable increase in their rate of movement in that fall (or the winter immediately following, as in 1977). The year of highest flow departure from normal over the period of record was 1999 (36%), closely followed by 1997 (35%). Moreover, it can be observed that the potential threshold criterion of 3,400 Mm³ has been exceeded 15 times in the 96 years of record between 1913 and 2011 as indicated in Table 4.1 (river flow data was not recorded in years 1932, 1933 and 1934). This is equivalent to a likelihood of occurrence of approximately 15.6% or a 1:6.4 event. The threshold criterion of 3,400 Mm³ captures 14 of the 17 landslide events (82%) shown on Figure 4.6.

The three landslides not captured by the criterion all occurred in the winter of 1976/77; this winter was associated with a dramatic shift in the North Pacific climate conditions with widespread implications; this event was subsequently described as a “regime shift” of the Pacific Decadal Oscillation and is discussed in Section 4.5 below. The 3,400 Mm³ threshold criterion was exceeded in five years when no landslides were recorded: 1928, 1935, 1954, 1960, 1968 and 1996. Whether the lack of reported landslides in these years represents a lack of slope movements or a lack of record keeping is difficult to ascertain, as they are primarily pre-1970, when, according to Eshraghian et al. (2005), railway records of slope movements were not reliably maintained. While further research is needed to verify the validity of the threshold, it demonstrates the value of utilizing the Thompson River flow records as a potential proxy for estimating the frequency of historic landslide events in the corridor, and potentially as a tool for forecasting future landslide activity.

4.4. Annual Basin-Wide Snow Pack

Many rivers in western North America are dominated by snowmelt runoff, to the extent that snow survey programs collect snow data for spring and summer water supply forecasting (Cayan 1996). An article appearing in The Daily Colonist newspaper in 1907 anecdotally correlated the Thompson River flow to the regional snow pack (Daily Colonist 1907):

“There is much speculation as to whether traffic on the C.P.R. will suffer interruption from floods this season. Should a warm wave come suddenly, it is anticipated that damage will surely be done, as a result of the great mass of snow in the mountains melting rapidly.” (p. 6)

Septer (2007) affirmed that spring runoff flooding in central/southern British Columbia typically occurs following a winter with an above-normal snow pack, combined with a cold and late spring. A sudden warm spell in May, especially when accompanied by above-average precipitation, may be portend serious spring runoff flooding, which can last for weeks (Septer 2007). Septer (2007) also noted that record snowfalls and great flooding of the Thompson River took place in 1894 and 1948, when cool spring temperatures were suddenly succeeded by warm, wet weather in late May. This facilitated rapid melting of the higher-than usual snowpack and resulted in snowmelt plus rainfall induced flooding (Septer 2007). On June 3, 1894, it was reported that every bridge along the Cariboo road had been swept away and the road itself destroyed for a considerable distance (Septer 2007). Half a century later, the 1948 flood was called the most devastating since 1894 (Septer 2007).

In his model of the regional hydrogeology, Bishop (2008) found that the transient application of precipitation had a greater impact on the pore pressure distribution in the valley slopes compared to modern irrigation levels or variation in the Thompson River stage, and concluded that the regional groundwater flow regime was much more sensitive to climatic changes, than to the effects of river stage or irrigation. However, Bishop’s (2008) study did not consider regional water inputs due to snow melt.

Quinn et al. (2012) demonstrated that the seasonal peak Thompson River flow levels correlate with the peak winter snow pack measured across the watershed. They presented a temporal comparison of the mean annual snow pack and the subsequent peak flow levels for the Thompson River measured at Spences Bridge for the years 1984 to 2009. I postulate that melting of the snow pack on the basin-wide scale may provide considerable input to the regional groundwater flow regime. Quinn et al.’s (2012) data were limited to the 16-year period of 1984 to 2009, as they considered only the active automated snow pillow monitoring stations present in the North and South Thompson River basins. However, numerous additional inactive and active manual snow survey sites also exist in the North and South Thompson

River basins, as shown in Figure 4.7. The manual snow survey sites are subject to discreet measurements of snow pack depth at intervals of approximately 2 to 4 weeks at the height of the season, as compared to the continuous measurements collected by the automated snow pillow stations (Province of British Columbia 2014). The size of the drainage basin of the Thompson River at Spences Bridge is approximately 55,000 km².

I accessed and analyzed data for all the active and inactive manual and automated snow survey sites within the North Thompson and South Thompson River basins of the British Columbia Snow Survey Network. Snow monitoring records present the peak snow pack depth as an equivalent height of water (snow water equivalent or SWE), which can then be normalized to the average peak value over the period of record for that site. Details for the name, location, and period of record for each station are given in Table 4.2. The spatial distribution of the active and inactive snow survey sites is shown in Figure 4.7. Snow survey measurements date back as early as 1938 at some sites. To investigate the relationship between the peak snow pack across the Thompson River watershed and the peak and cumulative Thompson River flow, only those snow stations with a minimum of 15 years of data were included in the analysis, to ensure a representative mean value for each station to be normalized against. Ideally, a 30 year period of record, as recommended by the World Meteorological Organization would be used in the calculation of the mean, but this would limit the total number of snow pack monitoring stations to 7, as opposed to 10 (Government of Canada 2014). Where manual and automated snow surveys were conducted at the same site in the same year, only one of the surveys (that with the longer period of record) was included in the analysis, to avoid bias in the results.

Using the basin-wide average of normalized snow pack and the daily Thompson River discharge measurements at Spences Bridge, Figure 4.8 presents the relationship between the average normalized peak snow pack and normalized annual and peak Thompson River flow for the hydrologic years (October to September) 1950 to 2011. Figure 4.8 presents a persuasive relationship between the normalized peak snow pack, averaged between the active monitoring stations (3 to 14 stations, depending on the year), and the subsequent normalized peak and annual Thompson River flow measured at Spences Bridge. Depending on the station elevation,

the maximum snow pack typically occurred in late winter to early spring, with the peak river flow typically occurring in mid to late summer. River discharge records for Station 08LF051 near Spences Bridge indicate that the mean monthly river discharge rate varied from a low of 224 m³/s in February, to a high of 2300 m³/s in June, presumably driven by melting of the snow pack (Environment Canada 2014). When the average normalized peak snow pack is plotted versus the normalized maximum and annual river flow, a linear relationship is evident. Comparing the peak snow pack to the maximum (annual) Thompson River flow, a linear regression coefficient of $r^2=0.58$ ($r^2=0.45$) is obtained for the period of 1952 to 2011, and is improved to $r^2=0.68$ ($r^2=0.62$) for the period of 1970 to 2011, due to an increased number of active snow monitoring sites. From 1970 to 2011, there were 11 to 14 active snow monitoring stations, resulting in a more representative basin-wide average value for the peak normalized snow pack over this period of record (compared to 3 to 10 active sites during 1952 to 1969).

D. Campbell (personal communication, 2016) confirmed that the winter snow pack contributes the bulk of the Thompson River annual flow volume (in the order of approximately 70-80%); though peak summer flows in June/July coincide with the rainy season in the B.C. Interior, the upstream influence of Kamloops Lake serves to attenuate the effects of flash precipitation events. Notwithstanding the potential for significant interannual variability in river discharge, the Thompson River is a relatively stable river system (D. Campbell, personal communication 2016). During extreme spring runoff events, areas hit first with “flash” floods are those situated near narrow, shallow rivers close to the snow packs, compared with the Fraser or Thompson Rivers that are filled by tributaries (Septer 2007). Moreover, the attenuating effect of Kamloops Lake (outlet located approximately 30 km upstream of Ashcroft), reduces the likelihood of flash flooding downstream (D. Campbell, personal communication, 2016). Antecedent precipitation likely accounts for most of the discrepancy between the peak annual snow pack and the peak annual river flow values shown in Figure 4.8; antecedent weather conditions affecting the timing and duration of the snow melt will also influence the subsequent peak river flow produced by the freshet. The B.C. River Forecast Centre conducts flood forecasting for the Thompson River which is published in online Snow Survey Bulletins for the current year (Province of British Columbia 2016b). These forecasts are based on a multivariate statistical approach which considers multiple factors including snow pack,

antecedent river flow and antecedent precipitation (D. Campbell, personal communication, 2016).

The height of the winter snow pack measured across the Thompson River basin plays a significant role in controlling the subsequent peak and cumulative Thompson River flow levels. The snow pack monitoring stations have not been active as far back in history as the river discharge monitoring stations, so the correlation of peak river flow to peak snow pack does not improve the historic frequency analysis of the landslide movements. However, the correlation does serve the important purpose of linking the peak Thompson River flows to the regional climate conditions, which could in turn, serve as a potential early-warning tool for predicting slope movements in the corridor, as suggested by Quinn et al. (2012). Moreover, the compelling link between the peak Thompson River discharge and the peak snow pack may serve to explain the lack of success that the author and others (Eshraghian et al. 2005, Quinn et al. 2012) have had in attempting to relate landslide movements to historic rainfall records. Given Ashcroft's semi-arid climate, with an annual average rainfall of only 232 mm (Bishop 2008), this apparent lack of correlation between landslide movements and rainfall records is not surprising.

Viewed on a basin-wide scale, the Thompson River represents a formidable force of nature that is both reflective of, and in turn contributes to, the overall climate conditions. Wade (1979) described the powerful force of the Thompson River during spring freshet in his accounts of the building of the bridge across the river at Cook's Ferry (later known as Spences Bridge). The bridge was first completed in the spring 1864, only to be completely swept away by the spring freshet (Wade 1979). The bridge was re-built by the following year, and stood until the "extraordinary freshet of 1894, which overwhelmed and utterly destroyed every vestige of it"; the bridge was ultimately rebuilt, for the third time, as a "more substantial" structure (Wade 1979).

4.5. Pacific Decadal Oscillation (PDO)

4.5.1. Introduction

It is evident in examining the past 100 years of discharge data in Figure 4.5 that the cumulative Thompson River flow is affected by multiyear cycles of abundance and deficit in the measured daily departures from normal. While interannual fluctuations exist, there also appears to be a strong component of interdecadal trends in the cumulative river flow departures from normal. A possible explanation for these stream flow trends may be higher-level multi-decadal climate phenomena, expressed in indices such as the Pacific Decadal Oscillation (PDO). Fluctuations in the PDO have been correlated by others to substantial changes in the snow pack and stream flow regimes in the Pacific Northwest; the implications of the PDO for the Thompson River landslides are investigated in the following subsections.

4.5.2. Definition of the Pacific Decadal Oscillation

Mantua (2002) described the Pacific (inter) Decadal Oscillation (PDO) as a long-lived El Niño-like oscillatory pattern of climate variability centered over the Pacific Ocean and North America. It is defined as the first empirical orthogonal function (EOF) of the anomalies of monthly mean sea surface temperature (SST) poleward of 20°N in the Pacific Ocean (Mantua et al. 1997). The PDO has been shown to exert considerable influence on climate-sensitive natural systems in the Pacific and over North America, including the water supplies and snow pack in selected regions in North America, and major ecosystems from the coast of California north to the Gulf of Alaska and the Bering Sea (Mantua 2002). Fisheries scientist Steven Hare first coined the term Pacific Decadal Oscillation in 1996 while researching connections between Alaskan salmon production cycles and the Pacific climate (Mantua 2002).

PDO fluctuations over North America are primarily a cool season phenomena, most energetic in the winter and spring, from October to March (Mantua 2002). Anomalously cool sea surface temperatures (SSTs) in the central North Pacific coincident with anomalously warm SSTs along the west coast of the Americas are associated with the warm phase of the PDO (Mantua

2002). From October to March, warm PDO sea level pressure (SLP) anomalies vary in a wave-like pattern, with low pressures over the North Pacific giving rise to enhanced counter-clockwise winds, while high SLP over western North America and the subtropical Pacific cause enhanced clockwise winds in those regions (Mantua 2002). Tracking PDO variations is therefore typically achieved using indices constructed from observed Pacific SST and SLP patterns (Mantua 2002). Cool PDO anomalies are the opposite of those observed during warm PDO phases (Mantua 2002).

There are three main characteristics, as summarized by Mantua (2002), which distinguish the PDO from the more well-known El Niño/Southern Oscillation (ENSO). First, PDO events are much more persistent than ENSO events—PDO regimes in the 20th century have persisted for 20-30 years, while typical ENSO events persisted for 6-18 months; second, the climatic effects of the PDO are most pronounced in the North Pacific/North American sector, with secondary effects in the tropics, while the opposite is true for ENSO; and third, the mechanisms which give rise to the PDO are not currently known, while causes for ENSO are relatively well-understood (Mantua 2002).

4.5.3. PDO Regimes

In the early 1990's, an array of evidence began accumulating that a major climate event had transpired in the mid-1970's, which had widespread impacts on the biota of the North Pacific Ocean and Bering Sea; this event was eventually termed a climatic "regime shift"⁵ (Hare and Mantua 2000). Hare and Mantua (2000) cited numerous scientific studies documenting the climatic and ecosystem changes that accompanied the event. Particularly influential was the study of Ebbesmeyer et al. (1991) who used a composite time series assembled from a diverse cross section of 40 multi-disciplinary environmental variables to demonstrate that a statistically significant step change occurred in the winter of 1976-77 (Hare and Mantua 2000).

⁵ Minobe (1997) defines a climatic regime shift as "a transition from one climatic state to another within a period substantially shorter than the lengths of the individual epochs of each climate states." According to Hare and Mantua (2000), "A shift suggests an abrupt change, in relation to the duration of a regime, from one characteristic behavior to another. Although climate variability occurs across a broad spectrum of spatial and temporal scales, ...a regime spans a decade or more, whereas a shift occurs within a year or so."

Mantua et al. (1997) were among the first to identify the 1976/77 regime shift as one event in a series of a robust, recurring pattern of ocean-atmosphere climate variability centered over the midlatitude North Pacific basin, with an interdecadal signature detectable in a variety of Pacific basin climate and ecological systems. In examining the instrumental record of climate data, they found evidence of reversals in the prevailing polarity of the oscillation occurring around 1925 and again in 1948, in addition to the event of 1977; the last two reversals were also coincident with substantial shifts in salmon production regimes in the North Pacific Ocean (Mantua et al. 1997).

Minobe (1997) independently arrived at the same time periods exhibiting coherent interdecadal climate trends by examining instrumental records including spring air-temperature anomalies in western North America and spring sea-surface temperature (SST) anomalies in the eastern North Pacific. As shown in Figure 4.9, he identified interdecadal “warm” periods of 1870-1889, 1925-1947, and 1977-(at least) 1990; the alternating periods of 1890-1924 and 1948-1976 were identified as anomalously “cool” (Minobe 1997). In association with the regime shifts of 1947/48 and 1976/77, significant cooling and warming were observed, respectively, in surface air-temperatures over western North America in spring (Minobe 1997) and over Alaska and Western Canada in winter (Zhang et al. 1997). The Ashcroft Thompson River landslides are located within the geographical extents of Minobe’s (1997) study, as shown in Figure 4.10. The earliest “warm” period on the instrumental record of 1870-1889 (Minobe 1997) followed the ending of the global “Little Ice Age” in the mid-1800’s, as indicated by proxy records (Moore et al. 2010).

Minobe’s (1997) further analysis of tree ring reconstructed continental surface temperatures suggested that PDO-like interdecadal climate variabilities, characterized by a 50-70 year recurrence interval, have been prevalent in North America from at least the eighteenth century to the present. Individual epochs or “regimes” would therefore have been of 25-35 years in length, since the period of each regime consists of two epochs with opposite tendencies (Minobe 1997). Minobe (1999) later showed that 20th century PDO fluctuations were most energetic in two general periodicities—one from 15-25 years, and the other from 50-70 years. He suggested that the 50-70 year variability was likely due to an internal oscillation in the

coupled atmosphere-ocean system, although it could be modulated by the external solar radiation heating in the 20th century (Minobe 1997). Gedalof and Smith (2001) independently analyzed a transect of climate sensitive tree ring-width chronologies from coastal British Columbia and Alaska, confirming that abrupt regime shifts in the North Pacific climate have occurred 11 times since the year 1650, with an average duration of 23 years. Gedalof and Smith (2001) suggested that the PDO may be distinct from other forms of climate variability in that it does not appear to be truly oscillatory in nature, but rather shifts abruptly between relatively warmer and cooler states.

Bovis and Jones (1992) documented the impact of regional hydroclimatic changes on the mass movements of earthflows in south-central British Columbia. They presented evidence relating regionally consistent earthflow movements to the hydroclimatic history on three time scales (Holocene, using the paleobotanical record; the past 300 years, using the tree-ring record; and the past 60 years using air photographs and instrumental records of cumulative precipitation departures from normal) (Bovis and Jones 1992). They hypothesized that recurring cooler, wetter intervals within the Holocene, documented by the paleobotanical record, resulted in periods of increased groundwater recharge and reactivation of dormant earthflows driven by a combination of increased precipitation and decreased evapotranspiration (Bovis and Jones 1992). Their study showed a generally consistent relationship between compression-wood development (as a proxy for slope movements) at the Pavilion earthflow and the local tree ring-width sequence (as a proxy for climate), suggesting increased earthflow activity corresponding to the cooler, wetter period of 1790-1810, and decreased activity during warmer, drier periods of 1840-1860 and 1920-1940 (Bovis and Jones 1992). Elements of this pattern were repeated at two other sites studied (Bovis and Jones 1992). While these time periods do not correspond directly to the PDO regimes identified by Mantua et al. (1997) and Minobe (1997), which is likely due to the localized nature of Bovis and Jones' (1992) study and their use of proxy records, their study underscores the relationship between climate-driven fluctuations in groundwater recharge and slope movements in south-central British Columbia.

4.5.4. Impacts of PDO on Snow Pack and Streamflow in North America

The warm phase of the PDO is correlated with anomalously warm and dry winter/spring conditions in the northern half of North America (El Niño-like), while the cool phase of the PDO is correlated with the opposite climate patterns (cool and wet, La Niña-like) (Mantua 2002). PDO variability is also strongly expressed in regional snow pack and stream flow anomalies in western North America, as identified in Cayan (1996) and Mantua et al. (1997). In examining snow course records in the Rocky Mountains, Changnon et al. (1991) demonstrated that spring snow accumulation serves as a regional climatic indicator, while Cayan (1996) showed that marked “runs” of positive and negative anomalies in the April 1st snow water equivalent (SWE) were generally coincident with the warm/cool phases of the PDO as articulated the following year by Mantua et al. (1997).

Cayan’s (1996) time-series of snowpack variability from 1937 to 1989 for the “Idaho” pattern, centered in the Pacific Northwest, is consistent with the PDO-related wintertime air temperature and precipitation patterns presented in Mantua et al. (1997): relatively warm (cool) winter air temperatures and anomalously low (high) precipitation during positive (negative) PDO years contributed to reduced (enhanced) snowpack in the Pacific Northwest. In particular, the shift in climate in the Pacific North American sector in 1976/77 with a series of winters having a deepened Aleutian low resulted in a shift towards a diminished snowpack in the Northwestern United States extending to the Pacific Coast, and a coincident increased snowpack in the Southwestern United States extending into Arizona and New Mexico (Cayan 1996). This inversion is consistent with the findings of Changnon et al. (1993), who noticed a pivotal zone in the central Rockies with decreasing snowpack in the northern Rockies (Idaho and Montana) and increasing snowpack in the southern Rockies (Utah and southern Colorado). Cayan (1996) asserted that SWE anomaly patterns are strongly organized by the atmospheric circulation, and that snow accumulation appears to show more sensitivity to large-scale fluctuations in atmospheric circulation than do precipitation and temperature. Specific to British Columbia, Stahl et al. (2006) demonstrated that positive phases of the PDO were associated with positive winter temperature anomalies throughout western Canada and with negative precipitation anomalies in the mountains and Interior, resulting in a reduced

snowpack, as shown in Figure 4.11.

Mantua et al. (1997) determined that during positive PDO years, the annual water year (October to September) discharge in the Skeena, Fraser, and Columbia Rivers was on average 8%, 8%, and 14% lower, respectively, than during negative PDO years (Figure 4.12). The reverse was true further north, where discharge from the Kenai River in the central Gulf of Alaska region was on average about 18% higher in positive PDO years compared to negative PDO years (Mantua et al. 1997). Table 4.3 summarizes the climate anomalies associated with the PDO. Pizarro and Lall (2002) identified the importance of the PDO for flood forecasting in the western United States. They found statistically significant correlations of the annual maximum flood with January–April averages of the ENSO (NINO3) and PDO indices over large, contiguous areas in the region, irrespective of the dominant season of occurrence and the operative climate mechanism. Their study underscores the importance of the PDO in affecting the non-stationarity of the flood hazard on an interdecadal time scale, such that knowledge of the PDO regime may significantly improve regional flood frequency estimates and provide information on their temporal variation (Pizarro and Lall 2002).

Substantiating the effects of the PDO on ecological systems, several studies have also shown that fish populations over the North Pacific were significantly impacted by the interdecadal climate regime shifts of the past century. Francis and Hare (1994) and Mantua et al. (1997) showed that the Alaskan salmon stock decreased with the PDO shift from positive to negative in the 1940's and increased in the 1970's. Generally speaking, the reverse was true for Pacific Northwest salmon (Mantua et al. 1997). The catch of the Japanese sardine was affected by all three regime shifts of the 1920s, 1940s, and 1970s, with larger catch amounts in the regimes with the deepened Aleutian low (positive PDO) (Minobe 1997, citing I. Yasuba, personal communication). Baumgartner et al. (1992) found a similar periodicity of 60-year variability in the populations of sardine and northern anchovy in the eastern North Pacific, from examining sediments in the Santa Barbara basin off California dating back to AD 270 (Minobe 1997).

4.5.5. Impacts of PDO on Snow Pack and Thompson River Flow

As described above, fluctuations in the PDO have been correlated to substantial changes in the snow pack and stream flow regimes in the Pacific Northwest. As a result of warmer, drier winters during positive PDO years, Mantua et al. (1997) determined that the annual discharge of the Fraser River was on average 8% lower than during negative PDO years. The Thompson River is a tributary of the Fraser River, which it joins south of Spences Bridge. It therefore stands to reason that the annual Thompson River flow would likely be affected by the PDO in a manner similar to the Fraser River. Based on the daily discharge readings (m^3/s) for stations 08LF051 and 08LF022 on the Thompson River at Spences Bridge, compared to the calculated daily average flow rates for each station's respective period of record, I calculated the Thompson River average flow departure from normal for the hydrologic years of 1925-1947 (warm/dry PDO phase) to be, on average, 7% lower than for the years 1948-1976 (cool/wet PDO phase) (0.97 and 1.04 normalized departure from station average over period of record, respectively). Data are missing from hydrologic years 1932, 1933, and 1934, so these years were omitted from the analysis. As snow survey measurements for the Thompson basin are only available from about the mid-century onwards, there is not a long enough period of record to make a comparison of snow pack for the established PDO regimes of 1925-1947 and 1948-1976.

Figure 4.13 plots the Thompson River normalized annual flow departures from normal for the years 1913 to 2011 with running averages overlain (years 1932, 1933 and 1934 are omitted due to missing data). Annual fluctuations are evident throughout the time series in both the positive and negative directions; regimes of prolonged wetter and dryer periods are more evident when examining the multi-year running averages.

Perhaps more salient, however, in visually relating the Thompson River discharge to the effects of the PDO, is Figure 4.14. The daily Thompson River discharge at Spences Bridge is plotted in the lower pane as a continuous departure from normal over the period of record from 1912 to the end of 2011; this is compared to the average winter (October to March) PDO indices for the corresponding years, plotted in the upper pane; the shifts in the PDO regimes are indicated

by the dashed lines. Monthly PDO Index values were retrieved from the online databased maintained by Mantua (2015). An increasing slope in the cumulative river flow departure from normal indicates an abundance of flow compared to the daily station averages for the period in question, while a negative slope indicates a deficit in the measured daily river flows.

Figure 4.14 vividly illustrates an increasing trend in the cumulative discharge of the Thompson River during the cool/wet PDO periods of (pre-)1912-1924 and 1948-1976, and a generally decreasing trend or deficit in river discharge during the warm/dry PDO periods of 1925-1947 and 1977-(at least) 1998. The possible reversal from a warm to cool PDO phase in 1997/1998 is marked with a dashed line and a question mark; observed changes in the Pacific climate following the exceptional El Niño event of 1997–1998 are postulated to potentially represent a shift in the PDO regime, but there is not consensus in the literature as to whether these changes mark the beginning of a 20–30 year long cool phase of the PDO (Mantua and Hare 2002). Bond et al. (2003) attribute the lack of a consistent sense to the PDO since 1998, at least in part, to the concurrent fluctuations in ENSO, citing the transition from a very strong El Niño in the winter of 1998 to the moderate La Niña of 1999/2000, then again to a moderate El Niño in the winter of 2003.

Gedalof and Smith (2001) noted that while the pre-instrumental (dendroclimatic) fluctuations in the PDO showed pronounced interdecadal variability, the secular portion of the record is more strongly interannual in nature. Hare and Mantua (2000) noted a shift in some components of the North Pacific ecosystem which took place in 1989, although these were not as pervasive as the 1977 changes—relative clarity was expressed by changes in biological records, but not so clearly in the Pacific climate indices. Litzow (2006) also noted changes in the Pacific climate in 1988/89 and in 1998/99, but his analysis rejected the hypothesis that the events of 1988/89 and 1998/99 constituted a reversal in the polarity of the PDO, suggesting these were due to a spatial pattern distinct from either positive or negative values of the PDO. Recent research by Hartmann (2015) and Bond et al. (2003) suggests that a single indicator such as the PDO alone may not be sufficient to characterize the variability of the North Pacific climate. They noted that the second empirical orthogonal function (EOF) of North Pacific SST, termed the North Pacific Mode (NPM), provides valuable insights into the SST anomalies that are

distinct from, and not captured by, the PDO. While ongoing research into the effects of the North Pacific Mode may serve to improve the climate relationships discussed in this chapter, further discussion is outside the scope of the current study.

4.5.6. Association of PDO with Landslide Activity

The effects of the alternating cool and warm regimes of the PDO on the snow pack and stream flow in the Pacific Northwest offer an explanation for the temporal clustering of landslide activity observed along the Thompson River Valley over the past approximately 150 years. The cluster of landslide movements which occurred in the early 1970's and up until the winter of 1977 (evident in Figure 4.14) coincides with the cool/wet regime of the PDO which persisted from approximately 1947/48 to 1976/77. The regime shift in the PDO which took place in the winter of 1976/1977 may offer an explanation for the unusual level of landslide activity which was reported in the winter of 1976/77. Although all the movement rates were extremely to very slow, the Goddard landslide moved in the fall of 1976, followed by the CN 50.9, South and Nepa Crossover slides in the winter of 1977 (refer to Table 3.1). The abrupt regime shift in the PDO from wet/cool conditions in 1976 to warm/dry conditions in 1977 likely contributed to the anomalous winter landslide activity. Blocking of groundwater outlets by freeze/thaw as per Hutchinson (1987) is a physical process that may have contributed to the anomalous slope movements in the winter of 1977. A period of relative inactivity followed, in correspondence with the warm/dry PDO regime of 1976/77 to (at least) 1997/98. The obvious anomaly during this time period was the 1982 rapid reactivation of the Goddard landslide. Judging from Figure 4.14, this event is associated with a localized rapid rise in the Thompson River discharge during a generally downward-trending regime. The sharp rise in cumulative discharge observed in 1997 corresponds to a return to a more active phase of landslide activity (events of 1997, 1999 and 2000 in Table 3.1), which is coincident with the postulated 1997/98 regime shift from a warm to cool phase of the PDO.

To the extent that the 20th century activity of the Ashcroft Thompson River landslides are associated with years when the Thompson River exhibits anomalously high discharge preceded by higher winter snow pack measurements, the relationship between the landslide activity and

cool/wet regimes of the PDO is a logical extension. Fourteen of the seventeen landslide events shown on Figure 4.14 occurred during the cool/wet PDO regimes of 1947/48-1976/77 and post 1997/98; the remaining three events took place in the high-flow years of 1921 and 1982 that occurred during warm/dry PDO regimes. The threshold criterion of 3400 Mm³ proposed in Section 4.3 above was exceeded 15 times between 1913 and 2011; two-thirds or 10 of these exceedances occurred during the cool/wet PDO regimes of 1947/48-1976/77 and post 1997/98 as shown in Table 4.1; the remaining five exceedances took place in 1921, 1928, 1935, 1982 and 1996. This is equivalent to a 22.7% (1:4.4) likelihood of exceedance during the cool/wet PDO regimes shown in Figure 4.14, and a significantly lower probability of only 9.6% (1:10.4) likelihood of exceedance during warm/dry PDO regimes.

Moreover, the spate of rapid landslides which occurred in the corridor during the late 1800's, attributed to irrigation of the arid upland areas, coincide with the warm/dry PDO regime of 1870 to 1889/90 identified by Minobe (1997) (Figure 4.14). In keeping with the working hypothesis that these 19th century landslides were caused by primitive irrigation of the upland areas, the clustering of these events within a dry regime of the PDO makes sense—unusually dry conditions would likely correspond to unusually high levels of water input through anthropogenic irrigation.

4.6. Hydrologic Effects of the El Niño Southern Oscillation (ENSO)

The empirical study of Gershunov and Barnett (1998) suggests that ENSO influences on North American climate are also strongly dependent on the phase of the Pacific Decadal Oscillation. They found that the PDO exerts a modulating effect on ENSO teleconnections, such that typical ENSO signals tend to be stronger and more stable during preferred phases of the PDO. Typical El Niño patterns (dry northwest) are strong and consistent only during the high phase of the PDO; the generally reversed precipitation patterns during La Niña winters are consistent only during the low PDO phase. Accordingly, climate anomalies tend to be weak and spatially incoherent during low PDO-El Niño and high PDO-La Niña winters (Gershunov and Barnett 1998).

Environment Canada issues seasonal climate bulletins for British Columbia and the Yukon. According to Environment Canada (2015c), there is a high degree of variability in the historic snow pack records for El Niño years in British Columbia. While strong El Niño conditions in the Pacific Ocean typically favor warmer than normal (+2 to +3°C) and drier than normal (– 10%) winter periods, years of extreme high and extreme low snow packs have been observed in previous El Niño years (Environment Canada 2015c). The warmer than normal temperatures associated with El Niño tend to result in a higher proportion of precipitation falling as rain versus snow, which may produce a shallower snowpack in the mountains and possible drought conditions in the following year (MacDonald et al. 2016). Climatologists caution, however, that while temperature associations with ENSO events show coherent trends (+/- 2 to 3°C for El Niño/La Niña, respectively, beginning in mid-January) precipitations anomalies associated with ENSO events are less predictable; the association of La Niña with higher snow packs may be slightly stronger than the association of El Niño with drier conditions, but both are variable (MacDonald et al. 2016). Local experience would suggest that El Niño imparts drier winter conditions to low- to mid-elevation sites (el. <1200 m), with less coherent effects on snow pack at higher elevations (MacDonald et al. 2016).

I obtained historic Oceanic Niño Indices for 1950 to 2011 from the American National Oceanic and Atmospheric Administration (NOAA, 2016). The Oceanic Niño Index (ONI) is the standard used by the NOAA for identifying (warm) El Niño and (cool) La Niña events in the tropical Pacific, representing the running 3-month mean sea surface temperature (SST) anomaly for the Niño 3.4 region (5°N to 5°S, 120°W to 170°W) (Null 2016). An El Niño (La Niña) event is defined as five consecutive overlapping 3-month periods at or above the + (–) 0.5°C SST anomaly. Events are further categorized as weak, moderate, strong, and very strong based on the threshold exceeded for at least three consecutive overlapping 3-month periods (weak, 0.5 to 0.9 SST anomaly; moderate, 1.0 to 1.4; strong, 1.5 to 1.9; and very strong, ≥ 2.0) (Null 2016). In accordance with this definition, since 1950 there have been five strong/very strong El Niño events and three strong La Niña events. Strong El Niño events were recorded in 1957/58, 1965/66 and 1972/73, and very strong El Niño events in 1982/83 and 1997/98; strong La Niña events occurred in 1973/74, 1975/76 and 1988/89 (Null 2016).

Figure 4.15 displays the strong/very strong El Niño and La Niña events along with the cumulative Thompson River flow departure from normal, the number of landslides in the corridor, and the phase of the Pacific Decadal Oscillation (PDO) for the years 1950 to 2011. The lengths of the red (green) bars correspond to the persistence of the El Niño (La Niña) events, and the vertical positions of the bars are indicative of the corresponding maximum (minimum) ONI value achieved. Comparing the temporal occurrences of the strong/very strong El Niño events with the indicated PDO regimes, the very strong El Niño events of 1982/83 and 1997/98 were in phase with the warm/dry PDO regime which prevailed from 1976/77-1997/98; the strong El Niño events of 1957/58, 1965/66 and 1972/73 were out-of-phase with the cool/wet PDO which persisted from 1947/48 to 1976/77. The strong La Niña events of 1973/74, 1975/76 were in phase with the prevailing cool/wet PDO regime, while the 1988/89 La Niña event was out-of-phase with the dry/wet PDO regime.

It is evident from Figure 4.15 that since 1950, landslides were recorded during every strong La Niña event that was *in phase* with a cool PDO regime—that is, in 1973/74 and 1975/76. The strong La Niña event of 1988/89 occurred within the warm phase of the PDO, which may explain the lack of observable effect on landslide activity in the corridor. However, somewhat confounding this explanation is the fact that landslides also occurred in the corridor in 1972, 1982 and 1997 during strong/very strong El Niño events that were both in- and out- of phase with the prevailing PDO regime, though in conjunction with above-normal river flows. Though no landslides were recorded during the strong El Niño events of 1957/58 and 1965/66, it is difficult to say whether this is due to a lack of landslide activity or a lack of record keeping. The Thompson River flow in these years, was, however, near or below average conditions, and as such, it is quite plausible that landslides did not occur in these years. The strong/very strong El Niño events appear to have less coherent effects on landslide activity in the Thompson River Valley compared to the strong La Niña events of the last half-century. D. Campbell (personal communication, 2016) confirmed that, anecdotally, ENSO signatures in British Columbia tend to be stronger for La Niña years than for El Niño years.

The 2015/16 El Niño is the strongest recorded event since recordkeeping began in 1950 (MacDonald et al. 2016); the next strongest El Niño on record was 1997/98 (van Aalst 2006).

The record-breaking El-Niño of 1997/98 was followed by a record-breaking La-Niña winter in 1998/99; research and experience suggests a strong El-Niño event is likely to be followed by a strong La-Niña, which may have implications for a cold/wet 2016/17 season and attendant landslide activity (MacDonald et al. 2016).

4.7. Weather and Climate Conditions Associated with the 1982 Goddard Landslide

1982 is a year of significant importance as it marks the most recent occurrence of a rapid landslide in the Ashcroft corridor—the rapid reactivation of the Goddard landslide on September 24, 1982—and the only rapid landslide to have occurred in the corridor since the adoption of modern irrigation techniques (Figure 3.2). Figure 4.8 shows that the peak snowpack in 1982 was 19% above the average peak snowpack for the Thompson Basin. While this was not a particularly unusual snow season overall, in examining the station-specific snow monitoring records more closely, an interesting anomaly is apparent for the spring snow records of 1982. There was a localized late-season persistence of snow on the ground in the vicinity of Ashcroft (Middle Fraser basin) in mid- to late- April 1982. Snow water equivalent measurements for several stations in the basin of up to 1333% of normal were recorded by manual snow surveys conducted at five sites within approximately 100 km of Ashcroft between April 29 and May 14, 1982. I postulate that this late-season persistence of snow on the ground and associated late melting may have contributed a significant input to the local groundwater system, aggravating the slope instability at the Goddard landslide. A general statement to this effect was made in the expert report by Thurber Consultants Ltd. (1984), which was submitted as part of the court proceedings associated with the Goddard slide. A summary of the manual snow survey sites within 100 km of Ashcroft with snow survey measurements greater than 500% of normal for the spring of 1982 is given in Table 4.4 below. The locations of these particular snow monitoring sites are presented in Figure 4.16; they are located within the boundaries of the Middle Fraser basin. In addition, the federal weather station located at Spences Bridge, which functioned from 1981-2002, recorded an extreme snow depth of 23 cm on January 24, 1982—the highest for the station’s 22-year period of record (Environment Canada 2015b).

As previously mentioned in Section 4.4, Septer (2007) noted that spring runoff flooding in southern BC is typically preceded by three factors: (1) a winter with an above-normal snow pack, (2) a cold and late spring, and (3) a sudden warm spell in May, especially when accompanied by above-average precipitation. The late-season persistence of snow on the ground at monitoring sites in the vicinity of Ashcroft in 1982 is consistent with Septer's (2007) first condition for spring flooding; the second condition, a rapid swing from cool to warm temperatures and associated rapid melting of the snow pack, may have also been enacted that year. It is of interest to note that there was a substantial surge in the cumulative river flow departure from normal during the spring and summer of 1982 (Figure 4.14). This occurred in conjunction with the strong El Niño event commencing in the spring of 1982, as indicated by the red bar on Figure 4.15. It is possible that the warm characteristics of El Niño, in phase with the positive PDO, may have produced unusually warm spring temperatures and rapid melting of the higher-than-normal winter snowpack which was recorded in spite of the prevailing dry PDO phase. With respect to Septer's (2007) third condition, spring precipitation in 1982 was exceptionally low, but as others (EBA Engineering Ltd. (1984) and Thurber Consultants Ltd. (1984), e.g.) have noted, the summer of 1982 was wetter than usual, and Figure 4.3 bears this out. During the months of July, August and September, Ashcroft received 41, 41, and 31 mm of precipitation respectively, which were 32% to 64% higher than the respective 20-year averages recorded for those months at the Spences Bridge station (Figure 4.4). It is plausible that all these factors conspired to produce high summer river flow conditions (increased toe erosion) in conjunction with high local groundwater conditions (increased porewater pressure within and below the slide mass), ultimately resulting in the rapid reactivation of the Goddard landslide on September 24, 1982.

4.8. Climate Change and Hydrologic Impacts in British Columbia

Given the preceding discussion relating the Thompson River flow to landslide activity in the corridor, the potential impacts of climate change on snowpack and streamflow in British Columbia are relevant to forecasting landslide risk. This is especially true for high-latitude regions such as Canada where climate change signals are projected to be stronger and the impacts may be more severe (Zhang et al. 2001). As previously discussed, many weather and climate extremes are the result of natural climate variability (including phenomena such as ENSO and the PDO); even if there were no anthropogenic changes in climate, a wide variety of natural weather and climate extremes would still occur (IPCC 2012). These natural decadal or interdecadal variations in climate provide the backdrop for anthropogenic climate changes, which may alter the frequency, intensity, spatial extent, duration, and timing of weather and climate extremes, and can result in unprecedented extremes (IPCC 2012). Demonstrated changes in the mean state of Canadian climate reflected in temperature and precipitation have had attendant impacts on the hydrology of Canadian rivers, such as volume and timing of streamflow and river ice conditions (Zhang et al. 2001).

The Intergovernmental Panel on Climate Change (IPCC) defined climate change as “any change in climate over time, whether due to natural variability or as a result of human activity⁶” (IPCC 2007). Climate change thus refers to a measureable change in the state of the climate that can be identified by changes in the mean and/or the variability of its properties, and that persists for an extended period of time as a result of natural internal processes or external forcings such as persistent anthropogenic changes in the composition of the atmosphere or in land use (IPCC 2014). There are two methods generally employed in peer-reviewed research for quantifying the effects of climate change; one is the detection and attribution of past trends for the understanding of potential future climate change; the other is the use of global climate models and emissions scenarios for forecasting future climate conditions. Both approaches

⁶ This definition is adopted in this thesis; it differs from the United Nations Framework Convention on Climate Change, where climate change refers to a change of climate that is attributed directly or indirectly to human activity (IPCC 2007).

have inherent uncertainties and limitations. The detection of historic trends is strongly affected by the length of the record, the magnitude of the trend relative to inherent interannual variability, and the window of data relative to decadal-scale shifts such as the PDO (Moore et al. 2010). The accuracy of climate change forecasts, on the other hand, is affected by uncertainties in the global climate model(s) and emission scenarios used (Morrison et al. 2002). Using multiple scenarios and an array of global climate models produces a range of equally-plausible outcomes, illustrating the inherent uncertainties in the estimates (Moore et al. 2010). The following sections discuss climate studies of both types which deal specifically with British Columbia: the detection and attribution of past trends by Zhang et al (2001), and the modelling of future climate conditions by Shrestha et al. (2012) and Morrison et al.(2002). These studies are by no means comprehensive, but for the purposes of this discussion they serve to illuminate the anticipated impacts of global climate change on streamflow and snowpack in central British Columbia.

4.8.1. Historic Trends in Canadian Climate and Streamflow

Zhang et al. (2001) investigated trends in Canadian streamflow between 1947-1996 for three study periods of 30, 40, and 50 years length, analyzing trends in 11 hydroclimatic variables obtained from 243 stations within the Canadian Reference Hydrometric Basin Network (RHBN). They found negative trends suggesting a reduction in annual mean streamflow across southern Canada, particularly in southern British Columbia (Zhang et al. 2001). This finding is consistent with changes in climate observed over the same periods, whereby positive trends in temperatures (and hence potential evapotranspiration) combined with almost no change in precipitation (Zhang et al. 2000) explain the generally negative trends in streamflow (Zhang et al. 2001). Maximum daily streamflow appears to be decreasing where temperature is rising (Zhang et al. 2001). Over southern British Columbia the strongest decreases in mean monthly streamflow occurred in the months of August through October, while showing significant positive trends in March and April (Zhang et al. 2001).

This trend of increasing streamflow in the spring and decreasing streamflow in the autumn may be indicative of a larger shift in the annual hydrologic cycle—an earlier snow melt

attributable to warmer spring temperatures (Zhang et al. 2000) resulting in less water remaining in the basin later in the year, and lower streamflows in summer and autumn. Peak streamflows, especially those in large basins, are generally associated with snowmelt, and the earlier warming in spring results in earlier but more gradual snowmelt because of shorter days and lower sun angle (Zhang et al. 2001). Increased proportion of spring precipitation falling as rain versus snow also accelerates melting of the snowpack as the wet snow absorbs more radiation (Zhang et al. 2001). During the last 30–50 years, the beginning of the freshet season in many basins has advanced by more than a month, particularly in British Columbia (Zhang et al. 2001). Zhang et al. (2001) argued that Canada has *not* experienced more extreme hydrological events with increasing temperature; they asserted that overall trends in annual streamflow were similar to trends in the higher quantiles of daily mean streamflow, but were not as coherently reflected in trends for the median (fiftieth percentiles) of daily mean streamflow. The trends in river ice breakup are consistent with the findings of Skinner (1992, cited in Zhang et al. (2001)). Notwithstanding, in western Canada, especially in British Columbia, the earlier freshet has been accompanied by an earlier freeze-up associated with decreasing November mean temperatures, resulting in no significant change in the length of ice cover period (Zhang et al. 2001). These results are in agreement with the study of Lettenmaier et al. (1994) who also found significant negative trends in autumn streamflow for the Northwestern United States. Hamlet et al. (2005) note that recent studies have shown substantial declines in snow water equivalent (SWE) over the last half-century for much of the western United States, accompanied by earlier spring snow melt and earlier peak streamflows.

Due to the limited 30–50 years of data in the study of Zhang et al. (2001), it is difficult to ascertain whether the trends in hydroclimatic variables reflect their long-term tendencies or simply interdecadal variations. The Pacific Decadal Oscillation is known to impact climate over western North America in particular, and the strongest trends in all of the hydroclimatic variables analyzed in Zhang et al.'s (2001) study were along Canada's the west coast. Hamlet et al. (2005) concatenated two warm period PDO epochs and found that declining trends in 1 April SWE in the western United States were not well explained by decadal climate variability associated with the PDO, but rather most strongly affected by widespread warming temperature trends. Precipitation variability also affected Apr 1 SWE but was attributed to

decadal variability rather than long-term trends (Hamlet et al. 2005).

4.8.2. Climate Change Forecasts for British Columbia

The IPCC uses multiple scenarios to model potential future climate conditions; each scenario is based on a story line about developments in technology, economic growth and international cooperation; emissions of greenhouse gases are estimated for each scenario, and used as input to global climate models (GCMs) (Moore et al. 2010). A range of future climates is possible, depending on the emissions scenario and the GCM used; the realism of the climate change forecasts must be treated as conditional on the realism of the global climate model(s) and emission scenarios used (Morrison et al. 2002). For the Province of British Columbia, all models and emissions scenarios used by the IPCC suggest an increase in temperature that grows with time (Moore et al. 2010). Southern and central British Columbia are expected to become drier in the summer and wetter in the winter, with greater warming and changes in precipitation than the global average (see Table 4.5).

Shrestha et al. (2012) modelled the spatial and temporal variability of climate-induced hydrologic changes in the Fraser River basin, British Columbia, including the discharge of the Thompson River at Spences Bridge. They simulated base-line (1970's) and future (2050's) hydrologic regimes based on climate forcings derived from eight global climate models run under three emissions scenarios (Shrestha et al. 2012). The most significant temporal projections included earlier onsets of snowmelt-driven peak discharge, consistent with the other studies mentioned above; as well as increased winter and spring runoff and decreased summer runoff most pronounced in the Central Plateau region (Shrestha et al. 2012). The modelling also revealed increases in the total annual discharge and decreases in the 30-year mean of the peak annual discharge (Shrestha et al. 2012). Table 4.6 summarizes the median projections by Shrestha et al. (2012) for changes in snow water equivalent and streamflow for the Central Plateau region and for the Thompson River at Spences Bridge, specifically.

Figure 4.17 shows Shrestha et al.'s (2012) modeled baseline (1970's) hydrograph and projected future (2050's) monthly discharge ranges at Spences Bridge for the global climate

models utilizing three emissions scenarios. The projected increase in the winter discharge is related to warmer temperatures and an increased percentage of winter precipitation falling as rain versus snow (Shrestha et al. 2012). Winter runoff that is *higher* than autumn runoff is projected to occur in some other areas of the Fraser River basin, indicating a shift from a hybrid to a rain-dominant regime in some parts of the region (Shrestha et al. 2012). An earlier onset of peak discharge was simulated for all sub-basins including Thompson-Spences, which can be explained as the effect of earlier snowmelt driven by warmer temperatures (Shrestha et al. 2012). Moreover, Shrestha et al. (2012) suggest the timing of the peak runoff for the Interior Plateau will occur earlier, in May, indicating an earlier depletion of seasonal snow storage, and decreased summer (June 1st) soil moisture in the Central Plateau region. In spite of increased winter and spring precipitation, peak discharge is projected to decrease, illustrating the temperature-driven change in snow storage affects both the timing and magnitude of the discharge (Shrestha et al. 2012). Shrestha et al. (2012) warned that the reduction in summer discharge could have especially adverse effects on water availability in the dry Central Plateau region.

The hydrologic responses to climate change projected by Shrestha et al. (2012) are corroborated by previous studies of the Fraser River basin by Morrison et al. (2002); in examining discharge records since 1912 for the Fraser River at Hope, B.C., the days by which one-third and one-half of the annual discharge is reached have been transpiring earlier, at rates of 0.11 and 0.09 days per year, respectively. They also found that the summer water temperatures have been increasing at a rate of approximately 0.02°C per year, which could have a substantial adverse effect on salmon spawning processes if this trend continues with future climate change (Morrison et al. 2002). In addition to the analysis of historical trends, Morrison et al. (2002) extended their study to include future climate predictions using two global climate models. Figure 4.18 shows the modeled and historical hydrographs for the Fraser River at Hope, B.C.; “base” refers to the baseline established using hydrometric data from the years 1961-1990 (Morrison et al. 2002). Figure 4.18 shows the average daily mean flows for each of the 30-year periods⁷ in the study; it can be seen that the peak flow decreases

⁷ Base refers to years 1961-1990; 2020: years 2010-2039; 2050: years 2040 to 2069; 2080: years 2070-2099.

with time and occurs progressively earlier in the year (Morrison et al. 2002). They also found significant seasonal changes in the future scenarios compared to the baseline; the 2080 curve shows a significant increase in spring flow, however, the largest absolute change in flow is the decrease in June at the time of the freshet (Morrison et al. 2002). Relative changes were 200% in March and – 40% during the freshet (Morrison et al. 2002).

Currently, the Fraser River discharge is dominated by the freshet resulting from melting of the snow pack; winter months are characterized by lower, relatively constant flows of about 1000 m³/s, which reach a peak of approximately ten times that amount by mid-June (Morrison et al. 2002). Flow in the Thompson River at Spences Bridge follows a similar pattern; winter discharge is low and relatively consistent in the range of 250-500 m³/s, then peaks in mid-June at nearly ten times the base amount (2,400 m³/s range). The projections by Morrison et al. (2002) suggest that by the end of the 21st century, 13% of the years will no longer be snowmelt dominated; peak flows in the Fraser River may occur as early as the first week of April, or as late as the second week of October; winter flows are predicted to be continually increasing, rather than stable, throughout the season, such that the modeled April 1 flow rate is double the January 1 flow rate (Morrison et al. 2002). By 2080, there is predicted to be a modest increase (300 m³/s) in the minimum flow compared to the baseline values, accompanied by a more substantial decrease (1600 m³/s) in peak flow; the total volume of flow, represented by the annual mean discharge, is only expected to increase by 150 m³/s, or about 5% by 2080 (Morrison et al. 2002). Morrison et al. (2002) observed that the smooth transition between the historical trends in flow and temperature and their forecasts lends weight to the argument that the historical trends may be related to climate change that has already transpired.

Morrison et al. (2002) also modeled stream temperature projections for the Thompson River at Spences Bridge; by 2080 the water temperature is predicted to be above the baseline high for nearly 10 weeks; in addition the water temperatures also exceed the 20°C temperature considered harmful to salmon spawning for approximately 4 weeks (Figure 4.19). Unless the salmon can adapt by adjusting the timing of their migration, these increasing temperatures may be expected to have dramatic impacts on spawning success and survival of the species in the Thompson River (Morrison et al. 2002).

4.8.3. Implications of Climate Trends and Forecasts for the Thompson River

There is consensus among several studies that warming temperatures in British Columbia are likely to produce earlier and lower peak flows and less disparity between high- and low-flow conditions in the Thompson and Fraser Rivers. In contrast, the years of historic landslide activity in the Thompson River Valley south of Ashcroft are associated with sustained, high peak river flows resulting in a cumulative flow departure from normal of at least 14% (Figure 4.6), and rapid change from low flow to high peak river flow conditions (Figure 4.5), preceded by high snow pack (Figure 4.8) and cool spring temperatures resulting in a late, rapid freshet (Septer 2007). If snow pack in central British Columbia is diminished and spring thaw continues to occur earlier with more gradual snow melt, it is possible that climate change may have an attenuating effect on landslide activity in the Thompson River Valley south of Ashcroft.

Collison et al. (2000) modelled future changes in the slope hydrology and attendant stability of a 4-km escarpment in southeast England as a result of predicted increases in rainfall and temperature due to climate change. They found that in spite of a predicted increase in mean annual rainfall of 11%, increased temperature and evapotranspiration rates will maintain a high soil moisture deficit in the escarpment, resulting in a generally decreasing trend in porewater pressure and the associated occurrence of deep-seated landslides (Collison et al. 2000). They noted that other factors such as land use change and human activity are likely to have a greater impact on landslide frequency along the escarpment than climate change over the next 80 years (Collison et al. 2000).

4.9. Conclusion

In analyzing the discharge records for the past century at Spences Bridge, it is evident that the cumulative flow of the Thompson River is subject to interannual and interdecadal cycles. The 20th century activities of the Ashcroft Thompson River landslides mirror the interannual and interdecadal variations in river flow. To the extent that the 20th century activity of the Ashcroft

Thompson River landslides are associated with years when the Thompson River exhibits anomalously high discharge preceded by higher winter snow pack measurements, the apparent clustering of landslide activity within the cool/wet regimes of the Pacific Decadal Oscillation (PDO) is a logical extension. Identifying regime shifts in the PDO is still, essentially, a retrospective exercise; notwithstanding the absence of a theoretical understanding, PDO climate information improves season-to-season and year-to-year climate forecasts for North America because of its strong tendency for multi-season and multi-year persistence (Mantua 2002).

Taking the long view of hazard phenomena and seeking to understand the higher-level interactions between the hazards and the surrounding environment lies at the heart of the resilience paradigm for coping with complex risks. By understanding how and why the system as a whole is changing, we are better positioned to foresee and build capacity to cope with change, rather than falling victim to it (Walker and Salt 2006). An awareness of climate variations and their effect on the snow pack and stream flow in the Thompson River Valley is an essential component of a well-balanced understanding of past landslide frequency and the likelihood of future landslide events. Correlations of landslide activity to river flow and regional snow pack could potentially serve as an early-warning tool for anticipating slope movements in the corridor, while monitoring broader climate patterns such as the PDO may be beneficial for longer-term (interdecadal) forecasting of periods of increased landslide activity. Peak snow pack departures from normal of approximately 20% and cumulative river flow departures from normal of approximately 14% (3,400 Mm³) have historically portended seasonal landslide activity in the corridor; in the 20th century, these criteria were exceeded once every 4.4 years during the cool/wet PDO regimes and only about once per decade during warm/dry phases of the PDO.

The cluster of rapid landslides which occurred in the corridor during the late 1800's coincided with the warm/dry PDO regime of 1870 to 1889/90 identified by Minobe (1997). In keeping with the working hypothesis that these 19th century landslides were largely related to the introduction of ditch-and-furrow irrigation, the clustering of these events within a dry regime

of the PDO makes sense—unusually dry climate conditions would likely correspond to unusually high levels of water input through anthropogenic irrigation.

As evidenced by Figure 4.5, there has been a down cycle in the Thompson River flow departure from normal since 2001, and a corresponding absence of noticeable landslide activity in the corridor. The 20th century periodicity of the PDO would suggest that we should anticipate an upswing in cumulative river flow and a worsening of slope stability conditions in the corridor within the coming years. Looking further into the future, several climate change studies (Zhang et al. 2000, 2001, Morrison et al. 2002, Shrestha et al. 2012) have suggested that warming temperatures in British Columbia are likely to produce earlier and lower peak flows and less disparity between high- and low-flow conditions in the Thompson River. In contrast, the years of historic landslide activity in the Thompson River Valley south of Ashcroft have been associated with sustained, high peak river flows resulting in a cumulative flow departure from normal of at least 3,400 Mm³, and a rapid change from low flow to high peak river flow conditions that is preceded by high snow pack and cool spring temperatures resulting in a late, rapid freshet. If snow pack in central British Columbia is diminished and spring thaw continues to occur earlier with more gradual snow melt, it is possible that climate change may have an attenuating effect on landslide activity in the Thompson River Valley south of Ashcroft—though this should be the subject of ongoing study as more information emerges.

Table 4.1: Summary of hydrologic years with cumulative flow departure from normal exceeding 3400 Mm³ for Thompson River flow at Spences Bridge from 1913 to 2011.

Hydrologic Year (October—September)	Cumulative Flow Departure from Normal (Mm ³) at Spences Bridge	Flow Departure Normalized to Annual Station Average (%)
1921	3924	17 %
1928	4782	20 %
1935	4311	18 %
1948	6546	28 %
1954	4464	18 %
1960	4129	17 %
1968	3628	15 %
1972	5125	21 %
1974	3474	14 %
1976	6296	26 %
1982	4978	20 %
1996	5392	22 %
1997	8485	35 %
1999	8772	36 %
2000	4127	17 %

Table 4.2: Snow survey sites utilized in snow pack versus river flow analysis; modified from Province of British Columbia (2014)

Site Number	Basin	Station Name	Elevation (m)	Latitude	Longitude	Period of Record
1E01	N. Thompson	Blue River	690	52°08'	119°15'	1938-79
1E01A	N. Thompson	Blue River Town	670	52°08'	119°15'	1971-87
1E01B	N. Thompson	Blue River	673	52°08'	119°17'	1983-present
1E02	N. Thompson	Mount Cook	1830	52°11'	119°20'	1950-75
1E02A	N. Thompson	Mount Cook	1580	52°11'	119°19'	1974-2004
1E03	N. Thompson	Trophy Mountain	1900	51°49'	119°56'	1950-80
1E03A	N. Thompson	Trophy Mountain	1907	51° 48'	119°56'	1974-present
1E04	N. Thompson	Mount Albreda	1920	52°30'	119°03'	1950-91
1E05	N. Thompson	Knouff Lake	1189	50°59'	120°07'	1955-present
1E06	N. Thompson	Cook Forks	1390	52°10'	119°19'	1963-2004
1E07	N. Thompson	Adams River	1769	51°35'	119°25'	1970-present
1E08	N. Thompson	Azure River	1620	52°37'	119°43'	1970-2005
1E08P	N Thompson	Azure River	1310	52°37'	119°43'	1996
1E10	N. Thompson	Kostal Lake	1770	52°12'	120°02'	1974-94
1E10P	N Thompson	Kostal Lake	1770	52°12'	120°02'	1984-2011
1E13	N. Thompson	North Clemina Creek	1860	52°34'	118°57'	1989-2005
1F01A	S. Thompson	Aberdeen Lake	1262	50°08'	119°03'	1938-present
1F02	S. Thompson	Anglemont	1168	50°59'	119°11'	1956-present
1F03	S. Thompson	Park Mountain	1890	50°27'	118°37'	1957-95
1F03P	S. Thompson	Park Mountain	1890	50°27'	118°37'	1984-2011
1F04	S. Thompson	Enderby	1948	50°39'	118°55'	1963-present

Table 4.3: Summary of Pacific and North American climate anomalies associated with extreme phases of the PDO (Mantua 2002). Reproduced with permission.

Climate anomalies	Warm phase PDO	Cool phase PDO
Ocean surface temperatures in the northeastern and tropical Pacific	Above average	Below average
October–March northwestern North American air temperatures	Above average	Below average
October–March Southeastern US air temperatures	Below average	Above average
October–March southern US/Northern Mexico precipitation	Above average	Below average
October–March Northwestern North America and Great Lakes precipitation	Below average	Above average
Northwestern North American spring time snow pack and water year (October–September) stream flow	Below average	Above average

Table 4.4: Summary of snow monitoring stations with readings in excess of 500% of normal for the spring of 1982.

Snow Course Name	Number	Elev.	Date of Survey	Snow Depth	Snow Water Equivalent, SWE	% of Normal
Lac Le Jeune	1C07	1370	1982-04-29	32	87	791 %
Highland Valley	1C09A	1457	1982-05-14	11	29	967 %
Bralorne	1C14	1382	1982-05-12	29	80	727 %
Gnawed Mountain	1C19	1617	1982-05-13	35	122	530 %
Spahomin	1C30	1450	1982-04-30	14	40	1333 %

Table 4.5: Climate change projections for British Columbia (seven models and eight emission scenarios). Data are the changes from 1961 to 1990 climate as a change in mean temperature or a percentage change in total precipitation (PPT) (Moore et al. 2010).

	2020		2050		2080	
	Temperature (°C)	PPT (%)	Temperature (°C)	PPT (%)	Temperature (°C)	PPT (%)
Southern British Columbia						
Winter	0 to 2	-5 to +15	1.5 to 3.5	0 to +20	2 to 7	0 to 25
Summer	0.5 to 2	-30 to +5	1.5 to 4	-35 to 0	2.5 to 7.5	-50 to 0
Central British Columbia						
Winter	0 to 2	-5 to +15	1.5 to 4	0 to +30	2.5 to 6	+5 to +40
Summer	0.5 to 1.5	-10 to +5	1.8 to 3.5	-20 to 0	2.5 to 6.5	-20 to +5
Northern British Columbia						
Winter	0 to 2.5	0 to 20	1.5 to 5.5	0 to +25	2.5 to 9	0 to +45
Summer	0.5 to 1.5	-10 to +10	1.5 to 3.5	-10 to +15	2 to 6	-15 to +25

Table 4.6: GCM ensemble medians of April 1st SWE volume and annual discharge changes (2050s versus 1970s) for emissions scenarios B1, A1B and A2 (modified from Shrestha et al. (2012)).

Region/Sub-basin	April 1 st SWE change (%)			Flow volume change (%)		
	B1	A1B	A2	B1	A1B	A2
Central Plateau	-30	-44	-44	4	0	-4
Thompson–Spences Bridge	-28	-35	-41	9	6	2

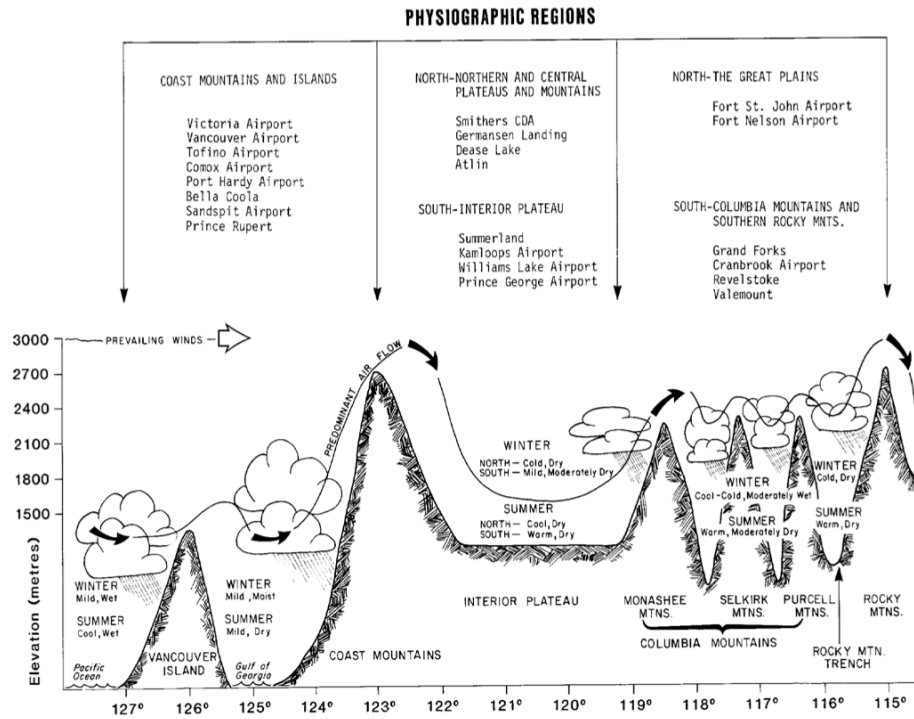


Figure 4.1: Latitudinal cross-section of southern British Columbia, illustrating the physiographic diversity and associated climatic regimes (Chilton 1981).

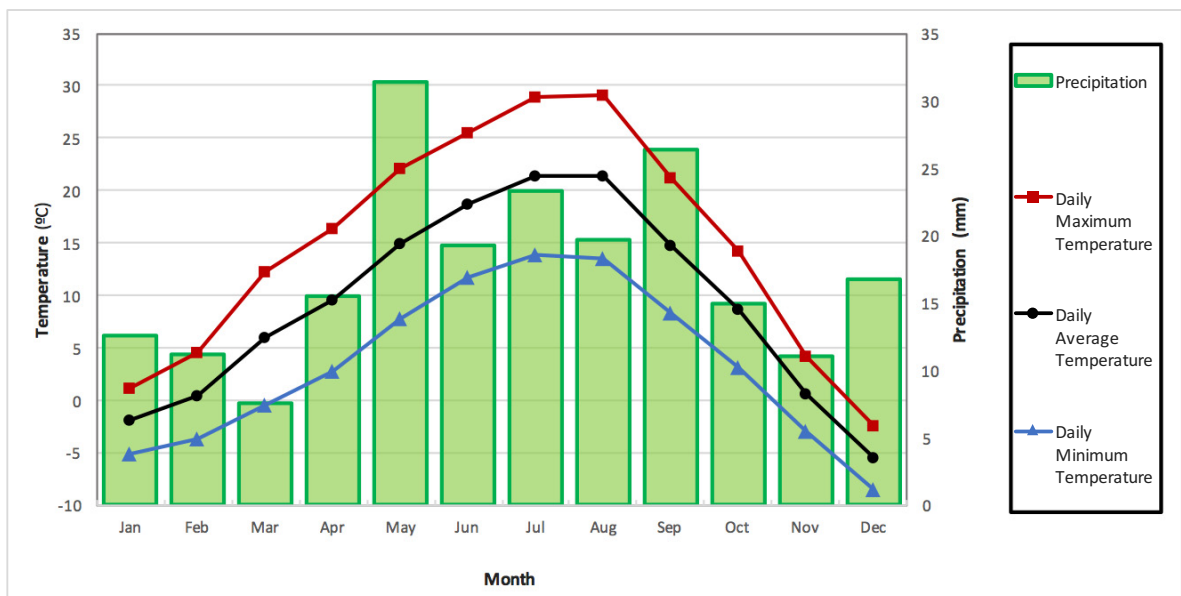


Figure 4.2: Ashcroft North weather station; temperature and average precipitation, 1980-1986 (Environment Canada 2015b).

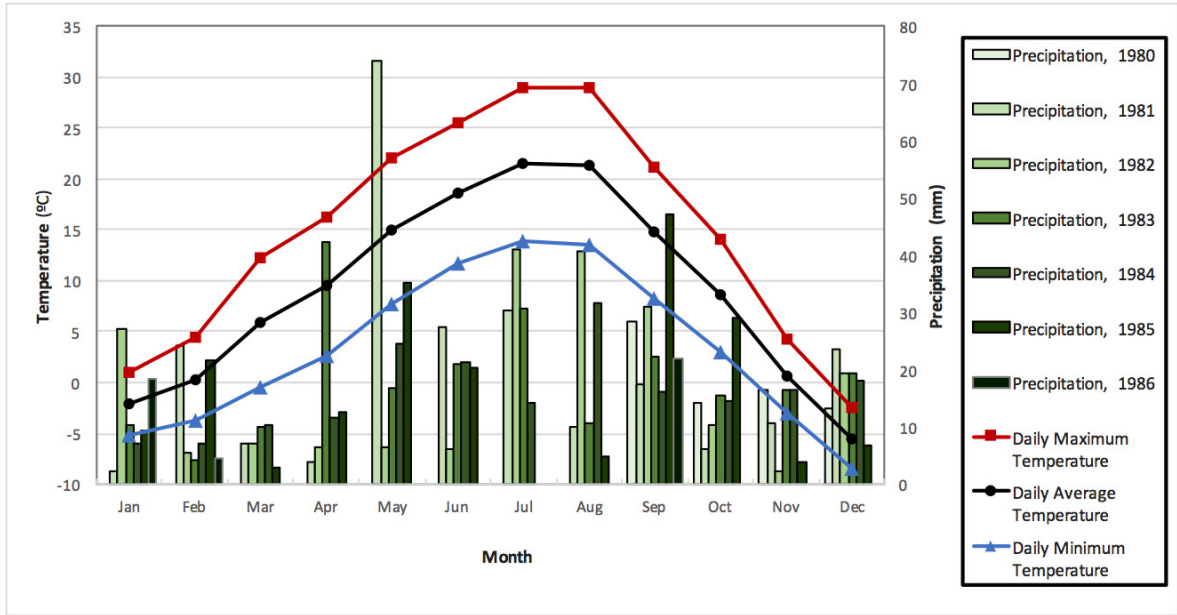


Figure 4.3: Ashcroft North weather station; temperature and annual precipitation, 1980-1986 (Environment Canada 2015b).

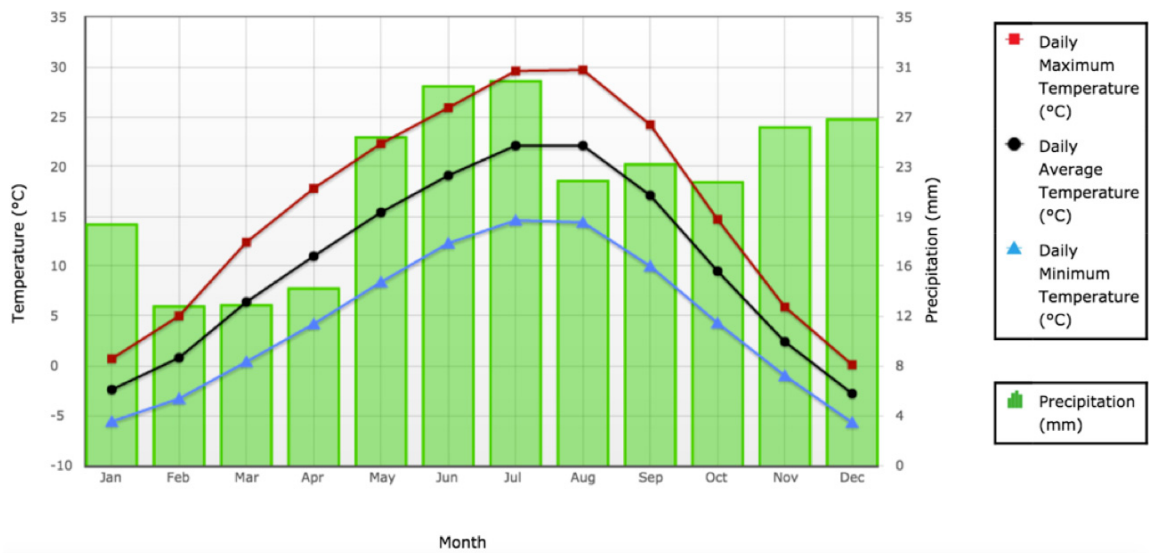


Figure 4.4: Spences Bridge Nicola weather station; temperature and precipitation normals, 1981-2002 (Environment Canada 2015b).

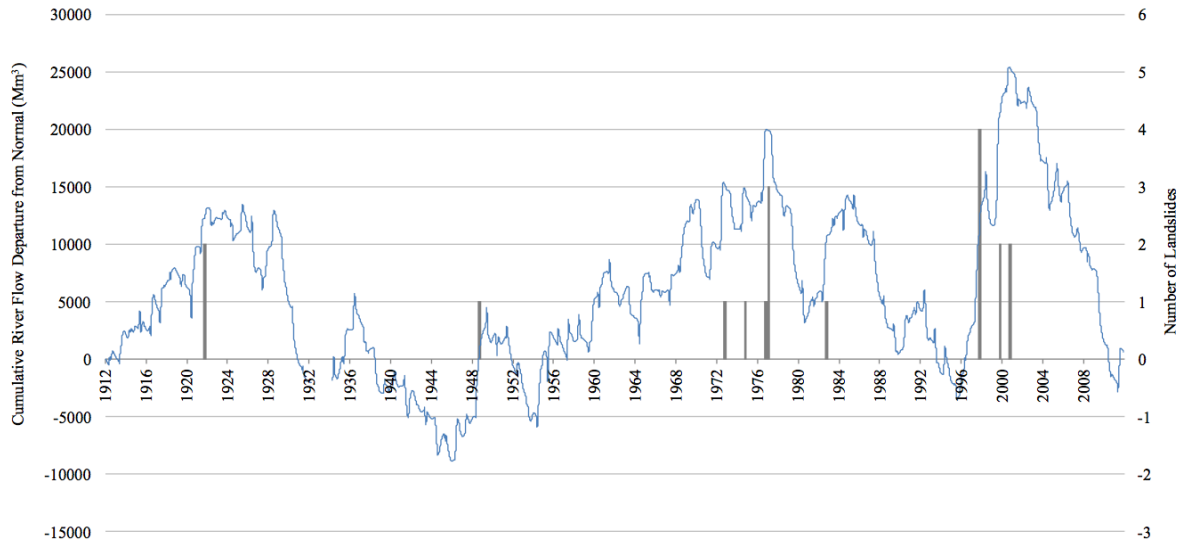


Figure 4.5: Thompson River cumulative flow departure from normal, Spences Bridge station 08LF022 (1912-1951) and station 08LF051 (1952-2011), with 20th century landslide activity indicated.

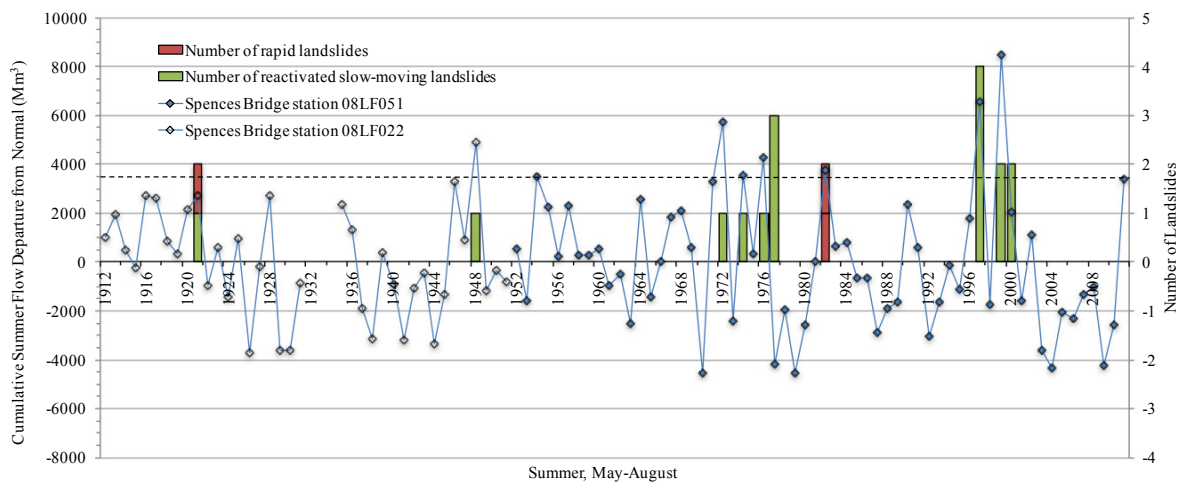


Figure 4.6: Annual cumulative flow departure from normal by hydrologic year (October – September), Thompson River at Spences Bridge; 1913-2011.

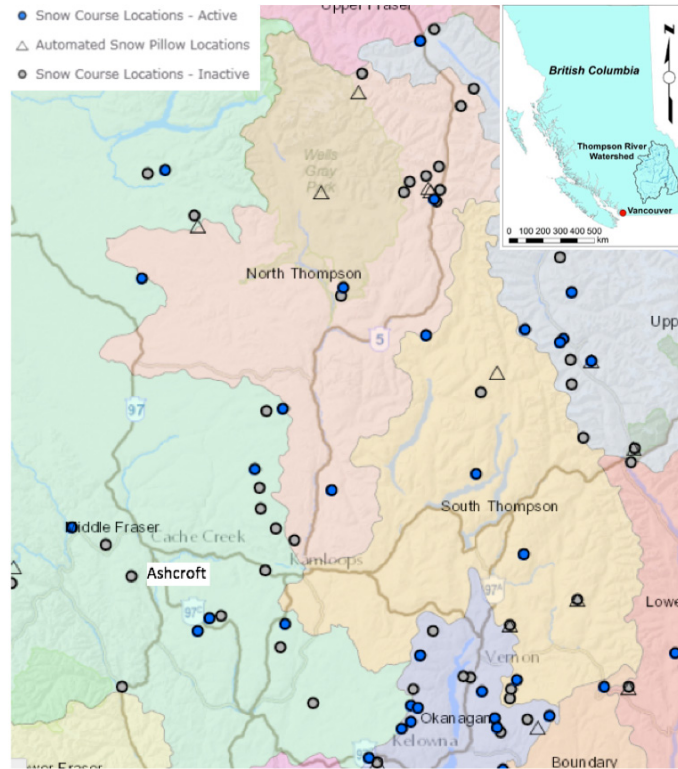


Figure 4.7: Overview of manual and automated snow survey sites, with boundaries of the North Thompson and South Thompson administrative basin areas as shown; modified from the Province of British Columbia (2016c), and Quinn et al. (2012).

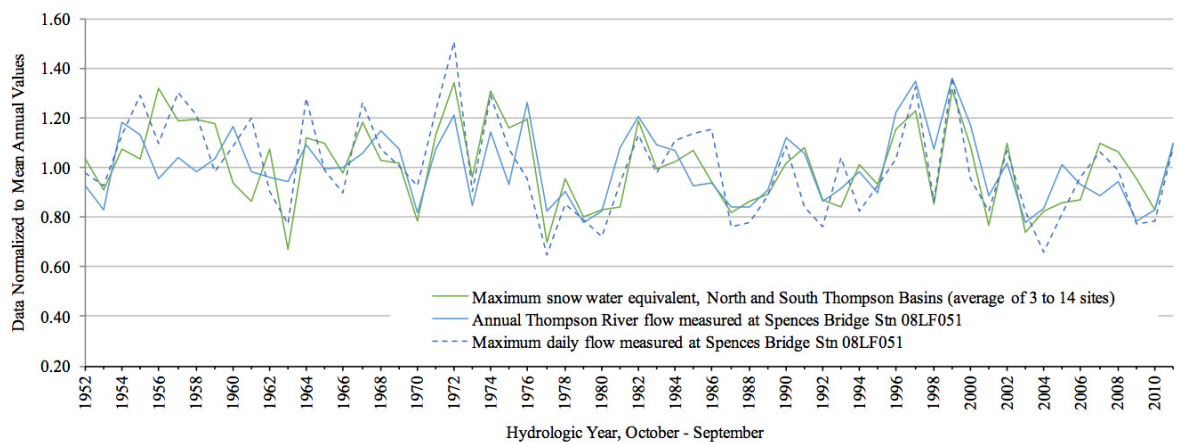


Figure 4.8: Relationship between peak snow pack (snow water equivalent) measured in the North and South Thompson River basins and annual and maximum Thompson River flow, 1952-2011.

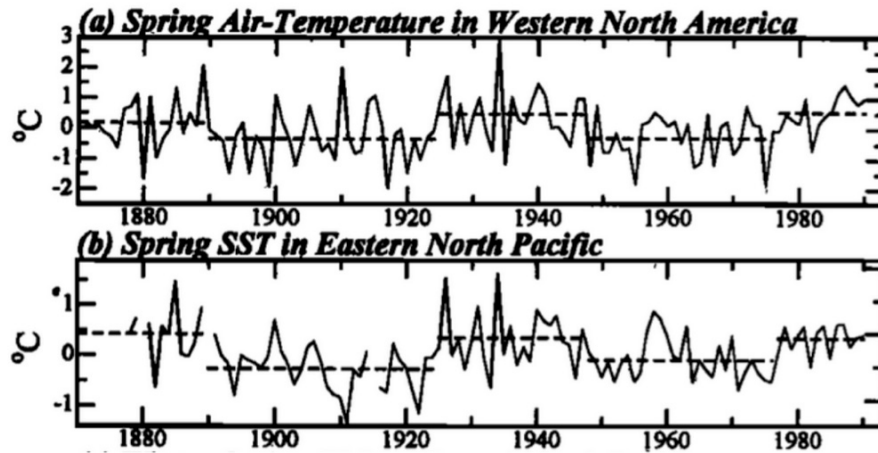


Figure 4.9: Time series of anomalies exhibiting coherent inter-decadal climate changes (thin solid curve), with temporal averages of the anomalies for the periods 1870-1889, 1890-1924, 1925-1947, 1948-1976 and 1977-1990 (thick dashed lines). (a) Spring (Mar-May) air-temperature anomalies in western North America averaged over 130°W-105°W, 30°N-55°N. (b) Spring SST anomalies in the eastern North Pacific average over 140°W-110°W, 30°N-55°N. All differences in the temporal average between successive periods are significant at the 95% confidence level in each time series (Minobe 1997). Reproduced with permission.

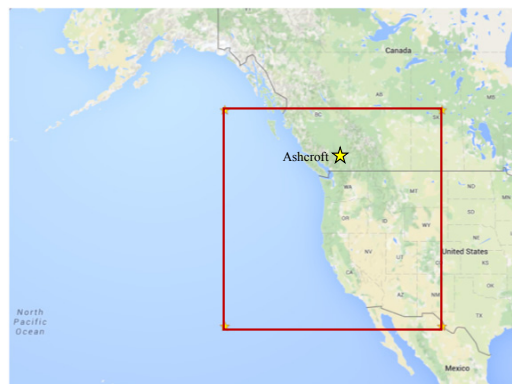


Figure 4.10: Outer extents of Minobe's (1997) study area (140°W-105°W and 30°N-55°N), with location of Ashcroft indicated.

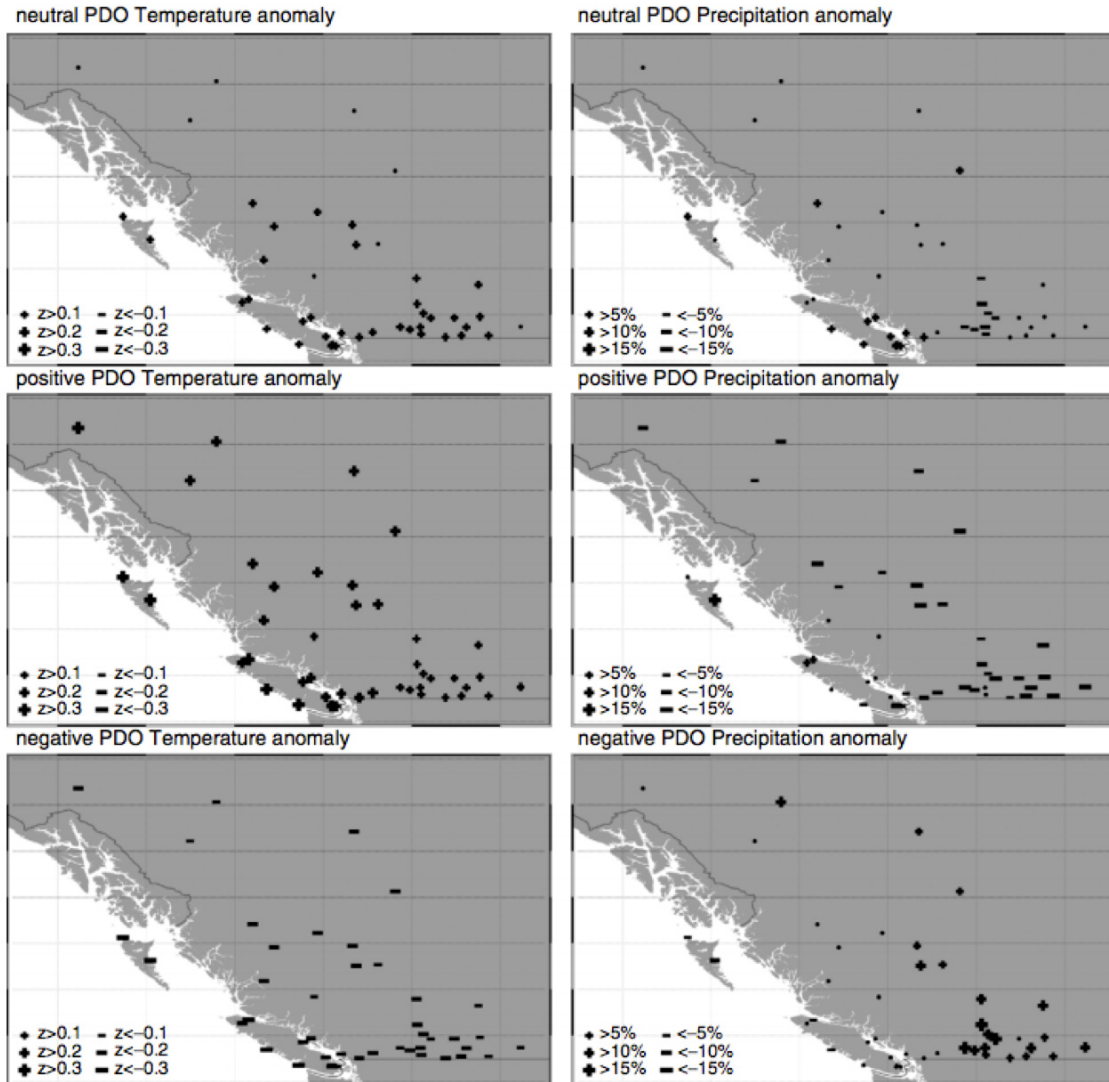


Figure 4.11: British Columbia winter (Dec-Feb) temperature and precipitation anomalies during neutral, positive and negative phases of the PDO (Stahl et al. 2006). Reproduced with permission.

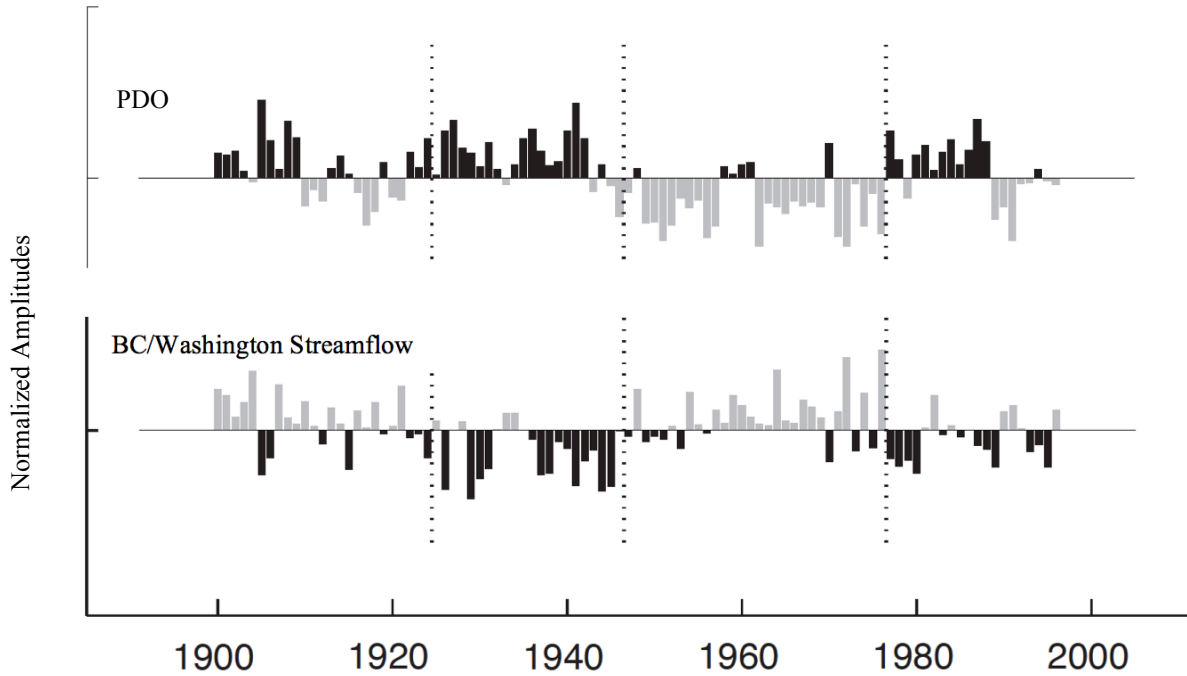


Figure 4.12: Normalized winter mean (November—March) time histories of Pacific Climate indices, with stream flow time series for Skeena, Fraser and Columbia Rivers (shading convention is reversed). Dotted vertical lines are drawn to mark the PDO polarity reversal times in 1925, 1947, and 1977 (Mantua et al. 1997). © American Meteorological Society; reproduced with permission.

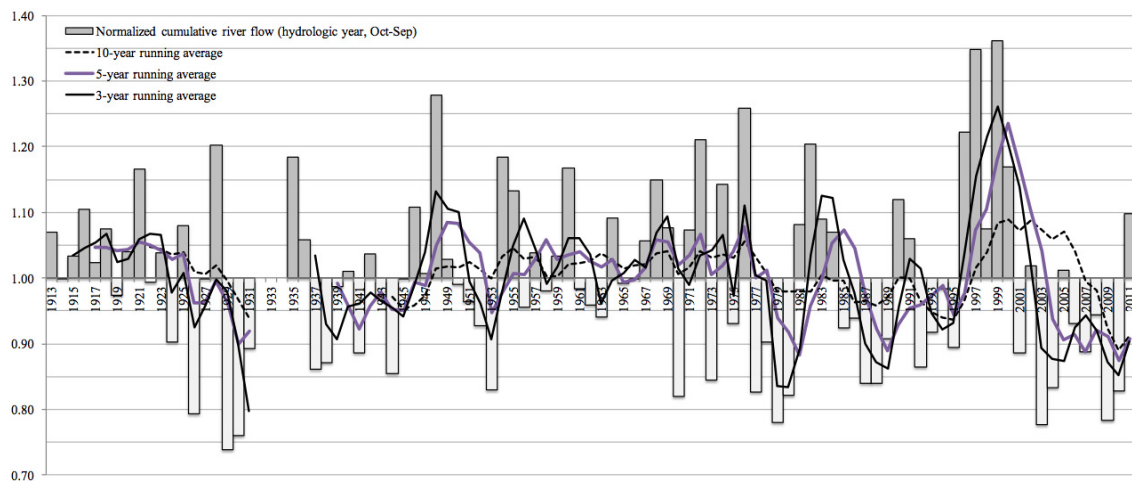


Figure 4.13: Times series of normalized annual flow departure from normal for hydrologic (October to September) years 1913 to 2011, with 3-, 5-, and 10-year running averages overlain.

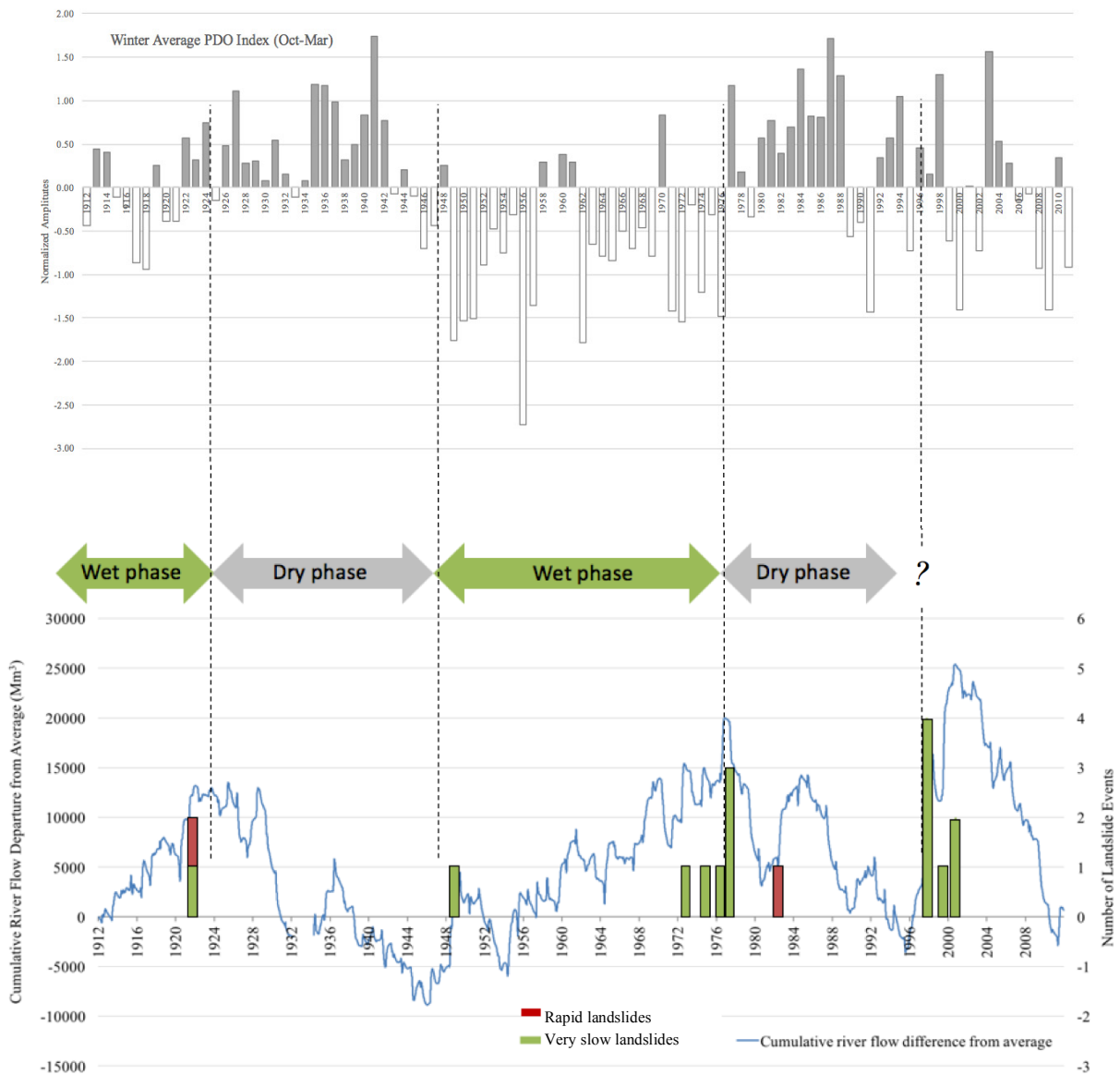


Figure 4.14: Comparison of Pacific Decadal Oscillation (PDO) index to Thompson River cumulative flow departure from normal at Spences Bridge, with number of landslides indicated; 1912-2011.

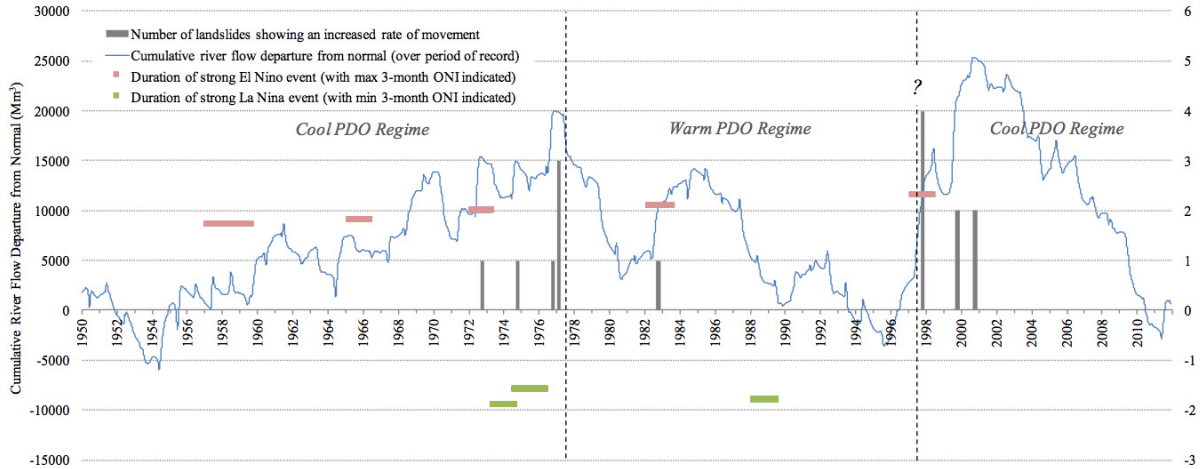


Figure 4.15: Strong/very strong ENSO events, landslide activity, and cumulative Thompson River flow departure from normal, with PDO regimes indicated; 1950-2011.

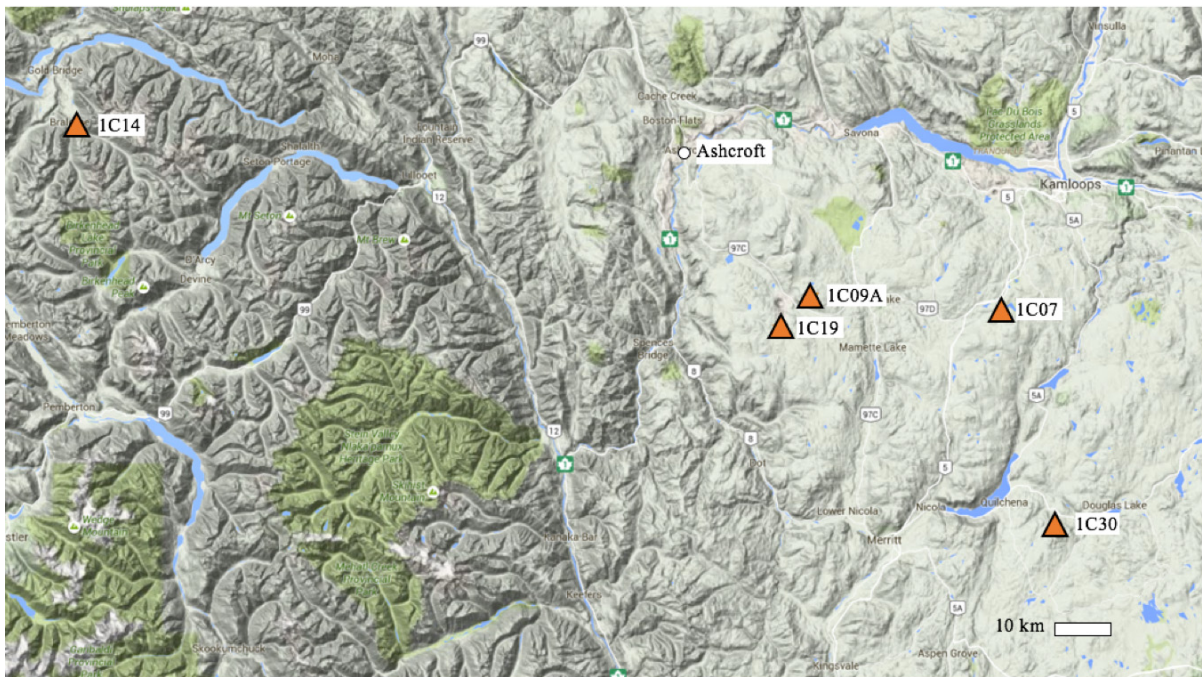


Figure 4.16: Locations of snow survey sites within approximately 100 km of Ashcroft with SWE in excess of 500% of normal on May 1, 1982. Province of British Columbia (2016c).

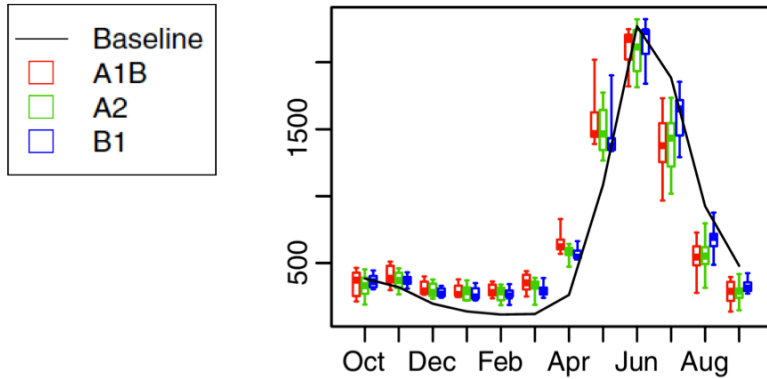


Figure 4.17: Baseline (1970's) and future (2050's) discharge for three emissions scenarios for the Thompson River at Spences Bridge. Each box plot shows the median and inter-quartile range, with whiskers denoting upper and lower limits of the 30-year means of GCM ensembles (Shrestha et al. 2012). Reproduced with permission.

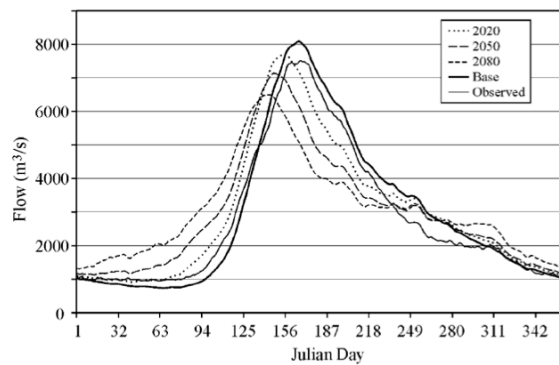


Figure 4.18: Fraser River average daily flows at Hope, B.C.; base, observed and projected (Morrison et al. 2002). Reproduced with permission.

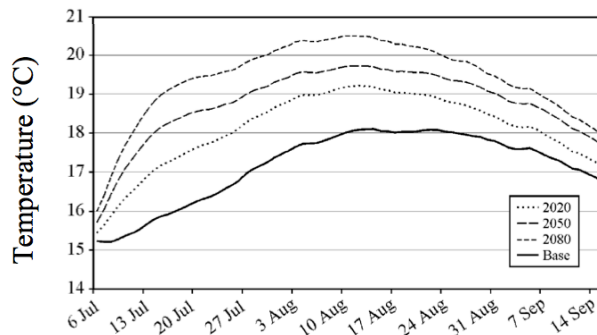


Figure 4.19: Thompson River summer temperatures at Spences Bridge; base and projected (Morrison et al. 2002). Reproduced with permission.

5. LANDSLIDE MECHANICS

“Large landslides seldom have a single and unambiguous cause.”

— Morgenstern (1986)

5.1. On Accelerations of Slow-Moving Landslides

In general, first-time landslides tend to exhibit considerable, and sometimes rapid, displacements during failure while renewals of movement in landslides on pre-existing rupture surfaces are usually associated with modest speed and travel (Skempton and Hutchinson 1969, Hutchinson 1988). Notwithstanding, rapid renewals of movement (or reactivations exhibiting a brittle mode of failure) may arise on existing rupture surfaces due to a variety of causal factors, which to quote Hutchinson (1988) “... are the more dangerous for being unexpected.” The catalyst for accelerating a dormant or extremely slow moving landslide towards rapid failure is conventionally understood to be a sudden change in external loading/boundary conditions or in the internal distribution of porewater pressure or soil strength (Hutchinson 1987, D’Elia et al. 1998, Leroueil 2001). Those causal factors which are extrinsic to the slope itself may include increased groundwater pressure due to variation in climate conditions on the local and regional scale (Chapter 4), intensive irrigation of river terraces, and stress change due to removal of material from the base of the landslide resulting from river erosion or construction activities. Internal causes are generally understood to be related to the microstructure of the soil, including a change in strength and corresponding brittleness along the shear surface due to cementation, chemical alteration or geomorphologic processes.

The causes of the Ashcroft Thompson River landslides are complex, and have varied spatially and over time. Preparatory factors which predispose the valley walls to movement, including ground conditions and geomorphologic processes were described in Chapter 2. Given the evolution of natural and anthropogenic impacts to the Thompson River Valley slopes, causal factors identified for the historical landslide movements can be grouped according to abandoned and active conditions.

Historic (abandoned) causal factors include:

- Inundation of river terraces with water via ditch-and-furrow irrigation methods;
- Original railway construction impacts to slope geometry and river hydrology/erosion.

Active factors contributing to slope instability include:

- Elevated porewater pressures and seepage forces induced by local and regional groundwater flow— related to regional climate conditions (typically portended by basin-wide snowpack 20% above normal, cumulative river flow departure more than 14% above normal, as described in Chapter 4);
- River erosion— estimated maximum rates of approximately 300 mm/year of loosely-deposited material at the feet of unprotected slides (Section 5.2.2.1);
- Human interference— including modification of slope geometry by excavation or fill placement (Ripley siding construction, Huntley et al. (2016)), in-stream construction activities (South slide and CN 50.9 slide, Section 7.2) and ongoing irrigation (though contemporary water-efficient irrigation systems are unlikely sufficient to trigger rapid renewals of movement (BC Court of Appeal 1990)).

Popescu (1994) suggested there is a clear distinction between preparatory factors (those causes which bring a slope into a state of marginal stability) and triggering factors (those which initiate movement); I would argue that for natural hillslopes of complex geology, these lines are blurred. As per Sowers and Sowers (1970):

“In most cases a number of causes exist simultaneously and so attempting to decide which one finally produced failure is not only difficult but also incorrect. Often the final factor is nothing more than a trigger that set in motion an earth mass that was already on the verge of failure. Calling the final factor the cause is like calling the match that lit the fuse... the cause of the disaster” (p. 506).

In their book *Resilience Thinking*, Walker and Salt (2006) suggest that natural systems exist in multiple dynamic states of equilibrium, or “regimes”, separated by thresholds which may be crossed. This concept is somewhat analogous to Hutchinson’s (1975) writings on the cyclical nature of landslide reactivations subject to differing rates of toe erosion. Acknowledging that the Ashcroft Thompson River landslide deposits may exist in multiple dynamic states, separated by kinematic thresholds, is a powerful concept for understanding their long-term

behavior. The different modes of failure and associated velocities which have been documented for these landslides over the past 150 years suggest that the nature of the slope movements may change abruptly, not only in response to changes in external boundary conditions induced by factors such as irrigation and climate, but also in response to the internal kinematics of the slope movement itself. A threshold is crossed when a landslide exhibiting stepped, extremely slow seasonal displacements, accelerates suddenly towards rapid failure. The internal kinematics of a compound translational landslide, associated with the formation and coalescence of cracks delineating the active and passive blocks, can evolve gradually over many years (see Figure 5.1). The formation of the active block may constitute the kinematic threshold which ushers a slow-moving landslide into the state of rapid reactivation.

In the case of the Goddard landslide, a rapid compound translational movement was preceded by minor precursory events; these served the detrimental function of developing minor scarps and corresponding extension near the toe of the slide, which permitted the progressive formation of the major upslope backscarp, followed by formation and growth of the counterscarp, and ultimately the rapid translation of the slide driven by the fully-formed active block (Figure 5.1). I would contend that these precursory movements perform the critical functions of achieving a kinematically admissible failure mechanism through internal shearing of the slide mass (Hutchinson 1987), which may culminate in large slope movements when the counterscarp, which has taken years to grow, penetrates to the depth of the rupture surface. An integrated understanding of the interplay of causal factors and kinematic thresholds accounts for the sometimes perplexing behavior of natural slopes that appear to fail as a result of a seemingly innocuous event, or during a year of unremarkable weather conditions.

5.2. Interpreted Modes of Movement

Three modes of movement are proposed for classifying the large landslides which have occurred along the Thompson River Valley south of Ashcroft since the late-1800's, as documented in Chapter 3. These modes of movement are subsequently treated as separate hazard scenarios for the risk assessment that follows in Chapter 6; they are: I) complex, very rapid earth slide–debris flow; II) reactivated, rapid, compound earth slide; and III) reactivated,

very/extremely slow earth slide. The following sections describe how these classifications were arrived at, with reference to selected landslide events from the Thompson River Valley south of Ashcroft representing each hazard scenario. Hungr et al. (2005) noted that the best way to assess a landslide's potential for catastrophic failure is to compare it to similar case histories whose failure stages have already taken place; the following sections also draw comparisons between the hazard scenarios and contemporary case studies of similar landslides which have occurred elsewhere. Classification of landslide type follows the terminology of Cruden and VanDine (2013), and landslide velocity (movement rate) is categorized according to Cruden and Varnes (1996).

5.2.1. Complex⁸ Earth Slide–Debris Flow (North Slide, Spences Bridge Slide)

As described in Chapter 3, the North Slide occurred on the east bank of the Thompson River on October 14, 1880, and was the largest of the landslides along the subject corridor, with an estimated volume of 21 Mm³ (Eshraghian et al. 2007). A field visit to the North slide in June 2016 facilitated the observation of many uphill-facing scarps/ridges in the main body and towards the toe of the North slide, as indicated in Figure 5.2. The persistence of these features is typical of (semi-)arid climates; they correspond to the internal shears necessary for a kinematically-admissible compound slide in brittle materials, according to Hutchinson (1987). The orientation of the blocks so delineated within the disturbed mass are sub-parallel to the slope, suggesting sliding along a rupture surface that is slightly inclined towards the river. A cross-section through the North slide is presented at natural scale in Figure 5.3. The surface contours are based on 2015 LiDAR data provided by CN and processed by R. Macciotta (personal communication, 2017); the stratigraphic information and rupture surface elevation (at track level) is based on Eshraghian et al. (2007).

Stanton (1904) observed of the North slide that “In dropping and pushing out toward the river, the whole tract was broken into sections by great cracks, which still exist. The larger cracks

⁸ According to Varnes (1978), *complex* refers to slope movements that exhibit more than one of the major modes of movement.

run parallel with the river and at right angles to the line of movement...” (p. 311). Though weathering has obscured some of the salient features of the North slide, these extension cracks are readily detectable along the upper portion of the disturbed mass in the 1928 air photo (Figure 5.4). As evident in Figure 5.2, substantial weathering of the main scarp of the slide has occurred in the intervening 136 years since 1880, when the scarp and lateral margins of the North slide originally stood “vertically to a height of between 50 feet and 200 feet, ...where the vertical cliffs of boulder clay, and in places of the silt itself, extend round the whole slide...” (Stanton 1898, p.4).

Stanton (1904) describes the events leading up to the landslides of the late-1800’s (including the North slide) as follows:

“In every instance noted, these slides occurred from 3 to 6 years after irrigation began at each point. ...A very large quantity of water was necessary for raising crops, on account of the sandy nature of the soil and the nature of the subsoil. The topography of the several benches assisted materially toward the final result. Each field being in the form of a shallow basin, around which the irrigation ditches were built, little of the surplus water was drained off; hence the greater part of that not taken up by the plants or by evaporation ran towards the center of the field and soaked down in one channel.” And, *“...In the case of the larger one, the great north slide, the final catastrophe was hastened by the bursting of a small reservoir”* (p. 311).

A working hypothesis is that the North Slide was a complex, very rapid, very wet, earth slide-debris flow. Because it was the only slide that reportedly involved the breach of an irrigation reservoir, it differs in type from the other slides. Based on Stanton’s (1904) description, it is reasonable to assume that the piezometric surface at the North slide coincided with the ground surface, and that there was sufficient standing water available to drain into the slide and rapidly drive the displacing mass towards the river as it began to move. The travel angle of the North slide was approximately 8.5° , being the inverse tangent of the height of the crown, approximately 150 m (Stanton 1898a, 1904, Eshraghian et al. 2007), divided by the distance to the opposite bank of the Thompson River, approximately 1000 m (as measured from the 1928 aerial photos). The travel angle would likely have been even lower had the displaced material not run up against the opposite bank of the river, where it formed a dam approximately 50 m (160 feet) high (Stanton 1898a). In any case, the travel angle was lower than the range of residual friction angles measured on the unit 2 rupture surface materials of 10° – 15° (Bishop

2008), suggesting some additional driving forces may have contributed to the movement; these could include undrained loading and bedding inclined towards the river.

Undrained loading is a possibility as a result of the breaching of a nearby irrigation dam which preceded the North slide of 1880. According to Stanton (1898a): "...some time before the final catastrophe occurred a reservoir 2 miles distant in the hills from which the irrigation water came, broke its dam, and most of the water liberated spread over the upper benches of this land, already well soaked. The whole tract of 150 acres sank vertically in one movement to a depth, at the back edge, of over 400 feet" (p. 5). The risers of the terraces are abandoned slopes (in Hutchinson's (1975) terminology) so their toes would be protected by colluvial accumulations shed by the slopes due to desiccation and weathering in a dry state, below Proctor-optimum moisture contents. Saturation of this loose colluvium by overflowing irrigation water could cause the colluvium to contract and flow onto the alluvium which mantles the terrace flats. This undrained loading of the alluvial sediments could cause them to liquefy and flow into the active channel of the Thompson (liquefaction by undrained loading, Hutchinson and Bhandari (1971)).

Stanton (1904) characterized the North slide as consisting of large, back-tilted blocks which moved on a layer of "oozing" silt. Cambie (1902) described an experiment on a block of dry, indurated clay obtained from the site of one of the landslides south of Ashcroft:

"When a block of this dry indurated clay was placed in a soup plate and water dropped upon it, the clay absorbed 50 per cent of its own weight without any change of form or other visible effect, but when it had absorbed about 60 per cent of water, its structure completely collapsed, and it became as fluid as water" (p. 198).

Cambie's (1902) description suggests that some cementing agent, such as calcium carbonate, or interparticle clay forces which were destroyed by saturation of the sample, were responsible for the majority of its strength in the dry state. Lum (1979) concluded that the high strength of the South Thompson silts under low degrees of saturation, typical of the semi-arid environments in which they occur, is due to substantial apparent cohesion, the magnitude of which is controlled by the degree of saturation. While the overconsolidated glaciolacustrine clays and silts of units 2 and 3 would not exhibit the open fabric and conditionally-collapsible

nature of the surficial late-glacial silts studied by Lum (1979), it is still possible that similar carbonate cementation and interparticle forces may be responsible for the high apparent strength of these deposits in a dry (likely unsaturated) state, resulting in a substantial loss of strength when saturated. Carbonate cementation, as evidenced by white precipitates at the locations of groundwater seepage, can be readily observed along the Thompson River Valley south of Ashcroft (Figure 5.5). Ingress of ample irrigation water into unit 2 would promote softening and failure along pre-sheared clay layer(s). The availability of ponded water and the saturation of overlying sediments would serve to rapidly drive the displacing mass towards the river as it began to move.

Iverson et al. (2015) noted that high pore pressures may dissipate slowly in rapidly moving, water-laden landslides that contain even small amounts of silt and clay, allowing the moving sediment-water mixtures to retain high mobility. Rapid, undrained loading of loose, wet sediments on terraces or at river level has been hypothesized as contributing to unusually high landslide mobility, as in the contemporary case of the fatal Oso landslide in Washington which occurred on March 22, 2014 following a period of unusually wet weather. Observational evidence and numerical simulation of the landslide, documented by Iverson et al. (2015), supported the hypothesis that the high mobility of the landslide resulted from liquefaction of water-saturated sediment at its base. The impacts of the landslide were severe because it was more mobile than prior landslides at the site; the approximately 8 Mm³ of material originated on a gentle (< 20°) riverside bluff 180 m high, yet traveled across the entire 1 km floodplain and spread laterally a similar distance, resulting in 43 fatalities (Iverson et al. 2015). The slope had been periodically undermined by the North Fork Stillaguamish River, with evidence of abundant landslide deposits mantling a thick sequence of Pleistocene glacial till and outwash sediments forming the walls of the river valley (Iverson et al. 2015). At the base of this stratigraphic sequence lies a glaciolacustrine silt-and-clay unit, similar to the Thompson River Valley unit 2, that is associated with abrupt failure and landsliding (Iverson et al. 2015).

Owing to its high mobility and varied deposits, Iverson et al. (2015) described the landslide at Oso as a debris avalanche-flow, or alternatively, a flowslide. They suggested that a smaller landslide occurred on a lower segment of the slope first, which withdrew support from the

mass above it and resulted in retrogressive collapse of the upslope bluff, leading to the high-speed debris avalanche-flow (Iverson et al. 2015). Seismological evidence supported the hypothesis that rapid loading of unstable, wet sediment by material collapsing from upslope may have been an important factor contributing to the behavior of the Oso landslide in which drier, stronger material likely rode atop a wetter, liquefied basal layer (Iverson et al. 2015).

Iverson et al.'s (2015) description of the 2014 Oso landslide bears comparison to the North Slide of 1880, and to the catastrophic 1905 landslide on the Thompson River at Spences Bridge (approximately 40 km downstream of Ashcroft). Similar to the North slide, I hypothesize the 1905 Spences Bridge slide was a complex, extremely rapid, very wet, earth slide-debris flow. The *Daily Colonist* (1905b) newspaper described the slide as "...a vast cloud of dust... rolling down the bluff toward the river.... As it reached the water, the spray and debris were flying right by, the terrific force affording an awful spectacle and one rarely witnessed by so many people." This account lends credence to the hypothesis that basal liquefaction occurred and likely enhanced the mobility of the slide, as Iverson et al. (2015) postulated for Oso. Moreover, like the Oso landslide, the Spences Bridge slide was preceded by a least two prior landslides, as described in Chapter 3, both of which had limited mobility compared to the 1905 event, when the very rapid slope failure produced a displacement wave, dammed the Thompson River, and caused at least 15 fatalities. Sediment dilation may have occurred during prior episodes of landsliding at the Spences Bridge site, as Iverson et al (2015) postulated for the Oso slide; this disturbed sediment could have been saturated by a period of heavy rainfall which preceded the 1905 slide and by the irrigation of the delta terrace above the slide (Ryder 1981), on which the land owners had reportedly been "pouring large quantities of water ... in order to get a heavy second crop of hay" (Daily Colonist 1905b).

The Attachie landslide of 1973 is a second contemporary case study which is relevant to my interpretation of the North slide of 1880 and the Spences Bridge slide of 1905. Fletcher et al. (2002) describe the sudden acceleration of the Attachie landslide on the Peace River in northeastern British Columbia, which originated as a compound translational landslide of low mobility, and developed into an extremely rapid flow slide of 6.4 Mm³ in on May 26, 1973. The flow slide occurred during steady rain, which followed a wet April preceded by an

unusually high winter snowpack preserved by cool spring temperatures (Fletcher et al. 2002). The Attachie landslide bears comparison with the Thompson River landslides, as it is also situated in overconsolidated glaciolacustrine clay and silt sediments, with the body of the slide containing a considerable amount of non-plastic silt, which was likely unsaturated and/or cemented (Fletcher et al. 2002). The landslide inundated the Peace River Valley and temporarily dammed the river. Fletcher et al. (2002) proposed a failure mechanism for the Attachie slide based on a process of “macroscopic” brittleness, in which the slide mass was broken into blocks of intact material separated by open tension cracks as a result of slow, ductile displacements along a deep rupture surface (Fletcher et al. 2002). She proposed that these open cracks filled with loosely deposited material released by loosening and weathering of the exposed crack walls, and that prior to rapid failure, inflowing surface water resulted in saturation and liquefaction of this loosely-deposited matrix (Fletcher et al. 2002). The heavy fluid pressure so exerted on the crack walls would have served to suddenly increase the driving forces acting on the passive segment of the slide mass and produce rapid failure (Fletcher et al. 2002). The process is thus initiated by gradual mechanical disturbance of overlying non-plastic units due to slow deformations along a ductile rupture surface, leading to rapid slope failure of material that may be characterized as sensitive in its bulk behavior (Fletcher et al. 2002).

Similar to Fletcher et al.’s (2002) assessment of the Attachie slide, the brittle, non-plastic nature of the unit 3 sediments comprising the body of the North slide, which were also likely unsaturated and cemented, could facilitate a similar process of macroscopic brittleness initiated by the slow, pre-failure movements which might have occurred due to the introduction of water-intensive irrigation methods some years prior. Compounded by Ashcroft’s semi-arid climate, frost weathering of the crack walls below Proctor-optimum moisture contents would promote infilling of the tension cracks created by precursory movements with the requisite loosely-deposited (contractant) materials.

As demonstrated by the historical accounts of the North slide of 1880 and the Spences Bridge slide of 1905, and more recently by the Oso and Attachie landslides, the remobilization of previously-disturbed deposits can be particularly dangerous. Whether this remobilization takes

the form of liquefaction to the extent required for a complex, very rapid earth-slide debris flow, or is limited to producing a reactivated earth slide of lesser mobility, is difficult to explain due to the complex interactions of many causal factors, which, from a risk management perspective, leaves some “troubling questions unanswered” (Jibson 2006). Notwithstanding, in the case of the Thompson River Landslides south of Ashcroft, history would appear to indicate that the highly-mobile catastrophic movements of the North slide and Spences Bridge slide were facilitated by a substantial supply of ponded irrigation water. In Ashcroft’s semi-arid climate, it seems highly unlikely that this amount of water could be provided by modern irrigation systems or by natural sources, such as prolonged, intense rainfall, as was the case preceding the Oso landslide, which is located on the west coast of the United States and subject to extreme pineapple express precipitation events.

5.2.2. Reactivated Rapid Compound⁹ Earth Slide (Goddard)

The Goddard landslide of September 24, 1982 represents an important event from a railway risk management perspective, as it is the only rapid slope movement in the 10-km corridor south of Ashcroft which has severely damaged the railway since the historical landslides of the late-1800’s. No other documented rapid slope movement occurred in the corridor during the 20th century, except the Red Hill slide of 1921, which was located on the opposite bank of the river and did not affect the railway infrastructure. The Goddard landslide of 1982 was a reactivation of a landslide which occurred at the same location in 1886 (Eshraghian et al. 2007). While Eshraghian et al. (2007) suggested the 1886 event represented a retrogression along a new rupture surface, I am inclined to agree with the assessments of Thurber Consultants (1984), Brawner (1982) and Wood (1982), that the 1886 event was also a reactivation of the northern portion (approximately one-third) of an older, possibly ancient landslide, the outline of which can be clearly seen on aerial photographs of the area (Figure 3.6). The 1886 reactivation, which was probably rapid (Eshraghian et al. 2007), may have occurred in connection with cutting near the toe of the slope for construction of the CPR track

⁹ According to Skempton and Hutchinson (1969), *compound* describes a slope movement in which the rupture surface is formed of a combination of curved and planar segments, whereby the movements exhibit a part-rotational, part-translational character.

three years prior (Thurber Consultants Ltd. 1984). The volume of the 1982 Goddard landslide was approximately 2 Mm³ (Eshraghian et al. 2007). I estimated the travel angle of the landslide, based on the cross-section prepared by Eshraghian et al. (2007), to be approximately 14° (inverse tangent of scarp height to toe of the slide). This is within the range of residual friction angles of 10–15° measured in ring shear laboratory tests on the unit 2 glaciolacustrine clays comprising the rupture surface (Bishop 2008). As illustrated in Figure 5.6, for a wedge of frictional soil sliding on a horizontal rupture surface with a water-filled tension crack at the rear, the stable slope angle, β , is approximately equal to the internal friction angle of the soil, ϕ' . Movement requires that the rear crack be filled with water such that cleft water pressures are exerted (Cruden 2003).

The Goddard landslide of 1982 was preceded by very/extremely slow reactivations in 1974 (Morgenstern 1986) and October 1976 (Golder Associates 1977, Morgenstern 1986, Porter et al. 2002), and likely by other slow reactivations undocumented in the intervening 96 years between 1886 and 1982. Rapid compound landslides are often preceded by minor precursory events, related to the development of minor scarps and corresponding extension near the toe of the slide, which permit the progressive formation of the major upslope scarp and ultimately the rapid translation of the slide driven by the fully-formed active block. The altered kinematics of the landslide associated with the formation and coalescence of cracks forming the active and passive blocks can occur gradually over many years; Soe Moe et al. (2009) described deep compound translational landslides in Edmonton's North Saskatchewan River Valley, where the precursory movements to the major (relatively rapid) failures occurred over a period of two to 12 years prior. These precursory movements perform the critical functions of achieving a kinematically admissible failure mechanism through internal shearing of the slide mass (Hutchinson 1987), while simultaneously creating open cracks which facilitate the entry of surface water into the disturbed mass to promote the further destabilization of the slope.

Hungr et al. (2005) observed that while certain types of landslides tend to behave in a ductile manner, and others are typified by brittle failure, there is unfortunately a large “transitional” group that may exhibit either behavior, or both in sequence, as appears to have been the case at the Goddard landslide. The repeated, brittle reactivations of the Goddard landslide in 1886

and 1982 suggest that the slope exists in a state of limiting equilibrium which may be readily disrupted by seemingly innocuous changes in the slope geometry or environmental conditions. Regardless of whether these changes are human-induced or naturally occurring, they may produce a rapid, brittle failure despite the previously disturbed condition of the slope, which would generally be associated with slow and relatively limited displacements (Skempton and Hutchinson 1969). The rapid reactivations of the Goddard landslide in 1886 and 1982 have substantial implications for the risk management of the numerous other large compound translational landslides along the Thompson River Valley south of Ashcroft.

Soe Moe et al. (2006) suggested the development of a compound translational landslide can be described in five idealized kinematic stages, as illustrated in Figure 5.1. Soe Moe et al. (2006) and Cruden et al. (2003) described these kinematic stages as follows: In Stage 1 (Figure 5.1, (a)), tension cracks develop on the valley wall and behind the crest, corresponding to formation of minor scarps and the main scarp, as a result of minor movements at the toe of the slope, potentially due to river erosion or the discharge of artesian groundwater pressures. In Stage 2 (Figure 5.1, (b)), water pressure develops in the gaping main scarp, pushing the main body of the landslide along a weak seam at depth, which has been reduced to residual strength by prior failures or geomorphological processes. As movement enlarges the aperture of the main scarp, cleft pore water pressure drops and the rate of movement is reduced or ceases entirely. In Stage 3, the uphill-facing counterscarp develops over several months or more, as a result of the partial loss of support at the head of the landslide. The counterscarp delineates the downward-tapering wedge, or active block, as shown in Figure 5.1 (c). In Stage 4 (Figure 5.1, (d)), the active block is fully-formed, and a kinematically admissible failure mechanism is achieved. The increase in driving forces resulting from the weight of the active block triggers an acceleration of slope movement as the passive block moves outwards and the active block drops down until its tip comes to rest on the rupture surface, forming the graben. In Stage 5, the rapid slope movement is halted as the active block comes to rest on the rupture surface and a more stable slope geometry is achieved; ongoing minor movements may then resume, depending on erosion of the displaced material at the toe of the passive block and hydrogeologic processes such as groundwater discharge are re-established (Figure 5.1, (d)).

Hutchinson (1988) described compound slides as being of such geometry that failure is only made kinematically admissible by the development of internal displacements and shears, with the velocity of the slide reflecting the brittleness of these internal failures. Their geometry is otherwise locked in-place and generally reflects the presence of a heterogeneity, typically a weak layer (Hutchinson 1988). Several mechanisms which may lead to rapid failure along pre-existing rupture surfaces are discussed by Hutchinson (1987). Of these, the three factors which appear most relevant to the Goddard slide are: 1) unloading of the toe due to river erosion, 2) brittleness within the slide mass (as compared to the bounding slip surface), and 3) hydraulic thrust generated by the entry of surface water into open cracks. To these, I would add 4) groundwater seepage forces due to contrasting permeabilities of soil strata. These causal factors are discussed in the following subsections as they relate to the 1982 Goddard landslide. I would contend that these causal factors served to establish a kinematically admissible failure mechanism through differential slope displacements resulting in crack formation, coalescence and growth, culminating in the formation of the active block and the rapid compound translational landslide which occurred in 1982. The transition implicit in the progression from one kinematic stage to the next can be understood as a kinematic threshold, which, when crossed, may result in rapid acceleration depending on the stage of formation of the compound failure mechanism.

Given the complex interplay of several causal factors implicated in the rapid 1982 Goddard landslide, it is difficult, if not impossible to derive a predictive model of landslide behavior. However, presented in Section 5.2.4 are first-hand observations of the landslide characteristics and surface measurements of accelerating movement rates as recorded in an unpublished memorandum by Wood (1982), who was onsite during the Goddard 1982 landslide and the days leading up to the major movement. His observations are analyzed using an inverse-velocity approach in Section 5.2.4, and constitute an important part of the integrated monitoring strategy proposed in Chapter 6 for better anticipating and coping with the rapid acceleration of a landslide in the Thompson River Valley south of Ashcroft.

5.2.2.1. River erosion

During an inspection of the Goddard landslide on September 26, 1982, Brawner (1982) noted the role that river erosion may have played in triggering the slide two days prior:

“The C.N. Rail has had slide instability on the opposite side of the river [CN 53.4/53.7 slide] and have placed rip rap directly across from the [Goddard] slide. In addition, rip rap has been placed about 1500 feet upstream. This has pushed the river harder against the C.P. bank and increased scour” (p. 2).

Cruden et al. (2002) described a similar situation for Edmonton’s Lesueur landslide, where dumping of mine waste led to increased erosion and landsliding on the opposite bank of the North Saskatchewan River.

Morgenstern (1986) compared air photos from 1928 and 1976 and estimated that the Goddard landslide was subject to river erosion at a maximum rate of 0.25-0.33 m/year during this time period¹⁰. Wood (1982) observed at the time of the 1982 slide that “The original shoreline was almost intact and the toe movement extended some 50 ft. [15 m] into the river” (p.8)¹¹. Given the similar extents of the 1886 movement compared to the 1982 movement (Thurber Consultants Ltd. 1984, Eshraghian et al. 2007), it is likely that the 1886 slide deposits projected a comparable distance into the Thompson River, and as such the river erosion which subsequently occurred would have acted on this displaced material. Given the periodicity of the two major movements at the Goddard landslide, occurring 96 years apart (in 1886 and 1982), river erosion at a rate within the order of magnitude estimated by Morgenstern (1986) likely played a preparatory role in returning the previously-failed slope to a state of marginal stability on which additional preparatory and triggering factors acted to bring about the 1982 landslide (moving from a Type 1 to a Type 2 situation in Hutchinson’s (1975) terminology).

Citing an internal C.P. memorandum from L.A. Hill dated September 24, 1982, Morgenstern

¹⁰ Based on an inspection of aerial photographs dating from 1948-1982, Thurber Consultants (1984) asserted that little to no visible erosion had occurred at the base of the Goddard slide during this time period.

¹¹ Thurber Consultants (1984) estimated that the toe of the Goddard landslide was pushed out into the river by approximately 50 m immediately following the 1982 slope failure, based on aerial photographs before and after the movement.

(1986) argued that the 1982 movements originated at the bottom of the slope, coincident with the river level, underscoring the importance of river erosion in contributing to the reactivation of the slope. Hutchinson (1987) cited toe erosion as perhaps the most common trigger of landslides on pre-existing shears, noting that "... the removal of a given weight of material from the toe of a slide will cause a considerably larger reduction in factor of safety than the addition of the same weight at its head. This follows from the tendency of the stress systems at the toe and head of a slide to approximate to the passive and active modes, respectively" (p. 182). Other causal factors including high winter snowpack and late persistence of snow on the ground in 1982, as discussed in Section 4.7, likely acted in concert to produce higher-than-normal river flow levels (and resulting erosion) and abundant groundwater recharge (increased artesian porewater pressure below the rupture surface) that year.

The only other documented rapid landslide south of Ashcroft which occurred in the 20th century is the Red Hill slide of August 13, 1921. It temporarily dammed the Thompson River, though only for a few hours, as described in Section 3.2.8. The slide has not been investigated in detail, though several authors have referred to it as a rapid earth flow. Based on an examination of the 1928 air photos, I interpret the mode of movement to be a rapid compound translational earth slide (Figure 5.7). A contemporary composite photograph of the Red Hill slide is presented in Figure 5.8. Based on 2015 LiDAR data used with permission of CN, a cross-section through the Red Hill slide is presented in Figure 5.9; R. Macciotta retrieved the topographic data for the slope profiles from the 2015 LiDAR data of the Thompson River Valley (personal communication, 2017).

Irrigation was implicated at the time as the cause of the Red Hill Slide (Ashcroft Journal 1921); however, the narrative of the Ashcroft slides being the result of irrigation was well-entrenched by 1921, and may have obfuscated other potential contributing factors. River erosion at the base of the slope may have been one of these contributing factors. While most of the irrigation-induced landslides of the late 1800's took place in the dry climate regime of 1870-1889, the Red Hill slide occurred during the wet climate regime of 1890-1924, in a year of unusually high river flow (Chapter 4). A faint, but clearly evident scarp to the south suggests that this was not the first landslide of its kind in the immediate area (Figure 5.10). It is likely that the

natural river erosion at the base of the slide was accelerated in the preceding years by the rock groynes constructed below the South slide (immediately to the north on the opposite bank) and the recent construction of the CN railway on the opposite bank (completed in 1915). The 1928 air photo was taken only 7 years after the Red Hill landslide occurred, and constriction of the river is still evident (Figure 5.7). I examined aerial photographs of the Red Hill slide dating from 1928 and 2015 and estimated the rate of maximum rate of shoreline erosion which occurred to be approximately 0.3 m/year. This estimate at the Red Hill slide is in agreement with Morgenstern's (1986) estimate of river erosion at the Goddard slide, underscoring the potential similarities between these two rapid 20th century slope movements.

There is little documentation associated with the Red Hill slide, as both the CN and CP tracks are located on the opposite side of the river at this location in the corridor, and hence have not been directly impacted by the slope movement. However, what information can be gleaned from the earliest air photos, recent field inspections, and LiDAR data of the Red Hill slide lends credence to the argument that river erosion could produce a landslide of sufficient size and mobility to temporarily dam the Thompson River, and that this scenario could still occur in the present day in the absence of ditch-and-furrow irrigation.

5.2.2.2. Brittleness within the slide mass

Hutchinson (1987) noted the important effect of contrasting strength and brittleness within the slide mass (and hence along internal shears) to that on the bounding rupture surface for a landslide of general, non-circular, non-planar shape. Substantial movement in a slide of this type is not possible until a kinematically admissible mechanism is achieved through internal shearing of the slide mass, allowing the rear part of the slide to subside to form a graben and the main slide body to move forwards (Figure 5.1). It follows from energy considerations that the resistance on such internal shears can contribute significantly to the overall stability of the slide, and this contribution will be higher in more strongly non-circular slides with larger ratios of strength and brittleness on internal shears to those on the bounding slip surface (Hutchinson 1987).

A sketch of the Goddard landslide immediately prior to, and during, the 1982 reactivation was prepared by Wood (1982) based on his firsthand observations, and is presented in Figure 5.11. The slide has the non-circular form of a compound translational slide, with internal shearing of the slide mass evidenced by the numerous cracks forming scarps and grabens. David Wood (personal communication, 2016) described substantial internal deformation and “chaotic” behavior of the moving mass during the 1982 Goddard landslide. From the cross-section of the 1982 Goddard landslide prepared by Eshraghian et al. (2007) (Figure 5.12) it can be seen that the slope moved on two rupture surfaces as a multiple compound translational earth slide; the deeper rupture surface was located in unit 2, where clay seams within the varved glaciolacustrine deposit are likely pre-sheared (ductile) and exhibit low residual shear strengths, about 10 to 15 degrees (Section 2.2.1). The overlying unit 3, however, of which the main body of the slide was comprised, is described in borehole loggings as hard to very hard silt of low plasticity, with partings of fine sand and clay, having a high strength exhibited by Standard Penetration Test blow counts in the range of 42 to greater than 100 (refusal) (Klohn Leonoff Consulting Engineers 1986). Silt of this strength is likely cemented and unsaturated, typical of the semi-arid setting. The marked contrast between the strong, brittle, surficial silts of unit 3 comprising the slide mass, compared to the ductile, pre-sheared clay partings of unit 2 which form the bounding slip surface are compliant with Hutchinson’s (1987) criteria for mechanisms producing large displacements in landslides on pre-existing shears; the rapid velocity of the 1982 Goddard landslide reflected the brittleness of these internal failures.

5.2.2.3. Entry of surface water into open cracks

In spite of the prevailing dry and semi-arid conditions associated with British Columbia’s southern Interior, early summer is often relatively wet (Moore et al. 2010), with localized precipitation events that could fill surface cracks with water and exert the hydraulic thrust to trigger a landslide on a marginally-stable slope. In the case of the 1982 Goddard landslide, the winter preceding the failure had an unusually high snowpack, as previously discussed, with localized late persistence of snow on the ground (Section 4.7). 1982 also experienced the highest summer precipitation recorded at Ashcroft over the 10 years of record between 1973–1983 (Thurber Consultants Ltd. 1984). Morgenstern (1986) was of the opinion that antecedent

precipitation contributed very significantly to the magnitude of the 1982 slide, noting that substantial rain fell while the Goddard slide was in progress, and that the pressure of water-filled cracks likely contributed to the movements.

Wood (1982) was onsite during the Goddard 1982 landslide and the days leading up to the major movement. He observed that the 1982 failure originated in the same area as a smaller, 1976 reactivation, towards the north end of the slide where a corrugated steel pipe (CSP) culvert with flume was located (Wood 1982). As evidenced by the presence of the culvert, this area was presumably subject to regular seepage or surface runoff. Wood (1982) observed that the initial cracks heralding the 1982 landslide were in the same locations as those which occurred during the minor slope movement in 1976, as evidenced by the broken asphalt which had been placed over the cracks under the recommendation of Golder Brawner and Associates to minimize surface erosion and the percolation of surface water in the moving mass.

The Grierson Hill landslide of 1901 in Edmonton, Alberta, is believed to have been triggered by a period of heavy rainfall, which entered the surface cracks (due to subsidence caused by underground mine workings) and generated sufficient hydraulic thrust to trigger the slope movement (Martin et al. 1984). Martin et al. (1984) described the Grierson Hill landslide on the bank of the North Saskatchewan River as a compound translational slide on a deep-seated bentonite seam in the Cretaceous clay shale bedrock, which destroyed the Humberstone mine workings located in an overlying coal seam (Martin et al. 1984). Measured piezometric pressures along the failure surface of the Grierson Hill slide were uniformly low, and did not show a seasonal response (Martin et al. 1984). Hutchinson (1987) also described several cases where the entry of surface water into tension cracks generated sufficient hydraulic thrust to trigger a landslide. Terzaghi (1950) recounted a similar process leading to a landslide at Swir, in which ductile movements on a plastic clay layer broke the overlying glacial till in to large fragments; rain water then accumulated in the crevices and caused disintegration and collapse of the till fragments, which flowed into an open cut. Morgenstern (1986) noted that very low piezometric pore pressures were measured in the Goddard landslide mass following the 1982 reactivation, with pore pressure ratios (r_u) of 0.1 or less. It therefore stands to reason that the

infilling of cracks with surface water may have played a substantial role in the Goddard landslide reactivation, as illustrated by the force balance model in Figure 5.6.

5.2.2.4. Groundwater seepage forces due to contrasting permeability

In the hours following the 1982 Goddard slide Wood (1982) observed that “The complete soil mass was sheared and broken with ground water running from the face and collecting into small streams. Clay zones of soil were saturated” (p. 8). His observations suggest that groundwater seepage may have played a significant role in the 1982 reactivation. Wood (1982) also notes that he was told by CPR crews two days before the slide that there had been an “unusual amount of water introduced to the slope above the track” (p. 2) that year by the irrigation of the upslope terrace, but in the ensuing litigation, “the plaintiff [Canadian Pacific] ...failed to prove the irrigation practices of Highland caused or contributed to the [Goddard] landslide [of September 1982]” (p. 26) (BC Court of Appeal 1990). Brawner (1982) noted that the central portion of the 1982 slide area, in particular, was persistently wet, as evidenced by the presence of willows. The presence of a culvert in the vicinity where the initial cracks were observed, both in 1976 and 1982 (Wood 1982), suggests that groundwater seepage, regardless of its source, was concentrated in the area that failed. Moreover, Iverson and Major (1986) identified the rather slight distinction between Coulomb slip and liquefaction ($z \geq 1$), particularly for situations where there exists both a significant upward seepage component and a slope angle nearly equal to the angle of internal friction, ϕ' , as is typically the case for marginally stable slopes such as at the Goddard slide. Where an upward seepage component exists, Coulomb failure may occur under conditions close to those required for static liquefaction (Iverson and Major 1986). This may explain Wood’s (1982) observation of “silt boils” in the Thompson river during and after the failure of the Goddard slide in 1982; evidence of upward groundwater seepage due to confined groundwater pressures at the slide toe in excess of the critical gradient resulting from a low-permeability clay layer confining an underlying aquifer, as per Lafleur and Lefebvre (1980).

Terzaghi (1950) observed the periodicity of “certain types” of landslides, wherein a water-bearing strata of relatively high permeability is overlain by lower-permeability soils (p. 102).

He described a landslide in the Folkestone Warren, on the north coast of the English Channel, which was responsible for periodic disturbance of the Southern Railway approximately every 20 years. There, the water-bearing Lower Greensand, a soft sandstone, was overlain by Gault, a very stiff clay of Cretaceous age; the majority of the sliding mass advanced along the nearly horizontal boundary between the Gault and the Lower Greensand (Terzaghi 1950). Borings showed an artesian water level in the Lower Greensand, of up to 27 feet (8.2 m) above sea level, which was subject to variation in both the short- and long-terms (Terzaghi 1950). As the periodic reactivations of the landslide were not preceded by any change in the external slope conditions, Terzaghi (1950) mused that the displacements could only be accounted for by an increase of the hydrostatic pressure on the base of the sliding body. He postulated that abnormal rainfall recharge of the underlying Lower Greensand, where it reached the ground surface many miles distant from the site of the landslide, was responsible for periodic increases in the water pressure at the base of the landslide and the resulting displacement of the marginally-stable slope. The factor of safety of the slope with respect to sliding, he noted, thus varied with the elevation of the groundwater table in the aquifer a substantial distance from the slide (Terzaghi 1950).

Terzaghi's (1950) assessment of the Folkestone Warren slide underscores the importance of regional hydrogeology in controlling the displacements of periodically active slopes which are subject to artesian pore water conditions at depth. This same hydrogeologic scenario is played out in the periodic reactivations of the Ashcroft Thompson River landslides, wherein artesian pore water pressures in the buried sands and gravels (unit 1) are confined by the overlying varved clay and silt (unit 2), which contains the rupture surfaces of the landslides. I postulate that the Ashcroft slides are reactivated in years when the regional recharge of the underlying aquifer (unit 1 sand and gravel) is unusually high, as evidenced by a Thompson River flow departure from normal in excess of about 14%. These years of high recharge appear to be largely controlled by regional snow pack levels which are affected by high-level climate phenomena, including the Pacific Decadal Oscillation, which is itself periodic in nature (Chapter 4). Whether the reactivation of a particular landslide takes the form of slow, ductile movements or a rapid, brittle failure, would depend on the state of evolution of the landslide kinematics as described in Section 5.2.2.

As discussed in Section 2.3.1, the presence of a buried aquifer, such as unit 1 in the Thompson River Valley south of Ashcroft, has a profound effect on the movement of groundwater and hence the slope stability in the vicinity of the valley walls (Freeze and Witherspoon 1967, Lafleur and Lefebvre 1980, Bishop 2008). The central importance of hydrogeology and regional groundwater flow in the reactivation of the Ashcroft landslides is fundamentally lost in the deployment of limit equilibrium modeling (LEM) of the hillslopes. Limit equilibrium slope stability analysis does not capture the effect of seepage forces due to gradients present in the slope, considering only the buoyancy effect of the associated pore pressures (Harrison 2014), as the underlying assumptions of LEM preclude unbalanced body forces and internal deformation of the moving mass. Controversy exists over whether seepage forces can be explicitly incorporated by modifications to limit equilibrium formulations (King 1989, Morrison and Greenwood 1989, King 1990, Morrison and Greenwood 1990).

Morrison and Greenwood (1989) correctly pointed out that LEM presumes the equilibrium of the slope to be independent of the effective stresses resulting from strain within the slope. This assumption applies to the effective stresses both within the slices and on the inter-slice boundaries (Morrison and Greenwood 1989), such that the Mohr-Coloumb failure criterion is not violated along the interslice boundaries, and the line of thrust of the interslice forces lies within the mass that is circumscribed by the rupture surface (Morgenstern and Price 1965, Sarma 1973). An iterative procedure is employed to solve the basic equations to find a set of inter-slice shear and normal forces which do not violate the Mohr-Coulomb soil failure criterion along the inter-slice boundaries—this is achieved via an assumed distribution of the inter-slice forces and an additional unknown, λ , which scales the assumed distribution and is computed as part of the solution (Morrison 1988). The solutions effectively uncouple the forces on the inter-slice boundaries from those on the slip surface. By contrast, the Sarma (1979) method is a fully coupled solution in which both the distribution and magnitude of the forces on the rupture surface and the inter-slice boundaries are determined directly, and without iteration, from the equations for static equilibrium with the Mohr-Coulomb failure criterion is applied to all the internal wedge boundaries (Morrison 1988). In Sarma's (1979) method, the pore water forces acting on the inter-slice boundaries are provided as part of the

data specifying the stability problem, and hence the effect on the factor of safety of the seepage forces within the slide mass can be examined directly (King 1990).

Employing limit equilibrium analyses to assess the stability of the Ashcroft Thompson River landslides, several authors have reported overall factors of safety of greater than 1.0 for slopes that were moving (Eshraghian et al. 2006 & 2008, Porter et al. 2002). Several assumptions contained within the limit equilibrium methods of slices are fundamentally incompatible with the kinematics of a compound translational failure mechanism, and hence the factors of safety for a slope so computed should be viewed with an understanding of the following limitations. Limit equilibrium methods assume:

1. that the slope failure is governed and fully described by the soil properties and state of stress acting along the rupture surface, and that no failure occurs within the sliding mass itself, which is divided into a series of rigid slices. These assumptions are incompatible with the internal shearing that is required to produce a kinematically admissible failure mechanism for compound translational landslides according to Hutchinson (1987). David Wood (personal communication, 2016) recounted substantial internal deformation and “chaotic” behavior of the moving mass during the 1982 Goddard landslide;
2. that one uniform factor of safety exists along the entire rupture surface, which implies the entire sliding body moves simultaneously and without internal deformation; this is incompatible with a compound translational mechanism where the passive toe block moves out first, followed by subsidence of the active wedge at the head of the slope (Bromhead 1992);
3. arbitrarily the relative magnitude and orientation of the inter-slice shear and normal forces, which implicitly determine the effective stress state along the vertical slice boundaries; these assumptions produce implicit pore water conditions within the mass which are likely not representative of the actual pore water pressures induced by complex groundwater flow systems (Morrison and Greenwood 1989).

5.2.3. Alternate Hypotheses for the Rapid Acceleration of the Goddard Slide

5.2.3.1. Potential role of progressive failure

Progressive failure may be invoked as a possible alternate explanation for the rapid acceleration of the Goddard landslide which occurred in 1982. Progressive failure is a possibility in the case where all portions of the active rupture surface may not be at residual strength; there is then the danger that the accumulation of strain due to repeated, seemingly benign movements results in “creep fatigue” or straining of the remaining portions of the rupture surface to the point of peak strength followed by strain-weakening and rapid (brittle) failure (Lacerda 1989, Leroueil 2001). That is, where the potential failure surface may be only partly formed, with some areas having experienced sufficient deformation to produce residual strength conditions, while other areas which have experienced less deformation may have not yet attained peak strength, there exists the possibility for brittle failure and rapid movement on an existing rupture surface (Leroueil 2001). Moreover, even if an equilibrium exists at a given time, any modification of the slope may cause progressive failure to resume or continue. The main factors leading to this situation are (Leroueil 2001):

1. a change in the geometry of the slope and the resulting shear stresses (e.g. excavation/erosion at the toe or loading at the head);
2. a decrease in the normal effective stress (and thus in peak and residual strengths) due to pore pressure increase or excavation, for example;
3. a decrease in soil strength (lowering of the peak strength envelope) due to creep, fatigue or weathering.

An alternate explanation for the rapid landslide reactivations which have periodically occurred along the Thompson River Valley is the re-initiation of progressive failure due to a change in external boundary conditions, such as river erosion at the slide toe or the removal of material at track level (for the construction of a railway siding, for example, at the Ripley slide in 2005 (Hendry et al. 2013b)), or a modification of internal soil strength properties, such as a reduction in the residual friction angle on the rupture surface induced by changes in rate of shearing, temperature, or pore water chemistry. The progressive failure hypothesis is particularly

plausible where the rapidly-remobilized material comprises the lateral margin of a former slide area, suggesting that this material, though it has failed in the past, may not have been displaced as much as the central portion of the slide. Not yet having attained a residual strength/critical state condition, the material occupying the flank of the former (larger) slide would be susceptible to progressive failure given the necessary precursory changes in boundary conditions. However, for situations where the rupture surfaces are confined to very thin layers, as have consistently been observed at the Ashcroft Thompson River landslides (Eshraghian et al. 2007), the slope movements preceding failure (and the displacement required to reach residual strength) may be on the scale of millimeters (Terzaghi 1950). Laboratory shear strength tests on overconsolidated clay specimens reported by Skempton (1964) showed residual strength values were obtained at displacements of 25–50 mm. The argument that the residual strength value was not fully mobilized along the rupture surface at the Goddard landslide prior to 1982 is therefore rejected, given the rapid failure in 1886 and ongoing slow movements which would have affected at least this much displacement across the rupture surface, now fully formed by 1982.

5.2.3.2. Effect of changes in pore water chemistry on residual shear strength

While the rate of movement is known to have an effect on the residual strength of moving slopes (Wedage 1995), the relatively narrow range of velocities exhibited by slow-moving landslides generally produces limited effects in this regard. Wedage (1995) found the residual friction angle of Alberta's Clearwater clay shale increased by only 3.5% (or approximately 0.2°) for a ten-fold increase in the rate of strain. For strain rates that are comparable to the rate of movement for landslides on pre-existing rupture surfaces at low angles of inclination, rate dependence is essentially negligible (Bromhead 2013). Shibasaki et al. (2016) suggested that seasonal activity of shallow landslides may be initiated by a decrease in ground temperature affecting a reduction in residual strength of clay rupture surfaces, though their findings are not considered applicable to the Ashcroft Thompson River landslides due to the deep-seated nature of the rupture surfaces. Seasonal fluctuations in the pore water chemistry can also modify the residual strength of natural clay soils, with lower salt concentrations given rise to lower residual strengths (Moore 1991). Moore and Brunsten (1996) found that seasonal fluctuations

in groundwater chemistry had implications for the ongoing movements of the shallow Warbarrow mudslide on the south coast of England. Seasonal mudslide reactivations or periods of high activity were preceded by low pore water ion concentrations which resulted in decreased residual shear strength (attributed to the weakening of Van der Waals' forces and associated reductions in the residual cohesion intercept); the cessation of movement in spite of persistently high pore-water pressures was attributed to higher salt concentrations measured in the pore water after movement ceased, and the implied increase in the residual strength of the clay (regain of residual cohesion of 2–3 kPa) (Moore and Brunnsden 1996). It may be argued, however, that the surfeit of water is probably more important than any chemical effects imparted by its presence (Bromhead 2013).

While it is prudent from an engineering perspective to neglect the contribution of cohesion to the residual strength of disturbed soils, it may not be entirely reflective of reality in certain cases where appreciable cohesion may be the result of cementation or other chemical processes producing clay interparticle forces. Cambie (1902) described an experiment on a block of dry, indurated clay obtained from the site of the Ashcroft landslides:

“When a block of this dry indurated clay was placed in a soup plate and water dropped upon it, the clay absorbed 50 per cent of its own weight without any change of form or other visible effect, but when it had absorbed about 60 per cent of water, its structure completely collapsed, and it became as fluid as water.” (p. 198)

Cambie's (1902) description suggests that some cementing agent, such as calcium carbonate, or interparticle clay forces which were destroyed by saturation of the sample, were responsible for the majority of its strength in the dry state. Lum (1979) concluded that the high strength of the South Thompson silts under low degrees of saturation, typical of the semiarid environments in which they occur, is due to substantial apparent cohesion, the magnitude of which is controlled by the degree of saturation. While the overconsolidated glaciolacustrine clay and silts of units 2 and 3 would not exhibit the open fabric and conditionally-collapsible nature of the surficial late-glacial silts studied by Lum (1979), it is still possible that similar carbonate cementation and interparticle forces may be responsible for the high apparent strength of these deposits in a dry (likely unsaturated) state, as described by Cambie (1902). Carbonate cementation, as evidenced by white precipitates at the locations of groundwater seepage, can

be readily observed along the Thompson River Valley south of Ashcroft (see photo in Figure 5.5, e.g.).

Porewater isotope data from samples collected at the Ripley landslide were presented in the previous chapter. It bears repeating that the composition of the porewater within the bedrock was enriched in both deuterium and oxygen-18 compared to the porewater in the overlying Quaternary fill deposits, which was essentially identical to meteoric (and river) water. When the Thompson River level seasonally decreases in the autumn, and the groundwater flow is correspondingly out-of-the-slope (positive gradient from the bedrock to the river), it is possible that the enriched groundwater from the aquifer enters unit 2 as a result of the artesian pressure condition and the residual strength of the unit is improved due to the enriched ion concentration in the porewater. This may provide some explanation for cessation of movement ($< 1\text{mm/year}$) while the gradient remains positive (but decreasing) in the early spring, as exhibited by the seasonal step-wise movements at the CN 50.9 landslide between 2001–2004 (see Figure 5.16) and at the Ripley landslide between 2013–2014 (Schafer et al. 2015).

5.2.3.3. Effect of accumulated strain on residual shear strength

Petley and Allison (1997) conducted high-pressure triaxial tests on undisturbed samples of London Clay to elucidate the behavior of deep-seated landslides in the transition between ductile and brittle behaviour. Their results identify a distinct “transitional phase” in the progression from ductile to brittle deformation under high effective stresses (19–30 MPa). Upon attaining peak strength these samples did not undergo strain weakening but retained a constant strength for a considerable further accumulation of strain (Petley and Allison 1997). Such maintenance of peak strength is usually taken to indicate deformation in the ductile regime; however, while truly ductile deformation can continue to infinite strains, the samples displayed distinct strain-weakening at a fixed strain (Petley and Allison 1997). The continuing growth and coalescence of the micro-cracks eventually led to the formation of a continuous rupture surface and corresponding brittle failure (Petley and Allison 1997). Petley and Allison’s (1997) results have important implications for the behavior of deep-seated landslides, implying that sudden (brittle) failure can occur on a deep rupture surface under steady-state

conditions, as a result of the accumulation of strain. During this pseudo critical state (or “transition”) regime, deformation may be distributed throughout a larger zone, and manifest as “creep” type behavior corresponding to the pervasive growth of micro-cracks in a pseudo-stable state of deformation (Petley and Allison 1997). When the threshold strain is reached, brittle failure will occur as the microcracks coalesce to form a distinct shear surface (Petley and Allison 1997). Sudden failure can thus occur from a steady-state condition if the threshold strain is reached (Petley and Allison 1997).

Hendry et al. (2015) documented numerous fissures in core samples from below the rupture surface at the Ripley landslide; though these were interpreted to be evidence of glacial pre-shearing, it could be argued that they are indicative of deformation occurring throughout a larger, more diffuse rupture zone, as would be associated with the “transitional” regime described by Petley and Allison (1997). The experimental data suggest that some materials may show a combination of ductile and brittle deformation resulting in long periods of creep followed by sudden failure (Petley and Allison 1997). Záruba and Mencl (1976) also contended that where there exists a thick remoulded zone at significant depth and hence high overburden pressure, laboratory strength tests may not be reliable; in this case, the movement produces thick remoulded zones, altering the internal structure of the clay. Petley and Allison’s (1997) ductile-brittle experiments also suggest that as the confining pressure increases, the amount of strain that the sample can accumulate in the micro-cracking (transitional) phase, before brittle failure occurs, also rises. This may essentially be described as a delayed-onset progressive failure occurring over an extended period of time due to the large strains required for the actualization of brittle (strain softening) behavior. Their results, however, would pertain to first-time slides in undisturbed material, and as such, are not considered particularly relevant to the Ashcroft Thompson River landslides, most of which appear to be reactivations of landslides of ancient origin.

5.2.4. Use of Inverse Velocity Method for Forecasting Rapid Failure (Goddard)

On-site observations recorded first-hand in a memorandum by Wood (1982) beginning on September 23, 1982, following a train derailment at the location of the Goddard landslide, indicated movement rates at the north flank (most active area) of the slide were 24 to 40 mm/hour (0.44 to 0.95 m/day). These accelerated to a maximum rate of movement on September 24, 1982 of 6 m/hour according to Krahn (1984), constituting a rapid failure in the terminology of Cruden and Varnes (1996). Wood (1982) measured a maximum rate of movement in the early morning of September 25, 1982 of approximately 1.2 m/hour (29 m/day), or moderate speed, based on vertical offset measurements made at the north flank as the failure progressed. Notwithstanding the discrepancy between these reports, both maximum movement rates are three to four orders of magnitude larger than the maximum rate of movements initially observed in 1976, of approximately 10 mm/day (in the direction of movement), when open cracks were evident in the vicinity of a drainage culvert towards the north flank of the Goddard slide (Golder Associates 1977), and two orders of magnitude larger than those measured from approximately 48 hours before and to about 7 hours prior to the onset of rapid failure in 1982 (Wood 1982).

Wood (1982) made offset measurements during the progress of the 1982 Goddard landslide and documented these in an unpublished memorandum. His cumulative offset measurements at monitoring point MP-1, at the north flank of the landslide (as depicted in Figure 5.13), are plotted in Figure 5.14. Monitoring point MP-1 was the most readily accessible (D. Wood, personal communication, 2016) and showed the most activity during the landslide, so more frequent measurements were taken by Wood (1982) at this location. The offset measurements show a classic exponential form associated with the transition from decelerating to accelerating stages of deformation. Varnes (1978) suggested that deforming materials progress through three stages of strain development, characterized by a “primary” phase of accelerated creep related to initial elastic deformation, followed by a “secondary” phase of plastic creep deformation as cracks begin to grow and coalesce, culminating in an exponential increase in displacement rate as the “tertiary” phase of brittle failure occurs. Cruden (1974) demonstrated that for brittle materials, there is no reason to assume that a period of steady state or secondary

creep intervenes between the transient (decelerating) and tertiary (accelerating) creep phases. Rather, he suggested that the static fatigue of brittle materials is governed by a critical density of microcracks in the specimen; at such a time as the cracks begin to intersect, the intersections grow at an accelerating rate and lead to failure (Cruden 1974).

Established empirical methods exist for forecasting the approximate time of failure based on monitoring of precursory surface slope movements, based on the soil creep curves methods of Saito (1965). These are predicated on the assumption that the increment of the logarithm of acceleration is proportional to the logarithm of velocity of the surface displacement immediately before catastrophic failure (Saito 1965). Fukuzono (1985) proposed a simple graphical method for predicting the time of failure of an accelerating slope based on the reciprocal of mean velocity, v , which forms a negative linear trend immediately before catastrophic failure; failure time can be estimated as the time when the $1/v$ trend intersects the horizontal axis, forecasting the time at which $1/v$ equals zero and the slope acceleration is infinite. The method is empirical, overlooking the kinematics and cause(s) of failure, while relying on the surface manifestation of the instability—measurements of ground displacement (Hung et al. 2005).

I applied Fukuzono's (1985) inverse velocity method to Wood's (1982) surface offset measurements from the Goddard 1982 slide in Figure 5.15. As evident in Figure 5.15, the $1/v$ data initially do not show a coherent trend; the data then begin to linearize, commencing at approximately 23:40 hours on September 23, 1982, indicating that rapid failure may be imminent. The linear portion of the plot (from 23:40 hours on September 23 to 01:30 hours on September 25) is projected to intersect the horizontal axis at time 13:00 hours on September 25, 1982. The actual onset on rapid failure occurred just ten hours earlier at approximately 3:00 hours on September 25, 1982 (Wood 1982).

Crosta and Agliardi (2003) noted that inverse velocity methods should be viewed as giving an order of magnitude prediction of the failure time. The 1982 Goddard landslide demonstrates the utility of using the inverse-velocity method for predicting the approximate time to failure for the brittle failure of a reactivated, rapid compound translational landslide in the corridor.

Although it represents only one event, the 1982 Goddard landslide is the only rapid failure in the corridor for which surface displacement rates have been recorded. As previously described, the mechanics of the Goddard landslide are thought to be reasonably representative of potential future rapid reactivations which could occur in the Thompson River Valley south of Ashcroft, and hence it represents an important case study, with accompanying unpublished data that has herein been presented, analyzed and interpreted. The practical application of an empirical surface displacement monitoring approach, such as the inverse velocity method, requires that site-specific warning thresholds be set with respect to velocity or acceleration (Hung et al. 2005); these thresholds will be presented in Chapter 6 as part of an integrated risk management strategy.

5.2.5. Reactivated Very/Extremely Slow Earth Slide (CN 50.9)

As described in Chapter 3, several of the large landslides south of Ashcroft have demonstrated very/extremely seasonal reactivations associated with the loss of toe buttressing and the outward flow of groundwater due to the seasonal autumn decline in the Thompson River level. These reactivations have typically been preceded by characteristic climate conditions of high winter snow pack and unusually high cumulative river flow departure from normal, as discussed in Chapter 4, and amount to total annual displacements of millimeters to centimeters per year. The operational difficulties associated with these minor seasonal reactivations can be effectively managed during railway operations by regular maintenance activities, including track realignment, and tamping and replenishment of sunken ballast (Hendry et al. 2013b). The consequences associated with these slow renewals of movement are therefore relatively minor, due to the limited velocity and mobility of the displaced material. According to Bromhead (2013), bedding-controlled landslides with low-angle basal shear surfaces daylighting at or beyond the toe of the slope are likely to respond immediately to toe erosion, but generally in a “sedate” manner, often exhibiting continuous, slow movements. Notwithstanding, repeated reactivations can lead to a more serious situation by providing the necessary mechanical disturbance for a rapid remobilization in the manner of the Goddard landslide of 1982.

Lissak et al. (2014) examined historical antecedent rainfall records in an attempt to empirically define piezometric thresholds triggering renewals of movement for a slow-moving, deep-seated coastal landslide in Normandy, France. The landslide was characterized by annual displacements of approximately 10-100 mm/year, but was periodically subject to moderate accelerations of movement effecting several meters of displacement in a matter of weeks (Lissak et al. 2014). Based on slope monitoring since 1985, previous researchers qualitatively demonstrated that these accelerations were controlled by the slope hydrology, in particular the measured height of the groundwater table within the landslide (Lissak et al. 2014). Lissak et al. (2014) identified a two-tiered threshold for landslide activity based on antecedent hydro-climatic conditions: 1) discrete, accelerated landslide movements with a return period of 6–7 years, associated with successive rainfall events above mean precipitation levels, producing groundwater elevations of more than two meters above the mean annual level (1976-2013); and 2) moderate landsliding events associated with low intensity rainfall periods with a limited groundwater rise responsible for very/extremely slow seasonal surface displacements (return period every year).

While studies of thresholds for precipitation-induced landslides are plentiful (e.g. Squier and Versteeg 1971, Iverson and Major 1987, McSaveney and Griffiths 1987, Barton 2002, Guthrie and Evans 2004, Cheung et al. 2006, Lissak et al. 2014, Vallet et al. 2016), there is a paucity of literature investigating the reactivation of deep-seated landslides controlled by higher-level or regional climate factors. Sevi et al. (2014) suggested that periodic reactivations of complex earth slide–flows in varved glaciolacustrine deposits along the Brewster river, Vermont, were due to groundwater flow and pore pressures built up by snowmelt and rain over a long antecedent period. They postulated that increased toe erosion in the preceding wetter years, combined with the longer time period for groundwater flow and pore pressure build up at the deep rupture surface, resulted in landslide activity during comparably drier years (Sevi et al. 2014).

An empirical correlation was established in Chapter 4 between an unusually high annual Thompson River flow departure from normal and the reactivation of landslides along the corridor south of Ashcroft. The interannual and interdecadal variations in streamflow in the

Thompson River basin were in turn related to the basin-wide snow pack and the phase of the Pacific Decadal Oscillation (PDO). The small number of recorded landslide reactivations in the corridor over the last century, since hydrologic record-keeping began, does not lend itself to a rigorous statistical evaluation; notwithstanding, an empirical threshold of 3,400 Mm³ was proposed in Chapter 4 for the cumulative river flow departure from normal portending reactivation of one or more landslides in the Thompson River Valley south of Ashcroft. This threshold, however, does not discriminate between very/extremely slow reactivations (such as at the Goddard slide in 1974 and 1976), and rapid renewals of movement (as exhibited by the Goddard slide in 1982). A better understanding of the interannual and interdecadal variations in climate and streamflow in the Thompson River Valley, and its attendant effects on the activity of the Ashcroft Thompson River landslides, is an important component of risk management in the corridor for improved resilience through better anticipation.

5.2.5.1. Effect of artesian pore water pressure and groundwater recharge

As discussed in Chapter 2, numerous studies (Freeze and Witherspoon 1967, Záruba and Mencl 1976, Hodge and Freeze 1977, Lafleur and Lefebvre 1980, Tutkaluk et al. 1998, Clague and Evans 2003, Bishop 2008) have demonstrated the profound destabilizing effect that a low-permeability unit at depth may have on the stability of natural slopes, especially where it confines an underlying aquifer, which acts to transmit regional groundwater to the discharge area and may produce substantial uplift pressures due to the confined groundwater conditions. Iverson and Major (1987) demonstrated the importance of hydraulic gradients and transiently recharging groundwater flow in controlling the balance of forces that instigate seasonal landslide motion at the Minor Creek landslide in northwestern California.

Extremely slow seasonal movements recorded on the lower rupture surface at the CN 50.9 landslide, during a period of increased monitoring frequency from 2001–2004, demonstrated the interplay between the river level and the resulting artesian pore water pressure below the rupture surface, producing seasonal, though extremely slow, reactivations of the landslide movement (Figure 5.16). Incrementally-higher rates of movement observed when the river is falling (3 mm/year) as opposed to when the river is rising (<1 mm/year), affirm that the

seasonal movements are not simply due to erosion and saturation/rapid drawdown at the toe of the landslides, but are related to the direction of, and hence the force exerted by, the groundwater flow from the underlying permeable gravels and fractured bedrock. When the Thompson River level seasonally decreases in the autumn, and the groundwater flow is correspondingly out-of-the-slope (positive gradient from the bedrock to the river), movements at a rate of approximately 3 mm/year are initiated as soon as the gradient is greater than zero (Figure 5.16). This movement essentially ceases (< 1 mm/year) when the river level rises to an elevation of 282 m, while the gradient remains positive (but decreasing) in the early spring. Rupture surfaces in the CN 50.9 slide are located at 275.7 m and 280.9 m (Eshraghian et al. 2007).

A similar hysteresis in movement rates was recorded at depth in the Ripley landslide by Hendry et al. (2015) during continuous piezometric monitoring between 2011–2012. They reported that when the river elevation was below 265 m, the velocity of the landslide during drawdown was higher (reaching 0.5 mm/day, or 183 mm/year) than when the river was rising (reaching 0.3 mm/day, or 110 mm/year), with little difference in the very slow movement rates recorded when the river level was above 265 m. The primary rupture surface at the Ripley landslide is at elevation 256.5 m, with a secondary (upper) shear zone at 266.5 m (Hendry et al. 2015).

The findings of Bertini et al. (1986) also affirmed the importance of the groundwater seepage force and direction in contributing to the frequency and velocity of slope movements on pre-existing rupture surfaces in marginally stable slopes (Leroueil et al. 1996). They documented movement rates along a pre-existing shear surface at San Martino, Italy, and found these rates to be higher as a result of decreasing pore pressure conditions (when the river was falling), compared to movement rates during increasing pore pressure conditions (when the river was rising).

5.3. Conclusion

Three failure modes were proposed to capture the range of movement types and velocities which have been recorded over the last 150 years for slope failures in the Thompson River Valley south of Ashcroft:

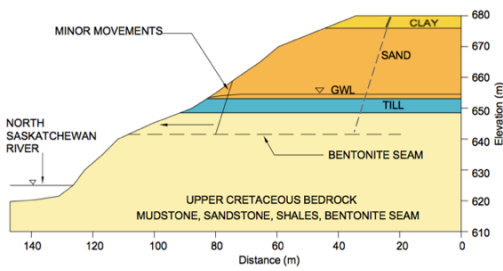
Mode I): complex, very rapid earth slide-debris flow;

Mode II): reactivated, rapid, compound earth slide;

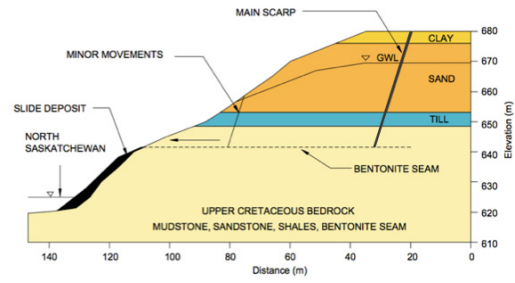
Mode III): reactivated, very/extremely slow, earth slide.

It was argued that a Mode I failure is contingent upon an ample supply of ponded water, as provided by now-abandoned methods of ditch-and-furrow irrigation. In the present day, Modes II and III failures may still occur, and have substantial consequences for the railway operations and numerous stakeholders in the Thompson River Valley.

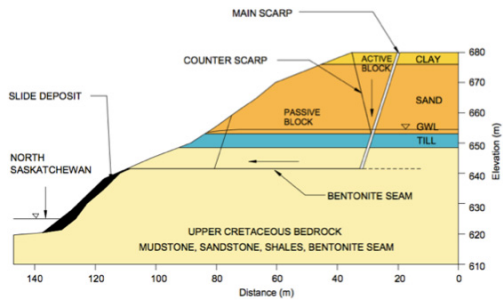
Compound translational earth slides, which have occurred along the corridor in more recent times and at locations untouched by irrigation, tend to display very/extremely slow seasonal displacements (Mode III); these precursory movements, however, may portend a future rapid acceleration, as demonstrated by the Goddard landslide of 1982 (Mode II). The catalyst for accelerating an extremely slow moving landslide into a rapid failure is conventionally understood to be a sudden change in external loading conditions, pore water pressure, or increase in brittleness on the rupture surface due to aging or chemical change. In the preceding analysis, it has been argued that kinematic threshold(s) exist for the compound landslides, which may produce rapid acceleration of a very/extremely slow moving mass resulting from the development of a kinematically admissible failure mechanism. The implications of kinematic thresholds are examined in the next chapter through a risk management lens.



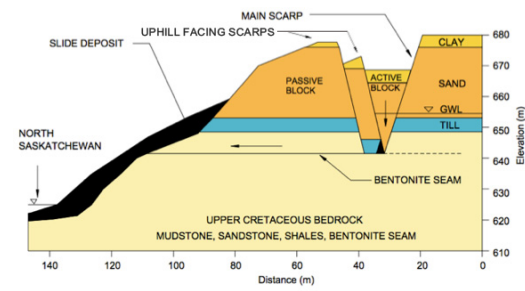
a) Stage 1: Development of tension cracks on valley wall and behind crest.



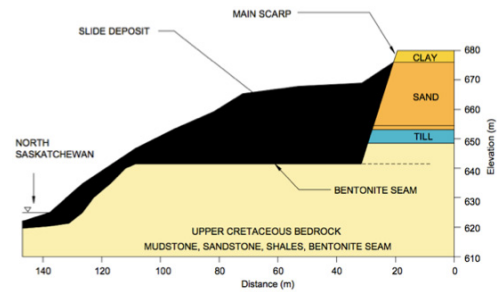
b) Stage 2: Aperture of main scarp enlarges due to cleft porewater pressure.



c) Stage 3: Counterscarp delineating active wedge begins to form.



d) Stage 4: Counterscarp penetrates to depth of rupture surface, facilitating outward movement of passive block and descent of active block.



e) Stage 5: Active block comes to rest on rupture surface, movement essentially ceases as a more stable geometry is achieved.

Figure 5.1: Five kinematic stages in the development of a compound translational slide (modified from Soe Moe et al. (2006)).



Legend (for Figures Figure 5.2, Figure 5.4, and Figure 5.7):

	Scarp- sharp; length of downslope lines to give an indication of length of feature
	Scarp- rounded
	Ridge
	Surface drainage in direction of arrow
	Extension cracks

Figure 5.2: Composite photograph (top) of the North slide, June 2016, with interpretation (bottom). Note weathered rear scarp and mid-slope uphill-facing scarps; irrigated plateau above the Goddard slide is visible in the background; vantage point is standing above the south flank looking north, as indicated on Figure 5.4.

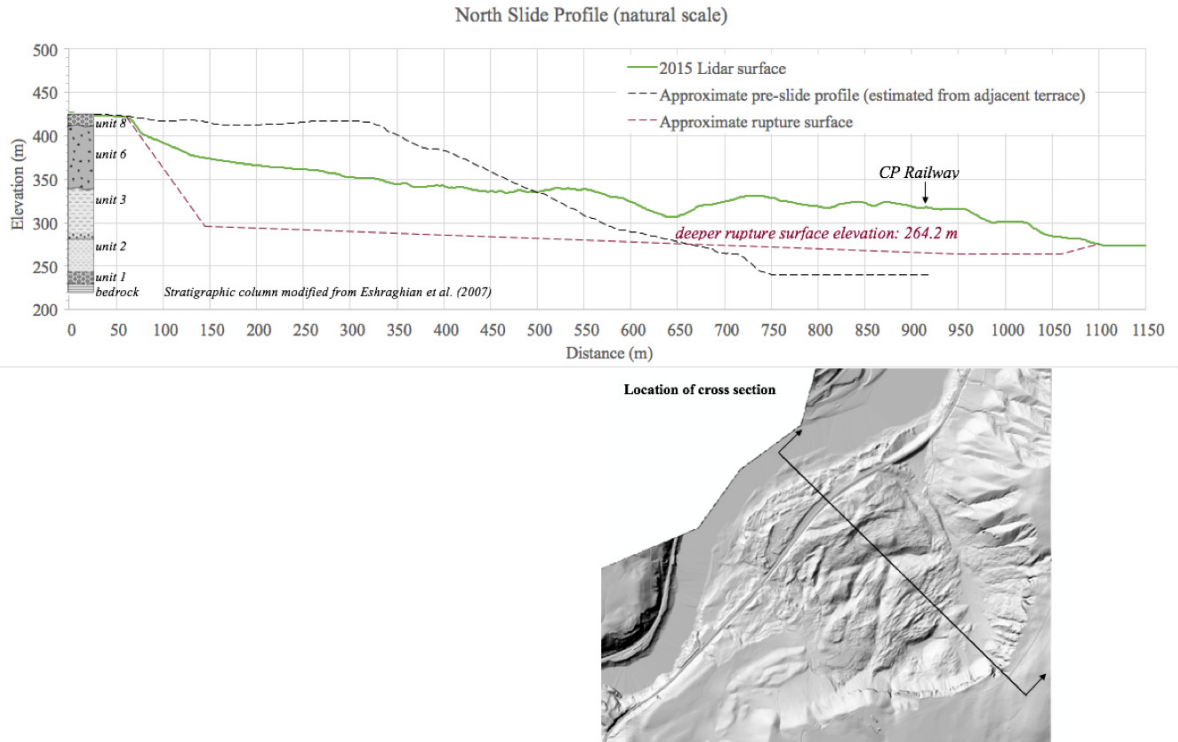


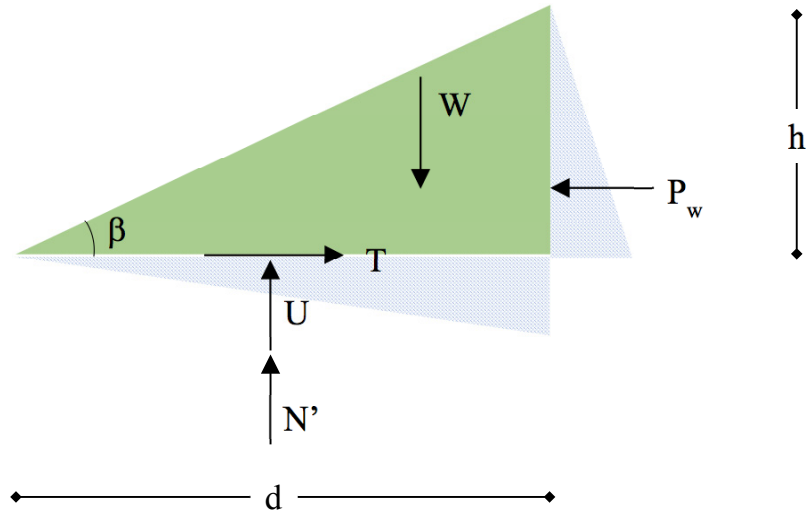
Figure 5.3: Cross-section through the North slide, based on 2015 LiDAR data (courtesy of CN). Stratigraphy and rupture surface after Eshraghian et al. (2007).



Figure 5.4: 1928 aerial photo of the North slide (left), with interpretation (right). Photo courtesy of Natural Resources Council (NRC), Roll A291, No. 54.



Figure 5.5: Carbonate (?) precipitates at slope face in seepage area south of the South slide; location shown in Figure 5.7 (June 2016).



- | | |
|------------------------------------------------|-----------------------------------------------------------------------------------------------------------------------|
| γ_w = unit weight of water | N' = effective normal force |
| γ_t = unit weight of soil | P_w = cleft pore water pressure = $\frac{1}{2} \cdot \gamma_w h^2$ |
| ϕ' = effective soil friction angle | U = pore water pressure acting on rupture surface
= $\frac{1}{2} \gamma_w h d = \gamma_w \frac{h^2}{\tan \beta}$ |
| β = slope angle | W = weight of wedge = $\frac{1}{2} \cdot \gamma_t h d$ |
| h = height of wedge | T = mobilized shear force at onset of movement in frictional material = $N' \cdot \tan \phi'$ |
| d = length of wedge = $\frac{h}{\tan \beta}$ | |

Force equilibrium in vertical direction:

$$(N' + U) = W \quad [5-1]$$

$$\left(N' + \frac{1}{2} \gamma_w h d\right) = \frac{1}{2} \cdot \gamma_t h d \quad [5-2]$$

Assume the unit weight of the soil is approximately twice the unit weight of water, i.e.:

$$\gamma_t = 2 \cdot \gamma_w \quad [5-3]$$

Then equation [5-2] becomes:

$$\left(N' + \frac{1}{2} \gamma_w h d\right) = \gamma_w h d \quad [5-4]$$

$$N' = \frac{1}{2} \cdot \gamma_w h d = \frac{1}{2} \cdot \gamma_w \frac{h^2}{\tan \beta} \quad [5-5]$$

Force equilibrium in horizontal direction:

$$T = P_w \quad [5-6]$$

$$N' \cdot \tan \phi' = \frac{1}{2} \cdot \gamma_w h^2 \quad [5-7]$$

$$\left(\frac{1}{2} \cdot \gamma_w \frac{h^2}{\tan \beta}\right) \cdot \tan \phi' = \frac{1}{2} \cdot \gamma_w h^2 \quad [5-8]$$

$$\left(\frac{\tan \phi'}{\tan \beta}\right) = 1 \quad [5-9]$$

$$\beta = \phi' \quad [5-10]$$

Figure 5.6: Derivation of the stable slope angle for a wedge of frictional soil sliding on a horizontal rupture surface, with cleft water pressure at the rear crack.

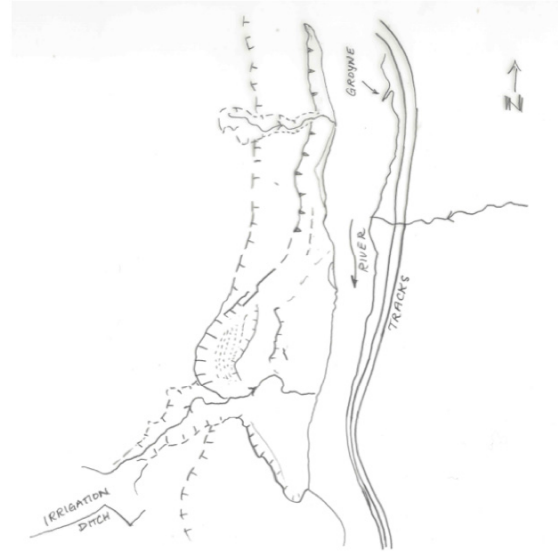
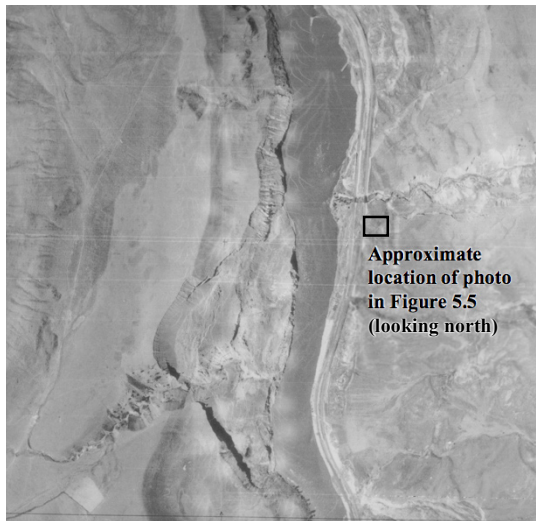


Figure 5.7: 1928 aerial photo of the Red Hill slide (left), with interpretation (right). Photo courtesy of Natural Resources Canada (NRC), Roll A291, No. 46.



Figure 5.8: Composite photograph of the Red Hill slide, taken from the opposite bank of the Thompson River, looking west (June 2016).

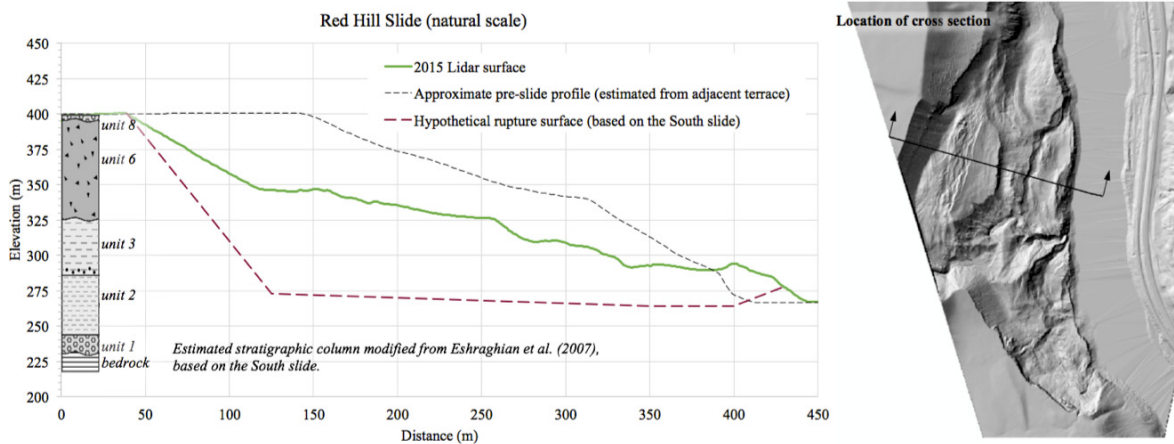


Figure 5.9: Cross-section through the Red Hill slide, based on 2015 LiDAR data (courtesy of CN). Stratigraphy and rupture surface interpolated from data at the South slide (after Eshraghian et al. (2007)).



Figure 5.10: Composite image of the Red Hill slide in 1928 (centre of image), with older scarp visible to the left (south) of the main slide area. Photos courtesy of Natural Resources Canada (NRC), Roll A0291, No. 45 & 46.

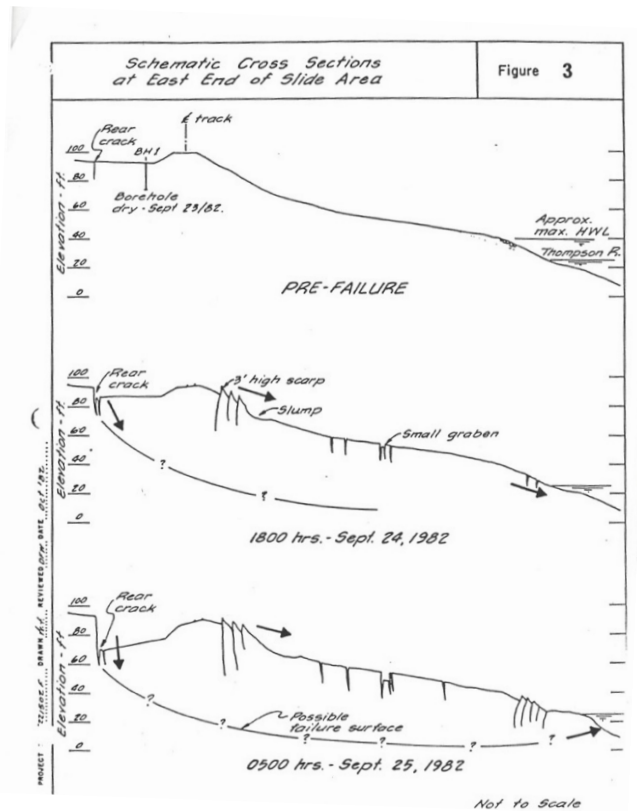


Figure 5.11: Schematic cross sections of the 1982 Goddard landslide before, during and after failure (from Wood (1982)); location shown on Figure 5.13.

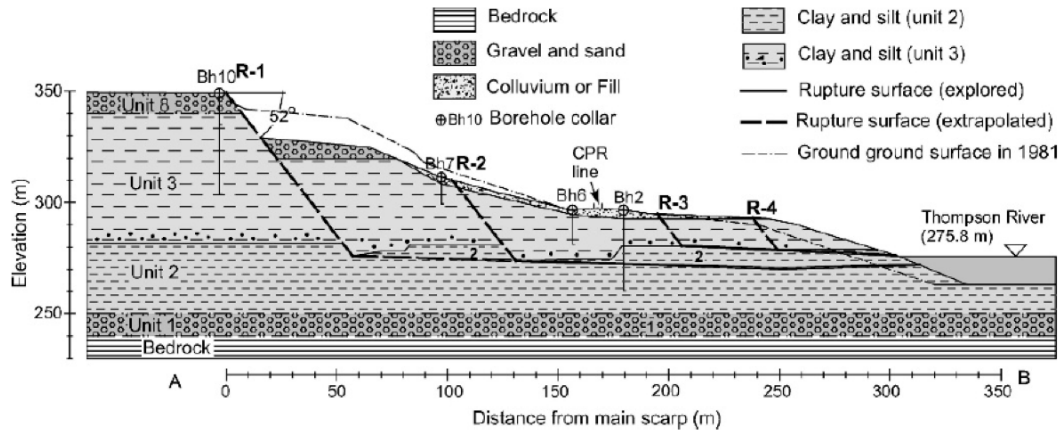


Figure 5.12: Simplified stratigraphic cross-section of the 1982 Goddard landslide, with pre-slide surface profile indicated by the dashed line (Eshraghian et al. 2007); location shown on Figure 5.13.

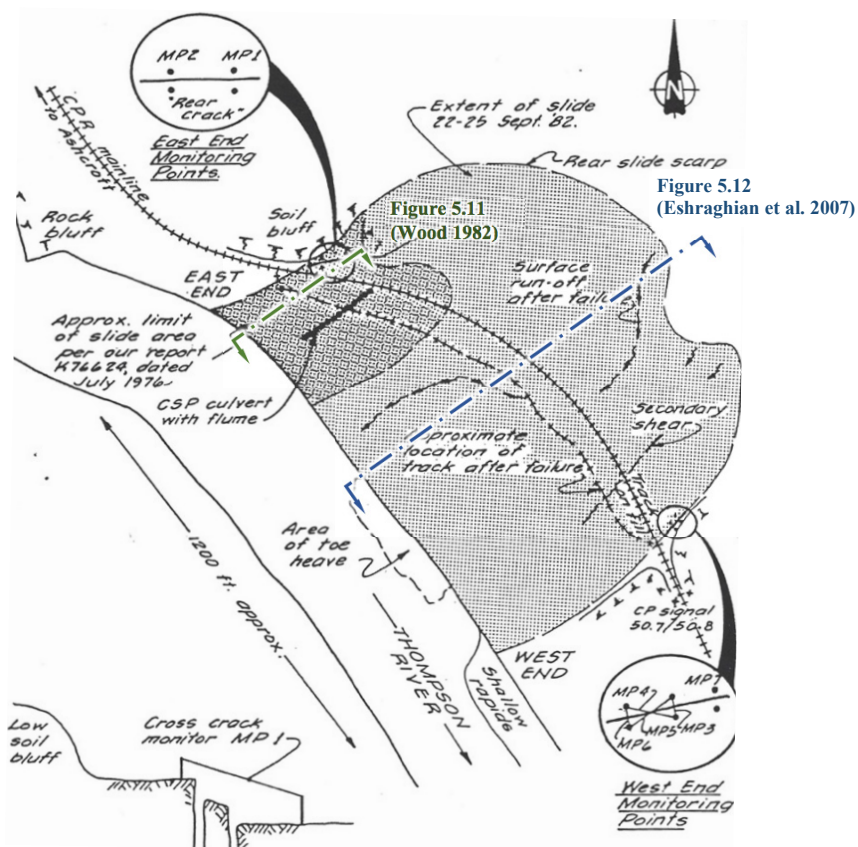


Figure 5.13: Sketch plan view of the 1982 Goddard landslide; note location of monitoring point MP-1 on the north flank of the landslide (modified from Wood (1982)).

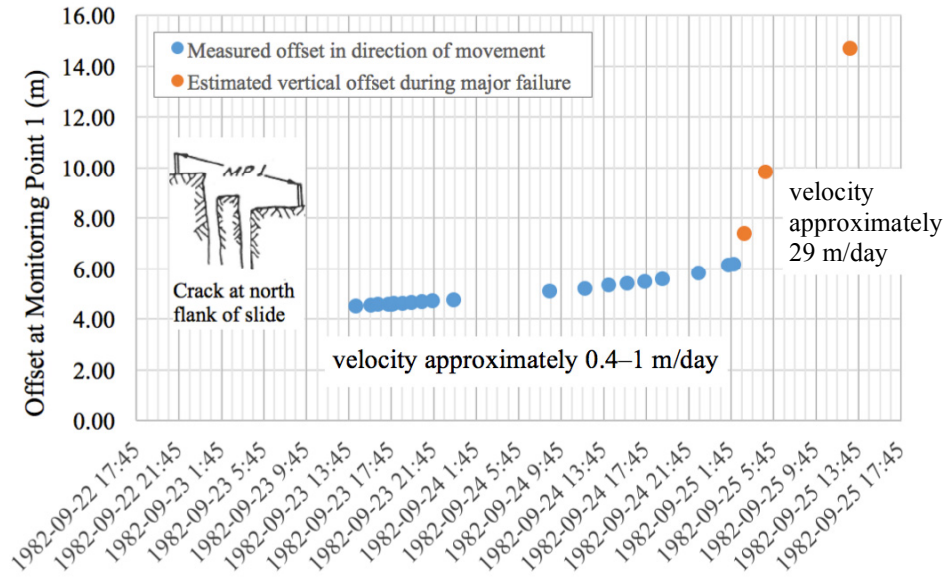


Figure 5.14: Cumulative surface displacement at north flank of 1982 Goddard slide, as determined from surface offset displacements recorded by Wood (1982); inset figure modified from Wood (1982).

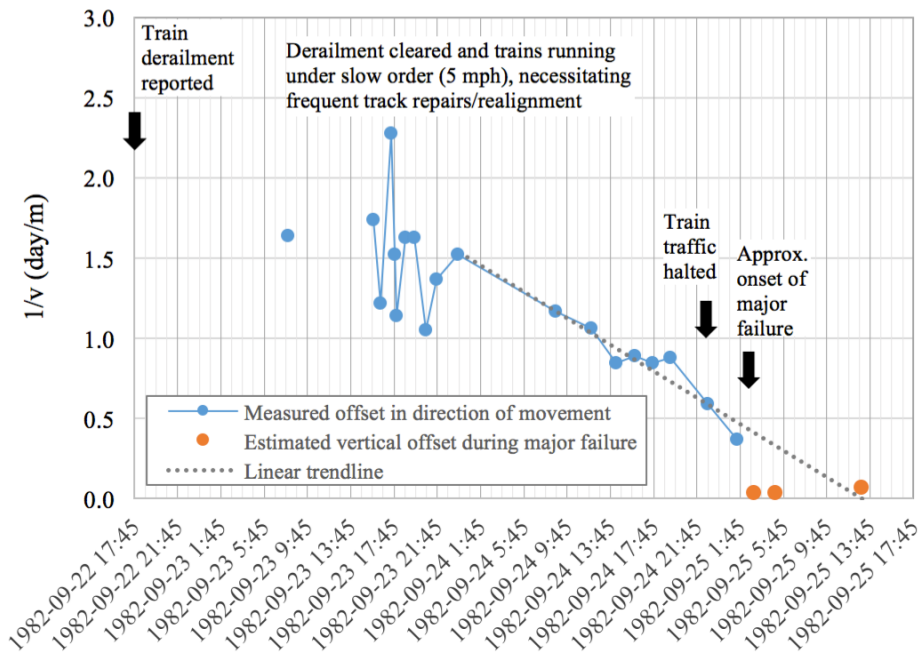


Figure 5.15: Inverse velocity of surface offset displacements during 1982 Goddard slide, with linear trendline established using surface displacements recorded by Wood (1982) from approximately 27 hours prior to onset of major failure.

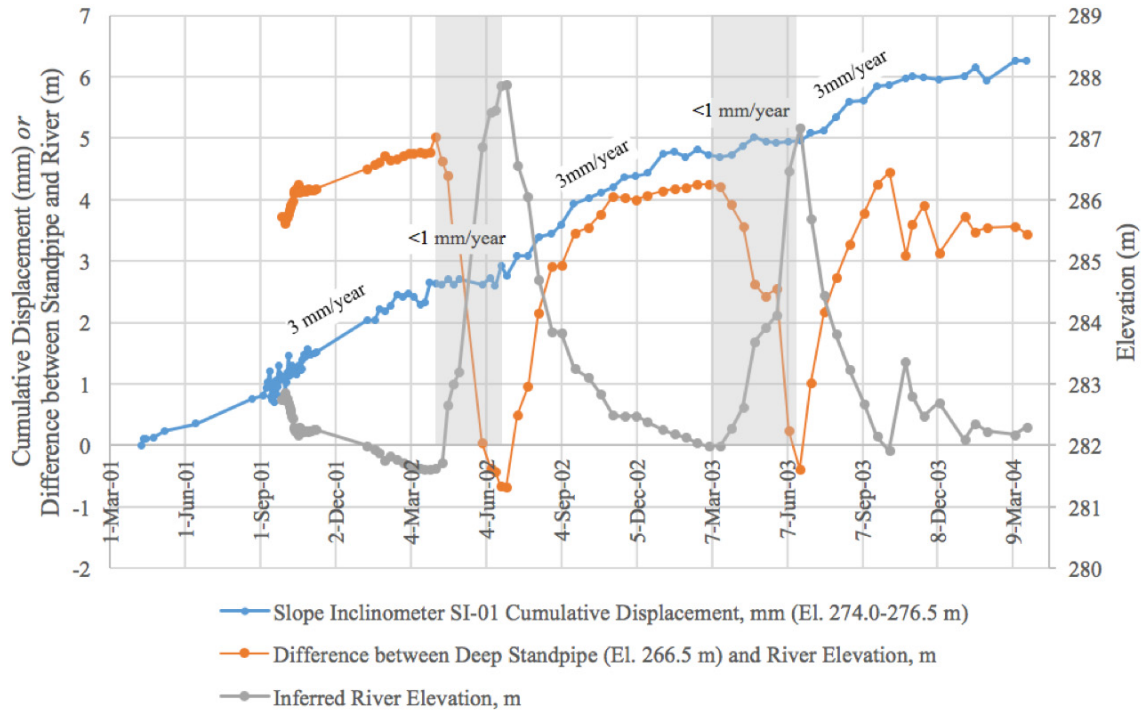


Figure 5.16: Relationship between CN50.9 landslide displacement (deep shear zone), Thompson River elevation, and deviation of bedrock pore pressure elevation from river level. Figure prepared based on instrumental data provided by BGC Engineering Inc., with the permission of Canadian National Railway.

6. LANDSLIDE RISK ASSESSMENT AND MANAGEMENT STRATEGY

“Whoever controls the definition of risk controls the rational solution to the problem at hand.”
— Slovic (1999)

6.1. Risk Assessment and Management Concepts

The Canadian Standards Association (1997) defines risk management as a systematic methodology for analyzing, evaluating, controlling and communicating about risks, as illustrated in Figure 6.1. The objective of risk management is to ensure that significant risks to a particular system are identified, and that appropriate actions are taken to minimize these risks to the extent reasonably achievable (Canadian Standards Association 1997). Risk assessment, which is a subcomponent of the risk management process, is the systematic identification of hazards, their probability of occurrence and their associated consequences to a particular system (Ayyub 2003). While the process of risk assessment is often viewed as a technical or scientific undertaking, in their *Risk Management Guideline for Decision Makers*, the Canadian Standards Association (1997) emphasized that risk involves three issues: the frequency of the loss, the consequences of the loss, and the perception of the loss—that is, how a risk is viewed by affected stakeholders in the larger socio-political-economic context.

It is insufficient for decision-makers to consider risk solely in terms of probability and consequence—the Canadian Standards Association (1997) Guideline stresses the importance of an effective communication strategy involving all stakeholders¹² in all phases of the risk management process. This includes the discussion of strategies for mitigating the risks, as these control measures may generate additional risks which ought to be evaluated in terms of the needs, issues and concerns of all interested and affected parties (Canadian Standards Association 1997). As illustrated in Figure 6.1, two-way communication and exchange of information between stakeholders is essential to all phases of the risk management process,

¹² Stakeholders are defined in accordance with the United States National Research Council (1996) as all “interested and affected parties.”

and decisions made should balance the technical aspects of risk assessment with the social and moral considerations that accompany the normative judgements of what constitute *acceptable* risk (Canadian Standards Association 1997). This chapter discusses strategies for assessing and managing the landslide risk to the railway corridor south of Ashcroft, while Chapter 7 focuses on models and case studies for stakeholder involvement in the risk decision-making process.

6.2. Importance of Railway Ground Hazards and Risk Management

In Canada, ground hazards pose a significant risk to the safety and reliability of railway operations. Railway ground hazards comprise a broad group of natural hazards that have the potential to directly or indirectly result in track failure, including landslides, ground subsidence, hydraulic erosion and snow and ice events; earth landslides were the highest frequency cause of ground hazard incidents on Canadian National (CN) track between 1922 and 2002 (Keegan 2007). Incidents arising from ground hazards may occur in isolated, high relief locations, often adjacent to a body of water, resulting in incrementally higher severities of injury, property loss, track outages, recovery time and costs, and environmental impacts; moreover, the frequency and severity of railway incidents stemming from ground hazards is incrementally higher in Western Canada compared to other parts of the country (Keegan 2007). Keegan (2007) found that on Canadian National (CN) track, the average direct cost per railway ground hazard incident between 1992 and 2002 was \$350,000—five times greater than the next most costly, rail defects.

In seeking to assess the landslide risk to rail operations in the Thompson River Valley south of Ashcroft, the previous chapter explicitly identified three modes of failure (landslide hazard scenarios as described in Chapter 5), and their underlying causes and associated consequences to railway operations. Strategies for failure detection (monitoring) and corrective measures (mitigation, coping or adaptation) flow naturally from the identified modes and consequences, or in this case, the landslide risk scenarios.

A risk scenario is a defined sequence of events with an associated frequency and consequences (Canadian Standards Association 1997). The following section builds on the slope failure modes identified in Chapter 5, capturing the spectrum of landslide movements that have been, or are presently, active within the approximately 10-km reach of the Thompson River Valley south of the village of Ashcroft. It is argued that the direct and indirect consequences associated with each failure mode are fundamentally related to the velocity of the slope movement; this velocity is a function of the failure mode and the underlying causes of movement. The limited and incomplete record of documented landslide events in the subject corridor over the last 150 years does not lend itself to a rigorous statistical evaluation; a conscious decision was therefore made to pursue a qualitative, rather than quantitative, assessment of the landslide risk to rail operations. The qualitative process of risk assessment and management broadly conforms to the following steps (modified from Ayyub (2003)): 1) define system; 2) identify potential failure modes; 3) identify failure mode causes and effects; 4) identify failure detection methods and corrective measures.

For situations where a quantitative risk assessment is deemed appropriate, examples have been produced by others for railways exposed to landslides (Bunce 2008), and in the form of a guidelines document for landslide risk management by the Australian Geomechanics Society (2007). Amongst the tools available for quantitative risk assessment, a Failure Mode and Effects Analysis (FMEA) could serve as a relevant tool for the logical elucidation of risk scenarios through the identification of potential failure modes or hazard scenarios, with consideration of their underlying causes and associated effects on the operation of the system as a whole (Ayyub 2003).

6.3. Spectrum of Landslide Failure Modes, Causes and Effects

As discussed in the preceding chapters, the morphology and mechanics of the landslides in the Thompson River Valley south of Ashcroft are consistent with reactivations of dormant landslides. The majority of the landslide movements appear to have occurred as reactivated, compound translational earth slides, though these may exhibit a remarkable range of velocities from extremely slow to rapid, with the associated effects ranging from undetectable to slope

failure and severance of railway infrastructure. Most of the landslides in the corridor appear to be of ancient origin, likely having originated during the post-glacial incision of the Thompson River, with renewed periods of activity coinciding with the introduction of agricultural irrigation in the mid-1800's, and the construction of railway infrastructure in the late-1800's/early 1900's. The largest, the North slide of 1880, is hypothesized to represent a unique failure mode: a complex earth slide-debris flow, which was precipitated by the breaching of an irrigation reservoir (Table 3.1). Three failure modes were proposed in Chapter 5 to capture the range of slope movement types and velocities which have been documented in the corridor over the last 150 years:

- Mode I): complex, extremely rapid earth slide-debris flow;
- Mode II): reactivated rapid compound translational earth slide;
- Mode III): active very/extremely slow earth slide.

The landslide failure modes and attendant risk scenarios are illustrated in Figure 6.2, and described in the following subsections. The causes of the landslides are complex, and have varied spatially and over time. As articulated in Chapter 5, several causal factors may conspire to move the mechanics of the landslide towards the kinematic threshold of rapid compound translational failure. Preparatory factors which predispose the valley walls to movement were described in Chapter 2. Given the evolution of natural and anthropogenic impacts to the Thompson River Valley slopes, primarily related to the introduction of agricultural irrigation and railway infrastructure in the valley, causal factors have evolved substantially over time and contemporary reactivations appear to be related to climate variations as described in Chapter 4.

Given the natural and built assets and diverse range of stakeholders in the Thompson River Valley, the direct and indirect effects of ongoing slope movements may have substantial economic, social and environmental implications. These potential outcomes are discussed in relation to the proposed monitoring and risk management strategy presented in Section 6.4. Evaluation of the acceptability or tolerability of the landslide risk so determined is an exercise which must be undertaken in concert with a representative cross-section of stakeholders.

Canadian case studies for stakeholder involvement in risk management decisions are presented in Chapter 7.

6.3.1. Mode III: Reactivated Very/Extremely Slow Earth Slide

At the lower end of the risk-spectrum, one or more of the Ashcroft Thompson River landslides may be seasonally active and exhibit very slow rates of step-wise movement, most notably in the fall and winter months when the river stage is lowest and the groundwater seepage direction is out-of-slope. The commencement of seasonal slope movements corresponds to the initiation of a positive gradient between the artesian groundwater in the bedrock and the falling river elevation in the autumn, with continuing very/extremely slow movements through the winter months. The effects of this type of activity have been documented at landslides traversed by railway infrastructure in the corridor over the last century, including the CN 50.9, Goddard, North, South, Ripley and Nepa Crossover slides (Table 3.1), as well as more recently at the southern extension of the South slide and the foot of the Red Hill slide, with the assistance of space-born InSAR technology (Huntley et al. 2017b). Huntley et al. (2017b) found very slow (but detectable) movements characteristic of seasonal landslide activity with the highest surficial movement rates in the fall/winter, of 60 mm/year at the foot of the Red Hill slide, 30–40 mm/year at the southern flank of the South slide, and about 50 mm/year at the Ripley slide.

Measurements of extremely slow movement rates have been undertaken at depth in the CN 50.9 slide and the Ripley slide, and related to the upward gradient produced by the interplay of the river stage and artesian groundwater pressure underlying the rupture surface, as described in Section 5.2.5.1. The measured rates of movement are millimeters to centimeters per year. Where in-situ displacement monitoring has been undertaken for discrete intervals of time, such as at the CN 50.9 and the Ripley landslide, it has been demonstrated that even in years where the Thompson River flow departure does not exceed the proposed threshold of 3,400 Mm³, very/extremely slow seasonal movements generally persist at rates detectable with instrumentation.

As described in Chapter 4, very/extremely slow landslide reactivations have historically produced noticeable slope deformations in years when the Thompson River's cumulative flow departure from normal has exceeded 3,400 Mm³ (or approximately 14% above average cumulative flow), as evidenced by surface cracks, railway track subsidence etc. While the database of very slow landslide reactivations is incomplete due to the relatively benign nature of many of these events, the river flow threshold for these movements was exceeded 15 times in the 96 years of record between 1912-2011, corresponding to a historic frequency of once every 6.4 years. It is evident from an analysis of 20th century river discharge records that the cumulative flow of the Thompson River is subject to interannual and interdecadal cycles. During the cool/wet phase of the Pacific Decadal Oscillation (PDO), the 3,400 Mm³ threshold was exceeded once every 4.4 years, with less-frequent exceedances (1 in every 10.4 years) during the warm/dry regimes of the PDO. The very slow landslide reactivations associated with these return periods have resulted in minor damage to railway infrastructure, prompting geotechnical investigations and necessitating more frequent track maintenance activities. Correlations of landslide activity with river flow and regional snow pack departures from normal could potentially serve as early-warning tools for anticipating the onset of Mode III slope movements in the corridor; peak, basin-wide, snow pack departures from normal of approximately 20% have historically preceded high river flow years and seasonal landslide activity in the corridor. Monitoring broader climate patterns such as the Pacific Decadal Oscillation (PDO) could be beneficial for longer-term (interdecadal) forecasting of periods of increased landslide activity.

6.3.2. Mode II: Reactivated Rapid Compound Earth Slide

Further along the risk spectrum, rapid reactivations of compound translational landslides have occurred along the corridor south of Ashcroft several times in the last century—at the Goddard slide in 1886, the CN 50.9 slide in 1897, the Red Hill slide in 1921, and again at the Goddard slide in 1982. While the frequency of these rapid reactivations is considerably lower than for the slow reactivations, the consequences of the movements are substantially more severe. CP rail's main line was shut down for 6 days of emergency construction after the 1982 Goddard slide (Porter et al. 2002); train derailments reportedly occurred at the Goddard slide in 1886

(Stanton 1898b) and in 1982 (Wood 1982); the Thompson River was temporarily dammed by the Red Hill slide in 1921 (Ashcroft Journal 1921), and at least partially dammed by the CN 50.9 slide in 1897 (Daily British Colonist 1897). Displaced material entering the waterway during the late summer and early fall can also have devastating effects on salmon spawning where displaced sediment covers the gravel in the river's salmon spawning beds or prevents the migration of salmon further upstream (Septer 2007).

Similar to the slow renewals of movement, these rapid reactivations have typically occurred in years when the Thompson River flow exceeded the 3,400 Mm³ threshold, but are hypothesized to have been exacerbated by some additional destabilizing activities such as change in slope geometry due to earthworks associated with the original railway construction (Goddard 1886, Red Hill 1921), increased river erosion due to constriction of the river by railway construction fill (Red Hill 1921, Goddard 1982) or landslide activity on the opposite river bank (CN 50.9), and/or increased groundwater pressures due to irrigation (Red Hill 1921, Goddard 1886 and 1982), rain or late persistence of exceptional snowfall (Goddard 1982).

Any re-profiling of the natural hillslopes in the subject corridor, especially by excavation, should be scrutinized. Even if the excavation flattens the toe of the slope, it may effectively produce unloading on a deeper rupture surface, as demonstrated by the simple physical model in Hutchinson (1984). Bromhead (1992) cited two examples where seemingly innocuous excavations near the toes of slopes caused the reactivations of pre-existing deep-seated failures due to unloading at the toe; these are a 1962 failure in the Lias Clays in Lyme Regis, Dorset (Pitts 1979), and a similar, but smaller slide in London Clay at Highlands Court in South London, where the excavation of only a metre or so of fill for site redevelopment triggered slope movements which required the installation of deep piles and shallow drainage works in order to arrest the movements (Allison et al. 1991).

It bears repeating that the CN 50.9 landslide of 1897, the Red Hill landslide of 1921, and the Goddard landslide of 1982 are important examples of rapid landslides in the corridor which cannot simply be attributed to ditch-and-furrow irrigation. They demonstrate the possibility that a landslide caused by factors other than ditch-and-furrow irrigation (factors such as river

erosion which persist to the present day) can be sufficient to dam the Thompson River (if only for a few hours); and that this sort of occurrence is still a contemporary possibility. Compound translational landslides are of a cyclic nature; the cumulative effects of a variety of causal factors may conspire to move the mechanics of the landslide towards the kinematic threshold for rapid compound translational failure. As articulated in Chapter 5, the formation of the active block through the growth and coalescence of cracks, facilitated by the cumulative effects of slow, precursory movements, can transpire over many years to dramatic effect.

6.3.3. Mode I: Complex Very Rapid Earth Slide-Debris Flow

The historic landslide failures which would today exert the highest consequences due to their large volume, very rapid rate of movement and high mobility, are the Mode I complex earth slide-debris flows, which include the North Slide of 1880 and the Spences Bridge slide of 1905. As discussed in the previous chapter, it is hypothesized that these complex slope movements were initiated by inundation of the river terraces with irrigation water, leading to saturation and sliding of the loose colluvium mantling the terrace slopes, which could have produced undrained loading and liquefaction of the contractant alluvial terrace deposits. This sequence of events supports the hypothesis that the high mobility of these landslides resulted from the liquefaction of saturated sediment at the base of the moving mass, with large quantities of ponded water available to drive the displacing material forward as it began to move. As demonstrated by the historical accounts of the North slide in 1880 and the Spences Bridge slide in 1905, and more recently by the comparable event in Oso, Washington, the remobilization of previously-failed deposits can be particularly dangerous. Notwithstanding, as concerns the Thompson River Landslides south of Ashcroft, history appears to indicate that the highly-mobile catastrophic movements of the North slide and Spences Bridge slide were facilitated by a substantial supply of ponded water related to intensive ditch-and-furrow irrigation of the upland areas. Given the evolution of irrigation methods, and Ashcroft's naturally semi-arid setting, it seems highly unlikely that this amount of surface water could be made available in the present day. From a risk management perspective, I would therefore argue that, barring substantial changes in precipitation and the climatic setting of the valley,

the Mode I type of complex rapid failure can be viewed as an artifact of now-discontinued irrigation practices which need not be revisited.

6.4. Risk Scenarios and Risk Management Strategy

6.4.1. Direct Operational Effects

Slope movements in the Thompson River Valley south of Ashcroft have a direct negative impact on the railway infrastructure located in the valley. Main lines of the Canadian National (CN) and Canadian Pacific (CP) railways traverse the lower portions of many of the active landslides on both the east and west sides of the corridor; these railways connect the bustling Port of Metro Vancouver to the rest of the country, and represent a vital artery of the national transportation network. Any impacts on the operational capacity of the railways have economic consequences for the railway companies themselves, but also have substantial implications for the national transportation of goods. Interruption of this transportation corridor can result in economic losses that grow exponentially with the duration of the outage (Bunce and Chadwick 2012), as demonstrated by the substantial losses associated with the 6-day closure for emergency remedial construction following the 1982 Goddard landslide (Porter et al. 2002). The magnitude of the impact of a slope movement on railway operations is directly related to the velocity of the slope displacement. Very or extremely slow seasonal slope movements are readily handled by regular track maintenance, which includes replenishing sunken ballast and re-aligning the tracks (Hendry et al. 2013b). A rapid reactivation, however, such as occurred at the Goddard landslide in 1982, can result in complete closure of the affected rail line(s) for several days, incurring substantial emergency repair costs in addition to the ongoing effects of reduced capacity resulting from slow orders which may persist for days or weeks. A sudden landslide reactivation could also produce a train derailment in the Thompson River Valley, with attendant implications for the safety of railway employees and environmental impacts to the Thompson River. Even when the Mode I type of complex earth slide-debris flows are removed from the picture of plausible future events, as I have argued they can rationally be, potential impacts of Mode II and III slope failures threaten both serviceability of the railway lines, and safety and protection of persons and the environment.

Figure 6.2 depicts the three landslide failure modes (I, II and III) and the risk scenarios (Stage 1, Stage 2 and Stage 3) which are derived from the recorded history of landslide events in the subject corridor (Table 3.1). The scenarios are termed Stage 1, 2 and 3, in order of increasing risk; they represent roughly order-of-magnitude differences in peak velocity and annual displacements. Moreover, each scenario corresponds to a particular stage in the kinematic evolution of a compound translational landslide (Soe Moe et al. 2006), which should be confirmed by regular field inspections. The corresponding kinematic stages are as follows:

- Stage 1: failure mode not yet declared—surface expressions of landslide movements not readily identifiable;
- Stage 2: failure mode forming—growth and coalescence of cracks leading to formation of active block via propagation of main scarp and counterscarp;
- Stage 3: failure mode declared—fully-formed counterscarp penetrates to depth of the rupture surface, producing a kinematically admissible failure mechanism through internal shearing producing a driving force associated with subsidence of the active block.

These risk scenarios are based specifically on experiences at the Thompson River landslides south of Ashcroft, and would not be generally transferable to other locations, though similar site-specific methodologies could be developed based on relevant experience at other locations. As shown on Figure 6.2 the risk scenarios pertain to Mode II and Mode III slope movements, and do not explicitly address the complex earth-slide debris flow type of movement (Mode I), which I have argued to be contingent upon now-arcane methods of ditch-and-furrow irrigation.

Operational maintenance experience over the last century suggests that Stage 1 events (extremely/very slow seasonal landslide reactivations) can be reasonably managed by the railways within the context of regular track maintenance activities. The accurate and timely recording of observed slope deformations and associated maintenance activities would be beneficial for enhancing the sporadic record of slow-moving landslide events which have taken place over the last century in the corridor, and for affirming and refining the proposed

correlations between the basin snow pack and Thompson River flow levels (Chapter 4) portending years of unusual landslide activity and reduced track serviceability in the corridor.

Based on the retrospective analysis of the rapid reactivation of the Goddard landslide in 1982 (Chapter 5), I would argue that Stage 2 events be managed by a strategy aimed at integrating real-time monitoring of surface displacements with field inspection and recognition of the evolution in the kinematic stages of a compound translational landslide. While the most representative indicator of damage potential to infrastructure may be the monitored landslide displacement rate, the risk assessment of complex landslides requires a more detailed analysis integrating an understanding of the kinematic behaviour underlying the slope movements, and the potential for future change (Lollino et al. 2016)—understanding the likelihood of progression from a Stage 2 to a Stage 3 scenario.

6.4.1.1. Impact of slope movements on railway track alignment

Several authors have studied the effects of very slow slope movements on the railway track alignment at the smaller Ripley landslide in the Thompson River Valley south of Ashcroft. While the estimated volume of the 750,000 m³ Ripley slide is comparatively small, it is currently the most active landslide in the corridor and is traversed by both CN and CP tracks (Macciotta et al. 2016). In their investigation of remotely-monitored movement rates at the Ripley landslide, Bunce and Chadwick (2012) proposed that trains be slowed when the total horizontal movement exceeded 25 mm; to protect against rapid acceleration trains would be stopped if movement exceeded 12.5 mm in 24 hours.

Due to localized ground displacements being accommodated by a lengthy section of track, Hendry et al. (2013b) found that slope displacement rates of approximately 80–100 mm/year at the Ripley landslide yielded annual track alignment deviations of less than approximately 25 mm/year, most within the 5–15 mm/year range. Real-time monitoring of the surface displacements (using GPS) and subsurface displacement (using an SAA) at the Ripley landslide showed an annual cycle of slope deformations most active between September and May, with cumulative horizontal displacements between approximately 80–120mm/year

(Hendry et al. 2013b, Macciotta et al. 2016). Elevation changes ranged between 25 and 80 mm for the north and south areas, of the slide, respectively (Macciotta et al. 2016). The average horizontal velocities during the active displacement period were between 0.2 and 0.35 mm/day; the Ripley slide was most active between September and May, with maximum horizontal rates of movement during the peak season of up to about 0.6 mm/day, as measured by GPS and Slope Accel Array (SAA) (Macciotta et al. 2016). Hendry et al. (2013b) indicated that seasonal movements of this magnitude were accommodated with normal track maintenance practices. Macciotta et al. (2016) suggested that sustained velocities over 1.5 mm/day should trigger a warning for intensified monitoring at the Ripley landslide to assess the potential for rapid acceleration of the moving mass. GPS can assess horizontal displacements with greater accuracy than vertical displacements, and given the primarily translational nature of the Ashcroft slides, the following discussions focus on horizontal movements.

Operating track speed in the corridor south of Ashcroft can exceed 64 km/h under normal conditions, which make this section a Class 4 track (Macciotta et al. 2016). Transport Canada's *Rules Respecting Track Safety* mandate that for a Class 4 track, deviations in alignment exceeding 38 mm require a slow order to be issued and repairs to be carried out within 72 hours (Transport Canada 2011). The alignment is evaluated as the midpoint offset of an 18.9 m (62 foot) chord; because differential slope deformations are accommodated by a large section of track, the incurred track deflection will be less than the horizontal displacement of the slope. Analysis of track deflection records at the Ripley landslide by Macciotta et al. (2016) suggest that horizontal slope displacements in the order of 150 mm would be required to exceed the Transport Canada criteria of 38 mm of track deflection. Their approach assumed a linear relationship between the horizontal slope displacement and the associated track deflection; moreover the Ripley landslide for which the relationship was derived is substantially smaller than the other landslides in the corridor. However, the translational kinematics of the Ripley slide are similar to those exhibited by the other larger landslides, where the slope translates seasonally along a sub-horizontal shear surface at a very slow velocity (Macciotta et al. 2016). Moreover, differential movements are generally confined to the flanks (or lateral margins) of the landslides (Hendry et al. 2013b) as illustrated on Figure 5.13 for the 1982 Goddard

landslide (Wood 1982); hence it is reasonable to assume that the track deflections associated with both slow and rapid reactivations will be somewhat independent of the circumscribed volume of landslide material.

6.4.2. Slope Monitoring Strategy and Kinematic Threshold Criteria

While remote sensing of surface displacements addresses certain economic realities in terms of what may be feasible for monitoring kilometers of unstable valley walls, criteria for failure prediction based on the rate of movement should also be contextualized within a broader understanding of the relevant rupture mechanics and state of the slope prior to failure (Hungr et al. 2005). Seeking to manage landslide risk only by means of monitoring the surficial slope displacement rates provides only partial information on the landslide hazard and attendant risk, since no indication of the landslide mechanics is obtained (Lollino et al. 2016). Based on a synthesis of the published experience concerning track deflections resulting from very slow displacements at the Ripley landslide (Hendry et al. 2013b, Macciotta et al. 2016), unpublished offset measurements taken during the rapid reactivation of the Goddard landslide in 1982 (Wood 1982), and general stages in the kinematic evolution of deep-seated compound translational landslides (Cruden et al. 2003, Soe Moe et al. 2009), Table 6.1 presents a recommended slope monitoring strategy for implementation in the Thompson River Valley south of Ashcroft. The table integrates real-time monitoring of surface displacements with field inspection and recognition of the evolution in the kinematic stages of a compound translational landslide; when a kinematic threshold is crossed, the landslide behaviour is ushered into the next stage as expressed by an order-of-magnitude increase in displacement rate. Two levels of management are proposed for addressing the direct effects of slope displacements on railway operations: ongoing track maintenance supplemented by documentation for identifying active areas of coherent deformation; and monitoring of surface displacements in more-active areas, supplemented by field inspections for assessing the kinematic evolution in the formation of a compound translational landslide.

Table 6.1 apportions slope movements into three risk categories derived from real-time monitoring of horizontal slope deformations, expressed as a maximum daily velocity, v_{\max} ,

and cumulative annual displacement. The categories are delineated based upon the landslide activity levels, associated kinematic stages, and their expected impacts on track performance. The risk categories (Stages 1, 2 and 3) correspond to annual slope displacements in the ranges of <100 mm, 100–1000 mm, and >1000 mm, respectively (Table 6.1). The mode of movement is implied from the previous discussions to be a compound translational earth slide exhibiting extremely/very slow seasonal activity (Stage 1), which may intensify to a Stage 2 reactivation where track deflections exceeding the Transport Canada criteria are likely. Macciotta et al. (2016) suggested horizontal slope deformations in excess of 130 mm to 170 mm would be required to produce a track deflection in excess of 38 mm at the Ripley slide; 100 mm was selected as the lower boundary for the Stage 2 risk scenario, in order to reflect the uncertainty associated with generalizing the findings at the smaller Ripley slide to the larger slides in the corridor. Finally, a Stage 3 scenario represents a landslide reactivation of moderate to rapid velocity which, based on Wood's (1982) experience at the Goddard slide, may portend imminent, massive slope failure.

The proposed annual displacement ranges and their associated effects to the railway infrastructure correspond reasonably well with the movement ranges documented by Mansour et al. (2011) for expected damage to highway infrastructure due to slow-moving landslides. Mansour et al. (2011) compiled numerous case studies to suggest that annual slope displacement rates in the order of 10–100 mm/year would produce minor cracks in pavement requiring minor maintenance (patching) on an annual basis and re-paving every 3 to 4 years; slope movements in the 100–1600 mm/year range were likely to produce wider cracking in pavements requiring frequent patching, and development of large fissures in embankment slopes which could result in slope failure; and at annual displacement rates greater than 1600 mm/year, their research suggested that severe infrastructure collapse, traffic obstruction, and possible loss of life may occur (Mansour et al. 2011).

The upper bound of maximum daily velocity given in Table 6.1 for a Stage 1 scenario ($v_{\max} \leq 2$ mm/day) is based on surface displacement measurements at the Ripley landslide by Macciotta et al. , who suggested that sustained velocities over 1.5 mm/day should trigger intensified monitoring (Section 6.4.1.1). The lower bound of maximum daily velocity given

in Table 6.1 for entering a Stage 3 scenario ($v_{\max} \geq 400$ mm/day) is based on the slope displacements measured by Wood (1982) in the days preceding the 1982 Goddard landslide, which increased from approximately 400 mm/day to 1000 mm/day prior to the onset of rapid acceleration and slope failure (Section 5.2.4). No daily maximum velocity range is specified in Table 6.1 for a Stage 2 scenario, as there is a paucity of slope displacement measurements for the Ashcroft landslides in this stage of behaviour. In 1976, Golder Associates (1977) documented slope displacements of up to 10 mm/day (in the direction of movement) at the site of the Goddard landslide, which were accompanied by open cracks near a drainage culvert towards the north flank of the slide.

Research by Carlà (2017) suggests that the *change* in velocity (or acceleration) of a moving slope is more indicative of impending failure than the absolute value of the velocity of the slope movement. Slope acceleration is implicit in Table 6.1, in that each category represents a one to two order-of-magnitude difference in the maximum seasonal displacement rate, v_{\max} , implying an intervening acceleration of the moving mass. All of the movement rates represented in the table fall within Cruden and Varnes' (1996) classification of very/extremely slow (Stages 1 and 2) to very slow/moderate (Stage 3) movements, but the finer distinction between categories implies an important evolution in the kinematics of the compound landslide. Based on historical experience concerning the Ashcroft Thompson River landslides, a Stage 1 scenario may evolve kinematically into a Stage 2 situation, producing track deflections which may require immediate attention in accordance with the Transport Canada (2011) criteria, progressing still further into a Stage 1 scenario, which may portend imminent rapid slope failure. The Stage 1, 2 and 3 scenarios each represent a unique stage in the kinematic evolution of a compound slide. These correspond broadly to the framework proposed in Giordan et al. (2013) for characterizing the Montaguto earth flow in southern Italy:

- Stage 1: *low activity*– landslide is active, but displacement trend is low; based on past experience, the possibility for local reactivations cannot be excluded;
- Stage 2: *moderate activity*– displacement may be high in localized areas but no clear trend is apparent; may require specific attention/additional maintenance activities for maintaining track alignment within the regulated tolerance and maintaining

uninterrupted railway operations; based on past experience the possibility for acceleration of a moderate to large volume cannot be excluded;

- Stage 3: *high activity*– displacements are high throughout the landslide and the trend is in acceleration. The evolution of the landslide must be actively monitored; passage of trains may be dangerous or impossible due to accumulated displacements; organizational strategies should be implemented to prepare for a disruption in service.

The derivation of the Stage 1, 2 and 3 scenarios was outlined on Figure 6.2. An example of a Stage 1 scenario would be the slope movements observed via InSAR immediately south of the South slide, in the order of 20 mm/year, for which Journalt et al. (2016) confirmed that no visible cracks or surface expression of movement could be readily observed on the ground surface. This may progress to a Stage 2 scenario where coherent crack formation and growth is evident, and intensified monitoring is called for, as is currently underway at the Ripley landslide as described in Huntley et al. (2016), for example. The most severe scenario, Stage 3, may result from the fully-formed counterscarp intersecting the deep rupture surface and initiating a rapid, compound translational slope failure as occurred at the Goddard landslide in 1982 (Wood 1982). The potential for a slope in a marginally stable condition to progress from a Stage 1 through Stage 2 to a Stage 3 event provides the motivation for intensified monitoring, should the threshold between Stage 1 and Stage 2 be evident, either by way of increased velocity of movement or coherent evolution in the kinematics of the landslide movement.

Table 6.1 and Figure 6.3 identify risk management strategies for each of the Stage 1, 2 and 3 risk scenarios. A Stage 1 scenario poses the lowest risk, due to very/extremely slow landslide activity with limited consequences that can be managed by regular railway maintenance. Remote sensing of slope movements is recommended for evaluation of annual change. A Stage 2 scenario poses higher risk to the railways due to increased velocity of the slope movements, with the potential for accumulated displacements to induce track deflections in excess of the Transport Canada (2011) criteria; in addition to more frequent and onerous track maintenance, intensified monitoring is justified to provide additional information on the possibility of the kinematic evolution to a Stage 3 scenario. Site specific remedial slope repairs may also be contemplated at this stage. If intensified monitoring implemented in the Stage 2

phase identifies the slope to be in acceleration, and the velocity of displacements enters the Stage 3 range, rapid slope failure may be imminent. The recommended risk management strategies shift to anticipation and coping, using an inverse-velocity estimation of the failure time from measured surface displacements, and deploying procedures to communicate and cope with the potential for an interruption of railway service and potential social, economic and environmental impacts.

6.5. Indirect Effects

Damming of waterways may result from landslides whose displaced material moves rapidly enough and is of sufficient volume to inundate the valley floor and block the flow of the watercourse (Cruden and VanDine 2013). The volume of the displaced material and its rate of movement upon entering the water are the main factors determining the energy of the moving mass and hence the size and propagation of the waves generated (Cruden and VanDine 2013). The effects of waves so created can be felt over distances many times the dimensions of the material displaced by the landslide. This phenomenon was evidenced by the Spences Bridge landslide of 1905, where five people were reportedly buried by the slide debris, but an additional ten people were killed by the resulting displacement wave, which also carried away village infrastructure on the opposite side of the river with considerable force (see description in Section 3.2.13). Landslide generated waves may not only affect bridges and other waterway infrastructure, but also extend to communities, railways, roads and other linear infrastructure in proximity to the waterway (Cruden and VanDine 2013).

I have argued the most mobile and devastating landslides in the Thompson River Valley south of Ashcroft were the result of complex earth slide-debris flows, which occurred in concert with ditch-and-furrow irrigation at the North slide in 1880, and at Spences Bridge in 1905. The availability of ample ponded water draining into the sliding mass could have provided the unbalanced driving forces necessary to produce high movement rates and long runout distances by acceleration of the soil mass (Leroueil 2001). I have argued that given the evolution of irrigation practices and imposed irrigation restrictions, the recurrence of a Mode I earth slide-debris flow in the present day is extremely unlikely. Full or partial damming of the Thompson

River, however, could be still be achieved by a Mode II compound earth slide, as demonstrated by the CN 50.9 landslide of September 1897, which was of sufficient magnitude and mobility to partially dam the Thompson River, despite the reported absence of any streams or active irrigation in the relative vicinity (Victoria Daily Times 1897). In addition, the Red Hill slide which occurred on August 19, 1921 entirely blocked the Thompson River and caused an upstream rise in the river level of about 3.7 m (12 feet) (Ashcroft Journal 1921). Though attributed at the time to irrigation, it is likely that the Red Hill slide was the result of several causal factors, as described in Section 5.2.2.

According to Cruden and VanDine (2013), smaller dams in large rivers are typically overtopped within a few hours or days, as was the case in the damming of the Thompson River in the late-1800's by several of the landslides south of Ashcroft, and the 1905 landslide at Spences Bridge, as previously described in Chapter 3. Evans (1986) observed that landslide dams in stratified Pleistocene deposits are typically breached by a gradual enlargement of a spillway following overtopping and do not exhibit catastrophic breaching behavior. Catastrophic breaching of landslide dams is typically associated with steep, high configurations, where displaced soils are fine-grained and loose, and the downstream slope of the dam may be rapidly eroded (Cruden and VanDine 2013). Though the most recent damming of the Thompson River by landslide material occurred nearly 100 years ago, at the Red Hill slide in 1921, the recurrence of such a phenomenon remains a contemporary possibility which stakeholders should be aware of and prepared to cope with.

Another important indirect effect of a landslide in the Thompson River Valley is the possibility for displaced sediment to cover the gravel in the river's salmon spawning beds (Septer 2007). As the largest tributary of the Fraser River, the Thompson is an important Pacific salmon spawning waterway (Clague and Evans 2003). Clague and Evans (2003) reported that up to four million sockeye salmon and one million pink salmon migrate up the Thompson each year, comprising a resource with an annual commercial value in excess of \$100 million. Displaced material entering the waterway can prevent salmon populations from migrating upstream to spawn, and such blockages can have a devastating impact on the population and its commercial value, which may persist for generations (Clague and Evans 2003). In 1913, dumping of waste

rock during the construction of the Canadian Northern Railway (later CN) at Hell's Gate blocked an important back eddy used by the salmon as a passage through the narrow gorge; as a result of the obstruction, and others upstream, millions of stranded sockeye and pink salmon died without spawning (Septer 2007). This was followed by a major rock fall at Hell's Gate in 1914, which blocked the Fraser River and CN's tunnel, producing devastating effects on the salmon population with substantial economic implications (Septer 2007). In 1913, the sockeye catch had been 31 million fish, but after the Hell's Gate disaster the average annual catch over a four-year period dropped to 5 million (Septer 2007). The persistent effects of the rock fall continued to reduce the numbers of spawning salmon year by year; by 1944, investigations had shown that the obstruction at Hell's Gate was the major reason for the continued poor Fraser sockeye runs (Septer 2007). A conservative estimate placed the loss to commercial fisheries at nearly \$300 million, due to the consequent depletion of the salmon stocks between 1917-1947 (McGill 1979). In an attempt to restore the sockeye and pink salmon runs to their historical abundance, Septer (2007) reported that fishways were constructed at a cost of \$1.36 million between 1944–1966 to provide passage for the salmon past the obstruction. In 1978 dollars and landed values, the loss to the sockeye fisheries alone, resulting from a diminished return in 1914, amounted to an estimated \$1.7 billion between 1951–1978 (Septer 2007).

In addition, valuable agricultural land may be lost due to a landslide which encompasses the benchlands above the river in the Thompson Valley. Much of this land is used to produce hay for cattle feed and ginseng for the Asian export market (Clague and Evans 2003). Cultural implications of landslide impacts to the natural environment may also be substantial, particularly for indigenous people who have a unique relationship to their natural environment (Harmsworth and Raynor 2004). These cultural implications are addressed more thoroughly in the following chapter on resilience.

6.6. Conclusion

The direct and indirect consequences of a compound translational landslide in the Thompson River Valley are related to the volume of displaced material of the landslide and the velocity at which it moves (mobility). Railway infrastructure may be damaged and operations temporarily halted; salmon stocks in the Thompson River may be indirectly impacted; valuable agricultural land could be lost, and public safety could be threatened by upstream flooding due to damming of the waterway or a downstream wave resulting from breaching of a landslide dam.

An integrated risk management strategy has been presented based on a synthesis of published information on railway track deflections resulting from very slow slope displacements at the Ripley landslide, an inverse-velocity analysis of unpublished offset measurements taken during the rapid reactivation of the Goddard landslide in 1982, and the incorporation of general stages in the kinematic evolution of deep-seated compound translational landslides. Three risk scenarios were delineated based upon the landslide activity levels, associated kinematic stages, and their expected impacts on track performance. A compound translational earth slide exhibiting very/extremely slow seasonal activity (Stage 1), may intensify to a Stage 2 reactivation where track deflections exceeding the Transport Canada criteria are likely. Finally, a Stage 3 scenario represents a landslide reactivation of moderate to rapid velocity which, based on Wood's (1982) experience at the Goddard slide, may portend imminent, massive slope failure, with the potential to impact a broader group of stakeholders.

Risk management strategies employing monitoring, mitigation and adaptation relevant to each identified scenario were presented in Table 6.1 and Figure 6.3. Increased intensity of monitoring and remedial efforts correspond to increasing stages of kinematic evolution and landslide risk, progressing from Stage 1, to Stage 2, to Stage 3 scenarios. Strategies for integrating stakeholder perspectives into the risk management approach will be discussed in the following chapter, with the aim of increasing the overall resilience of the railway system and the affected communities.

Table 6.1: Summarized landslide monitoring and risk management strategy for the Ashcroft Thompson River Landslides.

Risk scenario	Possible ranges of approximate ground surface displacements	Kinematic expression	Risk management strategy
Stage 1	$v_{\max} \leq 2$ mm/day; annual displacement ≤ 100 mm	Subdued kinematics— Failure mechanism not yet evident	InSAR/GPS change detection monitoring Seasonal accelerations within expected range for regular track maintenance
Stage 2	$100 \text{ mm} < \text{annual displacement} \leq 1 \text{ m}$	Coherent crack formation and growth (crack aperture opening near toe and at backscarp, counterscarp forming)— Failure mechanism developing	Intensify monitoring (SAA, frequent LiDAR) Onerous/more frequent track maintenance Slow orders may need to be implemented Derailment possible Remedial works may be beneficial
Stage 3	$v_{\max} \geq 400$ mm/day annual displacement $> 1 \text{ m}$	Crack coalescence (counterscarp extends to rupture surface)— Failure mechanism declared	Rapid slope failure may be imminent Inverse velocity estimation of failure date Consider necessity of halting passage of trains and implementing strategy for coping with service interruption

CAN/CSA Q850-97 Risk Management Framework

Initiation

- Define problem or opportunity and associated risk issue(s)
- Identify risk management team
- Assign responsibility, authority, and resources
- Identify potential stakeholders and begin to develop consultation process



Preliminary Analysis

- Define scope of the decision(s)
- Identify hazards using risk scenarios
- Begin stakeholder analysis
- Start the risk information library



Risk Estimation

- Methodology for estimating frequency and consequences
- Estimate frequency of risk scenarios
- Estimate consequences of risk scenarios
- Refine stakeholder analysis through dialogue



Risk Evaluation

- Estimate and integrate benefits and costs
- Assess stakeholder acceptance of risk



Risk Control

- Identify feasible risk control options
- Evaluate risk control options in terms of effectiveness, cost and risks
- Evaluate options for dealing with residual risk
- Assess stakeholder acceptance of residual risk



Action / Monitoring

- Develop and implementation plan
- Implement chosen control, financing and communication strategies
- Evaluate effectiveness of risk management decision process
- Establish a monitoring process, sunset, terminate as applicable

Figure 6.1: Risk management framework (modified from Canadian Standards Association (1997)).

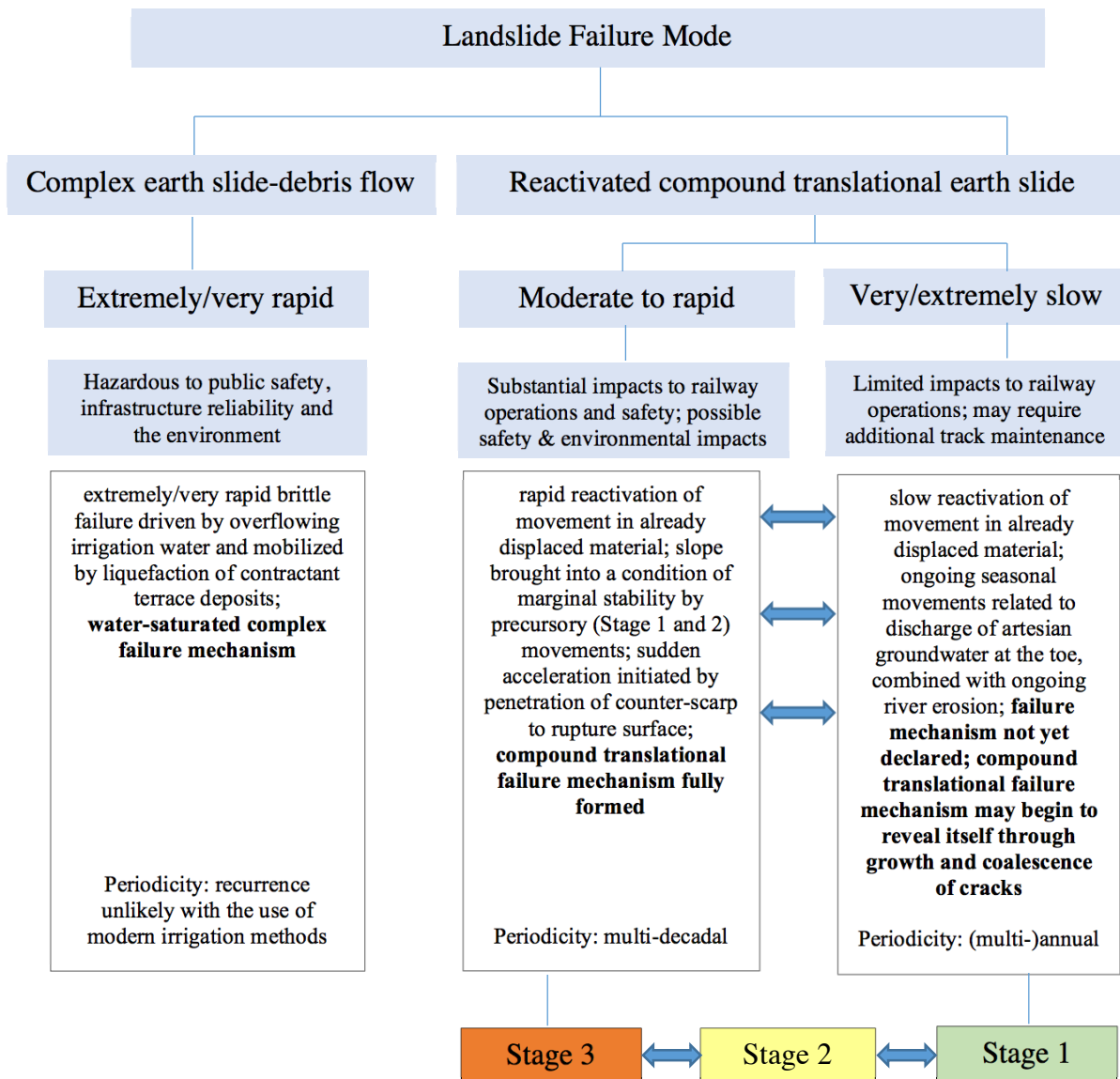


Figure 6.2: Landslide failure modes and attendant risk scenarios for the Ashcroft Thompson River Landslides.

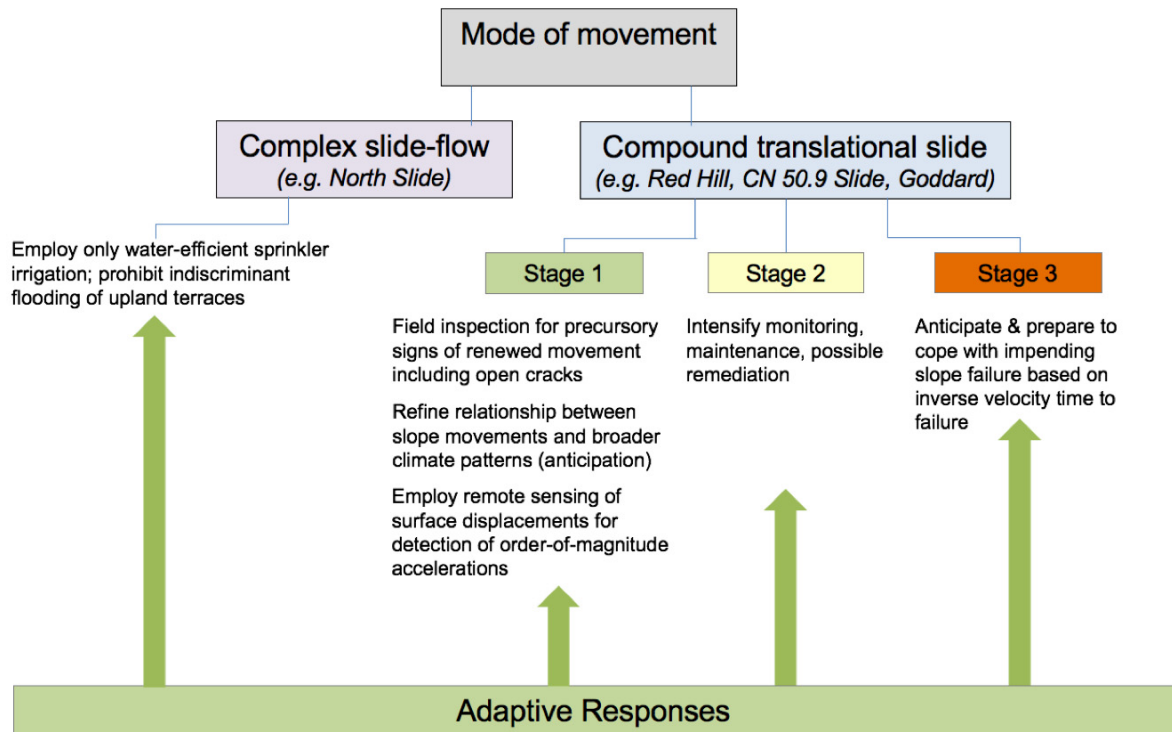


Figure 6.3: Landslide risk scenarios and adaptive responses.

7. RISK MANAGEMENT WITHIN A RESILIENCE FRAMEWORK

“The task that faces us is partly humanitarian and social, and partly technical, economic and political in character.”

— Hutchinson (2001)

7.1. Resilience Concepts and Frameworks for Managing Complex Risks

Portions of this chapter have been published in the journal paper *The District of North Vancouver’s Landslide Management Strategy– Role of public involvement for determining tolerable risk and increasing community resilience* (Tappenden 2014a) and the conference paper *Climatic influences on the Ashcroft Thompson River Landslides, British Columbia, Canada* (Tappenden 2014b).

Resilience may be described as the ability to cope with disruptions in a dynamic environment (Brunner and Giroux 2009). Rooted in the work of ecologist C.S. Holling (1979), the resilience paradigm recognizes that not all disasters can be predicted, nor avoided, and emphasizes the capacities of individuals, communities and corporations for adaptation, learning, and self-organization (Frommer 2013). While risk is often expressed as the static likelihood of an adverse event multiplied by its consequences, risk in the context of natural hazard management is a dynamic concept which manifests as fluctuating hazard levels and time-dependent consequences. This time dimension of risk is acknowledged in the concept of resilience, which may be understood as the collective ability to anticipate, cope with, resist, and recover from the impact of a natural hazard (Hufschmidt et al. 2005), as illustrated in Figure 7.1.

The levels of risk posed by the Ashcroft Thompson River landslides inevitably vary over time, both seasonally and in the long-term, due to the implicit relationship between the landslides and the climate described in Chapter 4. The potential consequences of a landslide, too, have a dynamic component; interruption of the railway transportation corridor can result in economic losses that have the potential to grow exponentially with the duration of the outage (Bunce and Chadwick 2012). Depending on the mobility of the landslide, the impacts to other stakeholders

may also be largely dependent on their ability to cope with the outcomes. The American National Infrastructure Advisory Council (2010) defined infrastructure resilience as the ability to reduce the magnitude and/or duration of disruptive events. In contrast to traditional risk management strategies focused on hazard mitigation and control, resilience strategies emphasize managing the outcomes of an adverse event through improved anticipation and coping capacities. Geotechnical engineers have always recognized the importance of the early warning concept as articulated in Peck's (1969) Observational Method; however, the resilience paradigm takes this notion a step further, underscoring "both the capacity of a system to react appropriately to moments of crises that have not been entirely anticipated, and its ability to anticipate these crises..." (Aguirre 2006). Resilience strategies take a transformed view of risk management which embraces long-term sustainability over short-term optimization, complexity over calculability, flexibility and creativity over predictability, and learning, coping and adaptation over control; these facets lie towards the centre-right of the risk management spectrum illustrated in Figure 7.2. Table 7.1 summarizes and contrasts various traditional engineering approaches to system management with concepts of resilience.

Following on the heels of the application of resilience in the context of social systems, several international government organizations are employing the concept of resilience in the assessment of their critical infrastructure, including the National Infrastructure Unit (NIU) in Wellington, New Zealand, and the National Infrastructure Advisory Council (NIAC) in Washington, D.C. NIAC (2010) defined infrastructure resilience as the ability to reduce the magnitude and/or duration of disruptive events, comprising four capacities: (1) Robustness—the ability to absorb shocks and continue operating; (2) Resourcefulness—the ability to skillfully manage a crisis as it unfolds; (3) Rapid Recovery—the ability to get services back as quickly as possible; and (4) Adaptability—the ability to incorporate lessons learned from past events (National Infrastructure Advisory Council 2010). This framework is illustrated in Figure 7.3, which powerfully illustrates the dynamic, ongoing and iterative nature of resilience. Similarly, the New Zealand National Infrastructure Unit (2011) defined infrastructure resilience as follows: "The concept of resilience is wider than natural disasters and covers the capacity of public, private and civic sectors to withstand disruption, absorb disturbance, act effectively in a crisis, adapt to changing conditions, including climate change, and grow over

time.” These definitions are effectively performance-based criteria, challenging the system to retain its basic structure and some level of function after a hazardous event has materialized, with anticipation, coping, recovery and learning (adaptation) all playing important roles in improving the resilience of the system over time.

7.2. Engineering Mitigation and Stakeholder Perspectives

As touched on in Chapter 3, landslide risk mitigation measures in the Thompson River Valley south of Ashcroft have primarily consisted of structural engineering measures supplemented by discrete periods of displacement and groundwater-level monitoring in areas where slope movements have adversely affected railway operations. Moving from north to south through the corridor, a rip-rap toe berm was constructed at the base of the CN 50.9 landslide in the 1970’s and enlarged in the early 2000’s, with the aim to reduce the rate of toe erosion and provide additional stability at the base of the slope. At the Goddard slide, following the rapid 1982 slope failure, the CP railway track was realigned and relocated upslope of the major failure. At the South slide, two large groynes (rock breakwaters extending into the river to protect against bank erosion) were constructed in the 1950’s and repaired in the late-1990’s (Edwards 2015), again with the view of reducing the rate of river erosion at the slide toe. A variety of in-situ and remote-sensing methods have been deployed for detecting slope movements and groundwater conditions, most recently at the Ripley landslide, as described in papers by Huntley et al. (2017a) and (2017b).

Perhaps the most innovative action that the railways have taken in the subject corridor has been the creation of a shared operating agreement, whereby all westbound trains run on the east bank (CP) track, and all eastbound trains run on the west bank (CN) tracks. While this action serves the economic interest of increasing capacity for both companies, because the tracks are located on opposite sides of the Thompson River for much (but not all) of the subject corridor, this agreement also permits both companies to continue operations in the event that a landslide severs the track on one side of the river. While this action increases the capacity of the system and hence the number of elements at risk, it also improves the redundancy and flexibility of operations for both companies, thus increasing their resilience.

Opportunities exist for more effective stakeholder involvement in the context of the Ashcroft Thompson River landslides. A multi-stakeholder workshop, sponsored by Transport Canada, was held in the village of Ashcroft on April 26, 2011, to elicit public input and provide information concerning the Ashcroft Thompson River landslides. 34 participants representing twenty organizations took part in the workshop, capturing a broad cross-section of interested and affected parties, including representatives of First Nations communities, CN and CP railways, agricultural associations, utility transmission industries, environmental agencies, local, regional and federal government officials, and technical experts. The Summary Report underscored the clear consensus among participants that more effective communication amongst stakeholders is needed, with a compelling argument that better communication would enhance trust and collaboration between parties (BGC Engineering Inc. 2012). Participants agreed that a proactive approach to risk management was preferable to simply reacting to emergency situations, with more effective communication on issues of public safety, emergency preparedness and environmental impacts (BGC Engineering Inc. 2012). Many of the concerns voiced by stakeholders centred on environmental impacts, not only of the landslides themselves but also of the associated structural mitigation measures enacted by the railways; these concerns focused on the preservation of water quality, fish and spawning habitat in the Thompson River, and respecting indigenous rights, title and traditional uses of resources (BGC Engineering Inc. 2012). Ensuring the safe and uninterrupted movement of people and goods by road and rail through the corridor was of importance to a range of stakeholders; potential landslide impacts to transmission infrastructure, agricultural land use were also expressed (BGC Engineering Inc. 2012).

The feedback from the multi-stakeholder workshop suggested that many stakeholders perceived slope stabilization measures enacted by the railways, especially the in-stream construction of rock groynes and rip rap berms, to be short-sighted and insensitive to deleterious impacts on salmon resources, and by extension, to the agency and autonomy of indigenous peoples. Comments from participants underscored the need for considering a broader set of issues and values beyond the technical information associated with the landslides, to also include the social, environmental and economic impacts of a large landslide

event (BGC Engineering Inc. 2012). Proponents of resilience emphasize a move away from a centralized, command-and-control style of crisis management toward a decentralized, holistic, participatory approach which utilizes and builds upon existing social networks and community resources (Wildavsky 1988, Aguirre 2006, Maguire and Hagan 2007, Lorenz 2010). In an ongoing and iterative process, a resilient community has the capacity to predict and anticipate disasters, to absorb, respond to and recover from the shock; and to learn from realized risks in order to refine risk management strategies and processes (Maguire and Hagan 2007). A more holistic approach to landslide risk management and mitigation that seeks to involve community members in a two-way exchange of information, and incorporate a broader set of values beyond the short-term optimization of railway operations, would serve to promote better trust and communication between parties and promote increased system resilience in the long term.

In their guidelines for Sustainability in Professional Practice, the Association of Professional Engineers and Geoscientists of British Columbia (APEGBC 2016) affirmed social, environmental, and economic considerations as the three pillars of sustainable decision-making in an engineering context. Where structural mitigation measures are contemplated, they should be designed, constructed and monitored in an environmentally sensitive manner, with appropriate advance communication to the public, at a minimum, in order to balance competing interests and promote sustainable, well-considered solutions (APEGBC 2016). In keeping with a resilience perspective on risk management, an awareness of the current regime in which the hazards are situated, both with respect to climate conditions and kinematic stage, is an essential component of a well-rounded analysis. We should not attribute periods of relative calm in the historical landslide record to the success of structural mitigation measures before considering the overarching roles that climate variations and climate change may play in accelerating or abating the landslide movements, as well as the cyclical nature of the landslides themselves. The formulation of risk management guidelines based upon the short-term (multi-annual) behavior of the system may ultimately fail in the long (multi-decadal) term.

With respect to the cultural implications of risk management, Place and Hanlon (2011) argued that First Nations people in Canada take a less empirical, more holistic approach to risk

assessment, and that technical risk assessments often miss the normative, spiritual, experiential, value-based and cultural aspects of risk which are so intrinsic to First Nations' identity and well-being. Harmsworth and Raynor (2004) underscored the importance of cultural differences in understanding risk perception, particularly for indigenous peoples who have a distinct dependence on or intimate relationship with their natural environment; they argued that "sustainable management solutions need to be holistic, and that risk reduction measures can be improved by understanding cultural traits and differences", noting also that an increased perception of landslide risk is based on memory and experience of a severe event. Wade (1979) recounted the harrowing landslide that took place south of the study site near Spences Bridge in the Thompson River Valley on August 13, 1905. A landslide occurred on the west bank of the Thompson River and with great force crossed the river and inundated an aboriginal village with a deluge of water and mud. Fifteen people were killed by the landslide and the resulting wave, and many more were injured (Wade 1979). Given the strong oral history of First Nations peoples in Canada, the collective local memory of this event likely forms an important component of their perception of landslide risk in the Thompson River Valley, and may be enlightening to explore further. Within the context of complex risks such as the Ashcroft Thompson River landslides, which impact and are in turn affected by the social and natural environments in which they occur, improved stakeholder engagement holds promise for linking scientific knowledge and anticipation with more traditional forms of learning to improve the overall resilience of the system. While scientific knowledge typically consists of synchronic, short term observations of natural phenomena such as landslides, stakeholder engagement has the potential to tap into the local, indigenous and traditional forms of knowledge and social memory which are diachronic and long term.

7.3. Case for Public Involvement in Risk Management

Public involvement in risk decision-making or "risk governance" to borrow from Renn's (2008) terminology, forms a central part of the resilience paradigm, implicitly acknowledging that all stakeholders have something to contribute to the risk management process and that the mutual exchange of ideas, assessments, and evaluations ultimately improves the final decisions, rather than impeding the decision making process or compromising the quality of

scientific input or the legitimacy of legal requirements (Renn 2008). Effective stakeholder engagement in the context of natural hazard risk governance may serve both the democratic purpose of gathering a community perspective on risk tolerance, and also encourage citizens to take more responsibility for emergency preparedness by engaging community members in the discussion of risks that affect them (Wachinger et al. 2013). In the wake of the tragic Oso, Washington landslide of 2014, David Montgomery, a geomorphologist and professor at the University of Washington in Seattle observed: “One of the things this tragedy should teach us is the need to get better information about geologic hazards out to the general public” (U-T San Diego Newspaper 2014).

While the estimation or assessment of risk might be described as a scientific undertaking, the acceptability or evaluation of a given level of risk is inherently political (Douglas and Wildavsky 1982). The public rightly takes a sinister view of so-called risk experts who attempt to decontextualize and desocialize an inherently political problem (Douglas and Wildavsky 1982). According to Perrow (1999):

“The new risks have produced a new breed of shamans, called risk assessors. As with the shamans and the physicians of old, it might be more dangerous to go to them for advice than to suffer unattended.we will examine the dangers of this new alchemy where body counting replaces social and cultural values and excludes us from participating in decisions about the risks that a few have decided the many cannot do without.” (p. 12)

A handful of international jurisdictions have developed and enacted legislated risk tolerance criteria concerning specific hazards affecting the public. These include pioneering risk tolerance criteria governing the development of landslide-prone areas in densely-populated Hong Kong (ERM-Hong Kong, Ltd. 1998), regulating land use planning near industrial sites in the United Kingdom (Health and Safety Executive (HSE) 2001) and the construction and operation of large dams in Australia (Australian National Committee on Large Dams (ANCOLD) 2003). All three jurisdictions implemented similar criteria for tolerable risk to the public, consisting of an annual risk of mortality of 1×10^{-4} (1:10,000) for existing developments, and a more stringent criterion of 1×10^{-5} (1:100,000) for new developments (Jakob and Porter 2007). The most relevant of these to the current study is the Hong Kong criteria, governing tolerable risk to life from landslides and rockfall on natural hillslopes. Each

of the criteria were developed for different hazard types, both human-induced and naturally-occurring, at different scales, and in different social, cultural, environmental, economic and political contexts. Their extension to different contexts should therefore be treated with some caution, as the question of risk tolerance is inherently a question of values, requiring social as well as scientific inputs (Douglas and Wildavsky 1982). As engineers involved in assessing risk due to natural hazards, Hutchinson (2001) challenges us to demonstrate "... a willingness to become involved in the social and economic consequences of [our] work."

Notwithstanding, public involvement in risk decision making is still a contentious subject in many sectors. The perception persists that public participation may be unproductive, time consuming and costly, delaying the decision process, over-emphasizing the interests of the active publics, and usurping the role of elected officials (Dorcey and McDaniels 2000). Despite the objective challenges of involving the public in risk decision-making, the influential U.S. National Research Council (1996) publication asserted that risk characterization ought to be viewed as an analytic deliberative process involving all interested and affected parties. Within this framework, analysis employs rigorous, replicable scientific methods to arrive at answers to factual questions, whereas deliberation involves such processes as "discussion, reflection and persuasion to communicate, raise and collectively consider issues, increase understanding, and arrive at substantive decisions" (United States National Research Council 1996). In this manner, the technical and social understandings of risk coexist in a recursive process, whereby deliberation frames analysis, and analysis informs deliberation (United States National Research Council 1996). Petts (2004) emphasized the importance of involving stakeholders at the problem formulation stage, such that the nature of the risks and the assessment required is determined through discussion with the public, not in advance of it. In this setting, public perspectives may serve to define or reframe what the problems or issues actually are, as well as identify appropriate solutions (Petts 2004). Horlick-Jones (1998) confirmed that the initial framing of the issue is of critical importance and should include a wider range of understandings than merely that of the expert. Slovic (1999) aptly observed that "Whoever controls the definition of risk controls the rational solution to the problem at hand."

Risk management decisions concerning the Ashcroft Thompson River landslides are likely to impact multiple stakeholder groups, whether directly or indirectly, in addition to having environmental, social and economic implications. Issues of traditional land use rights may come into play for indigenous peoples who fish for salmon on the Thompson River, where spawning habitat could be adversely impacted by technically-sound but environmentally-undesirable slope stabilization measures. Harmsworth and Raynor (2004) underscored the importance of understanding cultural differences in understanding differences in risk perception, particularly for indigenous peoples who have a distinct dependence on or intimate relationship with the natural environment. They explored landslide risk perception based on two indigenous group case studies, one from Aotearoa, New Zealand and one from Pohnpei, Micronesia. The case studies demonstrated that “sustainable managements solutions need to be holistic, and that risk reduction measures can be improved by understanding cultural traits and differences, including local authority, values, kinship relations, environmental relationship, land tenure and changes to or evolution of culture” (p. 220) (Harmsworth and Raynor 2004).

Renn (2008) affirmed public involvement as a necessary, although insufficient, prerequisite for tackling risks in a sustainable and acceptable manner. Moreover, while scientific knowledge typically consists of synchronic, short term observations of natural phenomena such as landslides, stakeholder engagement has the potential to tap into the local, indigenous and traditional forms of knowledge and social memory which are diachronic and long term. In the case of the Ashcroft Thompson River landslides, continuous monitoring of the slope movements at any given location has been limited to a few years, usually due to instruments becoming unserviceable after a certain amount of accumulated displacement; this is a very small window of observation compared to the approximately 150 years over which the landslides have been known to be active, as described in Chapter 3. It is possible that oral histories, especially surrounding the 1905 landslide at Spences Bridge which devastated the Cook’s Ferry aboriginal settlement, could serve to shed more light on our understanding of these landslides, and would perhaps be an enlightening subject of investigation if a relationship of trust existed between parties. The important role of memory and experience of a severe event in affecting landslide risk perception by indigenous peoples in New Zealand and

Micronesia was documented in the study by Harmsworth and Raynor (2004), who observed the cumulative nature of understanding historic landslide events which had been passed on through several generations.

Public engagement in policy decisions arising from engineering risk assessments is still an emerging and growing field. An important contribution to the knowledge base is the publication of case studies illustrating how public involvement can be carried out in the context of risk management decisions concerning natural hazards. The level of public engagement in risk management decisions can vary along a spectrum from essentially no consultation to empowering community members to directly impact policy decisions. Tappenden (2014a) presented four criteria against which public involvement efforts can be evaluated; they are: representative participation; early involvement; information availability; and impact on policy.

The following discussion considers two case studies of public involvement in natural hazard risk decision making at the municipal levels. The first is a brief discussion of the Town of Canmore, Alberta's Mountain Creek Hazard Mitigation Program. The second, more detailed case study focuses on the of the District of North Vancouver's Landslide Management Strategy; it is an abbreviated version of the full paper published in Natural Hazards (Tappenden 2014a). While the Town of Canmore engaged residents in conversations about natural hazard risk and sought to obtain public feedback and perspectives on policy decisions, the District of North Vancouver engaged a community task force in the creation of the policy itself, empowering these residents to arrive at quantitative risk tolerance criteria upon which mitigation actions were based.

7.3.1. Mountain Creek Hazard Mitigation Program, Canmore, Alberta

The Town of Canmore, Alberta, sought to formulate and implement a Mountain Creek Hazard Mitigation Program following devastating debris flooding which impacted several neighborhoods in their community in 2013. While there were no fatalities, many homes were damaged or destroyed by the floods, including more than 80 homes in the vicinity of Cougar Creek alone, which was the neighbourhood most affected (A. Esarte, personal communication

2016). The Town engaged an engineering consultant to conduct risk assessments and evaluations for the five major creeks affected, and to recommend engineering mitigation options. A commitment to open dissemination of information, with all engineering reports and related documents publically available on-line, constituted an important component of these efforts. Providing timely updates and reporting on progress of engineering assessments and mitigation measures was achieved through the regular publication of a Mountain Creek Hazard Mitigation newsletter. In addition to the webpage, newsletters and resident mail-outs, the Town held frequent open houses (bi-weekly to monthly) and provided regular updates to council in the aftermath of the flooding (J. Eisl, personal communication 2016). Public input/feedback on proposed changes to the Municipal Development Plan (MDP) was collected and compiled from the open houses into a publically-available document, from which themes emerged for incorporation into the draft MDP (Town of Canmore 2015).

Given the pristine mountain setting of the town, implementation of engineering mitigation measures, including the realignment of Cougar Creek and the construction of a massive upstream debris containment structure, were not without controversy (Rocky Mountain Outlook (Rocky Mountain Outlook 2014)); opportunity for public feedback on the proposed measures included an online survey. While responses were mostly supportive of the conservative mitigation approach, there were others who felt the dam was too imposing and were willing to accept a higher level of risk inherent in living in a mountainous environment (J. Eisl, personal communication 2016).

The Town officials were determined to learn from the past, and now require developers to provide similar mountain creek risk assessments for proposed development areas (J. Eisl, personal communication 2016). The Town of Canmore's response to the 2013 debris floods demonstrated commitment to engineering risk assessment, evaluation and control, while seeking to implement lessons learned into the planning of future developments. Though residents were given opportunities to provide feedback at various stages of the risk assessment and evaluation process, the flow of information was primarily from the expert to the public, and the policy decisions, including the tolerable level of annual risk to life from debris flooding, was determined without direct public input (J. Eisl, personal communication 2016).

The dissemination of information in this case was primarily for the purpose of educating the public on the assessment and evaluation of the risks, and getting public buy-in for proposed mitigation measures. Homeowners were given the agency to reduce their vulnerability to future flooding by re-grading their properties, and were compensated for these activities by the municipality, which also undertook re-grading of areas away from homes (J. Eisl, personal communication 2016). In summary, while there was early and ongoing public involvement, and ready access to information, direct public impact on policy was limited, due in part to tight timelines for remedial actions and budgetary constraints (J. Eisl, personal communication 2016).

7.3.2. Landslide Management Strategy, District of North Vancouver

Following a fatal landslide in the Berkley neighborhood in 2005, the District of North Vancouver (DNV) in British Columbia engaged a task force of community members to arrive at quantitative risk tolerance criteria on which to base local slope stabilization and remediation requirements, as described in Tappenden (2014a). In seeking to establish tolerable levels of risk to life from natural hazards, the District convened a community-based Natural Hazards task force in October 2007. To their knowledge, they were the only municipality in Canada at that time to assemble a community task force for the determination of tolerable risk due to natural hazards (District of North Vancouver 2011). This pioneering approach resulted in legislated risk-tolerance criteria that now govern the development of all sites exposed to landslide and debris flow hazards in the District of North Vancouver.

In the early morning of January 19, 2005, after prolonged and intense precipitation, a sudden slope failure occurred at the crest of the Berkley Escarpment in the District of North Vancouver, destroying two homes at the base of the slope. One woman, Eliza Kuttner, was killed, and her husband seriously injured (Porter et al. 2009, District of North Vancouver 2011). On June 21, 2005, a Statement of Claim was filed on behalf of Michael Kuttner, his daughter Amita and the Estate of Eliza Kuttner against the District of North Vancouver and the current and previous owners of the upslope property where the landslide initiated ((Statement of Claim 2005)). The claim contended that in addition to other anthropogenic

preparatory factors, the placement of excessive loads on a concrete retaining wall at the westerly edge of the upslope property resulted in its failure and triggering of the fatal landslide. The Kuttner claim squarely blamed the actions (and inactions) of the District and the upslope property owners for the fatal Berkley slide—characterizing it not as a natural hazard at all, but rather as an anthropogenic one. The claim was settled out of court in January of 2009 for an undisclosed amount (North Shore News 2009).

In the wake of the Berkley tragedy, concerns over the potential for future landslides in the District prompted the DNV Municipal Council to implement a Landslide Management Strategy in 2007, as part of an overall Natural Hazards Management Program (Porter et al. 2009). The strategy emphasized a risk-based approach for the management of landslide hazards, with a focus on public involvement and open, transparent dissemination of hazard and risk information. The Provincial Coroner’s report into the landslide fatality, issued in 2008, confirmed the need for an organized approach to managing landslide risks, stating that landsliding in the Berkley area was both “predictable and preventable” (BC Coroner’s Report 2008).

7.3.2.1. Natural hazards task force

A key component of the DNV’s Landslide Management Strategy was the convening of a community task force for the development of risk tolerance criteria for natural hazards. The purpose of the risk tolerance criteria was to set forth maximum levels of tolerable risk to life for new and existing developments within the community, providing a basis for clear, consistent and defensible decision making with respect to future land use planning (Dercole 2009). Concerning existing developments, the risk tolerance criteria would also facilitate the allocation and prioritization of public funds for slope stabilization works, in the spirit of “optimal risk management”—seeking to use limited resources to achieve the most overall benefit (Jardine et al. 2003).

Convened in October 2007, the Natural Hazards task force was comprised of eight volunteer District residents (six men, two women), with backgrounds in various related fields including

engineering, geology, emergency preparedness, outdoor education and ocean transportation (District of North Vancouver 2013a). The task force was to “gather input from an informed, broad-based community perspective regarding quantitative tolerable risk or risk acceptance criteria for landslides and other natural hazards” (Dercole 2009), with the mandate to recommend to Council the tolerable level of risk to life from natural hazards (District of North Vancouver 2013b).

To fulfill their mandate, the Natural Hazards task force participated in education sessions delivered by subject matter experts in the areas of natural hazards, risk assessment and mitigation, finance and law. The task force also reviewed the literature concerning risk tolerance criteria enacted in other jurisdictions with similar legal frameworks and natural hazard situations, including the United Kingdom, Hong Kong and Australia. In addition, the task force solicited input from the broader public through an open house, a public meeting and an online survey, before deliberating and preparing their recommendations to Council (Dercole 2009). The activities of the Natural Hazards task force are described in the following sections.

7.3.2.2. Definition of tolerable risk and comparison to other jurisdictions

Seeking to quantify tolerable risk is a contentious and emotional issue, and there are by no means any universally accepted definitions or processes for doing so. As Jardine et al. (2003) aptly observed, “Resolving risk tolerance conflicts involves an understanding of ... values and beliefs, coupled with open, honest communication and regulatory accountability.” of tolerable risk. While risk tolerance levels vary amongst jurisdictions, the DNV’s Natural Hazards task force was presented with the following general principles which may apply when seeking to define tolerable risk to the public from a particular hazard (Leroi et al. 2005):

- The incremental risk to an individual from the hazard should not be significant compared to other risks to which a person is exposed in everyday life;
- The ALARP (As Low As Reasonably Practicable) principle shall apply, such that the incremental risk from the hazard shall be reduced to the extent that is reasonably practicable;

- If there is a possibility of many lives lost from a single incident, the probability of its occurrence should be reduced accordingly;
- Higher levels of risk are more likely to be tolerated for existing developments than for newly proposed developments.

Tolerable risk in this context applies to risks that individuals are willing to accept in exchange for perceived benefits, and subject to ongoing monitoring and/or mitigation in accordance with the ALARP principle. This is differentiated from the concept of *acceptable* risk, which refers to those risks considered broadly acceptable and not requiring any further monitoring or management.

As part of the literature review process, the task force sought to learn from the experiences of other jurisdictions with similar legal frameworks and natural hazard situations (Dercole 2009). The task force examined risk tolerance criteria enacted for land use planning near industrial sites in the United Kingdom, for landslide risk from natural slopes in densely populated areas in Hong Kong, and for large dam failures in Australia. All three jurisdictions utilized similar criteria for tolerable risk to the public, consisting of an annual risk of mortality of 1×10^{-4} (1:10,000) for existing developments, and a more stringent criterion of 1×10^{-5} (1:100,000) for new developments (Jakob and Porter 2007).

7.3.2.3. Public meetings and survey

The Natural Hazards task force convened a public open house on November 22, 2007, with approximately 30 District residents in attendance. Seven of the eight task force members were on hand, along with five DNV staff and representatives from the engineering consulting firm engaged by the DNV. A second public meeting was held the following month. When discussing the concept of legislated risk tolerance criteria, District residents expressed concerns regarding (District of North Vancouver 2008):

- The impact on homeowners of potentially mandatory remediation costs and the possibility of reduced property values;

- The amount of assessment work versus the amount of mitigation work being performed by the District;
- The differing levels of risk tolerance among residents, in that some property owners may wish to accept a higher level of risk than others.

To supplement the feedback gathered at the public meetings, an online survey was conducted via the DNV website between November 20 and December 10, 2007. Seventy-eight survey responses were collected via the website, with an additional 12 responses gathered at the open house. The survey used risk comparisons to assist respondents in selecting quantifiable levels of tolerable risk for natural hazards. When compared to other mortality rates such as death from poisoning or death from a motor vehicle accident, 72% of respondents placed the tolerable level of risk of death from natural hazards between 1:10,000 and 1:100,000 per annum. 14% considered the tolerable risk of death from natural hazards to be higher (1:600 to 1:3,700), while 14% viewed the tolerable risk to be lower (1:200,000) (District of North Vancouver 2008).

In addition, the survey indicated that the majority of respondents felt the DNV should (District of North Vancouver 2008):

- Be responsible for managing natural hazard risks on public lands;
- Regulate and/or be responsible for risk mitigation on private lands;
- Spend no more than \$1,000,000 per year on natural hazards (the survey question correlated an expenditure of \$600,000 with a yearly tax increase of 1%).

The majority of respondents felt that personal emergency preparedness was the responsibility of the resident (District of North Vancouver 2008).

7.3.2.4. Task force recommendations

After discussion and deliberation, the Natural Hazards task force presented their recommendations to the District Council on April 14, 2008. The task force proposed the

following two-tier risk tolerance criteria for the District of North Vancouver (District of North Vancouver 2013b):

- 1:10,000 risk of death per year from natural hazards for existing developments;
- 1:100,000 risk of death per year from natural hazards for new developments.

The recommended risk tolerance criteria are similar to those used in other international jurisdictions, as outlined in Section 7.3.2.2. The criteria also reflect the public opinion gathered from the survey, where 72% of respondents placed the tolerable level of annual risk of mortality between 1:10,000 and 1:100,000 from natural hazards (Section 7.3.2.3). The two-tiered nature of the risk tolerance criteria acknowledges that it is generally more attainable to reduce risk by altering proposed developments, as compared to existing structures. The ALARP principle also requires that tolerable risks be subject to ongoing monitoring, and be further reduced below the stated tolerance levels when a significant reduction in risk can be reasonably achieved (District of North Vancouver 2013b).

On November 16, 2009, the District Council endorsed a policy implementing the recommended risk tolerance criteria for the District of North Vancouver, following an investigation by District staff into the various practical implications. The policy gives the District's Chief Building Official the discretion to apply the risk tolerance criteria to building permits, subdivision and development applications for sites exposed to landslide and debris flow hazards (District of North Vancouver 2013b). The District of North Vancouver also committed to providing in-kind assistance to the homeowners required to undertake remedial work on their properties, including construction coordination, on-site geotechnical support, arborist services, and the waiving of associated permitting fees (Ridge 2006). Through the cooperative efforts of the DNV and the affected homeowners, the required mitigation measures were implemented in a timely manner, resulting in the identified landslide hazards posing an annual residual risk of mortality of no more than 1:10,000 for the individuals most at risk (BGC Engineering Inc 2007, 2010, 2011).

District Council's report on the policy concludes with the commitment to continually revisit the risk tolerance criteria and make adjustments, as required, to meet the future needs of the

community, acknowledging, “Ongoing discussion with stakeholders is paramount, as risk tolerance criteria [are] determined more by social values than by technical advances” (Dercole 2009).

7.3.2.5. Ongoing communication with stakeholders

In addition to the work of Natural Hazards task force and the legislated risk tolerance criteria, the DNV has implemented several platforms for facilitating ongoing dialog and public education concerning landslide risk, including an educational website and brochure (Guide to Living Near Steep Slopes), a publicly-available GeoWeb Hazards Database with related risk assessment reports, and a Geotech on Demand program, which is funded by the DNV and connects property owners with geotechnical experts for improved understanding of personal landslide risk, and identification of mitigative measures that they can undertake on their own property.

The DNV’s Natural Hazards task force successfully utilized social, legal, and scientific information for informed decision-making, and their recommended risk-tolerance criteria were enacted into policy by the District of North Vancouver as a result of the process. While the quantitative risk-tolerance criteria recommended by the task force were in keeping with the status quo (i.e., similar to the DNV’s interim criterion and those enacted in other international jurisdictions), the public involvement process used to generate the criteria no doubt contributed to the legitimacy and public acceptance of the outcome. The DNV has also committed to ongoing public involvement and education efforts with respect to landslide risks, considering information accessibility and its usefulness for increasing individual capacity and community resilience. Overall, the District’s ongoing, dynamic approach to risk management promises to empower individuals and foster resilient communities in the aftermath of the tragic Berkley landslide (Tappenden 2014a).

The District of North Vancouver’s commitment to open, transparent dissemination of risk information, and commitment to involve the public in a meaningful dialog on tolerable levels of risk, no doubt aided in public acceptance and support of the process. This concept of social

license in risk decision-making is an important aspect of sustainable, robust operations. Acknowledging the importance of incorporating public perspectives in the management of risk, Leiss (2001) asserted that the resources devoted to the social management of risk should be equal to those employed in the technical assessment of risk, which is a tall order given the scope and nature of engineering risk assessments for natural hazards.

7.4. Adaptation Strategies for Risk Reduction

While mitigation strategies seek to reduce risk by reducing the frequency of hazards, or our exposure to them, adaptation strategies offer a complementary approach to risk reduction by reducing vulnerability to hazards which cannot be completely controlled or avoided (Figure 7.4). The long history of slope instability in the Thompson River Valley south of Ashcroft, the environmental sensitivity of the corridor and the substantial size of the landslides do not permit a reliance on traditional engineering mitigation strategies or structural approaches to risk reduction. Although knowledge will improve with ongoing monitoring and improved understanding of the landslide causes and effects, some level of uncertainty will remain inherent in when, where, and how fast a landslide will occur. The ability to cope with a landslide that has not been entirely foreseen, and to learn from the experience, are key components of resilience and adaptation. The International Panel on Climate Change (IPCC 2014) has identified that: “Overall, the transport sector will be highly exposed to climate change and will require ... a complex interaction between adaptation and mitigation efforts.”

Adaptive management involves the selection of risk management strategies that can be modified to achieve better performance as one learns more about the issues at hand and how the future is unfolding (European Climate Adaptation Platform 2017). These opportunities for learning include ongoing and enhanced slope stability monitoring for better understanding the causes of the landslides movements and their relationship to broader climate factors and anthropogenic influences, as well as an improved understanding of how climate change will impact the driving factors and resulting landslide activity in the corridor. The European Climate Adaptation Platform (2017) noted that “a key feature of adaptive management is that decision makers seek strategies that can be modified once new insights are gained from

experience and research.” Learning, experimenting and evaluation are key in this approach and are actively planned for in decision-making (European Climate Adaptation Platform 2017), corresponding to the post-incident learning phase of the NIAC’s (2010) resilience framework (Figure 7.3). Adaptive strategies work best in situations in which the decision time scales allow for incremental adaptation over time, such that decisions and strategies can be updated as new information becomes available; adaptation options that may be relevant in the context of the Ashcroft Thompson River landslides include (European Climate Adaptation Platform 2017):

- Ensuring the design of mitigation measures are ecologically sensitive and resilient to a range of future climate conditions, favouring reversible and flexible options which enable amendments to be made;
- Promoting so-called soft adaptation strategies, which could include building adaptive capacity through more effective forward planning;
- Delaying action (which should not be confused with inaction). This may be appropriate as part of an active monitoring and adaptation strategy where it has been determined that there is no significant benefit in taking a particular action immediately.

Ongoing monitoring to actively refine and improve understanding of the landslide mechanics and their relationship to causal factors such as climate variation and human interference, as described in Chapter 6, is an essential component of the adaptation strategy. Increased resilience and ability to cope with the landslide movements through better anticipation improves the flexibility and robustness of the system as a whole. The role of anticipation in a resilience context acknowledges the complex, inter-dependent nature of social and ecological systems, and utilizes anticipation for improved flexibility, coping capacity and adaptation, rather than as a means for achieving a false sense of system predictability or control. The continual evaluation and ongoing improvement of field monitoring and forecasting systems is critical to their effectiveness. The integration of new information as it becomes available through technical studies, research and public input will serve to improve the robustness of the strategy presented in Table 6.1. Moreover, the success of adaptation strategies rely on the continual assessment of monitoring results, internal processes which allow for decisions to be made with a minimum of delay, and timely and effective dissemination of risk information to the public and the relevant authorities (Hutchinson

2001). Internal processes and procedures should be established by the railways for collecting, assessing and communicating landslide hazard and risk information to Transport Canada and the public, utilizing a dynamic platform that facilitates the ongoing integration of new information, such as a web-based geographical information system, as was implemented by the District of North Vancouver (see Section 7.3.2.5 above).

As described in Section 7.2, engineering mitigation measures which have been implemented to-date consist of hard armoring techniques involving the construction of rock groynes in the waterway or placement of rip rap along the river bank. While these may be effective in slowing erosion in the area of application, they may have the undesirable effect of exacerbating scour and erosion on the opposite bank of the river, as suggested by the timing of several of the historical landslide reactivations described in Section 3.2. The role of surface water ingress in the 1982 Goddard landslide, described in Section 5.2.2.3, underscores the importance of surface water management on the valley slopes and the maintenance of culverts associated with the railway infrastructure. The effect of artesian pore water pressure on the landslide movement rates (Section 5.2.5.1), and the relationship of the landslide reactivations to the broader climate conditions (Chapter 4), provide a basis for the contemplation of drainage measures aimed at alleviating the excess pore water pressures near the toes of the landslides. Innovative erosion control techniques, such as live-staking, for example, could also provide a starting point for multi-stakeholder conversations on motivations and appropriate methods for attempting to minimize the landslide movements. Live staking involves the insertion of live woody plant and tree cuttings into a streambank, to reduce bank erosion by the eventual growth of roots and above-ground vegetation.

7.5. Conclusion

The economic consequences of a landside which impacts the railway infrastructure in the Thompson River Valley can grow exponentially with the duration of the outage (Bunce and Chadwick 2012). In addition to potential measures to reduce the likelihood of a rapid landslide occurrence, the capacity to cope with and adapt to the inevitable disruptions in the natural environment are also of critical importance for resilient systems. Resilience acknowledges the

dynamic nature of risk, and the ever changing natural and social environments which give rise to it. An awareness of the current regime in which the landslide hazards are situated, both with respect to climate conditions and kinematic stage, is an essential component of a well-rounded assessment of risk. We should not attribute periods of relative calm in the historical landslide record to the success of structural mitigation measures before considering the overarching roles that climate variations and climate change may play in accelerating or abating the landslide movements, as well as the cyclical nature of the landslides themselves. The formulation of risk management guidelines based upon the short-term behavior of the system may ultimately fail in the long term.

In addition to economic considerations, future landslides in the Thompson River Valley may have substantial safety, environmental and cultural impacts. Seeking to consider the diverse range of those who may be affected, and their sometimes conflicting interests, requires public involvement, and a willingness, on the part of risk assessors, to "... become involved in the social and economic consequences of their work" (Hutchinson 2001). The 2011 multi-stakeholder workshop sponsored by Transport Canada indicated that more trust and collaboration between parties is needed for effective risk management of the Ashcroft Thompson River landslides (BGC Engineering Inc. 2012). To this end, case studies summarizing and evaluating the public involvement efforts in Canmore, Alberta and the District of North Vancouver, British Columbia, were presented in this chapter for the benefit of conveying lessons learned and highlighting best practices for different levels of stakeholder involvement in risk management decision making. It is recommended that contemplated risk reduction measures favor flexible options which would be suited to a range of future climate conditions, improve adaptive capacity through more effective anticipation and forward planning, and integrate active monitoring and regular site inspections of slope movements with effective strategies for the documentation, communication and dissemination of hazard and risk information.

Table 7.1: Comparison of traditional engineering approach to system management with resilience concepts.

Traditional Engineering	Resilience Paradigm
Reductionist – break problem into component parts	Complex, adaptive system
Prevention and control	Absorption, adaptation, coping and transformation
Single stable state of static equilibrium	Multiple, dynamic states of equilibrium (regimes)
Short-term optimization of a component part	Long-term, sustainable strategy over space and time
Average, expected conditions emphasized	Importance of extreme events
Linear, incremental changes	Non-linear, interdependent changes
Striving for constancy	Embracing change and transformation
Rigid, efficient, optimized	Flexible, redundant, adaptable
Top-down, systematic, techno-centric approach	De-centralized, participatory, holistic approach

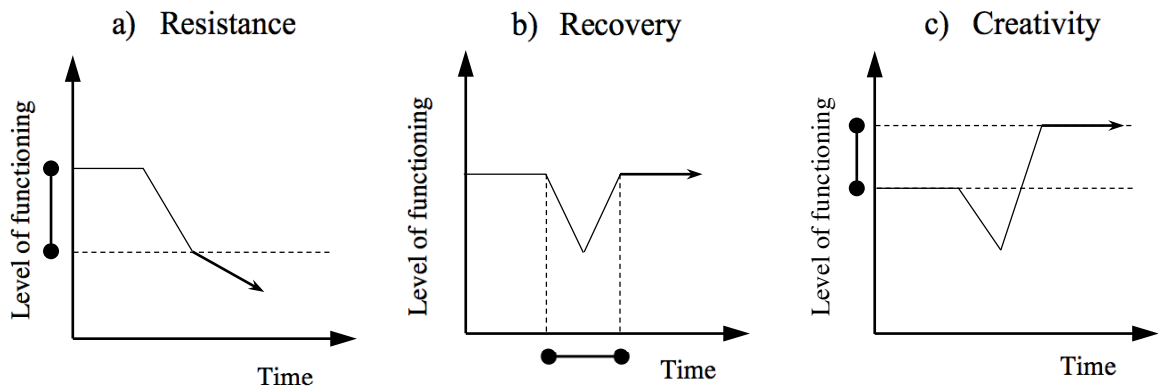


Figure 7.1: Properties of resilience (modified from Maguire and Hagan (2007), as adapted from Adger, 2000). Reproduced under: <https://creativecommons.org/licenses/by-nc/4.0/>

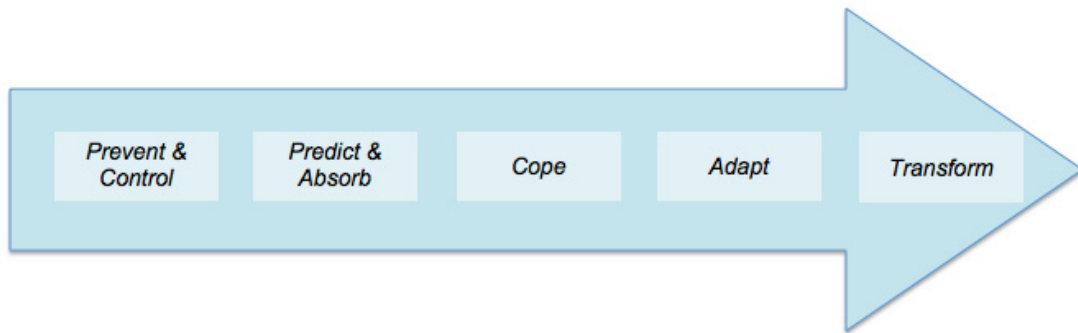


Figure 7.2: Spectrum of philosophical approaches to risk management.

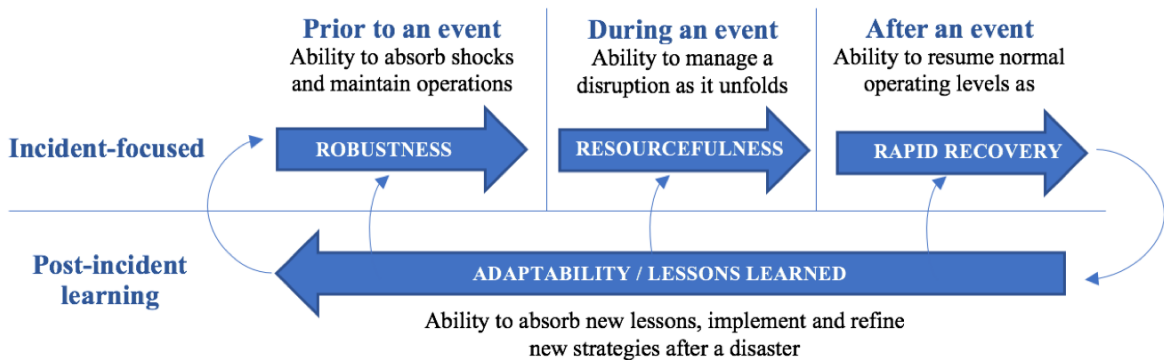


Figure 7.3: Resilience framework for managing critical infrastructure (modified from National Infrastructure Advisory Council (2010)).

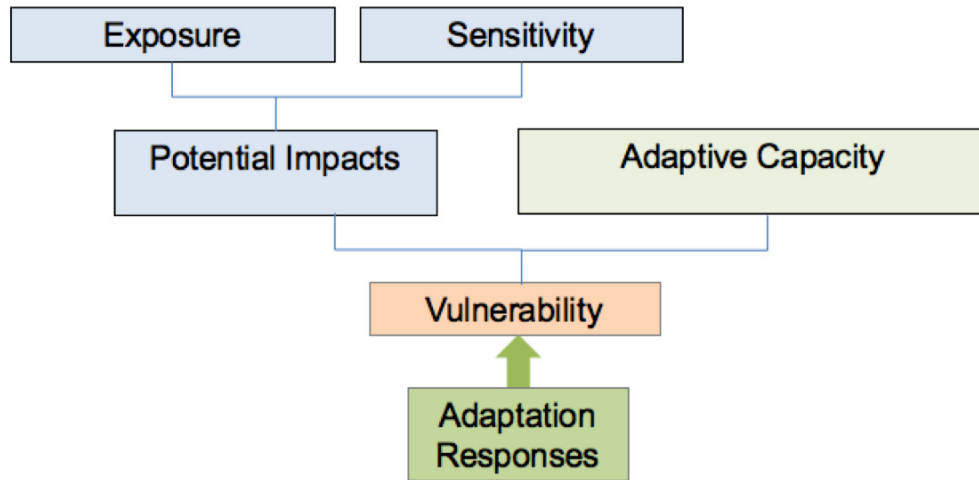


Figure 7.4: Role of adaptation responses for risk reduction through reduced vulnerability (modified from United Nations Environment Programme (2009)).

8. CONCLUSIONS AND FUTURE RESEARCH

8.1. Summary

This study employed an inter-disciplinary approach to assess the complex risks posed by landslides in the Thompson River Valley south of Ashcroft, British Columbia, with an emphasis on the impacts of climate variability, climate change and system resilience. In addition to a technical assessment of the Thompson River landslides and the likelihood of future landslide reactivations in the corridor, the thesis presented a risk management strategy for addressing operational impacts to the Canadian Pacific and Canadian Nation railways, which integrated ongoing monitoring of slope displacements with field-level observations of landslide morphologies. The level of risk posed by the landslides inevitably varies over time, both seasonally and in the long-term, due to the implicit relationship between the landslides and the climate described in Chapter 4. The potential consequences of a landslide, too, have a dynamic component; interruption of the railway transportation corridor can result in economic losses that have the potential to grow exponentially with the duration of the outage (Bunce and Chadwick 2012). The proposed risk management approach is flexible and should be refined as more experience is gained.

In addition to economic considerations, future landslides in the Thompson River Valley may have substantial safety, environmental and cultural impacts. Seeking to consider the diverse range of those who may be affected, and their sometimes conflicting interests, requires a level of public engagement in the risk management process, and a willingness, on the part of technical specialists, to "... become involved in the social and economic consequences of their work" (Hutchinson 2001). Current best practices for public involvement in risk decision making were presented based on two Canadian case studies– the District of North Vancouver's Landslide Management Strategy, and the Town of Canmore's Mountain Creek Hazard Mitigation Program. Considering the diverse cross-section of stakeholders involved and the corridor's strategic importance, the potential consequences of a large landslide in the Thompson River Valley today would include significant economic impacts, issues of public safety and environmental responsibility. It is hoped that a better understanding of the influence

of climate on landslide activity will facilitate early-warning of impending landslides and empower all stakeholders to improve their level of understanding and ability to prepare for, and cope with, the potential impacts of a large landslide. In an ongoing and iterative process, a resilient community has the capacity to predict and anticipate disasters, to absorb, respond to and recover from the shock; and to learn from realized risks in order to refine risk management strategies and processes (Maguire and Hagan 2007).

Recent Canadian railway disasters such as the derailment in Lac-Mégantic have served to underscore the urgent need for improved railway safety through an organized approach to managing complex risks. The research contributions in the area of risk management and system resilience will affect how Canada's railway industry and its regulator will monitor and mitigate landslides along the Thompson River Valley, with broader implications for risk management of natural hazards interacting with the built environment.

8.2. Conclusions and Significant Contributions

8.2.1. Landslide Failure Modes, Causes and Effects

- A detailed summary of known landslide events pertaining to 12 large landslides in the 10-km corridor of the Thompson River Valley south of Ashcroft was presented in Chapter 3, with reference to numerous contemporary and original sources. Inconsistencies and incompatibilities between sources were resolved to the extent possible. The probable origins and modes of movement for each landslide were presented based on the interpretation of historic aerial photographs, on-site inspections, and analysis of published documents and unpublished reports.
- The mode of movement for most of the landslides in the subject corridor appears consistent with compound translational slope failures of extremely slow to rapid velocity; most were likely reactivations of ancient landslides. It was argued that the largest, the North slide, represented a unique mode of failure, which was probably a complex earth slide-debris flow; it was preceded by the breaching of a nearby irrigation

reservoir, and was the most mobile of all the landslides, fully damming the Thompson River for nearly two days.

- Substantial changes in land use along the naturally semi-arid terraces of the Thompson River Valley occurred with European settlement of the area following the Cariboo gold rush of the mid-1800's. Flooding of the upland areas by ditch-and-furrow irrigation in the mid- to late-1800's probably served as the catalyst for dramatic landslides along these valley walls that were geologically predisposed to failure. The earliest documented landslide, the South slide, occurred between 1865 and 1877; this was followed by at least six (probably rapid) landslides recorded in the corridor between 1865 and 1898. The only reported rapid slope movements of the 20th century were the Red Hill Landslide of 1921 and the Goddard Landslide of 1982. Notwithstanding the connection between the historic landslides and primitive irrigation methods, the CN 50.9 landslide of 1897 occurred in the absence of any nearby irrigation indicating that other factors, including river erosion, undermined the stability of the valley walls and continues to exacerbate slope instability in the corridor.
- Analysis of the 20th century discharge records provided evidence that the cumulative flow of the Thompson River is subject to interannual and interdecadal cycles. The interdecadal cycles appear to be related to the phase of the Pacific Decadal Oscillation (PDO). An upward trend in the cumulative Thompson River flow departure from normal was apparent during the negative (cool/wet) phases of the PDO, while a downward trend (deficit) in the cumulative river flow departure from normal was associated with the positive (warm/dry) phases of the PDO. Correlations of landslide activity to river flow and regional snow pack could potentially serve as an early-warning tool for anticipating slope movements in the corridor, while monitoring broader climate patterns such as the PDO may be beneficial for longer-term (interdecadal) forecasting of periods of increased landslide activity.
- Peak snow pack departures from normal of approximately 20% in the Thompson River basin and cumulative river flow departures from normal of approximately 14% (3,400

Mm³) have historically portended landslide activity in the corridor; between 1912 and 2011, this criterion was exceeded on average once every 4.4 years during the cool/wet phases of the PDO and only about once per decade during the warm/dry phases of the PDO.

- The limited number of recorded landslide reactivations over the last century, since hydrologic record-keeping began, does not lend itself to a rigorous statistical evaluation; moreover, the proposed empirical threshold of 3,400 Mm³ does not discriminate between very/extremely slow reactivations (such as at the Goddard slide in 1976) and rapid renewals of movement (as exhibited by the Goddard slide in 1982). Notwithstanding, a better understanding of the interannual and interdecadal variations in climate and streamflow in the Thompson River Valley, and its attendant effects on the activity of the Ashcroft landslides, is an important component of risk management in the corridor for improved resilience through better anticipation.
- There is consensus among several climate change studies that warming temperatures in British Columbia are likely to produce earlier and lower peak flows and less disparity between high- and low-flow conditions in the Thompson River. Given the historic affiliation of landslide activity with years of high river discharge, if snow pack in central British Columbia is diminished and spring thaw continues to occur earlier with more gradual snow melt, it is possible that climate change may have an attenuating effect on landslide activity in the Thompson River Valley south of Ashcroft.
- Three failure modes were proposed to capture the range of movement types and velocities which have been documented in the corridor over the last 150 years:
 - Mode I): complex, very rapid earth slide-debris flow;
 - Mode II): reactivated rapid compound earth slide;
 - Mode III): reactivated very/extremely slow earth slide.

It was argued that a Mode I failure is contingent upon an ample supply of ponded water, as provided by now-abandoned methods of ditch-and-furrow irrigation. Modes II and

III may still have substantial implications for the railway operations and numerous stakeholders in the Thompson River Valley.

- The catalyst for accelerating an extremely slow moving landslide into a rapid failure is conventionally understood to be a sudden change in external loading conditions, porewater pressure, or increase in brittleness in the rupture surface due to aging or chemical change. It was argued that kinematic thresholds exist for the compound landslides, which may produce rapid acceleration of a very/extremely slow moving mass as a result of internal shearing and the development of a kinematically admissible failure mechanism. Whether the reactivation of a particular landslide takes the form of slow, ductile movements or a rapid, brittle failure, depends on the state of evolution of the landslide morphology as described in Chapter 5.

8.2.2. Integrated Risk Management Strategy and Adaptive Actions

- An integrated risk management strategy was developed based on a synthesis of published information on railway track deflections resulting from very slow slope displacements at the Ripley landslide, an inverse-velocity analysis of unpublished offset measurements taken during the rapid reactivation of the Goddard landslide in 1982, and the incorporation of general stages in the kinematic evolution of deep-seated compound translational landslides.
- Three risk categories were delineated based upon the order-of-magnitude velocity of slope movement, associated kinematic stage, and the expected impacts to track performance. A compound translational earth slide exhibiting very/extremely slow seasonal activity (Stage 1), may intensify to a Stage 2 reactivation where track deflections exceeding the Transport Canada criteria are likely. Finally, a Stage 1 scenario represents a landslide reactivation of moderate to rapid velocity which may portend imminent, massive slope failure, with the potential to impact a broader group of stakeholders.

- A risk management strategy employing monitoring, mitigation and adaptation relevant to Stage 1, 2 and 3 scenarios was presented in Chapter 6. Increasing intensities of monitoring and remedial efforts were recommended based on evolving kinematic expression and increasing risk of massive slope failure. Expected rates of surface displacements were specified for each scenario, and ranged from less than 2 mm per day (Stage 1) to up to 10 meters per day or more (Stage 3). Surface expressions of a landslide's progress through the identified kinematic stages will accompany the formation of a compound landslide and may provide warning of its potential for acceleration, moving from subdued kinematic expression to coherent crack formation, growth and coalescence.
- A 2011 multi-stakeholder workshop organized by Transport Canada indicated that more trust and collaboration between parties is needed for effective risk management of the Ashcroft Thompson River landslides (BGC Engineering Inc. 2012). To this end, case studies highlighting strategies for integrating stakeholder perspectives into natural hazard risk management in Canmore, Alberta, and the District of North Vancouver, British Columbia, were presented in Chapter 7, with the aim of disseminating lessons learned to improve the overall resilience of the railway system and the affected communities.
- It is recommended that contemplated risk reduction measures favor flexible options which would be suited to a range of future climate conditions, improve adaptive capacity through more effective anticipation and forward planning, and integrate active monitoring and regular site inspections of slope movements with effective strategies for the documentation, communication and dissemination of hazard and risk information.

8.3. Opportunities for Further Research

- The use of finite element modelling allows for explicitly incorporating factors affecting the landslide behaviour, including slope geometry, soil stratigraphy, piezometric regime and the soil geotechnical parameters, and would be a useful next step in refining the risk assessment and management strategy for the Ashcroft Thompson River landslides. Slope stability modeling of these landslides has so far been restricted to the use of limit equilibrium methods, which have several limitations as discussed in Chapter 5. Lollino et al. (2016) proposed a methodology for monitoring the evolution of the active Montaguto earthflow in southern Italy, which integrates the deformation monitoring of the landslide with the observed kinematic expressions and two-dimensional numerical modelling of the landslide deformation using PLAXIS-2D software.
- Ongoing study should be devoted to the evolving information concerning climate change implications for the hydrologic regime of the Thompson River, and its implications for the frequency and severity of future landslide activity in the corridor.
- The continual evaluation and improvement of field monitoring and forecasting systems is critical to their effectiveness. The integration of new information as it becomes available through technical studies, research and public input will serve to improve the robustness of the risk management strategy presented in Table 6.1.
- Internal processes and procedures should be established by the railways for collecting, assessing and communicating landslide hazard and risk information to Transport Canada and the public, utilizing a dynamic platform that facilitates the ongoing integration of new information, such as a web-based geographical information system. Web-based tools could also be used to facilitate multi-stakeholder conversations around contemplated engineering mitigation measures, including surface water management, sub-surface drainage, and erosion control as discussed in Section 7.4.

LIST OF REFERENCES

- van Aalst, M.K. 2006. The impacts of climate change on the risk of natural disasters. *Disasters*, **30**(1): 5–18.
- Aguirre, B.E. 2006. On the concept of resilience. University of Delaware Disaster Research Center Preliminary Paper #356. Available from <http://udspace.udel.edu/handle/19716/2517> [accessed 4 October 2013].
- Allison, J.A., Mawditt, J., and Williams, G.T. 1991. The use of bored piles and counterfort drains to stabilize a major landslide– a comparison of theoretical and field performance. *In Slope Stability Engineering– Applications and Developments*. Thomas Telford Publishing, London. pp. 347–354.
- APEGBC. 2016. Sustainability: Professional Practice Guidelines– The Association of Professional Engineers and Geoscientists of British Columbia. Available from <https://www.apeg.bc.ca/getmedia/91beda29-ad6f-4a6f-b302-ac60de0bab40/APEGBC-Sustainability-Guidelines.pdf.aspx> [accessed 20 January 2017].
- Ashcroft Journal. 1921, August 19. Landslide blocks Thompson river near Ashcroft. Ashcroft, British Columbia, Canada.
- Australian Geomechanics Society, Landslide Taskforce. 2007. Practice note guidelines for landslide risk management. *Australian Geomechanics*, **42**(1): 63–114.
- Australian National Committee on Large Dams (ANCOLD). 2003. Guidelines on risk assessment. Australian National Committee on Large Dams Inc., Melbourne, Australia.
- Ayyub, B.M. 2003. Risk analysis in engineering and economics. Chapman & Hall/CRC, Boca Raton, FL.

- Barton, M.E. 2002. Early warning of landsliding using weather station data. *In* Instability-planning and management: seeking sustainable solutions to ground movement problems. Proceedings of the international conference organised by the Centre for the Coastal Environment, Isle of Wight Council. *Edited by* R.G. MacInnes and J. Jakeways. Thomas Telford Publishing, Ventnor, Isle of Wight, UK. pp. 455–462.
- Baumgartner, T.R., Soutar, A., and Ferreira-Bartrina, V. 1992. Reconstruction of the history of Pacific sardine and northern anchovy populations over the past two millennia from sediments of the Santa Barbara basin, California. *CalCOFI Reports* 33.
- BC Coroner's Report. 2008. Coroner's Report into the death of Kuttner, Eliza Wing Mun. Case No. 2005:0255:0076.
- BC Court of Appeal. 1990. Reasons for Judgment of the Honourable Mr. Justice Toy. Canadian Pacific Limited versus Highland Valley Cattle Company Limited. Vancouver Registry No. CA007436. Vancouver, British Columbia, Canada.
- Bertini, T., Cugusi, F., D'Elia, B., and Rossi-Doria, M. 1986. Lenti movimenti di versante nell' Abruzzo Adriatico: caratteri e criteri di stabilizzazione. **Vol. I:** 91–100. Bologna, Italia. pp. 91–100.
- BGC Engineering Inc. 1998. Nepa Cross-Over and 1998 Slope Instrumentation. Report submitted to Canadian Pacific Railway, Calgary, Alberta, and Canadian National Railway, Edmonton, Alberta.
- BGC Engineering Inc. 2001a. Ashcroft 51 Landslide: September 2001 Instrumentation Installations. Report submitted to Canadian National Railway, Edmonton, Alberta. Kamloops, British Columbia.
- BGC Engineering Inc. 2001b. Geotechnical Evaluation of the North Slide - Mile 51.7 Thompson Subdivision. Report submitted to Canadian Pacific Railway, Calgary, Alberta.

- BGC Engineering Inc. 2003. Ashcroft 51 Landslide: June 2003 Instrumentation Installations. Report submitted to Canadian National Railway, Edmonton, Alberta. Vancouver, British Columbia.
- BGC Engineering Inc. 2005. Thompson 52.80 Westcap Geotechnical Investigation, Vol. 1-3. Report submitted to Canadian Pacific Railway, Calgary, Alberta. Kamloops, British Columbia.
- BGC Engineering Inc. 2007. District of North Vancouver, Berkley Landslide Risk Management- Updated Landslide Risk Assessment Following Stage 1 Mitigation. Report submitted to the District of North Vancouver.
- BGC Engineering Inc. 2010. District of North Vancouver Landslide Risk Summary. Report submitted to the District of North Vancouver.
- BGC Engineering Inc. 2011. District of North Vancouver Landslide Risk Assessment Update- Units 2871, 2873, 2875 and 2877, Cedar Village Crescent, Capilano Road. Report submitted to the District of North Vancouver.
- BGC Engineering Inc. 2012. Ashcroft Thompson River landslides evaluation of factors influencing risks of landslide hazard - Phase 1: Data gap analysis, stakeholder workshop report and Phase 2 plan. Report submitted to the Transportation Development Centre of Transport Canada.
- Bishop, N.F. 2008. Geotechnics and hydrology of landslides in Thompson River Valley, near Ashcroft, British Columbia. M.Sc. Thesis, Department of Earth Sciences, University of Waterloo, Waterloo, Ontario.
- Bond, N.A., Overland, J.E., Spillane, M., and Stabeno, P. 2003. Recent shifts in the state of the North Pacific. *Geophysical Research Letters*, **30**(23): 2183. doi:10.1029/2003GL018597.
- Bovis, M.J., and Jones, P. 1992. Holocene history of earthflow mass movements in south-central British Columbia: the influence of hydroclimatic changes. *Canadian Journal of Earth Sciences*, **29**(8): 1746–1755.

- Brawner, C.O. 1982. Slide Mile 50.4-50.6 Thompson Sub. Report submitted to CP Rail, Montreal.
- Brawner, C.O., and Readshaw, E.E. 1963. Drynoch landslide. British Columbia Department of Highways, Unpublished Technical Report, Victoria, British Columbia.
- Bromhead, E.N. 1992. The stability of slopes. 2nd ed. Blackie Academic & Professional, London. Available from <https://www.scribd.com/doc/93754887/Bromhead-1992-the-Stability-of-Slopes-2nd-Ed> [accessed 7 December 2016].
- Bromhead, E.N. 2013. Reflections on the residual strength of clay soils, with special reference to bedding-controlled landslides. *Quarterly Journal of Engineering Geology and Hydrogeology*, **46**(2): 132–155. doi:10.1144/qjegh2012-078.
- Brunner, E., and Giroux, J. 2009. Examining resilience- a concept to improve societal security and technical safety. Center for Security Studies (CSS), ETH Zürich.
- Bullock-Webster, H. 1879. Cambie [...] & survey party (photograph). University of British Columbia Library. Rare Books and Special Collections: H.Bullock-Webster fonds. Available from <https://open.library.ubc.ca/collections/bullock/items/1.0045057> [accessed 10 March 2016].
- Bunce, C.M. 2008. Risk estimation for railways exposed to landslides. Ph.D. Thesis, Department of Civil and Environmental Engineering, University of Alberta, Canada.
- Bunce, C.M., and Chadwick, I. 2012. GPS monitoring of a landslide for railways. *In* Proceedings of the Joint XI International & 2nd North America Symposium on Landslides. Banff, Alberta, Canada.
- Cambie, H.J. 1895, January 2. Letter to Mr. H. Abbott Esq., General Superintendent, CPR, Vancouver. Reproduced in: Geotechnical Evaluation of the Goddard Landslide, EBA Engineering Consultants Ltd., February 1984.

- Cambie, H.J. 1902. An unrecorded property of clay (with Discussion following).
Transactions of the Canadian Society of Civil Engineers, **XVI**(Part I, Paper 172):
197–215.
- Canadian Standards Association. 1997. CAN/CSA Q850-97- Risk Management Guideline
for Decision Makers. Canadian Standards Association, Ontario, Canada.
- Carlà, T., Intrieri, E., Di Traglia, F., Nolesini, T., Gigli, G., and Casagli, N. 2017. Guidelines
on the use of inverse velocity method as a tool for setting alarm thresholds and
forecasting landslides and structure collapses. *Landslides*, **14**(2): 517–534.
doi:10.1007/s10346-016-0731-5.
- Cayan, D.R. 1996. Interannual Climate Variability and Snowpack in the Western United
States. *Journal of Climate*, **9**(5): 928–948. doi:10.1175/1520-
0442(1996)009<0928:ICVASI>2.0.CO;2.
- Changnon, D., McKee, T.B., and Doesken, N.J. 1991. Hydroclimatic variability in the Rocky
Mountains. *Water Resources Bulletin*, **27**: 733–743.
- Changnon, D., McKee, T.B., and Doesken, N.J. 1993. Annual snowpack patterns across the
Rockies: Long-term trends and associated 500-mb synoptic patterns. *Monthly
Weather Review*, **121**: 633–647.
- Cheung, P.Y., Wong, M.C., and Yeung, H.Y. 2006. Application of rainstorm nowcast to
real-time warning of landslide hazards in Hong Kong. *In* WMO PWS workshop on
warnings of real-time hazards by using nowcasting technology. pp. 9–13. Available
from <http://www.hko.gov.hk/hko/publica/reprint/r673.pdf> [accessed 7 November
2013].
- Chilton, R.H. 1981. A summary of climatic regimes of British Columbia. Air Studies
Branch, Assessment and Planning Division, Ministry of Environment, Province of
British Columbia, Victoria, British Columbia.

- Clague, J.J. (*Editor*). 1998. Landslides and engineering geology of southwestern British Columbia. 8th Congress, International Association for Engineering Geology and the Environment: Technical Tour Guidebook, Trip 3. Vancouver, British Columbia, Canada.
- Clague, J.J., and Evans, S.G. 1994. Formation and failure of natural dams in the Canadian Cordillera. Natural Resources Canada, Minister of Energy, Mines and Resources.
- Clague, J.J., and Evans, S.G. 2003. Geologic framework of large historic landslides in Thompson River Valley, British Columbia. *Environmental & Engineering Geoscience*, **9**(3): 201–212.
- Clague, J.J., Evans, S.G., Fulton, R.J., Ryder, J.M., and Stryd, A.H. 1987. Quaternary geology of the southern Canadian Cordillera. XIIth Inqua Congress Field Excursion A-18. National Research Council of Canada.
- Clark, I.D., and Fritz, P. 1997. *Environmental Isotopes in Hydrogeology*. CRC Press/Lewis Publishers, Boca Raton, Florida.
- Collison, A., Wade, S., Griffiths, J., and Dehn, M. 2000. Modelling the impact of predicted climate change on landslide frequency and magnitude in SE England. *Engineering Geology*, **55**(3): 205–218. doi:10.1016/S0013-7952(99)00121-0.
- Crosta, G.B., and Agliardi, F. 2003. Failure forecast for large rock slides by surface displacement measurements. *Canadian Geotechnical Journal*, **40**(1): 176–191.
- Cruden, D.M. 1974. The static fatigue of brittle rock under uniaxial compression. *International Journal of Rock Mechanics and Mining Science & Geomechanics Abstracts*, **11**: 67–73.
- Cruden, D.M. 2003. The shapes of cold, high mountains in sedimentary rocks. *Geomorphology*, **55**: 249–261.

- Cruden, D.M., Martin, C.D., and Soe Moe, K.W. 2003. Stages in the translational sliding of 2 inclined blocks: observations from Edmonton. **1**: 823–830. Canadian Geotechnical Society, Ottawa, Winnipeg, Manitoba, Canada. pp. 823–830.
- Cruden, D.M., and VanDine, D. 2013. Chapter C: Classification, description, causes and indirect effects. *In* National Technical Guidelines and Best Practices on Landslides. Open File 7359, Geological Survey of Canada. Available from http://www.cgs.ca/geohazards_committee.php?lang=en [accessed 21 April 2016].
- Cruden, D.M., and Varnes, D.J. 1996. Landslide types and processes. *In* Landslides: Investigation and Mitigation. Transportation Research Board Special Report 247. pp. 36–75.
- Daily British Colonist. 1880a, August 19. Landslide near Cook’s Ferry. Victoria, British Columbia.
- Daily British Colonist. 1880b, October 21. The Great Land Slide. Victoria, British Columbia.
- Daily British Colonist. 1886, October 20. Landslide Near Aschroft. Victoria, British Columbia.
- Daily British Colonist. 1897, September 24. The Hills Gave Way. Victoria, British Columbia.
- Daily Colonist. 1905a, August 15. Avalanche Blots Out Rancherie. Victoria, British Columbia.
- Daily Colonist. 1905b, August 16. Tells of Slide at Spence’s Bridge. Victoria, British Columbia.
- Daily Colonist. 1907, May 17. Flood Season Nigh. Victoria, British Columbia.
- Daily Ledger. 1905, August 14. Landslide near Spences Bridge. Ladysmith, British Columbia, Canada.

- D'Elia, B., Picarelli, L., Leroueil, S., and Vaunat, J. 1998. Geotechnical characterization of slope movements in structurally complex clay soils and stiff jointed clays. *Italian Geotechnical Journal*, **32**(3): 5–32.
- Dercole, F. 2009. District of North Vancouver- Report to Council: Natural Hazards Risk Tolerance Criteria. Available from http://www.dnv.org/upload/documents/Engineering/CDNV_DISTRICT_HALL-%231311308-v1-risk_tolerance_criteria_-_RTC.PDF [accessed 6 December 2013].
- District of North Vancouver. 2008. Natural hazards task force, Report to Mayor and Council. Powerpoint presentation. Available from <http://www.dnv.org/article.asp?c=1024>. [accessed 28 February 2013].
- District of North Vancouver. 2011. Saskawa Award Nomination. District of North Vancouver, British Columbia, Canada.
- District of North Vancouver. 2013a. Natural hazards task force. Available from <http://www.dnv.org/upload/documents/Engineering/Taskforce.pdf>. [accessed 13 March 2013].
- District of North Vancouver. 2013b. Natural hazards management program. Available from <http://www.dnv.org/article.asp?c=1024> [accessed 27 February 2013].
- Dorcey, A., and McDaniels, T. 2000. Great expectations, mixed results: trends in citizen involvement in Canadian environmental governance. *In Environmental Trends in Canada. Edited by E. Parson*. Available from <http://tonydorcey.ca/governance/draft2.html> [accessed 6 June 2011].
- Douglas, M., and Wildavsky, A. 1982. *Risk and Culture: an essay on the selection of technological and environmental dangers*. University of California Press.
- Drever, J.I. 1997. *The geochemistry of natural waters: surface and groundwater environments*. 3rd ed. Prentice Hall, Upper Saddle River, New Jersey.

- Drysdale, C.W. 1914. Geology of the Thompson River Valley below Kamloops Lake, British Columbia. *In* Summary Report 1912. Geological Survey of Canada. pp. 115–150.
- EBA Engineering Ltd. 1984. Geotechnical Evaluation of the Goddard Landslide. Report submitted to Canadian Pacific Railway, Vancouver (Canyon) Division, Thompson Subdivision.
- Ebbesmeyer, C.C., Cayan, D.R., McLain, D.R., Nichols, F.H., Peterson, D.H., and Redmond, K.T. 1991. 1976 step in the Pacific climate: forty environmental changes between 1968-75 and 1977-1984. *In* Proceedings of the Seventh Annual Climate (PACLIM) Workshop, April 1990. *Edited by* J.L. Betancourt and V.L. Tharp. California Department of Water Resources. Interagency Ecological Studies Program Technical Report 26. pp. 115–126.
- Edwards, T. 2015, November 16. Public Geoscience Workshop: Ashcroft Thompson River Landslides - Railways Perspective. Powerpoint presentation. Ashcroft, British Columbia, Canada.
- Engineering News. 1909. The Salette landslide of 1908 and some earlier Quebec landslides. *Engineering News*, **61**(21): 576–578.
- Environment Canada. 2014. Archived hydrometric data- Thompson River near Spences Bridge, Stations 08LF051 and 08LF022. Available from <http://www.wsc.ec.gc.ca/applications/H2O/HydromatD-eng.cfm> [accessed 23 January 2014].
- Environment Canada. 2015a. Historical Climate Data. Available from <http://climate.weather.gc.ca/> [accessed 24 November 2015].
- Environment Canada. 2015b. Canadian Climate Normals. Available from http://climate.weather.gc.ca/climate_normals/index_e.html [accessed 24 November 2015].

- Environment Canada. 2015c. Integrated Seasonal Climate Bulletin, MSC-PYR: December 4, 2015.
- ERM-Hong Kong, Ltd. 1998. Landslides and boulder falls from natural terrain: interim risk guidelines. Geo Report No. 75.
- Eshraghian, A. 2007. Hazard analysis of reactivated earth slides in the Thompson River Valley, Ashcroft, British Columbia. Ph.D. Thesis, Department of Civil and Environmental Engineering, University of Alberta, Edmonton, Alberta.
- Eshraghian, A., Martin, C.D., and Cruden, D.M. 2005. Landslides in the Thompson River Valley between Ashcroft and Spences Bridge, British Columbia. *In* Landslide risk management: Proceedings of the International Conference on Landslide Risk Management. *Edited by* O. Hungr, R. Fell, R. Couture, and E. Eberhardt. Taylor & Francis Group, London. pp. 437–446. Available from <http://www.crcnetbase.com/isbn/978-1-4398-3371-1> [accessed 4 October 2013].
- Eshraghian, A., Martin, C.D., and Cruden, D.M. 2007. Complex earth slides in the Thompson River Valley, Ashcroft, British Columbia. *Environmental & Engineering Geoscience*, **13**(2): 161–181.
- Eshraghian, A., Martin, C.D., and Morgenstern, N.R. 2008. Movement triggers and mechanisms of two earth slides in the Thompson River Valley, British Columbia, Canada. *Canadian Geotechnical Journal*, **45**: 1189–1209. doi:10.1139/T08-047.
- European Climate Adaptation Platform. 2017. Uncertainty guidance topic 2 — Climate-ADAPT. Available from <http://climate-adapt.eea.europa.eu/knowledge/tools/uncertainty-guidance/topic2> [accessed 1 February 2017].
- Evans, S.G. 1982. Landslides and surficial deposits in urban areas of British Columbia: a review. *Canadian Geotechnical Journal*, **19**(3): 269–288.

- Evans, S.G. 1984. The 1880 landslide dam on Thompson River near Ashcroft, British Columbia. *In* Current Research, Part A, Geological Survey of Canada Paper 84-1A. pp. 655–658.
- Evans, S.G. 1986. Landslide damming in the Cordillera of Western Canada. *In* Landslide dams: processes, risk, and mitigation. *Edited by* R.L. Schuster. American Society of Civil Engineers, New York.
- Evans, S.G. 1992. High magnitude-low frequency catastrophic landslides in British Columbia. *In* Proceedings of the Geologic Hazards '91 Workshop, February 20-21, 1992. *Edited by* P. Bobrowsky. Open File 1992-15, British Columbia Geological Survey Branch, Victoria, British Columbia. pp. 71–98. Available from <http://www.empr.gov.bc.ca/Mining/Geoscience/PublicationsCatalogue/OpenFiles/1992/Documents/OF1992-15GeolHazards.pdf>.
- Evans, S.G. 2000. Catastrophic Landslides in Canada. *In* GeoCanada 2000- The Millennium Geoscience Summit, 29 May-2 June, 2000. Calgary, AB, Canada.
- Fletcher, L., Hungr, O., and Evans, S.G. 2002. Contrasting failure behaviour of two large landslides in clay and silt. *Canadian Geotechnical Journal*, **39**(1): 46–62. doi:10.1139/t01-079.
- Francis, R., and Hare, S.R. 1994. Decadal-scale regime shifts in the large marine ecosystems of the North-east Pacific: a case for historical science. *Fisheries Oceanography*, **3**: 279–291.
- Freeze, R.A., and Witherspoon, P.A. 1967. Theoretical analysis of regional groundwater flow. Part 2: Effect of water-table configuration and subsurface permeability variation. *Water Resources Research*, **3**(2): 623–634.
- Frommer, B. 2013. Climate change and the resilient society: utopia or realistic option for German regions? *Natural Hazards*, **67**(1): 99–115. doi:10.1007/s11069-012-0421-0.

- Fukuzono, T. 1985. A new method for predicting the failure time of a slope. *In* Proceedings of the IVth International Conference and Field Workshop on Landslides. Tokyo, Japan. pp. 145–150.
- Gedalof, Z., and Smith, D.J. 2001. Interdecadal climate variability and regime-scale shifts in Pacific North America. *Geophysical Research Letters*, **28**(8): 1515–1518.
- Gershunov, A., and Barnett, T.P. 1998. Interdecadal modulation of ENSO teleconnections. *Bulletin of the American Meteorological Society*, **79**(12): 2715.
- Ghiassian, H., and Ghareh, S. 2008. Stability of sandy slopes under seepage conditions. *Landslides*, **5**(4): 397–406. doi:10.1007/s10346-008-0132-5.
- Giordan, D., Allasia, P., Manconi, A., Baldo, M., Santangelo, M., Cardinali, M., Corazza, A., Albanese, V., Lollino, G., and Guzzetti, F. 2013. Morphological and kinematic evolution of a large earthflow: the Montaguto landslide, southern Italy. *Geomorphology*, **187**: 61–79.
- Golder Associates. 1977. Slide Area, Mile 50.6. Thompson Subdivision. Report submitted to Canadian Pacific Railway, Calgary, Alberta.
- Golder Associates. 2004. Application for Environmental Assessment Certificate: Ashcroft Ranch Landfill Project, Ashcroft, British Columbia (Appendix V – Groundwater). Report submitted to Greater Vancouver Regional District, Burnaby, British Columbia. Available from http://a100.gov.bc.ca/appsdata/epic/html/deploy/epic_project_doc_list_211_r_app.html [accessed 23 October 2015].
- Golder, Brawner & Associates Ltd. 1969. Report to Canadian Pacific Railway on Slide Investigation Mile 47.9 to 50.4, Mountain Subdivision, Ashcroft, British Columbia. Submitted to Canadian Pacific Railway, Vancouver, B.C.
- Goodman, R.E. 1999. Karl Terzaghi: the engineer as artist. American Society of Civil Engineers, Reston, Virginia.

- Government of Canada. 2014. Calculation of the 1971 to 2000 climate normals for Canada. Available from http://climate.weather.gc.ca/climate_normals/normals_documentation_e.html.
- Guthrie, R.H., and Evans, S.G. 2004. Magnitude and frequency of landslides triggered by a storm event, Loughborough Inlet, British Columbia. *Natural Hazards and Earth System Science*, **4**(3): 475–483.
- Haefeli, R. 1948. The stability of slopes acted upon by parallel seepage. *In Proceedings of the Second International Conference on Soil Mechanics and Foundation Engineering*. Rotterdam, 21-30 June, 1948. pp. 57–62.
- Hamlet, A.F., Mote, P.W., Clark, M.P., and Lettenmaier, D.P. 2005. Effects of Temperature and Precipitation Variability on Snowpack Trends in the Western United States. *Journal of Climate*, **18**(21): 4545–4561.
- Hare, S.R., and Mantua, N.J. 2000. Empirical evidence for North Pacific regime shifts in 1977 and 1989. *Progress in Oceanography*, **47**: 103–145. doi:10.1016/S0079-6611(00)00033-1.
- Harmsworth, G., and Raynor, B. 2004. Cultural consideration in landslide risk perception. *In Landslide Hazard and Risk. Edited by T. Glade, M. Anderson, and M.J. Crozier*. John Wiley & Sons, Ltd. pp. 219–249.
- Harrison, C. 2014. On the mechanics of seepage induced cohesionless soil slope instability. *In Proceedings of the 67th Canadian Geotechnical Conference*, 28 September-1 October, 2014. Canadian Geotechnical Society, Ottawa, Regina, Saskatchewan.
- Hartmann, D.L. 2015. Pacific sea surface temperature and the winter of 2014. *Geophysical Research Letters*, **42**(6): 2015GL063083. doi:10.1002/2015GL063083.
- Health and Safety Executive (HSE). 2001. Reducing risks, protecting people: HSE's decision-making process. Health and Safety Executive, United Kingdom, London.

- Hendry, M.J., Barbour, S.L., Novakowski, K., and Wassenaar, L.I. 2013a. Paleohydrogeology of the Cretaceous sediments for the Williston Basin using stable isotopes of water. *Water Resources Research*, **49**: 4580–4592. doi:10.1002/wrcr.20321.
- Hendry, M.T., Macciotta, R., Martin, C.D., and Reich, B. 2015. The effect of the Thompson River elevation on the velocity and instability of the Ripley Slide. *Canadian Geotechnical Journal*, **52**: 257–267.
- Hendry, M.T., Martin, C.D., Choi, E., Chadwick, I., and Edwards, T. 2013b. Safe train operations over a moving slide. *In Proceedings of the 10th World Congress on Railway Research*. Sydney, Australia.
- Hodge, R.A., and Freeze, R.A. 1977. Groundwater flow systems and slope stability. *Canadian Geotechnical Journal*, **14**(4): 466–476.
- Holling, C.S. 1979. Resilience and stability of ecological systems. *Annual Review of Ecology, Evolution, and Systematics*, **4**: 1–23.
- Horlick-Jones, T. 1998. Meaning and contextualisation in risk assessment. *Reliability Engineering & System Safety*, **59**(1): 79–89.
- Hufschmidt, G., Crozier, M., and Glade, T. 2005. Evolution of natural risk: research framework and perspectives. *Natural Hazards and Earth System Science*, **5**(3): 375–387.
- Hungr, O., Corominas, J., Eberhardt, E., Hungr, O., Fell, R., Couture, R., and Eberhardt, E. 2005. Estimating landslide motion mechanism, travel distance and velocity. *In Landslide Risk Management*. pp. 99–128.
- Huntley, D., Best, M., Bobrowsky, P., Bauman, P., Candy, C., and Parry, N. 2017a. Combining terrestrial and waterborne geophysical surveys to investigate the internal composition and structure of a very slow-moving landslide near Ashcroft, British Columbia, Canada. *In Proceedings of the 4th World Landslide Forum, 29 May-2 June, 2017 (Draft - In Print)*. Ljubljana, Slovenia.

- Huntley, D., Bobrowsky, P., Charbonneau, F., Journault, J., Macciotta, R., and Hendry, M. 2017b. Innovative landslide change detection monitoring: application of space-borne InSAR techniques in the Thompson River valley, British Columbia, Canada. *In* Proceedings of the 4th World Landslide Forum, May 29-Jun 2, 2017 (Draft - In Print). Ljubljana, Slovenia.
- Huntley, D., Bobrowsky, P., Parry, N., Bauman, P., Candy, C., and Best, M. 2016. Ripley landslide: the geophysical structure of a slow-moving landslide near Ashcroft, British Columbia. Open File 8062, Geological Survey of Canada.
- Hutchinson, J.N. 1975. The response of London Clay cliffs to differing rates of toe erosion. Building Research Establishment Current Paper, Reprinted from *Geologia Applicata e Idrogeologia*, Vol VII, Part 1, Bari, 1973, pp 222-239.
- Hutchinson, J.N. 1984. An influence line approach to the stabilization of slopes by cuts and fills. *Canadian Geotechnical Journal*, **21**(2): 363–370.
- Hutchinson, J.N. 1987. Mechanisms producing large displacements in landslides on pre-existing shears. *Memoir of the Geological Society of China*, number 9, Taipei, Taiwan. pp. 175–200.
- Hutchinson, J.N. 1988. Morphological and geotechnical parameters of landslides in relation to geology and hydrogeology. *General Report. 1*: 3–35. Lausanne. pp. 3–35.
- Hutchinson, J.N. 2001. Landslide risk; to know, to foresee, to prevent. *Geologia Technica*,.
- Hutchinson, J.N., and Bhandari, R.K. 1971. Undrained Loading, A Fundamental Mechanism of Mudflows and other Mass Movements. *Géotechnique*, **21**(4): 353–358.
doi:10.1680/geot.1971.21.4.353.
- IPCC. 2007. Summary for policymakers. *In* Intergovernmental Panel on Climate Change. *Climate change 2007: The physical science basis*. Available from www.ipcc.ch/publications_and_data/ar4/wg1/en/spm.html [accessed 25 February 2016].

- IPCC. 2012. Intergovernmental Panel on Climate Change. Managing the risks of extreme events and disasters to advance climate change adaptation. Cambridge University Press, Cambridge, UK.
- IPCC. 2014. Intergovernmental Panel on Climate Change. Climate change 2014: Mitigation of climate change. Contribution of Working Group III to the 5th Assessment Report of the Intergovernmental Panel on Climate Change. Cambridge University Press, Cambridge, UK.
- Iverson, R.M. 1992. Sensitivity of stability analyses to groundwater data. *In* Landslides, Proceedings of the Sixth International Symposium on Landslides, Christchurch, 10-14 February 1992. Edited by David H. Bell. Balkema. pp. 451–457. Available from https://profile.usgs.gov/myscience/upload_folder/ci2013Mar08191202246641991.Iverson%20ISL%20paper.pdf [accessed 8 November 2016].
- Iverson, R.M., George, D.L., Allstadt, K., Reid, M.E., Collins, B.D., Vallance, J.W., Schilling, S.P., Godt, J.W., Cannon, C.M., Magirl, C.S., Baum, R.L., Coe, J.A., Schulz, W.H., and Bower, J.B. 2015. Landslide mobility and hazards: implications of the 2014 Oso disaster. *Earth and Planetary Science Letters*, **412**: 197–208. doi:10.1016/j.epsl.2014.12.020.
- Iverson, R.M., and Major, J.J. 1986. Groundwater seepage vectors and the potential for hillslope failure and debris flow mobilization. *Water Resources Research*, **22**(11): 1543–1548.
- Iverson, R.M., and Major, J.J. 1987. Rainfall, ground-water flow, and seasonal movement at Minor Creek landslide, northwestern California: Physical interpretation of empirical relations. *Geological Society of America Bulletin*, **99**(4): 579–594.
- Iverson, R.M., and Reid, M.E. 1992. Gravity-driven groundwater flow and slope failure potential: 1. elastic effective-stress model. *Water Resources Research*, **28**(3): 925–938.

- Jakob, M., and Porter, M.J. 2007. Risk assessment and risk tolerance. Powerpoint presentation. Available from <http://www.dnv.org/article.asp?c=1024>. [accessed 28 February 2013].
- Jardine, C., Hrudey, S., Shortreed, J., Craig, L., Krewski, D., Furgal, C., and McColl, S. 2003. Risk Management Frameworks for Human Health and Environmental Risks. *Journal of Toxicology and Environmental Health, Part B*, **6**(6): 569–718. doi:10.1080/10937400390208608.
- Jibson, R.W. 2006. The 2005 La Conchita, California, landslide. *Landslides*, **3**(1): 73–78. doi:10.1007/s10346-005-0011-2.
- Johnsen, T.F. 2004. Late glacial lakes of the Thompson basin, southern interior of British Columbia: paleogeography and paleoenvironment. M.Sc. Thesis, Simon Fraser University, British Columbia, Canada.
- Johnsen, T.F., and Brennand, T.A. 2004. Late-glacial lakes in the Thompson Basin, British Columbia: paleogeography and evolution. *Canadian Journal of Earth Sciences*, **41**(11): 1367–1383. doi:10.1139/e04-074.
- Journault, J. 2016, March 30. Tracking the slow deformation of landslides in the Thompson River Valley using InSAR. Geotechnical Graduate Seminar Presentation, University of Alberta, Edmonton.
- Journault, J., Macciotta, R., Hendry, M., Charbonneau, F., Bobrowsky, P., Huntley, D., Bunce, C., and Edwards, T. 2016. Identification and quantification of concentrated movement zones within the Thompson River Valley using Satellite InSAR. Vancouver, British Columbia, Canada.
- Keegan, T.R. 2007. Methodology for Risk Analysis of Railway Ground Hazards. PhD Thesis, Department of Civil and Environmental Engineering, University of Alberta, Canada.

- Keegan, T.R., Abbott, B., Cruden, D.M., Bruce, I., and Pritchard, M. 2003. Railway Ground Hazard Risk Scenerio: River Erosion: Earth Slide. *In* 3rd Canadian Conference on Geotechnique and Natural Hazards. Edmonton, Alberta, Canada. pp. 269–277.
- King, G.J.W. 1989. Revision of the effective-stress method of slices. *Geotechnique*, **39**(3): 497–502.
- King, G.J.W. 1990. Discussion and reply for “Revision of effective stress method of slices.” *Geotechnique*, **40**: 651–654.
- Klohn Leonoff Consulting Engineers. 1986. Field Investigation Report: Goddard Landslide. Submitted to Alexander, Holburn, Beaudin & Lang, Vancouver, British Columbia.
- Kosar, K., Revering, K., Keegan, T., Black, K., and Stewart, L. 2003. Use of spaceborne InSAR to characterize ground movements along a rail corridor and open pit mine. *In* Proceedings of the 3rd Canadian Conference on Geotechnique and Natural Hazards. Canadian Geotechnical Society, Edmonton, Alberta, Canada, June 9-10, 2003. pp. 177–184.
- Krahn, J. 1984. Geotechnical Evaluation of the Goddard Landslide. Report submitted to Canadian Pacific Railway, Vancouver Division, Thompson Subdivision. EBA Engineering Consultants Ltd, Report 306-0950.
- Lacerda, W.A. 1989. Discussion leader’s contribution: Fatigue of residual soils due to cyclic pore pressure vatiation. **5**: 3085–3087. Rio de Janeiro, Brazil. pp. 3085–3087.
- Lafleur, J., and Lefebvre, G. 1980. Groundwater regime associated with slope stability in Champlain clay deposits. *Canadian Geotechnical Journal*, **17**: 44–53.
- Lambe, T.W., and Whitman, R.V. 1969. *Soil Mechanics*. John Wiley & Sons, Inc., New York.
- Leiss, W. 2001. *In the chamber of risks: understanding risk controversies*. McGill-Queen’s University Press, Montreal.

- Leroi, E., Bonnard, C., Fell, R., and McInnes, R. 2005. Risk assessment and management. *In* Landslide risk management: Proceedings of the International Conference on Landslide Risk Management, Vancouver, Canada, 31 May-3 June 2005. *Edited by* O. Hungr, R. Fell, R. Couture, and E. Eberhardt. Balkema. pp. 159–198. Available from <http://www.crcnetbase.com/isbn/9781439833711> [accessed 6 December 2013].
- Leroueil, S. 2001. Natural slopes and cuts: movement and failure mechanisms. *Geotechnique*, **51**(3): 197–243.
- Leroueil, S., Locat, J., Vaunat, J., Picarelli, L., Lee, H., and Faure, R. 1996. Geotechnical characterization of slope movements. *In* Landslides, Proceedings of the Seventh International Symposium on Landslides, Trondheim, 17-21 June 1996. *Edited by* K. Senneset. AA Balkema, Rotterdam. pp. 53–74.
- Lettenmaier, D.P., Wood, E.F., and Wallace, J.R. 1994. Hydro-climatological trends in the continental United States, 1948-88. *Journal of Climate*, **7**: 586–607.
- Lissak, C., Maquaire, O., Davidson, R., and Malet, J.-P. 2014. Piezometric thresholds for triggering landslides along the Normandy coast, France. *Géomorphologie: relief, processus, environnement*, **20**(2): 145–158. doi:10.4000/geomorphologie.10607.
- Litzow, M.A. 2006. Climate regime shifts and community reorganization in the Gulf of Alaska: how do recent shifts compare with 1976/1977. *ICES Journal of Marine Science*, **63**: 1386–1396.
- Lollino, P., Giordan, D., and Allasia, P. 2016. Assessment of the behavior of an active earth-slide by means of calibration between numerical analysis and field monitoring. *Bulletin of Engineering Geology and the Environment*,. doi:10.1007/s10064-016-0953-8.
- Lorenz, D.F. 2010. The diversity of resilience: contributions from a social science perspective. *Natural Hazards*, **67**(1): 7–24. doi:10.1007/s11069-010-9654-y.
- Lum, K.K.Y. 1979. Stability of the Kamloops Silt Bluffs. M.A.Sc. Thesis, Department of Civil Engineering, University of British Columbia, Vancouver, British Columbia.

- Macciotta, R., Hendry, M., and Martin, C.D. 2016. Developing an early warning system for a very slow landslide based on displacement monitoring. *Natural Hazards*, **81**(2): 887–907. doi:10.1007/s11069-015-2110-2.
- Macciotta, R., Hendry, M., Martin, C.D., Elwood, D., and Lan, H. 2014. Monitoring of the Ripley Slide, Thompson River Valley, British Columbia. Kingston, Ontario, Canada.
- MacDonald, M., Coldwells, L., Mo, R., Gardner, T., and Bramwell, G. 2016, March 10. Integrated Seasonal Climate Bulletin, MSC-PYR: Fall 2015 Summary & Winter '15-16 Outlook. Vancouver, British Columbia, Canada.
- Maguire, B., and Hagan, P. 2007. Disasters and communities-understanding social resilience. *The Australian Journal of Emergency Management*, **22**(2): 16–20.
- Mansour, M.F., Morgenstern, N.R., and Martin, C.D. 2011. Expected damage from displacement of slow-moving slides. *Landslides*, **8**(1): 117–131. doi:10.1007/s10346-010-0227-7.
- Mantua, N.J. 2002. Pacific-Decadal Oscillation (PDO). **1**: 592–594. John Wiley & Sons, Ltd. pp. 592–594.
- Mantua, N.J. 2015. PDO Index. Available from <http://research.jisao.washington.edu/pdo/PDO.latest> [accessed 4 September 2015].
- Mantua, N.J., and Hare, S.R. 2002. The Pacific Decadal Oscillation. *Journal of Oceanography*, **58**(1): 35–44. doi:10.1023/A:1015820616384.
- Mantua, N.J., Hare, S.R., Zhang, Y., Wallace, J.M., and Francis, R.C. 1997. A Pacific interdecadal climate oscillation with impacts on salmon production. *Bulletin of the American Meteorological Society*, **78**(6): 1069–1079.
- Martin, R.L., Williams, D.R., Balanko, L.A., and Morgenstern, N.R. 1984. The Grierson Hill slide, Edmonton, Alberta. *In* Proceedings of the 37th Canadian Geotechnical Conference. Canadian Geotechnical Society, Toronto, Ontario, Canada. pp. 125–133.

- McGill, D.E. 1979. 126 stops of interest in beautiful British Columbia. Frontier Publishing, Aldergrove, B.C. :
- McSaveney, M.J., and Griffiths, G.A. 1987. Drought, rain, and movement of a recurrent earthflow complex in New Zealand. *Geology*, **15**(7): 643–646.
- Minobe, S. 1997. A 50-70 year climatic oscillation over the North Pacific and North America. *Geophysical Research Letters*, **24**: 683–686.
- Minobe, S. 1999. Resonance in Bidecadal and Pentadecadal Climate Oscillations Over the North Pacific and North America. *Geophysical Research Letters*, **26**: 855–858.
- Moore, R.D. 1991. The chemical and mineralogical controls upon the residual strength of pure and natural clays. *Geotechnique*, **41**(1): 35–47. doi:10.1680/geot.1991.41.1.35.
- Moore, R.D., and Brunsden, D. 1996. Physico-chemical effects on the behaviour of a coastal mudslide. *Geotechnique*, **46**(2): 259–278. doi:10.1680/geot.1996.46.2.259.
- Moore, R.D., Spittlehouse, D.L., Whitfield, P.H., and Stahl, K. 2010. Weather and climate. **1**: 47–84. Forest Science Program / FORREX. pp. 47–84. Available from <http://www.for.gov.bc.ca/hfd/pubs/Docs/Lmh/Lmh66.htm> [accessed 9 January 2014].
- Morgenstern, N.R. 1986. Summary of the Opinion of Norbert R. Morgenstern; Goddard Landslide of September, 1982. Vancouver Registry No. C841694, British Columbia, Canada.
- Morgenstern, N.R., and Price, V.E. 1965. The analysis of the stability of general slip surfaces. *Geotechnique*, **15**(1): 79–93.
- Morrison, I.M. 1988. A note on the stability analysis of slopes. *Geotechnique*, **38**: 157–159.
- Morrison, I.M., and Greenwood, J.R. 1989. Assumptions in simplified slope stability analysis by the method of slices. *Geotechnique*, **39**(3): 503–509.

- Morrison, I.M., and Greenwood, J.R. 1990. Discussion and reply for “Assumptions in simplified slope stability analysis by the method of slices.” *Geotechnique*, **40**: 655–658.
- Morrison, J., Quick, M.C., and Foreman, M.G.G. 2002. Climate change in the Fraser River watershed: flow and temperature projections. *Journal of Hydrology*, **263**(1–4): 230–244. doi:10.1016/S0022-1694(02)00065-3.
- Moser, H., and Stichler, W. 1975. Deuterium and oxygen-18 contents as index of the properties of snow blankets. *In* Snow mechanics: Proceedings of the Grindelwald Symposium, April 1974, IAHS Publication 114. International Association of Hydrological Sciences (IAHS). pp. 122–135.
- National Infrastructure Advisory Council. 2010. A framework for establishing critical infrastructure resilience goals. Washington, DC. Available from <https://www.dhs.gov/xlibrary/assets/niac/niac-a-framework-for-establishing-critical-infrastructure-resilience-goals-2010-10-19.pdf>.
- National Infrastructure Unit. 2011. National Infrastructure Plan. New Zealand Government, Wellington, New Zealand. Available from <http://www.infrastructure.govt.nz/plan/2011/nip-jul11.pdf> [accessed 28 October 2014].
- National Oceanic and Atmospheric Administration. 2016. Historical El Niño / La Niña episodes, 1950-present. Available from http://www.cpc.ncep.noaa.gov/products/analysis_monitoring/ensostuff/ensoyears.shtml [accessed 3 February 2016].
- North Shore News. 2009, March 24. North Vancouver District settles Kuttner landslide suit. Available from http://www.canada.com/story_print.html?id=2ebab06e-9f5c-47a6-baf9-69edd59f7d1d&sponsor= [accessed 19 June 2013].

- Null, J. 2016. El Niño and La Niña years and intensities, based on Oceanic Niño Index (ONI). Available from <http://ggweather.com/enso/oni.htm> [accessed 3 February 2016].
- Peck, R.B. 1969. Advantages and limitations of the observational method in applied soil mechanics. *Geotechnique*, **19**(2): 171–187.
- Peckover, F.L. 1972. Treatment of Rock Falls on Railway Lines. A Study for the CN Main Line, Jasper - Vancouver. Part A: Policy and Planning. Office of the Chief Engineer, Canadian National Railways, Montreal, Quebec.
- Perrow, C. 1999. *Normal Accidents: Living with High-Risk Technologies*. 2nd ed. Princeton University Press, Princeton, N.J.
- Petley, D.N., and Allison, R.J. 1997. The mechanics of deep-seated landslides. *Earth Surface Processes and Landforms*, **22**(8): 747–758. doi:10.1002/(SICI)1096-9837(199708)22:8<747::AID-ESP767>3.0.CO;2-#.
- Petts, J. 2004. Barriers to participation and deliberation in risk decisions: evidence from waste management. *Journal of Risk Research*, **7**(2): 115–133. doi:10.1080/1366987042000158695.
- Pitts, J. 1979. Morphological mapping in the Axmouth-Lyme Regis Undercliffs. *Quarterly Journal of Engineering Geology and Hydrogeology*, **12**: 205–217.
- Pizarro, G., and Lall, U. 2002. El Niño-induced flooding in the U.S. West: What can we expect? *Eos, Transactions American Geophysical Union*, **83**(32): 349–352. doi:10.1029/2002EO000255.
- Place, J., and Hanlon, N. 2011. Kill the lake? kill the proposal: accommodating First Nations' environmental values as a first step on the road to wellness. *GeoJournal*, **76**(2): 163–175. doi:10.1007/s10708-009-9286-5.

- Popescu, M.E. 1994. A suggested method for reporting landslide causes. *Bulletin of the International Association of Engineering Geology-Bulletin de l'Association Internationale de Géologie de l'Ingénieur*, **50**(1): 71–74.
- Porter, M.J., Jakob, M., and Holm, K. 2009. Proposed landslide risk tolerance criteria. *In* Proceedings, in Proceedings of the Canadian Geotechnical Conference. Halifax. pp. 533–541.
- Porter, M.J., Savigny, K.W., Keegan, T.R., Bunce, C.M., and MacKay, C. 2002. Controls on stability of the Thompson River landslides. *In* Proceedings of the 55th Canadian Geotechnical Conference: Ground and Water: Theory to Practice. Canadian Geotechnical Society, Ottawa, Niagara Falls, Ontario. pp. 20–23.
- Province of British Columbia. 2014. Archived manual snow survey and automated snow pillow data. Available from <http://bcrfc.env.gov.bc.ca/data/>.
- Province of British Columbia. 2016a. Agricultural Regions: Thompson-Nicola - Overview. Available from <http://www2.gov.bc.ca/gov/content/industry/agriculture-seafood/agricultural-regions/thompson-nicola> [accessed 4 February 2016].
- Province of British Columbia. 2016b. Snow Survey Bulletins and Commentaries. Available from <http://bcrfc.env.gov.bc.ca/bulletins/index.htm> [accessed 2 March 2016].
- Province of British Columbia. 2016c. BC Water Resources Atlas. Available from <http://maps.gov.bc.ca/ess/sv/wrbc/> [accessed 2 February 2016].
- Quigley, R. 1976. Mineralogy, chemistry and structure of the Penticton and South Thompson silt deposits. Research Report to British Columbia Department of Highways, Faculty of Engineering Science, University of Western Ontario, London, Ontario.
- Quinn, P., Hall, I., Porter, M.J., and Savigny, K.W. 2012. Ashcroft Thompson River landslides- watershed scale controls. *In* Proceedings of the 65th Canadian Geotechnical Conference. Winnipeg, Manitoba, Canada.

- Reginatto, A.R., and Ferrero, J.C. 1973. Collapse potential of soils and soil water chemistry. *In Problems of Soil Mechanics and Construction on Soft Clays and Structurally Unstable Soils (Collapsible, Expansive and Others)*. pp. 177–183.
- Reid, M.E., and Iverson, R.M. 1992. Gravity-driven groundwater flow and slope failure potential: 2. effects of slope morphology, material properties, and hydraulic heterogeneity. *Water Resources Research*, **28**(3): 939–950.
- Renn, O. 2008. *Risk Governance- Coping with Uncertainty in a Complex World*. Earthscan, London.
- Ridge, J. 2006. Slope safety action plan: district response to the phase 2 BGC report. Powerpoint presentation. Available from <http://www.dnv.org/article.asp?a=3229&c=1030> [accessed 2 December 2013].
- Rocky Mountain Outlook. 2014. Cougar Creek mitigation misinterpreted, Town says. Available from <http://www.rmoutlook.com/Cougar-Creek-mitigation-misinterpreted,-Town-says-20140717> [accessed 3 March 2016].
- Ryder, J.M. 1976. Terrain inventory and quaternary geology, Ashcroft, British Columbia. Geological Survey of Canada Paper 74-49, and Map 1405A. Energy, Mines and Resources Canada.
- Ryder, J.M. 1981. Terrain inventory and quaternary geology, Lytton, British Columbia. Geological Survey of Canada Paper 79-25. Energy, Mines and Resources Canada.
- Saito, M. 1965. Forecasting the time of occurrence of a slope failure. *In Proceedings of the 6th International Conference on Soil Mechanics and Foundation Engineering*. pp. 537–541.
- Sarma, S.K. 1973. Stability analysis of embankments and slopes. *Geotechnique*, **23**: 423–433.
- Sarma, S.K. 1979. Stability analysis of embankments and slopes. *Journal of the Geotechnical Engineering Division, American Society of Civil Engineers*, **105**, **GT12**: 1511–1524.

- Schafer, M.B. 2016. Kinematics and controlling mechanics of the slow moving Ripley landslide. M.Sc. Thesis, University of Alberta, Canada.
- Schafer, M.B., Macciotta, R., Hendry, M., Martin, D., Bunce, C., Choi, E., and Edwards, T. 2015. Instrumenting and monitoring a slow moving landslide. *In* Proceedings of the 68th Canadian Geotechnical Conference, 20-23 September. Quebec City, Quebec, Canada.
- Schultz, C.B., and Smith, H.T.U. (*Editors*). 1965. Pacific Northwest: guidebook for field conference J. Nebraska Academy of Sciences.
- Septer, D. 2007. Flooding and landslide events: southern British Columbia, 1808-2006. Province of British Columbia, Ministry of the Environment, Victoria, British Columbia. Available from <http://www.for.gov.bc.ca/hfd/library/documents/bib106111south1.pdf> [accessed 10 July 2014].
- Sevi, A.F., Springston, G.E., and Kanat, L. 2014. A century of landslide activity in glaciolacustrine deposits in Jeffersonville, Vermont, USA. *In* Proceedings of the 6th Canadian Geohazards Conference, Kingston, Ontario. Canadian Geotechnical Society, Ottawa.
- Shibasaki, T., Matsuura, S., and Okamoto, T. 2016. Experimental evidence for shallow, slow-moving landslides activated by a decrease in ground temperature. *Geophysical Research Letters*, **43**(13): 2016GL069604. doi:10.1002/2016GL069604.
- Shrestha, R.R., Schnorbus, M.A., Werner, A.T., and Berland, A.J. 2012. Modelling spatial and temporal variability of hydrologic impacts of climate change in the Fraser River basin, British Columbia, Canada. *Hydrological Processes*, **26**(12): 1840–1860. doi:10.1002/hyp.9283.
- Skempton, A.W. 1964. Long-term stability of clay slopes. *Geotechnique*, **14**(2): 77–101.

- Skempton, A.W., and Hutchinson, J.N. 1969. Stability of natural slopes and embankment foundations. *In* Proceedings of the 7th International Conference on Soil Mechanics and Foundation Engineering, Mexico. State of the Art Volume. pp. 291–340.
- Skinner, W.R. 1992. Lake ice conditions as a cryospheric indicator for detecting climate variability in Canada. Canadian Climate Centre Report No. 92-4. Atmospheric Environment Service, Downsview, Ontario.
- Slovic, P. 1999. Trust, emotion, sex, politics, and science: Surveying the risk-assessment battlefield. *Risk analysis*, **19**(4): 689–701.
- Soe Moe, K.W., Cruden, D.M., Martin, C.D., Lewycky, D., and Lach, P.R. 2006. Delayed failure of a river valley slope: Whitemud Road Landslide. *In* Proceedings of the 59th Canadian Geotechnical Conference, 1-4 October 2006. Canadian Geotechnical Society, Ottawa, Vancouver, British Columbia. pp. 1476–1483.
- Soe Moe, K.W., Cruden, D.M., Martin, C.D., Lewycky, D., and Lach, P.R. 2009. Mechanisms and kinematics of river valley landslides in Edmonton. *In* Proceedings of the 2009 Annual Conference of the Transportation Association of Canada. Vancouver, British Columbia.
- Sowers, G.B., and Sowers, G.F. 1970. *Introductory Soil Mechanics and Foundations*. 3rd ed. Macmillan, USA.
- Squier, L.R., and Versteeg, J.H. 1971. The history and correction of the Omsi-Zoo landslide. *In* Proceedings of the 9th Annual Engineering Geology and Soils Engineering Symposium, 5-7 April 1971. Boise, Idaho. pp. 237–256.
- Stahl, K., Moore, R.D., and McKendry, I.G. 2006. The role of synoptic-scale circulation in the linkage between large-scale ocean-atmosphere indices and winter surface climate in British Columbia, Canada. *International Journal of Climatology*, **26**: 541–560.
- Stanton, R.B. 1898a. Great Land-slides on the Canadian Pacific Railway in British Columbia. *In* Proceedings of the Institution of Civil Engineers, Paper number 3074. pp. 1–20.

- Stanton, R.B. 1898b. Correspondence on “Great Land-slides on the Canadian Pacific Railway in British Columbia.” *In* Proceedings of the Institution of Civil Engineers. pp. 29–46.
- Stanton, R.B. 1904. Discussion on “Lateral Earth Pressures.” Transactions of the American Society of Civil Engineers, **LIII**(December 1904): 307–314.
- Stark, T.D., and Eid, H.T. 1994. Drained residual strength of cohesive soils. *Journal of Geotechnical Engineering*, **120**: 856–871.
- Statement of Claim. 2005. Supreme Court of British Columbia, Vancouver Registry No. S053396. Available from <http://www.seymourvalley.ca/Landslide/MichaelKuttnerClaim.pdf> [accessed 20 June 2013].
- Tappenden, K.M. 2014a. The district of North Vancouver’s landslide management strategy: Role of public involvement for determining tolerable risk and increasing community resilience. *Natural Hazards*, **72**(2): 481–501. doi:10.1007/s11069-013-1016-0.
- Tappenden, K.M. 2014b. Climatic influences on the Ashcroft Thompson River Landslides, British Columbia, Canada. *In* Proceedings of the 6th Canadian Geohazards Conference, 15-17 June 2014. Kingston, Ontario, Canada.
- Tappenden, K.M. 2016. Impact of climate variability on landslide activity in the Thompson River Valley near Ashcroft, B.C. *In* Proceedings of the 69th Canadian Geotechnical Conference. Vancouver, British Columbia.
- Terzaghi, K. 1950. Mechanism of landslides. *In* Application of geology to engineering practice: Berkey volume. Geological Society of America, New York. pp. 84–123.
- Thurber Consultants Ltd. 1984. Landslide at Mile 49 Thompson Subdivision, C.P. Rail. Report submitted to Highland Valley Cattle Company, British Columbia.

- Town of Canmore. 2015. Compilation of Public Input - Draft MDP 2015 Version 1 - Combined. Available from <http://www.canmore.ca/residents/mdp> [accessed 3 March 2016].
- Transport Canada. 2011, November 25. Rules Respecting Track Safety. Available from <https://www.tc.gc.ca/eng/railsafety/rules-tce54-830.htm> [accessed 13 September 2016].
- Tribe, S. 2002. Geomorphic evidence for Tertiary drainage networks in the southern Coast Mountains, British Columbia. Current Research 2002-A13, Geological Survey of Canada.
- Tribe, S. 2005. Eocene paleo-physiography and drainage directions, southern Interior Plateau, British Columbia. *Canadian Journal of Earth Sciences*, **42**(2): 215–230. doi:10.1139/e04-062.
- Tutkaluk, J., Graham, J., and Kenyon, R. 1998. Effects of riverbank hydrology on riverbank stability. *In* Proceedings of the 51st Canadian Geotechnical Conference. Canadian Geotechnical Society, Ottawa, Edmonton, Alberta. pp. 283–288.
- United Nations Environment Programme (UNEP). 2009. IEA Training Manual Volume Two– Vulnerability and Impact Assessments for Adaptation to Climate Change. Available from http://www.iisd.org/pdf/2010/iea_training_vol_2_via.pdf.
- United States National Research Council. 1996. Understanding risk: informing decisions in a democratic society. *Edited by* P.C. Stern and H.F. Fineberg. National Academy Press, Washington, DC.
- U-T San Diego Newspaper. 2014, March 26. More bodies found in mudslide; toll expected to hit 24– scientists warned in 1999 of danger. San Diego, USA.
- Vallet, A., Charlier, J.B., Fabbri, O., Bertrand, C., Carry, N., and Mudry, J. 2016. Functioning and precipitation-displacement modelling of rainfall-induced deep-seated landslides subject to creep deformation. *Landslides*, **13**(4): 653–670. doi:10.1007/s10346-015-0592-3.

- VanDine, D.F. 1983. Drynoch landslide, British Columbia – a history. *Canadian Geotechnical Journal*, **20**(1): 82–103. doi:10.1139/t83-009.
- VanDine, D.F., Nasmith, H.W., and Ripley, C.F. (n.d.). The emergence of engineering geology in British Columbia: “An engineering geologist knows a dam site better”! Available from <http://www.empr.gov.bc.ca/MINING/GEOSCIENCE/PUBLICATIONSCATALOGUE/OPENFILES/1992/Pages/OF1992-19-Engineer.aspx> [accessed 5 November 2015].
- Varnes, D.J. 1978. Slope movement types and processes. **176**: 12–33. National Academy of Sciences, Transportation Research Board Special Report. pp. 12–33.
- Veillette, J., and White, G. 1977. *Early Indian Village Churches: Wooden Frontier Architecture in British Columbia*. University of British Columbia Press, Vancouver, British Columbia, Canada.
- Victoria Daily Times. 1897, September 27. That Land Slide. Victoria, British Columbia.
- Wachinger, G., Renn, O., Begg, C., and Kuhlicke, C. 2013. The risk perception paradox- Implications for governance and communication of natural hazards. *Risk Analysis*, **33**(6): 1049–1065. doi:10.1111/j.1539-6924.2012.01942.x.
- Wade, M.S. 1979. *The Cariboo Road*. The Haunted Bookshop: Victoria, British Columbia, Canada.
- Walker, B., and Salt, D. 2006. *Resilience thinking: sustaining people and ecosystems in a changing world*. Island Press, Washington, USA.
- Wedage, A.M.P. 1995. Influence of rate effects on the residual strength of moving slopes. Ph.D. Thesis, Department of Civil and Environmental Engineering, University of Alberta, Edmonton, Alberta. Available from <http://search.proquest.com/pqdtlocal1006264/docview/230799795/abstract/5897D7B8A26D41D2PQ/1> [accessed 27 July 2016].
- Wildavsky, A. 1988. *Searching for safety*. Transaction Books, New Brunswick, USA.

Wood, D.F. 1982. Memorandum: CPR Landslide Mile 50.6-50.7 Thompson Subdivision. Submitted to CP Rail, Vancouver.

Záruba, Q., and Mencl, V. 1976. Engineering Geology. Elsevier Scientific Publishing Company, New York.

Zhang, X., Harvey, K.D., Hogg, W.D., and Yuzyk, T.R. 2001. Trends in Canadian streamflow. *Water Resources Research*, **37**(4): 987–998.

Zhang, X., Vincent, L.A., Hogg, W.D., and Niitsoo, A. 2000. Temperature and precipitation trends in Canada during the 20th century. *Atmosphere-Ocean*, **38**: 395–429.

Zhang, Y., Wallace, J.M., and Battisti, D.S. 1997. ENSO-like Interdecadal Variability: 1900–93. *Journal of Climate*, **10**(5): 1004–1020. doi:10.1175/1520-0442(1997)010<1004:ELIV>2.0.CO;2.